

# Twin Screw Wet Granulation of Pharmaceutical Powders: Role of Binder



The  
University  
Of  
Sheffield.

Mohammed Saleh

The University of Sheffield  
Department of Chemical & Biological Engineering

A thesis submitted in partial fulfilment of the requirements for the  
degree of Doctor of Philosophy

October 2016

## **Abstract**

Several manufacturing industries are looking into transferring from batch operation to continuous operations, due to advantages offered in ease of scale up and high throughput. The Twin Screw Granulator (TSG) offers continuous manufacturing. However, there is still a knowledge gap in completely understanding the mechanisms of the continuous granulation. This includes understanding the effect of the critical parameters on the granulation process and the product properties. This will enable optimizing the operation condition to obtain the desired granule properties (i.e. desired granulation) while minimizing powder caking onto the barrel surface (i.e. undesired granulation).

This research focuses on investigating the influence of the liquid binder viscosity at varying shear stresses, on both desired and undesired granulation. Different powders with different properties were considered to gain better appreciation of the importance of liquid-powder interaction. The research showed that both desired and undesired granulation was affected by the liquid binder viscosity. The effect of liquid binder viscosity varied as the shear stress applied was changed as well as the type of powder being used.

During low shear stress (i.e. conveying element only), increasing liquid binder viscosity limited the spreading of the liquid. This limitation showed to give similar trends for the desired granulation regardless of the powder property, while the undesired granulation showed to be influenced by the powder property. For desired granulation, the granules size distribution widens with increasing the liquid viscosity, with elongated granules. The primary particles on the surface remained unaffected, while loosely bonded, creating considerable air voids within its internal structure. For undesired granulation, the way the powder caked to the surface of the barrel showed to be independent of the powder property, while showing difference when the liquid binder viscosity is changed. Using low liquid binder viscosity resulted in powder caking, initiating from the side and advancing to the centre, while the high liquid binder viscosity resulted in powder caking to be initiated from the centre of the barrel. On the other hand, the mass of powder caking onto the surface of the barrel was influenced by both the liquid binder viscosity and powder

property. Increasing the liquid binder viscosity resulted in a reduction in the mass of powder caking for lactose and MCC. Whereas for the formulation, the amount of powder caking on the barrel surface, decreased first followed by a significant increase with increasing liquid binder viscosity.

Increasing the shear stress applied on the material (i.e. using conveying and kneading elements) resulted in different trends in the properties of granules (desired granulation) and powder caking (undesired granulation) as the liquid binder viscosity increased, when compared with their corresponding trends whilst applying low shear stress. The increase in shear stress helped to improve the spreading and mixing of liquid binder with the powder (particularly for higher liquid binder viscosity). For desired granulation, the lactose powder showed growth, in particular for the viscous liquid binder, due to the enhanced mixing while a reduction in big granules ( $\geq 3000 \mu\text{m}$ ) for MCC and formulation. Also, the granules tended to have a rougher surface as the liquid binder viscosity was increased, regardless of the material. The granule's surface topography showed to be more compacted and with less air voids within its internal structure. This was more influenced by the increase in the stress rather than the liquid binder viscosity or material property. For undesired granulation, the powder caking showed to give uniform behaviour (i.e. propagating from the side of the barrel) regardless of the liquid binder viscosity or the powder property. On the other hand, the mass of powder caking showed to be dependent on the powder property and the liquid binder viscosity. The ribbon of caked powder showed to have more compacted surface topography with less air voids internally, regardless of powder property and liquid binder viscosity. The tendency of powder caking showed possible influences in the integrity of the product, different powders within a blend showed a difference in tendency to adhere to the surface of the barrel.

Finally, the liquid binder viscosity and shear stress showed to influence the surface velocity of the granules which was measured using the PIV. The granules showed different surface velocity when moving from one screw to another, due to obstructions in the regions between the two screws. Generally, for low shear stress, depending on the liquid binder viscosity and the property of the material, obstruction between screws was more

prominent to occur. Increasing the shear stress reduced the level of obstruction, while reducing the difference in momentum gained as well as a lower surface velocity of the granules in both screws.

## **Acknowledgements**

Whilst I acknowledge the work was done by me, undertaking this Ph.D has been a life-changing experience. One that would have not been possible without the help and the inspiration of many people. Therefore, I would like to extend my sincerest gratitude and thanks to those who so generously and admirably stood by me.

Firstly, my greatest thanks and gratitude would go to my supervisor Prof. Agba Salman for all his support and guidance throughout. Without his faith in my ability, I would not have had the chance of presenting this thesis today. Also, I would like to extend my thanks to my beloved parents, my lovely Nannan and all of my dear family and friends (Majid, Amr, Maha, Marwa, Ali..etc) for supporting me throughout and tolerating my complaints and never failing to energise me as I was continually pushed to achieve more. You were the fuel to my engine, without you I would not have the energy to steer my life up to this point. Last but not least, I would like to express my gratitude to all of my colleagues (Chalak, Syed, Ranjit, Riyadh, Menan ..etc) from whom I learnt great deal of skills and knowledge. These were the infrastructure which enabled me to build the ladder to raise my intellectual skills a step higher.

## **List of Publications and Presentations**

Mohammed F. Saleh, Ranjit M. Dhenge, James J. Cartwright, Michael J. Hounslow, Agba D. Salman. Twin screw wet granulation: Binder delivery. *International Journal of Pharmaceutics*, 2015. 487(1–2): p. 124-134.

Mohammed F. Saleh, Ranjit M. Dhenge, James J. Cartwright, Michael J. Hounslow, Agba D. Salman. Twin screw wet granulation: Effect of process and formulation variables on powder caking during production. *International Journal of Pharmaceutics*, 2015. 496(2): p. 571-582.

Mohammed F. Saleh, Ranjit M. Dhenge, James J. Cartwright, Michael J. Hounslow, Agba D. Salman. Continuous Wet Granulation: Online monitoring the effect of Binder Delivery. 12th UK Particle Technology Forum, UK 2014.

Mohammed F. Saleh, Ranjit M. Dhenge, James J. Cartwright, Michael J. Hounslow, Agba D. Salman. Twin screw wet granulation: the effect of granulation liquid viscosity on the caking of lactose powder. 7<sup>th</sup> International Granulation Workshop, UK, 2009.

# Table of Contents

Abstract.....	I
Acknowledgements.....	IV
List of Publications and Presentations.....	V
Table of Contents.....	VI
List of Figures.....	XIII
List of Tables.....	XX
Nomenclature.....	XXI
Chapter 1 Introduction.....	1
1.1 Granulation background.....	1
1.2 Performance of Wet Granulation.....	2
1.2.1 Batch process.....	2
1.2.2 Continuous process.....	4
1.3 Thesis overview.....	5
Chapter 2 Literature review.....	7
2.1 Mechanism of Wet Granulation.....	7
2.1.1 Wetting and nucleation.....	7
Nuclei formation.....	7
Thermodynamics: Contact Angle.....	8
Thermodynamics: spreading coefficient.....	10
Nucleation kinetics:.....	11
2.1.2 Consolidation and Coalescence.....	14
Capillary and viscous forces.....	14
2.1.3 Breakage and attrition.....	15
2.2 Wet granulation behaviour.....	15
2.2.1 Desired granulation (Regime maps).....	15
2.2.2 Undesired granulation (powder caking).....	19
2.3 Background of Twin Screw Granulator.....	23
2.3.1 Application of the twin screw extruder in pharmaceutical field.....	23
2.3.2 Design of the Twin Screw Granulator (TSG).....	24
2.3.3 Fundamental of the screw elements.....	26

Mixing behaviour of screw elements.....	26
Distributive mixing behaviour.....	26
Dispersive Behaviour .....	28
Type of screw elements .....	29
Conveying Elements.....	29
Kneading Elements.....	30
2.3.4 Process and Formulation variables .....	31
Process variables.....	32
2.3.4.1.1 The effect of the Screw Configuration.....	32
2.3.4.1.2 The effect of the Screw Speed .....	35
2.3.4.1.3 The effect of the Powder Feed Rate .....	36
Formulation variables .....	38
2.3.4.1.4 The effect of the Liquid binder Viscosity .....	38
2.3.4.1.5 The effect of the Liquid/Solid (L/S) Ratio.....	40
2.4 Objectives.....	42
Chapter 3 Materials and Experimental methodology .....	44
3.1 Material.....	44
3.1.1 Lactose .....	44
3.1.2 Microcrystalline cellulose (MCC) .....	45
3.1.3 Crosscarmellose sodium .....	46
3.1.4 Hydroxypropyl methylcellulose (HPMC).....	46
3.1.5 First Intent formulation.....	47
3.2 Granule production.....	47
3.2.1 Powder conditioning.....	47
3.2.2 Liquid preparation.....	47
3.2.3 Blending .....	48
3.2.4 Twin screw granulator and screw configuration .....	48
3.2.5 Peristaltic pump .....	50
3.3 Granule analysis.....	51
3.3.1 Drying.....	51
3.3.2 Size distribution .....	51
3.3.3 Sieving .....	52



3.3.4 Shape.....	52
3.3.5 Surface topography.....	52
3.3.6 Structural characterization .....	53
Chapter 4 Desired Granulation: Influence of binder viscosity.....	54
4.1 Introduction .....	54
4.2 Experimental and analysis methodology.....	56
4.2.1 Droplet studies.....	56
4.2.2 Process and formulation parameters .....	59
4.2.3 Granule analysis.....	59
4.3 Results and discussion .....	59
4.3.1 The influence of binder viscosity on lactose powder .....	59
Droplet analysis.....	59
Size distribution .....	61
Granular shape.....	67
Surface topography.....	70
Structural characterization .....	71
4.3.2 The influence of binder viscosity on MCC powder .....	74
Droplet analysis.....	74
Size distribution .....	76
Granular shape.....	78
Surface topography.....	80
Structural characterization .....	81
4.3.3 The influence of binder viscosity on formulation .....	84
Droplet analysis.....	84
Size distribution .....	85
Granular shape.....	88
Surface topography.....	91
Structural characterization .....	92
4.4 Conclusion.....	94
Chapter 5 Desired Granulation: Binder Delivery .....	95
5.1 Introduction .....	95
5.2 Experimental and analysis methodology.....	98

5.2.1	Experimental plan .....	98
5.2.2	Droplet studies and process and formulation parameters.....	99
5.2.3	Binder spreading in Twin Screw Granulator (TSG).....	99
5.2.4	Granule analysis .....	100
5.3	Results and Discussion .....	100
5.3.1	Droplet analysis on static bed .....	100
5.3.2	Liquid spreading on a moving bed .....	102
5.3.3	Size distribution .....	104
5.3.4	Granular shape.....	106
5.3.5	Surface topography.....	108
5.3.6	Structural characterization .....	111
5.4	Conclusion.....	113
Chapter 6	Undesired Granulation: Powder Caking/Sticking.....	114
6.1	Introduction .....	114
6.2	Experimental and analysis methodology.....	117
6.2.1	Process and formulation parameters .....	117
6.2.2	Caking on Transparent Barrel .....	117
6.2.3	Caking on Stainless Steel barrel .....	118
6.2.4	Conductivity .....	118
6.3	Results and discussion- Part 1: Powder caking on the transparent barrel .....	120
6.3.1	Lactose .....	121
	Powder caking on the top barrel .....	121
6.3.2	MCC.....	125
	Powder caking on the top barrel .....	125
6.3.3	Formulation.....	128
	Powder caking on the top barrel .....	128
6.3.4	Binder delivery.....	131
	Powder caking on the top barrel .....	131
6.4	Results and discussion- Part 2: Powder caking on the stainless steel barrel.....	133
6.4.1	Lactose .....	133
	Powder caking/stickiness onto steel barrel .....	133
	Surface topography.....	134

Structural characterization .....	136
6.4.2 MCC.....	137
Powder caking/stickiness onto steel barrel .....	137
Surface topography.....	138
Structural characterization .....	140
6.4.3 Formulation.....	141
Powder caking/stickiness onto steel barrel .....	141
Surface topography.....	142
Structural characterization .....	143
6.4.4 Binder delivery .....	146
Powder caking/stickiness onto steel barrel .....	146
Surface topography.....	147
Structural characterization .....	148
6.5 Results and discussion- Part 3: The effect of caking on granule content .....	151
6.6 Conclusion.....	154
Chapter 7 Mechanistic understanding twin screw granulation.....	156
7.1 Introduction .....	156
7.2 Particle Image Velocimetry (PIV) background .....	157
7.3 Experimental and analysis methodology.....	158
7.4 Results and discussion .....	163
7.4.1 Lactose .....	163
Surface velocity.....	163
Granule size distribution and shape .....	166
7.4.2 MCC.....	168
Surface velocity .....	168
Granule size distribution and shape .....	170
7.4.3 Binder Delivery.....	171
Surface velocity .....	171
Granule size distribution and shape .....	173
7.5 Conclusion.....	175
Chapter 8 Conclusions .....	176
Chapter 9 Future work.....	179

9.1	Impact of change in screw configuration:.....	179
9.2	Powder caking/stickiness:.....	179
9.3	Surface velocity/material flow:.....	181
	References .....	182
	Appendix A.....	192
	A.1 Size distribution of primary particles .....	192
	A.2 Droplet analysis.....	192
	A.2.1 Lactose.....	192
	A.2.2 MCC .....	193
	A.3 Compressibility Index.....	193
	A.4 Independent process and formulation parameters:.....	195
	A.4.1 The effect of changing the L/S ratio .....	195
	Lactose .....	195
	MCC.....	197
	A.4.2 Powder Feed rate .....	199
	Lactose .....	199
	MCC.....	201
	A.4.3 Effect of Screw Speed.....	203
	Lactose .....	203
	MCC.....	205
	Appendix B .....	207
	B.1 Experimental set-up and process parameters .....	207
	B.1.1 Experimental set-up .....	207
	B.1.2 Size distribution:.....	209
	B.1.3 Further analysis for Experiment 3: .....	209
	B.1.3.1 Conveying elements only.....	209
	Size distribution .....	209
	Granular shape.....	211
	Granular's strength: .....	211
	Granules flowability: .....	212
	B.1.3.2 Kneading elements: .....	213
	B.2 Liquid binder spreading:.....	214

B.2.1 Methodology .....	214
B.2.2 Results and discussion .....	215
Appendix C .....	217
C.1 Size distribution .....	217
C.1.1 Lactose .....	217
C.1.2 MCC .....	218
C.1.3 Formulation .....	219
C.1.4 Binder delivery .....	220
C.2 Crushing force .....	221
C.2.1 Experimental method .....	221
C.2.2 Experimental method .....	222
Lactose .....	222
MCC .....	222
Formulation .....	223
Binder delivery .....	223
C.3 Powder caking/stickiness on the bottom barrel .....	224
C.3.1 Lactose .....	224
C.3.2 MCC .....	226
C.4 SEM .....	228
C.5 Thickness of caked ribbons .....	229
Appendix D .....	230
D.1 Visual On-line Sizing (VOS) .....	230
D.1.1 Method .....	230
D.1.2 Results .....	232
Appendix E .....	235
E.1 Effect of L/S on granule size .....	235
E.2 Effect of Viscosity on granule size .....	236
E.3 Effect of Feed-rate on granule size .....	237
E.4 Effect of screw-speed on granule size .....	238
Effect of screw-configuration on granule size .....	238

## List of Figures

Figure 1-1 Schematic representation of the wet granulation. ....	1
Figure 2-1 Schematic of the modern approach for granulation process [18]. ....	7
Figure 2-2 Droplet classification [22]. ....	9
Figure 2-3 Mechanisms of nucleation (a) Distribution, (b) Immersion [25]. ....	12
Figure 2-4 Nucleation zone regime [27]. ....	13
Figure 2-5 Granule growth regime map for twin screw granulation [36]. ....	18
Figure 2-6 Forms of liquid states with mobile bridges [38]. ....	21
Figure 2-7 Basic nomenclature of screw element [55]. ....	26
Figure 2-8 Distributive mixing behaviour [45]. ....	27
Figure 2-9 cross-section of the screws along the barrel ....	28
Figure 2-10 Dispersive mixing behaviour [45]. ....	29
Figure 2-11 Different common elements used to make up the configuration of the screw: (A) long pitch conveying element, (B) short pitch conveying element, (C) kneading element. ....	31
Figure 2-12 Growth and breakages of the granules. ....	31
Figure 2-13 the effect on mean residence time by the conveying capacity of each angle degree for the kneading element, while using varying the feed-rate and screw speed [17]. ....	34
Figure 2-14 Size distributions for changing powder feed rates [2]. ....	37
Figure 2-15 Median granule size with increasing amounts of HPC at different liquid to solid ratios [36]. ....	40
Figure 2-16 Schematic of research objective. ....	43
Figure 3-1 SEM image of primary particles of lactose monohydrate. ....	45
Figure 3-2 SEM image of primary particles of MCC. ....	46
Figure 3-3 Image of the parts the the twin screw granulator used in the current-experimental set-up. ....	49
Figure 3-4 illustrating the configurations of screw used in throughout the experiments: (A) conveying elements only (i.e. low stress) and (B) conveying elements with one section of kneading elements (i.e. high stress). ....	50
Figure 3-5 Calibration of peristaltic pump using water. ....	51
Figure 4-1 image of the droplet and surface bed (A), with the set-up used (B) used. ....	57
Figure 4-2 shows the spreading and penetration of the droplet once placed on a compact of powder. ....	57
Figure 4-3 Schematic drawing of (A) Projected area of the compressed bed (B) the actual (rough) area of the compress bed. ....	58
Figure 4-4 Effect of binder viscosity on maximum spread and penetration time on a static bed of lactose. ....	60
Figure 4-5 Shows the tablet's surface topography of compressed bed for the low (0%w/w HPMC) and high (15w/w HPMC) liquid binder viscosity. ....	61
Figure 4-6 Effect of liquid binder viscosity on size distribution; (a) low stress and (b) high stress. .	64

Figure 4-7 shows the span of size distribution as the liquid binder viscosity changed during low and high. shear stress. ....	65
Figure 4-8 schematic explanation of the spreading of binder of varying viscosity at a low shear stress. ....	65
Figure 4-9 schematically describes the function of the kneading elements .....	66
Figure 4-10 Effect of liquid binder viscosity on the aspect ratio of lactose granules as the stress varied. ....	68
Figure 4-11 Effect liquid binder viscosity on the shape of lactose granules as the stress varied.....	69
Figure 4-12 schematic diagram showing the flow of the material during low stress.....	70
Figure 4-13 Effect of low (0%) and high (15%) liquid binder viscosity on surface topography of lactose granules, as the stress varied. ....	71
Figure 4-14 Effect of liquid binder viscosity on the porosity of lactose granules, as the stress varied. ....	72
Figure 4-15 Shows X-ray of lactose granules produced as the liquid binder viscosity and the stress changed.....	73
Figure 4-16 effect of binder viscosity on maximum spread and penetration time on a static bed of MCC.....	75
Figure 4-17 Shows the tablet's surface topography of compressed bed for the low (0%w/w HPMC) and high (15w/w HPMC) liquid binder viscosity.....	76
Figure 4-18 Effect of liquid binder viscosity on size distribution; (a) low stress and (b) high stress.....	77
Figure 4-19 shows the span of size distribution as the liquid binder viscosity changed during low and high. shear stress. ....	78
Figure 4-20 Effect of liquid binder viscosity on the aspect ratio of lactose granules as the stress varied. ....	79
Figure 4-21 Effect liquid binder viscosity on the shape of lactose granules as the stress varied.....	80
Figure 4-22 Effect of low (0%) and high (15%) liquid binder viscosity on surface topography of MCC granules, as the stress varied.....	81
Figure 4-23 Effect of liquid binder viscosity on the porosity of MCC granules, as the stress varied.....	82
Figure 4-24 Shows X-ray of MCC granules produced as the liquid binder viscosity and the stress changed.....	83
Figure 4-25 effect of binder on maximum spread and penetration time on a static bed of formulation. ....	85
Figure 4-26 Shows the tablet's surface topography of compressed bed for the low (0%w/w HPMC) and high (15w/w HPMC) liquid binder viscosity.....	85
Figure 4-27 Effect of liquid binder viscosity on size distribution; (a) low stress and (b) high stress.....	87
Figure 4-28 shows the span of size distribution as the liquid binder viscosity changed during low and high. shear stress .....	88
Figure 4-29 Effect of liquid binder viscosity on the aspect ratio of lactose granules as the stress varied. ....	89
Figure 4-30 Effect liquid binder viscosity on the shape of lactose granules as the stress varied.....	90
Figure 4-31 Effect of low (0%) and high (15%) liquid binder viscosity on surface topography of lactose granules, as the stress varied. ....	91

Figure 4-32 Effect of liquid binder viscosity on the porosity of formulation granules, as the stress varied. ....	92
Figure 4-33 Shows X-ray of formulation granules produced as the liquid binder viscosity and the stress changed. ....	93
Figure 5-1 The change in granule size distribution for formulations containing pharmatose 200 M (A), impalpable (B), and supertab 30GR (C) as the lactose grade using dry binder (◆), 1:1 liquid:dry binder (■) and liquid binder (▲) at L/S = 0.3 [78]. ....	97
Figure 5-2 Illustration of the set-up to determine binder distribution over a moving bed.....	99
Figure 5-3 Effect of binder delivery on maximum spread and penetration time on a static bed. .	101
Figure 5-4 Shows surface topography for compressed bed from Set 1 and Set 3. ....	101
Figure 5-5 Images taken at $T_s$ of 4.17s (left) and 8.33s (right) for the three sections of the barrel (Beginning, Middle and End) for each set at low shear stress.....	103
Figure 5-6 Images taken at $T_s$ of 8.33s for the three sections of the barrel (Beginning, Middle and End) for two extreme sets (Set 1&3) at high shear stress. ....	104
Figure 5-7 Effect of binder delivery on size distribution: (a) low stress, (b) high stress.....	105
Figure 5-8 shows the span of size distribution as the binder delivery changed during low and high shear stress .....	106
Figure 5-9 Effect of binder delivery on the aspect ratio as stress varied. ....	107
Figure 5-10 Effect of binder delivery on granules' shape ( $\geq 2000\mu\text{m}$ ) as stress changed. ....	108
Figure 5-11 Effect of binder delivery on granular surface tomography, as the stress varied. ....	110
Figure 5-12 Effect of binder delivery on the porosity of granules, as the stress varied. ....	111
Figure 5-13 Shows X-ray of granules produced while varying the binder delivery and the stress. ....	112
Figure 6-1 Magnitude of the inter-particle forces as the primary particle size changes [116]. ....	115
Figure 6-2 Illustration an overhead view of the transparent barrel. The kneading zone is the location where the kneading elements will fit in the case of high shear stress.....	117
Figure 6-3 Imaged of undamaged ribbon of powder caking. ....	118
Figure 6-4 schematically indicating the three points of collecting the sample for conductivity....	120
Figure 6-5 shows the calibration of salt conductivity. ....	120
Figure 6-6 Effect of liquid binder viscosity on the mass (g) of lactose powder caking: low stress (■) and high stress (■).....	123
Figure 6-7 show the flow direction of the material within the granulator.....	123
Figure 6-8 Effect of liquid binder viscosity on the behavior of powder caking: (a) low stress (b) high stress. The material flows from screw No. 1 to screw No. 2. ....	124
Figure 6-9 Effect of liquid binder viscosity on the mass (g) of MCC powder caking: low stress (■) and high stress (■).....	126
Figure 6-10 Effect of liquid binder viscosity on the behavior of powder caking: (a) low stress (b) high stress. ....	127
Figure 6-11 Effect of liquid binder viscosity on the mass (g) of formulation powder caking: low stress (■) and high stress (■). ....	129
Figure 6-12 Effect of liquid binder viscosity on the behavior of powder caking: (a) low stress (b) high stress. ....	130



Figure 6-13 Effect of binder delivery on the mass (g) of formulation powder caking: low stress (■) and high stress (■).....	131
Figure 6-14 Effect of binder delivery on the behavior of powder caking: (a) low stress (b) high stress.....	132
Figure 6-15 extrude coming out at the end of the barrel at extreme conditions. ....	133
Figure 6-16 Effect of the low (0%) and high (15%) liquid binder viscosity on the mass (g) of lactose powder caking: low stress (■) and high stress (■).....	134
Figure 6-17 Effect of low (0%) and high (15%) liquid binder viscosity on the behavior of powder caking: (a) low stress (b) high stress. The material flows from screw No. 1 to screw No. 2. ....	134
Figure 6-18 6-19 Effect of low (0%) and high (15%) liquid binder viscosity on surface topography of lactose ribbon of cake, as the stress varied.....	135
Figure 6-20 Effect of low (0%) and high (15%) liquid binder viscosity on porosity of lactose ribbon of cake, as the stress varied.....	136
Figure 6-21 X-ray images of lactose ribbon as liquid binder viscosity and stress varied.....	137
Figure 6-22 Effect of the low (0%) and high (15%) liquid binder viscosity on the mass (g) of MCC powder caking: low stress (■) and high stress (■).....	138
Figure 6-23 Effect of low (0%) and high (15%) liquid binder viscosity on the behavior of powder caking: (a) low stress (b) high stress. ....	138
Figure 6-24 Effect of low (0%) and high (15%) liquid binder viscosity on surface topography of MCC ribbon of cake, as the stress varied. ....	139
Figure 6-25 Effect of low (0%) and high (15%) liquid binder viscosity on porosity of MCC ribbon of cake, as the stress varied. ....	140
Figure 6-26 X-ray images of MCC ribbon as liquid binder viscosity and stress varied.....	141
Figure 6-27 Effect of the low (0%) and high (15%) liquid binder viscosity on the mass (g) of formulation powder caking: low stress (■) and high stress (■).....	142
Figure 6-28 Effect of low (0%) and high (15%) liquid binder viscosity on the behavior of powder caking: (a) low stress (b) high stress. ....	142
Figure 6-29 Effect of low (0%) and high (15%) liquid binder viscosity on surface topography of formulation ribbon of cake, as the stress varied. ....	143
Figure 6-30 Effect of low (0%) and high (15%) liquid binder viscosity on porosity of formulation ribbon of cake, as the stress varied. ....	144
Figure 6-31 X-ray images of formulation ribbon as liquid binder viscosity and stress varied.....	145
Figure 6-32 Effect of binder delivery (Set 1 & 3) on the mass (g) of powder caking: low stress (■) and high stress (■).....	146
Figure 6-33 Effect of binder delivery (Set 1 & 3) on the behavior of powder caking: (a) low stress (b) high stress. ....	146
Figure 6-34 Effect of binder delivery (Set 1 & 3) on surface topography of ribbon, as the stress varied. ....	148
Figure 6-35 Effect of binder delivery (Set 1 & 3) on porosity of ribbons, as the stress varied.....	149
Figure 6-36 X-ray images of ribbon as binder delivery (Set 1 & 3) and stress varied.....	150
Figure 6-37 Size distribution granules with time produced with low liquid binder viscosity and high stress. ....	151

Figure 6-38 Mass (g) of powder caking with time. ....	152
Figure 6-39 Conductivity of salt coming from the feeding hopper with time (min).....	153
Figure 6-40 Conductivity of salt from the ribbon with time. ....	153
Figure 7-1 shows PIV set up (a) and an example of images taken (axis shown) (b). ....	159
Figure 7-2 Velocity in each integration area. ....	161
Figure 7-3 Steps of analyzing images for surface velocity (a) and the three areas of each image (b). .....	163
Figure 7-4 Effect of liquid binder viscosity on the surface velocity of lactose granules in the translational areas (TB and TA): (a) low stress and (b) high stress. ....	165
Figure 7-5 Effect of liquid binder viscosity on the channel fill as stress varied. ....	165
Figure 7-6 Describes the phenomena of the material build up prior to the kneading elements schematically.....	166
Figure 7-7 Effect of liquid binder viscosity on size distribution of lactose granules: (a) low stress and (b) high stress.....	167
Figure 7-8 Effect of liquid binder viscosity on the shape of lactose granules as the stress varied. ....	167
Figure 7-9 Effect of liquid binder viscosity on the surface velocity of MCC granules in the translational areas (TB and TA): (a) low stress and (b) high stress. ....	169
Figure 7-10 Effect of liquid binder viscosity on the channel fill as stress varied. ....	169
Figure 7-11 Effect of liquid binder viscosity on size distribution of MCC granules: (a) low stress and (b) high stress.....	170
Figure 7-12 Effect of liquid binder viscosity on the shape of MCC granules as the stress varied. .	171
Figure 7-13 Effect of binder delivery on the surface velocity of granules in the translational areas (TB and TA): (a) low stress and (b) high stress. ....	172
Figure 7-14 Effect of binder delivery on the channel fill as stress varied.....	173
Figure 7-15 Effect of binder delivery on the granules size distribution: (a) low stress and (b) high stress. ....	174
Figure 7-16 Effect of binder delivery on granules' shape as the stress varied. ....	174
Figure A-1: More images under the SEM showing the wet and dry section of the tablet after the droplet penetrated through the compact of Lactose material, at different magnification. ....	192
Figure A-2: More images under the SEM showing the wet and dry section of the tablet after the droplet penetrated through the compact of MCC material, at different magnification.....	193
Figure A-3: The Compressibility Index and Porosity of compressed beds Of Lactose and MCC change as the compression force varies.....	194
Figure B-1: The size distribution from each experiment may differ but the overall trends remain similar.....	209
Figure B-2: The effect of binder delivery in Set 1, 2 & 3 on Residence time (A), Torque (B) and Barrel Fill Level, while applying the condition in for experiment 2. ....	210
Figure B-3: shows the change in granular's shape as more HPMC delivered in the liquid phase. .	211
Figure B-4: the strength of granules in the big and small classes produced at different binder delivery.....	211

Figure B-5: The effect of binder delivery on the Angle of repose (A), and Compressibility Index (B.).	212
Figure B-6: The effect of binder delivery in Set 1 & 3 on the Residence time (A) & Torque (B), while applying the condition in for experiment 2, with kneading element	213
Figure B-7: The effect of binder delivery on the angle of repose, while using kneading element.	213
Figure B-8: calibration of light absorption to the concentration of red dye in the solution.	214
Figure B-9 Concentration of the dye in the three different classes of each set.	216
Figure C-1 Effect of variation of HPMC (% w/w) in the granulation liquid on size distribution of granules using lactose powder. (a) Using conveying elements only and (b) using conveying and kneading element as screw configuration.	217
Figure C-2 Effect of variation of HPMC (% w/w) in the granulation liquid on size distribution of granules using MCC powder. (a) Using conveying elements only and (b) using conveying and kneading element as screw configuration.	218
Figure C-3 Effect of variation of HPMC (% w/w) in the granulation liquid on size distribution of granules using lactose powder. (a) Using conveying elements only and (b) using conveying and kneading element as screw configuration.	219
Figure C-4 Effect of variation of binder delivery on size distribution of granules. (a) Using conveying elements only and (b) using conveying and kneading element as screw configuration.	220
Figure C-5 images of the indenter used to break the ribbon of cakes.	221
Figure C-6 Crushing forces required to break the ribbon of lactose cakes as the viscosity of the granulation liquid and screw configuration changes.	222
Figure C-7 Crushing forces required to break the ribbon of MCC cakes as the viscosity of the granulation liquid and screw configuration changes.	222
Figure C-8 Crushing forces required to break the ribbon of formulation placebo cakes as the viscosity of the granulation liquid and screw configuration changes.	223
Figure C-9 Crushing forces required to break the ribbon of formulation placebo cakes as binder delivery and screw configuration changes.	223
Figure C-10 Effect of granulation liquid viscosity on Lactose powder caking/stickiness on the bottom of the barrel after 6 minutes, using conveying elements only.	224
Figure C-11 Effect of granulation liquid viscosity on Lactose powder caking/stickiness on the bottom of the barrel after 6 minutes, using conveying elements and kneading elements.	225
Figure C-12 Effect of granulation liquid viscosity on the mass of caking on the bottom of the barrel using: conveying elements only (■) and conveying with kneading elements (■).	225
Figure C-13 Effect of granulation liquid viscosity on MCC powder caking/stickiness on the bottom of the barrel after 6 minutes, using conveying elements only.	226
Figure C-14 Effect of granulation liquid viscosity on MCC powder caking/stickiness on the bottom of the barrel after 6 minutes, using conveying elements and kneading elements.	227
Figure C-15 Effect of granulation liquid viscosity on the mass of caking on the bottom of the barrel using: conveying elements only (■) and conveying with kneading elements (■).	227
Figure D- 1 system set-up for VOS with overhead mixer.	230

Figure D- 2 system set-up for VOS with vibrator .....231  
Figure D- 3 image taken using overhead mixer. ....232  
Figure D- 4 image of granules as the fall off the vibrator. ....233

## List of Tables

Table 3-1 The first intent formulation. ....	47
Table 3-2 change in liquid binder viscosity with increase in the mass percentage of HPMC in the granulation liquid. ....	48
Table 3-3 the screw element coding. ....	50
Table 4-1 Contact angle using the Wenzel approach ( $\theta_w$ ) on compressed bed of lactose at 500N. ....	60
Table 4-2 Contact angle using the Wenzel approach ( $\theta_w$ ) on compressed bed of MCC at 500N. ..	74
Table 4-3 Contact angle using the Wenzel approach ( $\theta_w$ ) on compressed bed of formulation at 500N. ....	84
Table 5-1 Formulation composition and process conditions used in three sets .....	98
Table 5-2 Contact angle using the Wenzel approach ( $\theta_w$ ) on compressed bed at 500N. ....	101
Table 6-1 Experiment conditions for the conductivity of ribbon adhered to steel surface. ....	119
Table 6-2 shows the average mass (mg) of salt present in the powder cake as time varied. ....	154
Table 7-1 Position of the translational areas in the Y-direction. ....	163

## Nomenclature

$\phi_y$	Young's contact angle
$\gamma_{sl}$	Solid-liquid surface tension
$\gamma_{sv}$	Solid-vapour surface tension
$\gamma_{lv}$	Liquid-vapour surface tension
$\phi_w$	Wenzel's angle contact angle
$r_{RF}$	Roughness ratio
$W_c$	Work of cohesion
$W_A$	Work of adhesion
$\lambda_{ls}$	Liquid spreading coefficient over solids
$\lambda_{sl}$	Solid spreading coefficient over liquid
$P_c$	Laplace capillary suction pressure
$R_{pore}$	Radius of the pore within a powder bed
$\phi$	Solid-liquid contact angle
$\Psi_a$	Dimensionless spray flux
$\tau_p$	Penetration time
$St_v$	Viscous Stokes number
$U_c$	Colliding velocity of the particles
$U_{ci,j}$	Relative velocity of particle i on the particle j
$r$	Radius of particle
$\rho_s$	Density of particles
$\mu$	Viscosity
$S_{max}$	Maximum granule pore saturation
$De$	Deformation number
$w$	Mass ratio of liquid to solid
$\varepsilon_{MIN}$	Minimum porosity
$\rho_l$	Density of liquid
$\rho_g$	Density of gas
$Y_g$	Dynamic yield stress of material
$L/S$	Liquid/Solid ratio
$\beta$	Deformation value
L/D ratio	Length/Diameter ratio of the barrel
$D_o$	Screw diameter
K60°	Kneading elements staggered at 60° degree
$A_{particle}$	Actual area
$A_{projected}$	Projected area
$d_{max}$	Maximum spreading on compressed bed
$D_0$	Droplet initial diameter
$T_s$	Spreading time
$\dot{m}$	Mass flow rate

$\rho_B$	Bulk density
$V_F$	Conveyer free volume
$S_L$	Lead length of the screw
TA	Translational Area A
I	Intermeshing Area
TB	Translational Area B
$U_{aver}$	Average resultant surface velocity

## Abbreviation

2DSB	Two-dimensional spouted bed
API	Active pharmaceutical ingredient
COR	Cross Correlation Algorithm
MQD	Minimum Quadratic Difference
FBG	Fluidized bed granulation
FDA	Food and Drug Agency
GSK	Glaxosmithkline
HPMC	Hydroxypropyl methylcellulose
HSM	High Shear Mixer
LPCE	Long pitch conveying element
MCC	Microcrystalline cellulose
PIV	Particle Image Velocimetry
PEPT	Positron Emission Particle Tracking
PFN	Powder flow number
QbD	Quality by Design
RH	Relative Humidity
SEM	Scanning Electron Microscopy
SPCE	Short pitch conveying element
TSG	Twin screw granulator

# Chapter 1 Introduction

## 1.1 Granulation background

Granulation, also known as agglomeration (size enlargement), is the process in which particles are brought into contact with each other to form larger, or semi-aggregate, granules [1-3]. Granulation aims to improve the flow of materials as well as enhancing their compaction/homogeneity, reduce the production of dust (which minimizes losses, inhalation and explosion risks), increase the bulk density and prevent segregation of downstream blend of materials. Therefore, the application of granulation is used by a wide range of industries, such as pharmaceutical, food, chemical, ceramics, detergents, and fertilizers [4]. Such a technology is broadly classified into two classes; dry and wet granulation.

1. *Dry granulation*: is a process that applies mechanical compression to bring the powder particles into contact to form a granule without using any liquid solution e.g. roller compaction. This technique is ideal for products that may be sensitive to moisture or heat [5].
2. *Wet granulation*: is a process that depends on the use of liquid (water alone or with binder), to act as an adhesive to form a wet mass from the powder, as illustrated schematically in Figure 1-1. The particles are brought together by the use of the combination of capillary and viscous forces in the wet state. The wet mass is dried, where the permanent bonds are formed to give agglomerates [6].

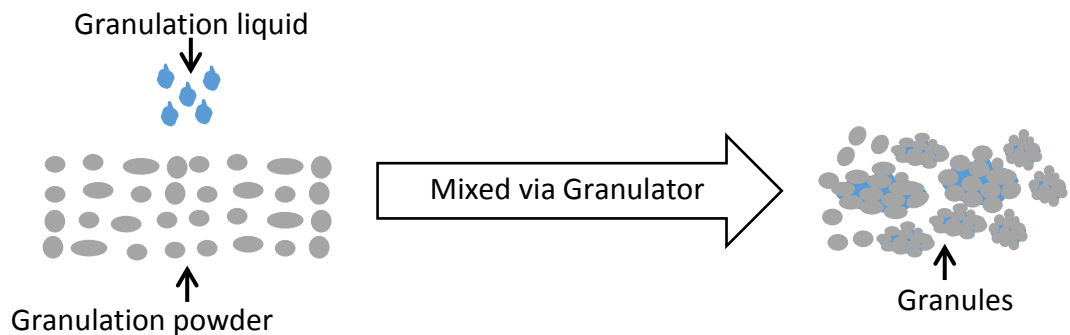


Figure 1-1 Schematic representation of the wet granulation.



Both methods of granulation (wet & dry) have some advantages and disadvantages. Granulation importance has grown fast in the industrial world. Wet granulation is well-established and accounts for more than 70% of the global industry's granulation [7].

In the pharmaceutical field, drug products are produced using an active pharmaceutical ingredient (API). API powder has a relatively small particle size ( $<100\mu\text{m}$ ), while tending to possess high cohesivity and poor flowability [8]. Such characteristics (of API) can present difficulties while intending to use a simple direct compaction technology to produce tablets. Therefore, granulation process becomes of a necessity in the pharmaceutical field as an intermediate process for the production of granules, which are subsequently compressed into tablets. However, the API materials are usually used in a formulation with one or more excipient materials (inert material). Excipient materials are pharmacologically inert as their inclusion as a part of drug formulation is to improve various functional roles. The functional roles of the excipient can be to regulate the quantity of API, enhancing compatibility of the formulation as well as aiding the binding of primary particles, lubrication source during processing, taste masking, or modifying the drug release. Such function makes these excipient have a great influence during the design and development of dosage form [9]. Moreover, the materials (active and inert materials) will have to be mixed homogeneously before granulation, as the purpose of granulation is to maintain the homogeneous mixture and prevent segregation, due to different primary particles properties (such as size), while also improving their flowability and compactibility [8].

## **1.2 Performance of Wet Granulation**

Wet granulation techniques can be carried out continuously or on a batch basis, where each one offers different advantages [2].

### **1.2.1 Batch process**

The pharmaceutical industry has depended largely on the batch processing for most of its granulation operations. This is due to a number of reasons; such as that the batch process is ideal for small volumes of material, which are routinely processed within the

pharmaceutical industry [10, 11]. The batch process is considered as a suitable method for materials that are heat-sensitive as well as being a flexible procedure for variety of productions [12]. Such advantages are considered the easiest way to comply with regulation and minimizing any production of off-specification materials. Some of the most frequently used batch granulation techniques are briefly discussed below.

**High shear granulation (HSG)** is widely used in the pharmaceutical industries for blending and granulation. Within the granulator, the mixing between the primary solid particle and granulation liquid is performed using an impeller to keep the particles moving, and a chopper; which is used to break large lumps into smaller fragments. The granulation liquid, used in this technique, can be added in variety of methods such as pouring, pumping, melting or spraying from the top. HSG has shorter processing time and uses a small amount of granulation liquid binder in comparison with that used during fluidized bed granulation. Furthermore, HSG technique allows for a highly cohesive material to be granulated [11]. Such technique is commonly known to give granules with a high density and uniform size and shape. However, the disadvantages of the high shear granulator (HSG) are; the possibility of variation in granule properties from batch to batch, difficulty to optimize the process, the requirement of a frequent cleaning as well as the high power consumption [13].

**Fluidized bed granulation (FBG)** is commonly used in the pharmaceutical industries, chemical and food. A powder bed within such a granulator is aerated by fluidizing air/gas. The fluidized air is passed through a bed of solid particles at a certain velocity, which cause solid particles to act as fluid or a free mobility. This creates a turbulent mixing in the granulator, which improves the mixing and hence resulting in the formation of granules. The granules produced obtain sufficient strength to sustain themselves within the granulator, while having an adequate porosity allowing for a quick dissolution. The fluidized bed granulation offers a major advantage in eliminating the need for an additional drying process, as the entire process can be carried out in a single unit.

However, the disadvantage of such technique are; the de-fluidizing of the solid particles, the need of dust recovery equipment and problems of powder caking to the surface of the equipment [10, 14].

### **1.2.2 Continuous process**

Although, the aforementioned batch techniques (FBG &HSG) are well established within the pharmaceutical field, each technique offers some limitations. The size of each batch will be restricted by the capacity of the given equipment. To scale-up such granulator (to allow for a high throughput) comes with many complications. This will inflict an increase in both time and cost of the process making such a technique an inefficient choice. Furthermore, monitoring and controlling batch equipment can present many difficulties. The continuous process can offer a potential solution to overcome such limitations. Some of the advantages, offered by a continuous process, are as follows:

- Continuous process can ensure a higher throughput of materials, with considerably smaller equipment footprint in comparison with that of the batch process, as well as being easy at changing process parameters during production.
- Such a process can be fully automated and has lower associated costs, as it requires less space and workers.
- Continuously processes present less complexity during scaling up into a commercial scale installation takes place and hence reduction on capital costs.

The continuous process can be considered more efficient as it allows for higher throughput in a short time [2, 12, 13, 15, 16]. Though, the drawbacks to the continuous process could be the waste of drug materials lost at start, as the system will need to reach steady state prior to production of the desired granules at the given process variables. This is not the case in the batch process as no material is wasted at the start. Twin screw extruders can be used as wet continuous granulation [12].

***Twin screw granulator (TSG)*** is a continuous process, which is rapidly growing in importance in the pharmaceutical industry, as it is more efficient and the granules it produces have improved properties [17]. The emergence of twin screw granulator, as a desirable choice for continuous wet granulation is owed to the advantages offered by such a technique. This equipment allows for a continuous granulation of primary particles, with high productivity, automated control and energy efficiency, and therefore, results in a reduction of the operational cost. Furthermore, the twin screw granulator allows more consistency within the granule properties (e.g. size and shape), while ability to change process variables more easily.

### **1.3 Thesis overview**

- ✓ Chapter 2: The scope of this chapter focuses on the literature of wet granulation, back ground information on twin screw granulation and previous work done within twin screw granulation.
- ✓ Chapter 3: This chapter focuses on the material used during this study and the experimental and analysis methodology of the main experiments conducted during this study.
- ✓ Chapter 4: This chapter explores the influence of liquid binder viscosity on the granule properties, as the shear stress and the material varied. The material used during this chapter are; lactose, MCC and formulation (the composition of the formulation is present in section 3.1.5). The shear stress was varied by changing the screw configuration, i.e. conveying elements only (low shear stress) and conveying with kneading elements (high shear stress).

- ✓ Chapter 5: In this chapter, the formulation is used where the effect of binder delivery, on the granule properties, is investigated as the shear stress applied was varied.
- ✓ Chapter 6: This chapter focuses on undesired granulation. It involves optically monitoring the behavior of powder caking as the liquid binder viscosity and shear stress varied. The material used within this chapter is the same as that in Chapter 4 & 5. Furthermore, the mass and the properties of ribbon of cakes (such as surface topography, structural characterization) were considered. Finally the uniformity within the ribbons is studied as lactose and salt used for as powder mixture.
- ✓ Chapter 7: This chapter studies the material flow within the barrel by considering its surface velocity using Particle Image Velocimetry (PIV). Three material considered (lactose, MCC and formulation) with a lowered operation condition (such as powder feed rate and screw speed).
- ✓ Chapter 8: The overall conclusion of the main findings from each study will be presented within this chapter.
- ✓ Chapter 9: Within this chapter, areas for further work which could be conducted in relation to the twin screw granulation are recommended.

## Chapter 2 Literature review

### 2.1 Mechanism of Wet Granulation

Although, the mechanism of wet granulation is still not comprehensively understood, the most modern approach to describe the mechanism can be split into three stages; wetting and nucleation, consolidation and coalescence, attrition and breakage [18], as illustrated in Figure 2-1.

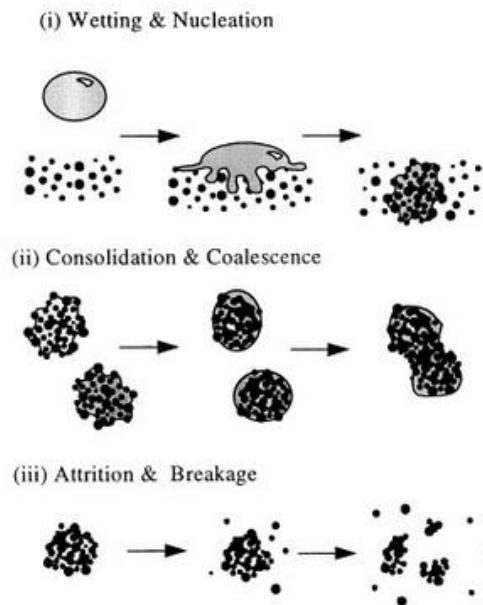


Figure 2-1 Schematic of the modern approach for granulation process [18].

#### 2.1.1 Wetting and nucleation

Wetting and nucleation is the first stage of the mechanisms during wet granulation. Within this stage, the liquid binder firstly comes into contact with the dry powder to form weak and loosely held cluster of particles (called nuclei). The nucleation step will depend on two processes; nuclei formation and binder dispersion.

##### ***Nuclei formation***

The nuclei formation process depends upon the wetting thermodynamics and kinetics to determine whether the process will be energetically favorable or not. Two of the aspects that describe the wetting thermodynamics are the contact angle (between the liquid and the solid) and the spreading coefficient [18].

**Thermodynamics: Contact Angle**

Wetting is the interaction between liquid and solid particles, where it involves the formation of three different interfacial boundary surfaces (solid-air, solid-liquid and liquid-air). The difference of interfacial tensions between these three different boundary surfaces acts within the local area of contact to create a contact angle. During the process of wetting, the area of the solid-liquid interface replaces a solid-air interface depending on the specific surface energy contents of the interface. Therefore, wetting is a thermodynamic process; where the extent of wetting and whether it will be spontaneous or not, will depend on the free energy available as a result from the difference in surface energies of the three interfaces [19, 20]. The contact angle value can be used as a parameter to indicate the wettability; though, the contact angle itself is not a primary thermodynamic quantity. The degree of wettability between liquid binder and primary particles of the powder influences the structure and strength of the produced granules [19, 21].

The conditions of the surface of solid powder led to a number of definitions of contact angle (intrinsic, actual and apparent contact angle). Intrinsic contact angle is the angle formed on an ideal smooth solid surface defined by Young's Equation ( $\theta_y$ ) (Equation 2-1), where  $\gamma$  (mN/m) is surface tension (surface energy) at the local area of contact, where the interfaces boundaries (solid, liquid and vapor) are denoted by the s, l, v subscripts respectively [19, 20].

$$\text{Cos}\theta_y = \frac{(\gamma_{sv} - \gamma_{sl})}{\gamma_{lv}} \qquad \text{Equation 2-1}$$

The Young's contact angle ( $\theta_y$ ) is based on an ideal solid surface, which is assumed to be smooth, homogeneous, rigid and both chemically and physically inert with respect to the liquid droplet deposited on the surface. Generally, if the contact angle is less than 90°, then the wetting of the solid surface of the powder bed will be good, as the droplet will tend to spread over a large surface area of the solid. In the case of water, the material will be classified as hydrophilic. The material will be considered as hydrophobic, if the contact

angle is greater than 90°. The wetting of the surface will be poor and hence the spreading of the droplet will be over a smaller area of the solid surface. This is schematically show in Figure 2-2. This affinity between the liquid and solid is an important factor during the wetting and nucleation stage, as it will have an effect on the strength of the granules produced [19].

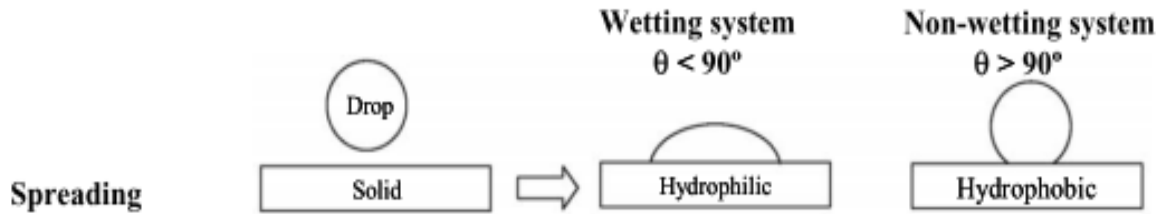


Figure 2-2 Droplet classification [22].

The contact angle measurement can vary substantially when performed on a powder bed. This is due to many factors that can affect the outcome, such as the roughness of surface of the powder bed and the viscosity of the droplet.

Such roughness in solid surface of the powder bed, can cause the base of the droplet to deviate from attaining circular shape once placed on the solid surface. This causes different contact angles values given, e.g. advancing, receding [20, 23]. The contact angle that can be measured is referred to as the 'apparent contact angle'. This is the angle between the apparent surface of the solid and the tangent to liquid interface [23]. A model by Robert Wenzel [21] has been proposed to relate the 'apparent contact angle' in a real system to the Young's contact angle (intrinsic/ideal angle) [22-24]. This model accounted for the surface roughness, where the system is homogeneous (no pocket of air between the liquid and the material), Wenzel proposed the following model:

$$\cos \theta_w = r_{RF} \cos \theta_y \quad \text{Equation 2-2}$$

where  $\theta_w$  is the observed angle on the rough surface of powder bed (Wenzel's angle),  $r_{RF}$  is the roughness ratio and  $\theta_y$  is the contact angle on a smooth surface (Young's contact angle). Wenzel's roughness ratio compares the real area of the rough surface available in a system with the area of the smooth surface area. This will always be greater than one and



because of this, if the material was to be hydrophilic, the roughness will make it more hydrophilic, and if it was a hydrophobic, then it will be more hydrophobic [21, 23, 24].

The most fundamental implications of this theory are that, it gives a single value for the 'apparent contact angle'. In the case of non-uniform roughness of solid surface, there is a range of 'apparent contact angles' (the hysteresis range). It has been proven that, mathematically, the 'apparent contact angle' can be calculated using Equation 2-2 (Wenzel's theory), when the size of the droplet is infinitely large in comparison with the scale of the surface roughness of the solid [19, 23].

***Thermodynamics: spreading coefficient***

The extent at which the liquid and solid will spread over each other can also be described by considering the surface free energy, using the spreading coefficient ( $\Lambda$ ). The spreading coefficient takes into consideration the difference between the work of cohesion ( $W_C$ ) and the work of adhesion ( $W_A$ ). The work of cohesion is the energy required to separate a unit cross sectional area of a material from itself (Equation 2-3 and Equation 2-4). The work of adhesion is the energy required to separate a unit area of an interface (Equation 2-5). [18].

$$\text{Work of cohesion of solid, } W_{Cs} = 2 \gamma_{sv} \qquad \text{Equation 2-3}$$

$$\text{Work of cohesion of liquid, } W_{Cl} = 2 \gamma_{lv} \qquad \text{Equation 2-4}$$

$$\text{Work of adhesion, } W_A = \gamma_{sv} + \gamma_{lv} - \gamma_{sl} = (\cos \theta_y + 1) \qquad \text{Equation 2-5}$$

The spreading coefficient is the difference between the work of adhesion and cohesion. This can be used to determine if the spreading is thermodynamically favorable or not, as there will be three different possible ways for spreading between the solid and liquid to take place [18, 19]:

1. Liquid will spread over the solid ( $\Lambda_{ls}$ ), creating a film on the solid surface. This will result in dense and strong granules.
2. Solid will adhere to liquid ( $\Lambda_{sl}$ ), without the creation of the film. This will result in porous and weak granules.

3. Both the solid and liquid will have a high work of cohesion, which results in minimising the interfacial area.

The spreading coefficient of each phase can be calculated using Equation 2-6 and Equation 2-7.

$$\Lambda_{ls} = W_A - W_{Cl} \quad \text{Equation 2-6}$$

$$\Lambda_{sl} = W_A - W_{Cs} \quad \text{Equation 2-7}$$

***Nucleation kinetics:***

Generally, the droplet will tend to reach equilibrium when the maximum spread is achieved during static bed of powder, where there is no extra energy added to influence the kinetic of the droplet. On the other hand, the wetting thermodynamic may not have enough time to reach equilibrium state, during granulation, due to the mixing/agitation from granulator that takes place simultaneously. In the wetting process, the droplet will penetrate through the pores of the powder to form a nucleus, and as the nucleus grows, the excess liquid migrates to the surface. This makes the nuclei size distribution a function of both the wetting thermodynamic and kinetic [18].

There are two proposed nucleation mechanisms, which depend on the size of the droplet in relation to the size of the particles. *Distribution* mechanisms; this occurs when the size of droplet is smaller than the particles causing a coalescing between particles, which gives nuclei with trapped air [18], as illustrated in Figure 2-3a. *Immersion* mechanisms; this occurs when the size of the droplet is larger than the size of the particles. The liquid will tend to penetrate through the capillary pores forming highly saturated initial agglomerates, as shown in Figure 2-3b.

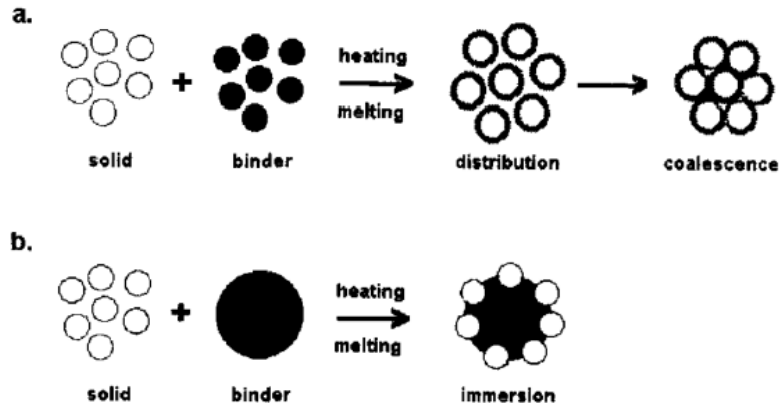


Figure 2-3 Mechanisms of nucleation (a) Distribution, (b) Immersion [25].

Furthermore, the penetration of the droplet through porous powder bed is driven by the Laplace capillary suction pressure,  $P_c$ , given in Equation 2-8 [19], where the  $R_{pore}$ ,  $\gamma_{lv}$ ,  $\phi$  characterize the size of pore within the bed, liquid surface tension and actual solid-liquid contact angle respectively [18, 19].

$$P_c = \frac{2 \gamma_{lv} \cos \phi}{R_{pore}} \quad \text{Equation 2-8}$$

Droplet penetration time is the time taken for the drop to penetrate through the porous bed until it is no longer appears on the solid surface of the powder bed. This can vary significantly, where the penetration through a loosely packed porous bed is shown to be complex and greatly dependent on the microstructure of the bed. Monitoring the penetration of the droplet on a static powder is useful to indicate how readily the liquid wets the powder and, hence nucleation [18, 19, 26].

The liquid viscosity, surface tension, contact angle as well as the pore radius will influence the penetration of the liquid into the pores of the powder bed. The viscosity of the droplet will act against flowing through the powder pores. During granulation, limited movement of the liquid will require a mechanical dispersion of the binder as otherwise it will reduce the production of nuclei [18]. The pore radius will also dictate the surface curvature of the liquid as it flows through the pores. As the pore widens the surface curvature of the liquid

will reduce causing a reduction in advancing. If the pore widens further so that the curvature of the liquid disappears, this results in a cease of flowing of the liquid through the pore [26].

So during granulation to achieve ideal nucleation conditions; short penetration time (can be achieved by small droplets), low liquid binder viscosity and porous powder (without macrovoids), must be achieved [19]. The wetting and nucleation process can be split into three different regimes as shown in Figure 2-4. The figure describes the relationship between dimensionless spray flux ( $\Psi_a$ ) and penetration time ( $\tau_p$ ). Dimensionless spray flux ( $\Psi_a$ ) is governed to describe the powder surface which is covered by the liquid binder [27].

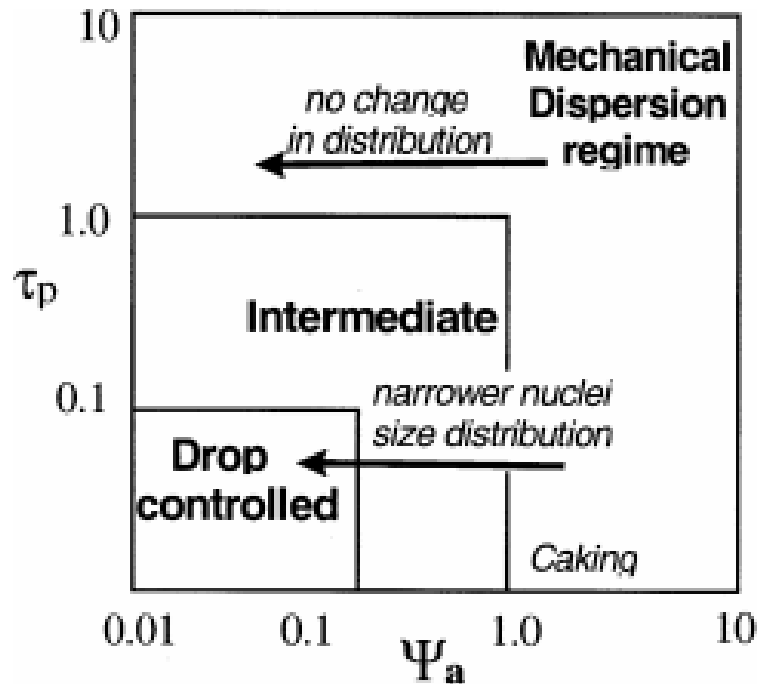


Figure 2-4 Nucleation zone regime [27].

In the drop controlled regime, the liquid binder penetrates immediately through the pores, as binder comes into contact with a powder bed. The lower the liquid binder viscosity the quicker it will penetrate (e.g. distilled water). This is predicted to produce a narrow size distribution range[27].

In the mechanical dispersion regime, the nuclei formation is expected to be reduced. This is due to the increase in liquid binder viscosity, where it causes a delay in the penetration time/spreading. This is predicted to produce a broader size distribution range, where it will be vital to control the mechanical mixing and agitation and delivery method of granulation liquid such as drop size, nozzle height etc [27].

### **2.1.2 Consolidation and Coalescence**

The nuclei (or initial granules), may undergo a further processes known as consolidation and coalescence. During the consolidation process, the granules collide with each other or on the wall of the granulator. These collisions result in consolidation, which may subsequently deform the granules and reduce their size and the porosity while squeezing out the entrapped liquid binder to their surface [18].

#### ***Capillary and viscous forces***

The migration of the liquid into the surface of the nuclei/initial agglomerate, promotes growth. The main process of growth in the nuclei is by coalescence. Coalescence process is the sticking/binding of two different nuclei/granule. Generally, coalescence can be successful if sufficient deformation and granulation liquid are available on the contact surface of colliding granules in order to form strong binding forces that will resist breakage [28, 29]. This can be illustrated by viscous Stokes number ( $St_v$ ) (shown in Equation 2-9), where the colliding granules must dissipate their energy in order to coalesce. This can be achieved if the colliding velocity of the particles ( $U_c$ ) results in their relative kinetic energy being insufficient to overcome the retarding force of the particles with a given density ( $\rho_s$ ). This could be challenging, as particles of the material will have different velocity within the granulator.

The presence of liquid on the surface of particles/granules during collision can also aid in dissipating energy. The liquid binder during granulation will give rise to capillary forces ( $f_{Lc}$ ) and viscous forces ( $f_{Lvn}$ ), as shown in Equation 2-10 and Equation 2-11, respectively. These forces will depend on the radius of the particle ( $r$ ), surface tension ( $\gamma$ ) and viscosity ( $\mu$ ) of the liquid as well as the relative velocity of particle  $i$  onto particle  $j$  ( $U_{ci,j}$ ). Increasing the liquid binder viscosity will increase the strength of the liquid bridges which will also

result in higher energy dissipation, during collision, and hence growth due to coalescence [30].

$$St_v = \frac{8\rho_s U_c}{\mu} \quad \text{Equation 2-9}$$

$$f_{Lc} = \frac{\pi r_2^2 \gamma}{r_1} \quad \text{Equation 2-10}$$

$$f_{Lvn} = 6\pi\mu r_0^* U_{ci,j} \frac{r_0^*}{2H} \quad \text{Equation 2-11}$$

### 2.1.3 Breakage and attrition

Due to the collisions and impact (i.e. stress) in the granulator, the wet granules can undergo breakage and attrition. Breakage process occurs when wet or dry granules impacted, where the stress cause a fracture within the granules. The extent of this breakage will depend on the strength of the initial granule, where the strength of the granule can be controlled by the formulation variables (e.g. amount of the liquid and the viscosity of the liquid) and processing condition (e.g. impeller/mixer speed). Furthermore, attrition of the granules is when the surface of the granules is gradually worn away in an opposite process to coalescence. Therefore, the breakage and attrition of the granules will have an influence on the final granule size distribution [18].

## 2.2 Wet granulation behaviour

### 2.2.1 Desired granulation (Regime maps)

Wet granulation process is performed using liquid binder to form liquid bridges between the primary particles producing larger granules. The liquid binder brings primary particles together by a liquid bridges via a combination of surface tension, capillary and viscous forces [31]. Such process can be achieved using a variety choices of equipment including twin screw granulator (TSG), high shear mixers (HSM) and fluidized bed (FB), [2, 27].

The extent of granulation of primary particles, during wet granulation, will depend upon process variables (which determine the stress imparted on the material), and formulation

variables (determine the strength of the bond formed). The stress applied by the system can ensure a better distribution of the liquid binder, which influence the strength of the aggregates/granules and eventually determine its size. This is indicated by the size distribution reported by many different researches on different equipment, i.e. production of granules and fine/un-granulated powder at a given conditions [32-35].

To understand the influence of these variables (process and formulation) on the extent of granulation, number of researchers have developed a regime map for different equipment such as high shear mixer [31] and twin screw granulator [36]. The regime map aims to characterize the growth behavior of granules within the granulator, based on wet granulation mechanisms [31].

Iveson and Litster [31] proposed that there are many types of growth behavior exhibited by the High Shear Mixer (HSM). The different exhibited behaviour were categorized as “dry”, “Nucleation”, “crumb”, “Steady Growth”, “Induction”, “Rapid Growth” and “slurry/over-wet mass”.

The granulation can result in no or little growth (during “dry” and “Nucleation”) due to insufficient use of liquid. Further increase in liquid binder show a slow growth initially and followed by a rapid growth (i.e. going through the “induction”, “steady Growth” to finally “Rapid Growth”). At given stress (i.e. process conditions) depending on the formulation used (i.e. amount of binder and viscosity) weak aggregates could be formed, i.e. loose *crumb*, which will undergo constant breakage and reforming as a result of cushion with a larger granule. Excess of liquid binder addition to the system could lead to overwetting of the powder forming an oversaturated slurry. Further details on the types of growth behavior is discussed in more detail elsewhere in the literature [31].

The author [31] hypothesized that these behaviors can be considered as a function of the pore liquid saturation and the degree of deformation imparted on the

aggregates/granules within the granulator [31]. To measure the liquid saturation they used the maximum granule pore saturation ( $S_{max}$ ), Equation 2-12, as the granule pore liquid saturation could change with time due to the consolidation of granules and evaporation of liquid binder and the dissolution of soluble components into the liquid phase. To account for the degree of deformation, they introduced the deformation number ( $De$ ), Equation 2-13:

$$S_{max} = \frac{w\rho_s(1 - \varepsilon_{MIN})}{\rho_l\varepsilon_{MIN}} \quad \text{Equation 2-12}$$

$$De = \frac{\rho_g U_c^2}{Y_g} \quad \text{Equation 2-13}$$

where  $w$  is mass ratio of liquid to solid,  $\rho_s$  is density of the solid particles,  $\varepsilon_{MIN}$  is the minimum porosity,  $\rho_l$  is density of liquid,  $\rho_g$  density of materials,  $U_c$  is particles collision velocity and  $Y_g$  is the dynamic yield stress of material.

Although, twin screw granulator (TSG) produces granules via wet granulation, the mechanism is different to that in high shear granulator. TSG is a continuous system where the mechanisms of wet granulation are assumed to be physically separated [36], whereas in HSM (batch system) they occur simultaneously [31]. Another key difference is that TSG has a smaller free volume, hence the wet powder mass may undergo higher stresses. These stresses will further assist the distribution of liquid binder, to form the initial granules, and deform, consolidate or break the granules. The stress can be related to the torque produced by the motor to convey the material, which can change with a change of fill level [36]. Dhenge et al. [36] proposed a slightly altered regime map, as shown Figure 2-5.



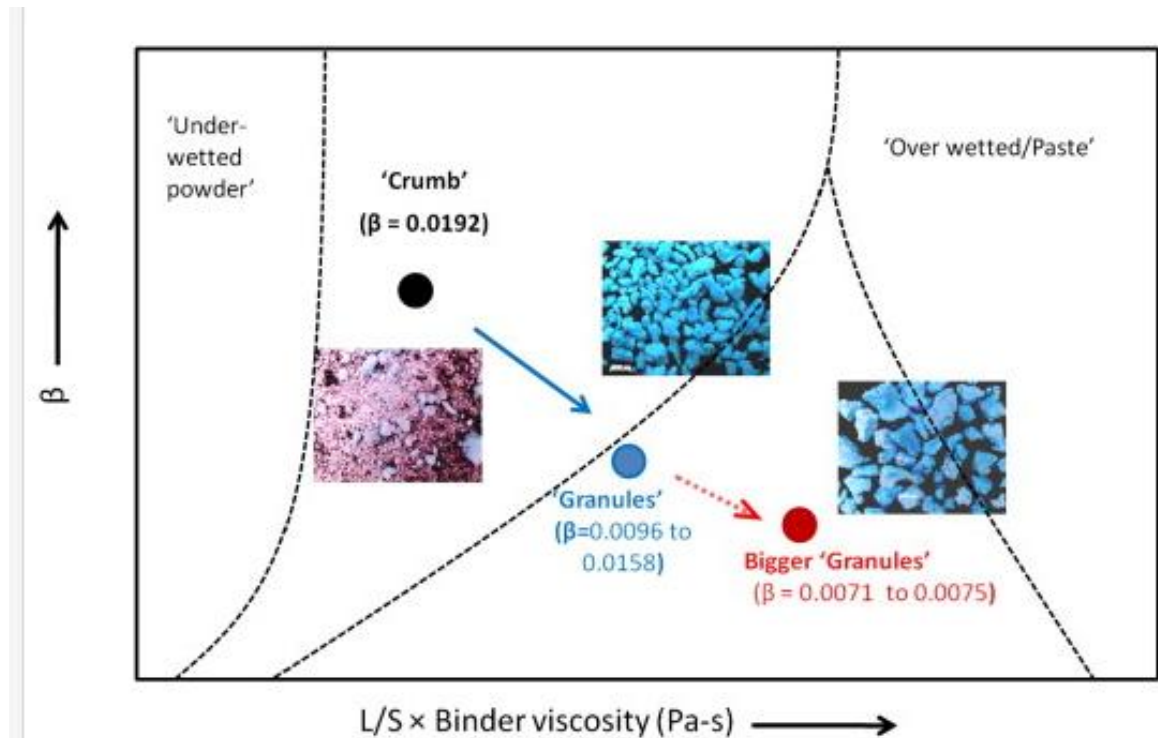


Figure 2-5 Granule growth regime map for twin screw granulation [36].

The regime map, Figure 2-5 shows a relationship between Deformation value ( $\beta$ ) and liquid/solid ( $L/S$ )  $\times$  Binder viscosity. Deformation value ( $\beta$ ) is the ratio of the stresses acting on the powder/granules over the strength of granules. This indicates the level of deformation in the granulation system. The combined product of ( $L/S$ )  $\times$  Binder viscosity is used to indicate the pore saturation, as they found that varying the viscosity of the liquid at the same  $L/S$  ratio will vary the pore saturation [36].

Although the addressed factors by Dhenge et al. [36], ultimately resulted in proposing altered equations to Equation 2-12 & 13, it marked an essential step forward to understanding the granulation within twin screw granulation. These equations describe the relationships between level of liquid and the mechanical property of the material on the product outcome, which are fundamental to understanding the wet granulation mechanisms. However, further amendments to those equations and to that proposed by Dhenge et al. [36] is necessary to allow such equations to be more applicable to the twin screw granulation. Such improvement should take into consideration the screw

configuration variable and how it influences the liquid-powder uniformity. This variable is hugely important to the liquid distribution, as well as shear stress which would be imparted on the given particles.

### **2.2.2 Undesired granulation (powder caking)**

Agglomeration is a natural phenomenon, where fine powder particles can be agglomerated via various granulation techniques (dry or wet). The outcome from such a phenomenon, i.e. granules is considered as a desired product and hence many techniques have been developed to intentionally agglomerate, fine particles into granules, in a controlled manner. However, under certain conditions, agglomeration of particles can take place where it would be considered undesired, and usually referred to as powder caking/stickiness [37, 38] (During this work, it will be referred to as powder caking).

Powder caking is an undesired widespread phenomenon in the process industries, where it involves the transformation of solid powder into coherent mass that resists the flow of materials. Such a problem is frequently encountered by various equipment dealing with particulate material; such as granulation equipment (roller compactor, high shear mixer, and spray drying), and during storage in silos and bags [39-42].

The tendency of the powder to cake could be related to the cohesion and the adhesion forces of the powder. The cohesion forces are an internal property of the material, which is a measure of the forces holding the powder particles together. The particles will tend to form bonds to stick to each other as they come into contact, unless there is a force greater than the cohesive force which has the ability to break the bond between them.

The adhesion forces are interfacial property of the material, which is a measure of the tendency of the material to stick/form a bond with the surface of the wall. The particles will tend to adhere to the surface unless a force greater than the adhesion force is applied [38, 42].

Nevertheless, the formation of powder caking during processing, transportation and storage may vary in a change in powder, material composition, particle size, particle shape, moisture content, pressure, and variation in temperature and humidity, as well as the nature of the physical process in which these particles of powder are brought into contact. This dependence on so many factors, implicated the understanding and defining the mechanisms of powder caking in a given powder system [39-42]. Yet, the cohesive and adhesives mechanisms are exploited to provide a better understanding of the powder caking/stickiness [38].

The cohesive and adhesive mechanisms are similar, although, the high cohesion force is not always associated with the high adhesion force (and vice versa). Generally, the mechanisms for the inter-particle attraction can be accounted for by considering five major groups (shown below) for forming inter-particle bond. These five inter-particle bonding mechanisms will vary on dominance in a given system, though; more than one mechanism can apply to powder caking/stickiness. These mechanisms are shown as followed [38, 41, 43]:

*1. Intermolecular and electrostatic forces:*

These are surface forces. Among these forces is the Van der Waals attraction force, which depends on the dipole attraction on molecular level, and it becomes more effective over a very short distance. Other forces, such as electrostatic forces act on a longer range in comparison with the Van der Waals forces [41]. Such forces are generally less effective during wet granulation as opposed to dry granulation. During wet granulation, the bonds formed to bind particles together are mainly resulted from mobile binding (such as capillary forces) [38].

*2. Mobile liquid bridges:*

When the liquid is added to a powder bed, the liquid tends to be mobile between the primary particles, forming liquid bridges. Most of the wet agglomerates are formed due to

the liquid bridges forces, holding the primary particles together. The formation of agglomerate due to these liquid bridges can be categorized into three ways, due to the distribution of the liquid between the primary particles. These are illustrated as follows:

**Pendular state:** this state occurs when the voids between primary particles are partly filled with the liquid, i.e. in low moisture level, as shown in Figure 2-6 (a). During this state, the primary particles are held together by lens-shaped rings of liquid. This results in adhesion of particles due to the surface tension forces of the liquid-air interface and the hydrostatic suction pressure in the liquid bridge.

**Capillary state:** this state occurs once all the air, present between primary particles, has been displaced where the primary particles become adhered to each other by the capillary suction at the liquid-air interface, as illustrated in Figure 2-6 (c). This state can be achieved by either increasing the liquid or decreasing the space between the particles. The formed liquid bridges at this state give the agglomerate a certain tensile strength.

**Funicular state:** This state represents the intermediate stage between the two states (pendular and capillary states). As, the liquid advances to displace the air, between the primary particles, the particles tend to arrange in a funicular state as shown in Figure 2-6 (B).

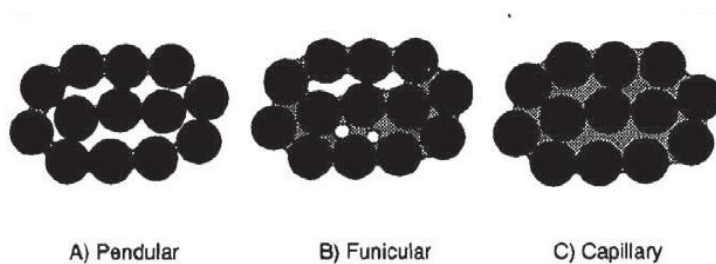


Figure 2-6 Forms of liquid states with mobile bridges [38].

### *3. Immobile liquid bridges:*

The immobile liquid bridges are formed as result of a thin layer of viscous binder present on the surface of the particle. Such a film tends to adhere particles together and reducing the distance between them as well as increasing the contact area (this will also increase the Van der Waals attraction as the particles get close). The immobile liquid bridges can form a strong bond between the particles (could be stronger than the bonds formed due to mobile liquid in the case of a very viscous binder), however, as the liquid level increases beyond the thin film then the liquid can become a mobile liquid to form liquid bridge, where interfacial tension and capillary pressure tend to create a strong bond between the particles.

### *4. Solid bridges:*

The solid bridges within agglomerate can be formed via various mechanisms. The solid bridges can be formed as particles come into contact, at a temperature high enough to cause the surface of the particle to melt and causing a molecular diffusion mutually at the point of contact (this is called sintering). Furthermore, the solid bridges can be formed by chemical reaction and hardening binder, which will depend solely on the participating materials, their reactivity and tendency to harden. The fluctuation in temperature can give arise to solid bridges due to crystallization of dissolved materials. The structure of the bond tends to be porous; therefore, the strength of the bond will depend on the amount of solid deposited and the crystal structure.

### *5. Mechanical interlocking.*

The mechanical interlocking of particles tends to contribute to overall strength of agglomerate. The tendency of such bonding will depend largely on the particle/granule shape. The needle shaped crystal and fibers can give arise to a mechanical interlocking. The resulted lumps can be very strong, where the particle will be required to broken to break such a bond.

## **2.3 Background of Twin Screw Granulator**

The twin screw granulator evolved from the extrusion process. Extrusion is a process in which a continuous feed of material is mixed with a continuous flow of granulation liquid, aided by the rotation of the twin screws. The material is then forced through an orifice by means of pressure, where the orifice is referred to as an extruder die and the end product is called extrudate, where it tends to obtain the shape of the die.

The twin screws are built modularly using modular blocks referred to as elements. The elements come in different geometries and they impact the material differently. This allows for a vast difference in design within twin screws, which can in principle operate differently and produce different properties of the product (i.e. granules). Likewise, the removal of the die, at the end of the extruder, and replacing it with conveying elements resulted in changes of product property, where granules are produced instead of extrudates [44, 45].

### **2.3.1 Application of the twin screw extruder in pharmaceutical field**

Extrusion is used as a process of converting raw materials (fine primary particles) into products (granules) with more desirable properties (e.g. size, shape, density etc.). Extrusion can be ideal for the high throughput production of consistent product as it is a continuous process.

Extrusion was primarily designed for cooking and processing of food. It since gained some importance in other fields such as pharmaceutical field. Within the pharmaceutical field, the extruder can be performed on two applications, namely; hot melt extrusion and cold extrusion. The use of cold extrusion (i.e. wet granulation) is more desired as most of the drugs and excipients are heat sensitive, except in the case of the production of sustained release tablets where melt extrusion is used [46-48].

The first introduction of the twin screw granulation from the cold extrusion, in the pharmaceutical industry, was made by Gamlen and Eardley (1986)[49]. Continuous wet

granulation using a twin screw granulator is ideal for a wide range of drug production. Twin screw granulation is also used to produce other products that are heat-sensitive and enables retention of heat labile components, such as vitamins (cold extrusion) [50-52]. It can be used to produce effervescent paracetamol granules [53] and the granulation of lactose and microcrystalline cellulose powder [54]. It was also noted by Keleb et al [47] that using  $\alpha$ -lactose monohydrate in the twin screw granulation, has improved the tableting of materials with poor compaction properties.

### **2.3.2 Design of the Twin Screw Granulator (TSG)**

The twin screw granulator (TSG) consists of a feeding hopper, two screws (identical in design, i.e. twin) inside the confined barrel, with an external cooler and a pump for driving the liquid media [48, 55]. The twin screw granulator offers a major attribute due to the variety of designs, which can be obtained by changing the type and sequence of the elements to create a certain screw configuration in addition the other process variables (such as powder feed rate, screw speed, and liquid flow rate).

The direction of the twin screw rotation and arrangement inside the barrel is considered to be the basis for classifying different type of twin screw granulators. Such classifications can be summarised as follows:

- Co-rotating Intermeshing
- Co-rotating Non-intermeshing
- Counter-rotating Intermeshing
- Counter-rotating Non-intermeshing

The two screws within the granulator can rotate in the same direction (co-rotating) or in opposite directions (counter-rotating). Regardless of the directions of screws rotation, the two screws can be arranged in a way to form a closed/semi-closed compartments (intermeshing) or separated (non-intermeshing), where the compartments between the screws are not closed. The intermeshing and non-intermeshing can be further classified

into self-wiping (cleaning deposited powder/material on the screws by themselves) and non-self-wiping [45, 46, 56].

Within a given twin screw granulator, its dimensions can be used to describe it. Its element can also differ in dimensions, even if they are the similar type. This is illustrated in Figure 2-7 for the conveying elements. The conveying element can come in different sizes (this will be described later on in more details). The description of the key dimensions (which are considered when distinguishing between them) is presented as follow:

- ***L/D ratio of barrel*** - the twin screws are enclosed inside a barrel with a distinct length (L) and diameter (D), where L/D ratio represents the Length/Diameter of the barrel. Furthermore, the L/D ratio of the barrel is considered to be one of the most referenced terms in defining the granulator as such dimensions can define many operating characteristic of granulator. This ratio is also considered to have a great influence in the effectiveness of the granulator as well as the material, which it can process [48].
- ***Flight*** - it is the space given by rotation of a screw to give one complete revolution.
- ***Flight width*** - It is the thickness of edge of the flight.
- ***Pitch***- this describes the angle of flight relative to the axis of the root.
- ***Pitch length*** - It is the distance between consecutive flights.
- ***Channel width*** – It is the space between flights.
- ***Screw diameter ( $D_o$ )*** – it represents the distance between the furthest flights across the screw shaft.
- ***Helix angle*** –It is an angle, which the flights create from a line that is perpendicular to the screw shaft.



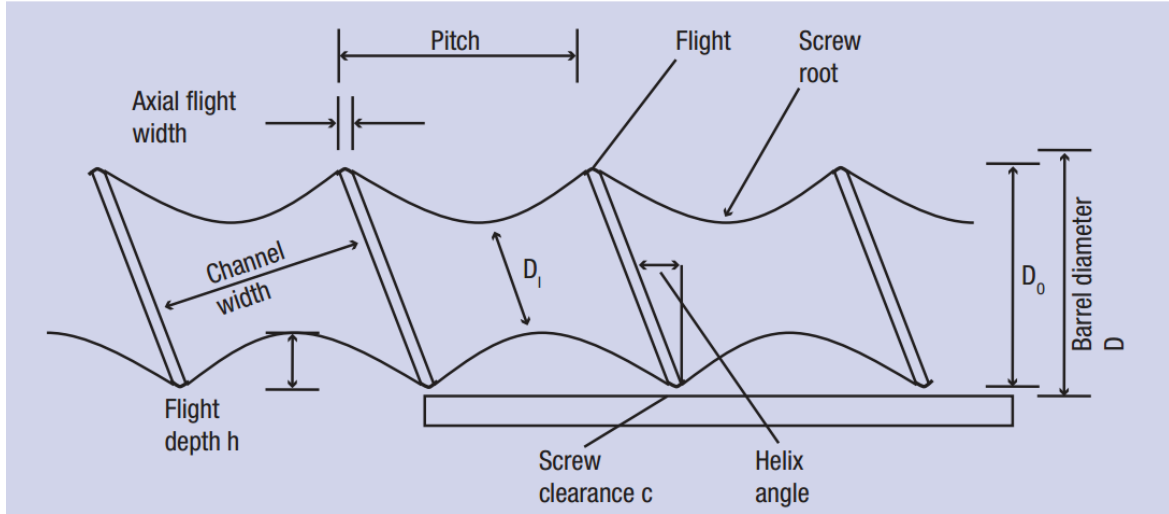


Figure 2-7 Basic nomenclature of screw element [55].

### 2.3.3 Fundamental of the screw elements

As previously mentioned, the twin screw granulator is built modularly, where the screw configuration can consist of different type of elements, such as conveying and kneading elements (these will be described in more details later). These elements will be intended for a different application. More than one type of element can be weaved into the shaft to give variety of different screw configurations, and hence alerting flow of the material and the properties of the product. The screw element will induce different mixing behaviour and subsequently changing the mechanisms in which the product are formed by, i.e. resulting in changes of product property.

#### **Mixing behaviour of screw elements**

The twin screw granulator is generally considered as a mixing machine, where two phases are mixed together (one or more components of powder and granulation liquid). Depending on the type of the screw element used, a different type of mixing can be imparted on the material. The mixing behavior of the screw elements can be considered as following:

#### **Distributive mixing behaviour**

Distributive mixing behaviour refers to the spatial rearrangement of the material as the screw elements divide and recombine the material while maintaining the morphological of

the primary particles. Such repeated rearrangement of the material is important to maintain the homogeneity of the components within the blend, as shown in Figure 2-8.

Although, the cross-section of the screws regardless of the elements used will be the same as shown in Figure 2-9, the flight and its design will vary. This change will result in differing amounts of free volume being available, for the material to reside onto. Furthermore, some elements will have a wider flight, giving a higher contact area with material at the clearance point and hence, more stress will be imparted on the material.

The screw elements that tend to distribute the material will have a high free volume and narrower flight (e.g. free volume between the two consecutive flights as illustrated in Figure 2-7). A given screw design can cause more than one mixing behaviour of the material within a granulator, the extent of the free volume offered by the element and the level of stress exerted (which can be influenced by the flight of the element) on the material can determine which mixing behaviour is more dominant [45, 57-59].

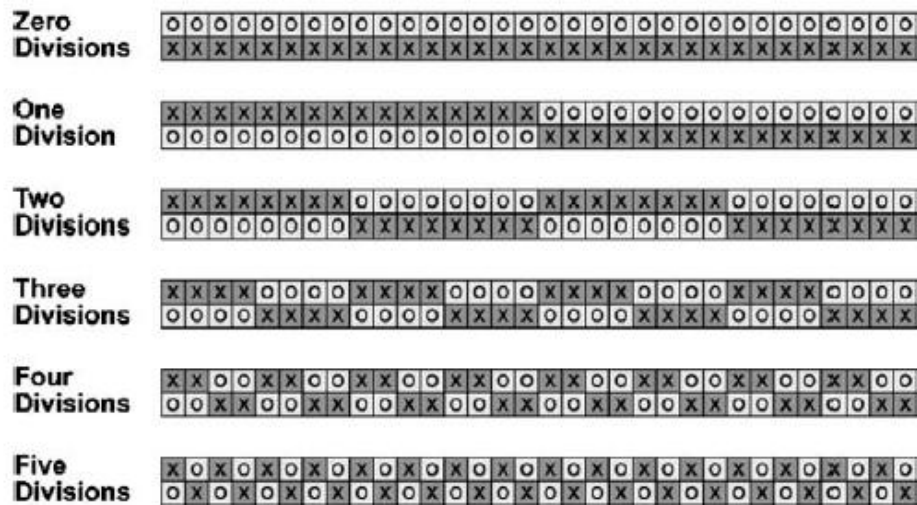


Figure 2-8 Distributive mixing behaviour [45].

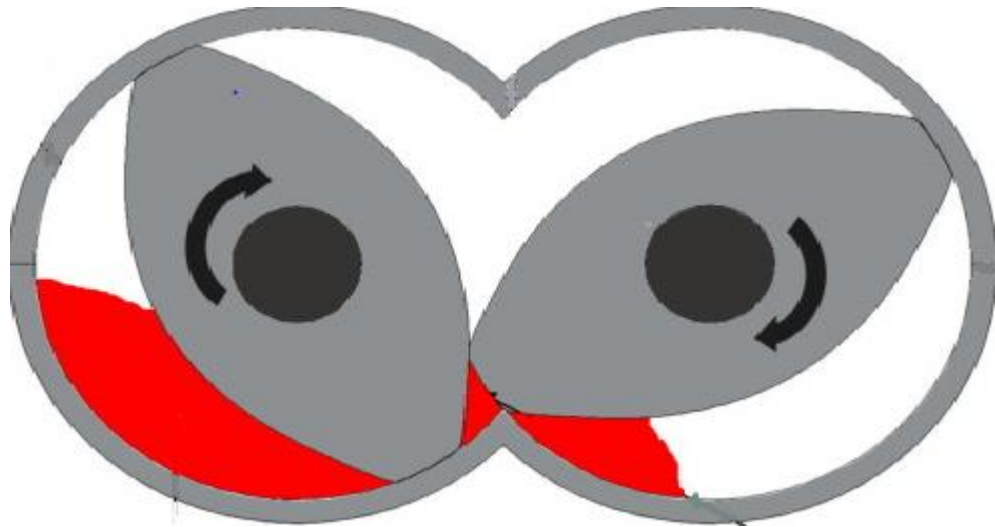


Figure 2-9 cross-section of the screws along the barrel

### ***Dispersive Behaviour***

The dispersive mixing behaviour is experienced when the material is trapped in area of high pressure (e.g. when the free volume is small as the distance between the screw element and barrel wall is small). This will result in the material being sheared and elongated. The dispersive mixing causes a reduction in size and deformation of the morphology of the primary particles, as illustrated in Figure 2-10 . For the material to undergo a dispersive mixing, the screw element must exceed a certain shear stress (this will be dependable on the property of the material) [45, 57-59].

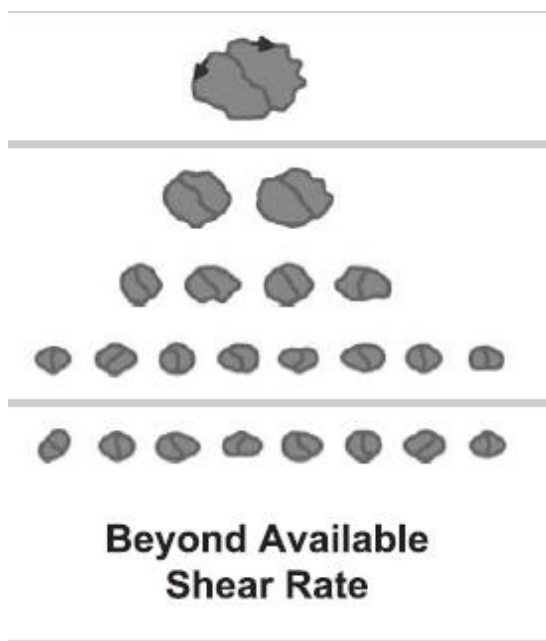


Figure 2-10 Dispersive mixing behaviour [45].

### ***Type of screw elements***

The modularity of screw design has provided the user with a tremendous flexibility. Such attribute allows the manipulation of the intensity in distributive and dispersive mixing within the granulator. This enables the user to generate granules with desired characteristic by controlling the degree of the particle buildup, agglomeration and homogenization [59]. There are many screw elements, which are available and new elements with different geometry are continuously emerging in the market. The most commonly used elements within the pharmaceutical field are conveying and kneading elements (the following different elements were used during this study).

### ***Conveying Elements***

Conveying elements are a type of the classical elements, where they are used to transport the material forward from the feed point. Such elements are available in many sizes and forms, where their use may differ. The pitch length and number of flights can be used to describe the conveying elements. The conveying element differ from each other by the channel width, where the greater the pitch length the more free volume available and hence more material to be conveyed. Figure 2-11 shows long pitch conveying element (LPCE) (A) and the short pitch conveying element (SPCE) (B).

Vercruyse et al [60] found that the conveying elements require minimal mechanical energy, where they provide a degree of distributive mixing, hence a poor consolidation as the granulation liquid will not be forced to the surface of the powder [45, 46, 52, 60].

### ***Kneading Elements***

These elements are another classical element type. The kneading elements produce shear stress on material, which helps to mix, distribute and disperse the components within a formulation. The arrangement of a stack of kneading elements can result in different outcomes. The length of the element, number of kneading discs and the offset angle between the kneading discs can be used to differentiate between different kneading zones within a screw configuration.

The number of the kneading discs and the offset angle at which they are staggered can have a great influence in the role of kneading elements and ultimately the product properties. There are three different offset angles 30°, 60° and 90° at which the kneading discs can be weaved into the shaft. The larger the offset angle, the more axially open the kneading elements will be. Therefore, the material will be well mixed; however, its conveying ability will reduce as a result [17, 52].

A study conducted by Lee et al [17], showed that varying the angle can vary the conveying ability of the kneading element. At 30° screw configuration, the fill level increases slowly and remains steady in the mixing zones. The 60° screw configuration, which has a slightly higher fill level, is less steady through the mixing zones, whereas at 90°, the mixing zone has no conveying capacity and, therefore, might be expected to be fully filled for any process conditions. Therefore, the components of the formulation at this zone are subjected to dispersive and distributive mixing [17, 45]. Four of kneading element discs with an offset angle of 60° used during this study as shown in Figure 2-11 (C). The

kneading element discs are thinner than the conveying element, 1/4 of element length (1 kneading element zone has 4 discs= 1SPCE).

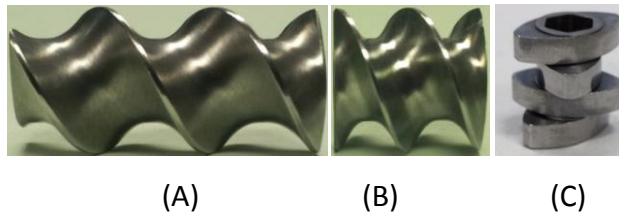


Figure 2-11 Different common elements used to make up the configuration of the screw: (A) long pitch conveying element, (B) short pitch conveying element, (C) kneading element.

### 2.3.4 Process and Formulation variables

It was highlighted previously, that the collision of granules may result in coalescence to give a further growth (e.g. granules) within the granulator. If the stress imparted on the material is relatively high the bond between the primary particles may break resulting in breakage. The balance between the growth and breakage will depend on the stress acting on the material as well as the strength of the bonding, as schematically illustrated in Figure 2-12. The stress acting on the wet granules will be manipulated by the process variables such as screw configuration, screw speed and powder feed rate. The strength of the wet granules will be influenced by the strength of the liquid/solid bridges between the particles, the amount of liquid used as well as the material properties (such as the deformability of material upon collision to help dissipate the kinetic energy).

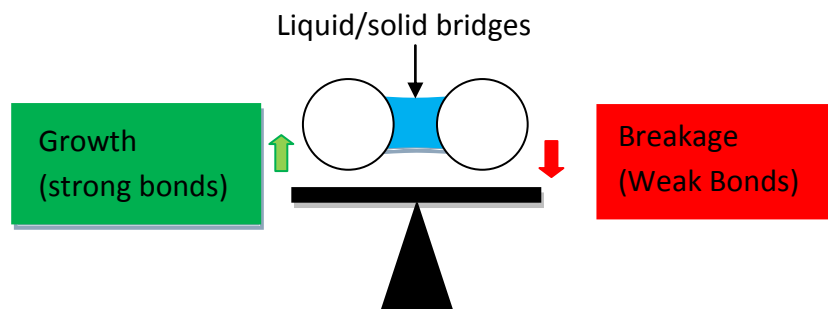


Figure 2-12 Growth and breakages of the granules.

The granulation process is not limited to achieving growth only (size), as other properties such as shape, strength and porosity will influence the downstream process. Such an

influence can affect the final product (i.e. tablet). Therefore, during the development of pharmaceutical products, the changes in mechanisms as the process and formulation variables modified needs to be understood. Such understanding will enable the manipulation of the variables to obtain the production of granules with the desired and consistent properties [61, 62].

The growth and breakage phenomena during granulation could result in a wide size distribution [62]. A wide range of size distribution can present a challenge in the downstream process. These processes could include drying (where the small granules will dry quicker). On other circumstances, a wide size distribution can be considered desirable depending on the application. For example if the purpose is to have a better packing of the granules then a broad size distribution might be more applicable.

The shape of the granules will also influence the flowability of the granules and packing density, which makes such a property of considerable value and must be taken into consideration while assessing the quality of the granules. The porosity of the granule will have a significant effect on the granule performance, as a low porosity within a structure of granule will result in resistance to disperse when placed in water [62].

### ***Process variables***

#### ***2.3.4.1.1 The effect of the Screw Configuration***

One of the main attributes of the twin screw granulator is its flexibility. This advantage arose due to the fact that the twin-screw granulator is built up modularly. This allowed for the achievement of a desired product with minimal downstream processes required.

The understanding of twin screw configuration is vital as different elements could lead to different mixing behavior and while imparting different level of stresses on the material. The screw configuration can also be altered to give a regime-separated process, to enable more control over the granule properties, which is unavailable in the other conventional granulation methods [32, 63-65].

This was demonstrated by Dhenge et al [36], who used a formulation (consisting of  $\alpha$ -lactose monohydrate, microcrystalline cellulose, crosscarmellose sodium and hydroxypropyl-methyl cellulose), where it was observed that using kneading elements, changes the consistency (thickening) of the material while using viscous granulation liquid. This is due to an increase in the cohesiveness and frictional resistance of the material to flow, i.e. due to the strength of the bonds. This also resulted in an increase in the residence time in which the granules spend within the barrel of the twin screw granulator, while also requiring higher torque, which reflects the increased stress on the granules from the process.

Lee et al [17] supported the results by illustrating that the kneading elements generally have a higher residence time and wider residence time distribution compared with the conveying zones as well as the fill level, although they used different material (microcrystalline cellulose). This is due to the high conveying capacity of the conveying elements in comparison to the kneading elements. However, the author also stated that at high powder feed-rate and screw speed, the effect of screw arrangement of 30° and 60° on the mean residence time becomes less significant. Additionally, staggering the kneading element at 90° can cause a blockage in the granulator. This is because the net of movement of materials only depends on the gradient fill, since the conveying element has no preferential direction as the screw moves the material to the adjacent (forward and backward). This can be shown in Figure 2-13, where kneading elements at staggering angle of 90° showed the least conveying capacity by having the longest residence time [17, 66].



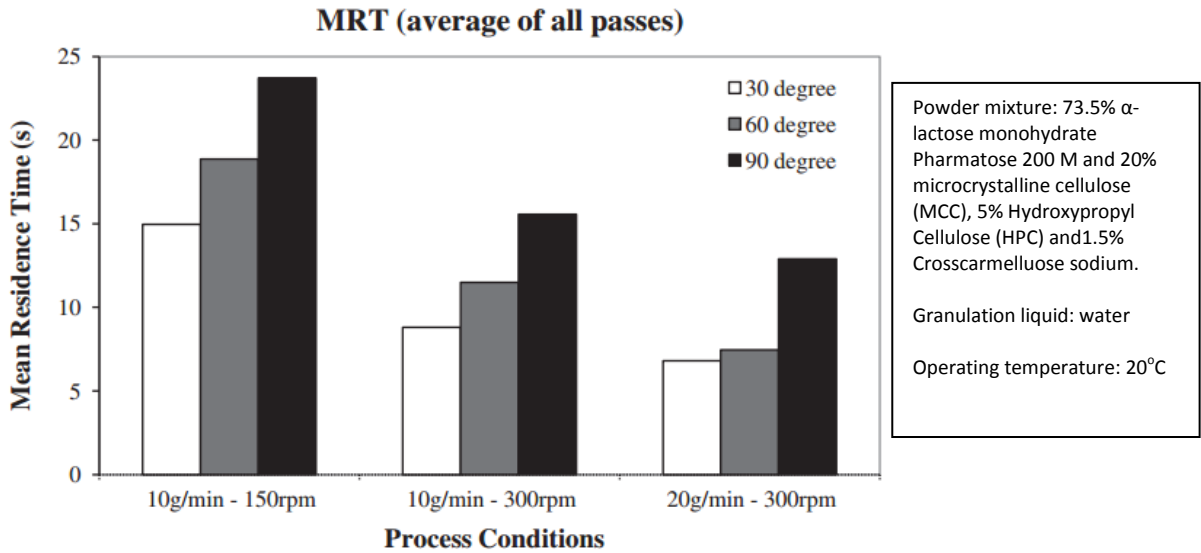


Figure 2-13 the effect on mean residence time by the conveying capacity of each angle degree for the kneading element, while using varying the feed-rate and screw speed [17].

J. Vercruyse et al [52] also found that using the kneading element instead of the conveying element created more friction between particles resulting in a higher resistance to movement. This accumulated the powder prior to the kneading element zone, where the particles are expected to experience a higher stresses. Consequently, the torque produced by the granulator was increased to maintain screw speed, as the load on it increased.

The increase in the number of kneading elements gives a decreased level of fines and shows a growth in size, while consuming higher power as they produce more stress on the material. Dhenge et al [36] found that the kneading elements in the screw configuration exert both shear and compressive stresses on the wetted powder mass inside the barrel. This caused in an increase in the particle packing/densification and consolidation of the powder mass. Though, the extent of the densification was found to be depending on the binding ability and the amount of granulation liquid (i.e. resistance to the applied stresses).

Furthermore, increasing the stresses applied on the material, i.e. using kneading elements, was generally found to give stronger granules, as Vercruyssen et al [52]; observed such a trend as they increased the number of kneading elements.

#### *2.3.4.1.2 The effect of the Screw Speed*

Screw speed is another influential parameter on the granule's properties. The speed of screw can affect the fill level of the material within the granulator. Such an effect can have an influence in the residence time and torque, i.e. the stresses experienced by the material will vary.

Dhenge et al [2] found that the screw speed has a reverse proportional relationship with residence time. An increase in the screw speed increases the conveying capacity, hence a decrease in the residence time and torque. This was shown to be in accordance with many other studies, as well as the model proposed by Baron et al [2, 67-70]. The screws will be starved of powder leading to a decrease of the powder load on the screws and, hence decrease in the torque required [2, 68, 71].

In general, the effect of screw speed on the size distribution was seen as minimal. However, the screw speed influence becomes greater with a change in the amount of liquid used (i.e L/S ratio), as the granules strength will vary. Dhenge et al [2] found that using a slow speed of the screw (250rpm) showed an increase in the size of the granules. This size increase can be related to the increase in residence time and the degree of fill level within the granulator. The additional time allowed more solid particles to bind together resulting in the granule growth. This was in accordance with other studies [2, 7, 64, 68, 72]. Lee et al [3] also found that the screw speed did not affect the granule growth when the L/S ratio is low. However, when increasing the L/S ratio, the screw speed showed an influence on the  $d_{50}$  of the granules, where increasing the screw speed gave a decrease in the  $d_{50}$  value [3, 17, 64].

Additionally, increasing the screw speed resulted in more rough and elongated granules as result of the higher shear stresses and the lower fill level [2]. However, Lee et al [3] showed insignificant effect on the granule porosity as the screw speed was varied using microcrystalline cellulose.

#### *2.3.4.1.3 The effect of the Powder Feed Rate*

The feed-rate is one of the processing parameters that can be altered to attain desired granule properties. This refers to the amount of solid powder fed from the hopper into the barrel accommodating the twin screws. Varying the powder feed rate will change the conditions inside the barrel, which can bring about a different interaction between particles within the barrel. The change in the feed rate will give a change in the channel fill which will experience a difference in the stresses applied on the material.

Dhenge et al [2, 68] found that an increase in powder feed rate results in a decrease in the residence time. This was due to the degree of fill level, where increasing the powder feed-rate increased the amount of powder in the barrel. This resulted in a higher compaction of granules, where the throughput forces to convey the granules forward is much stronger (at the same screw speed), which restricted the back-mixing of the powder while continuously pushing the material forward reducing its residence time in the granulator. This agrees with the model proposed by Ziegler & Aguilar [73]. The increase of feed rate will cause increase on the load of the powder on the screws forcing the drive of the screw to produce more power to ensure the conveyance of materials at the same screw speed. This was also found by Vercruysea et al [52], as it was shown this increase of load brought about the increase of torque [2, 52].

The change of barrel fill has led to a change of the size distribution. Dhenge et al [2] found that increasing the feed rate from 2 kg/h to 5 kg/h, resulted in small sized granules as there was a shift from bimodal to mono-modal size distribution as shown in Figure 2-14, while using the pharmaceutical formulation. This was due to the reduction of residence time, which led to production of a lower percentage for the fraction of big granules [2, 74,

75]. These findings were in accordance with those found by Lee et al who used similar formulation [17].

However, D. Djuric et al [76] found that increasing the feed rate resulted in a reduction of fine powder production, which increased median size of granules. The contradiction in the result was related to the difference in the size of the granulator, the screw configuration and materials used. The change in granulator size and screw configuration may have changed the fill level of the barrel and therefore, resulted in different stresses applied on the material. Furthermore, Vercruyssen et al [52] observed that increasing the feed rate did not show a significant effect on the size distribution of granules. Although, they noticed a variation in the degrees of barrel filling and torque values. This insignificance could be related to the fill level not exceeding the limit before it can show an effect on the granule size as well as using different formulation.

Increasing the fill level (through higher feed rate) increases the shear forces on the granules which resulted in an increase of the strength of the granules while also improving their sphericity (i.e. becoming more spherical) [2].

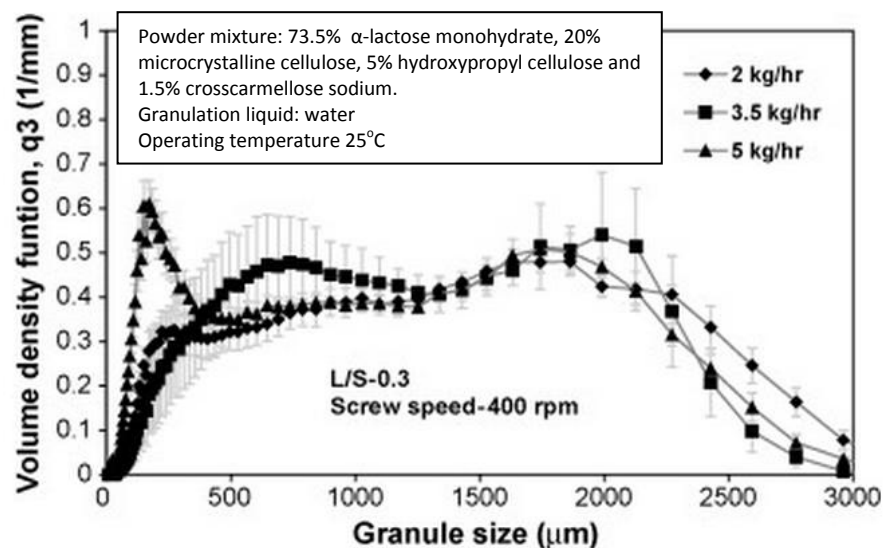


Figure 2-14 Size distributions for changing powder feed rates [2].

### ***Formulation variables***

This involves the type and size distribution of the primary powder, binder properties (viscosity) and liquid/solid ratio (L/S ratio). These variables will determine the strength of the granule and their ability to resist breakage under the stresses imparted on them by the process variables.

The composition and the type of the powder (or a mixture) has an effect on the granules strength, as different materials will deform differently as well as interacting with granulation liquid. A prime example was shown by a study on the lactose-MCC mixture conducted by Chitu et al [77] using the high shear mixer (HSM), where it was found that changing the MCC contents within the mixture results in a change of binder requirement for the granulation. El Hagrasy et al [78] concluded that using a different lactose grade in the twin screw-granulator has influenced the final granule physical properties.

Despite such influence, there are limited studies showing the effect of varying material during twin screw granulation.

#### *2.3.4.1.4 The effect of the Liquid binder Viscosity*

Numerous studies have reported that the liquid viscosity (i.e. solid binder quantity dissolved in the granulation liquid) has an effect on the granulation behaviour in a high shear granulator and a fluidized bed granulator. This generally results in growth in size of granules as the strength of the bond is stronger and able to resist the breakage due to stress imparted on them from the granulator. Despite the importance of such variables, there are limited number of studies of such parameter and its effect while using a twin screw granulator [33].

The effect of granulation liquid viscosity on the granule properties was looked at by Keleb et al [74]. They observed that increasing the viscosity of the granulation liquid reduced the minimum requirement of liquid for granulation to take place. This is due binding strength of the liquid bridges when compared to water; this meant granules can be formed with fewer liquid bridges [33, 74].

The variation of granulation liquid viscosity showed to affect the granulation differently depending on the screw configuration. Dhenge et al [33, 36] has found that in the absence of the kneading elements, increasing the granulation liquid viscosity results in a decrease in both residence time and torque, while using the pharmaceutical formulation. The author related this decrease to the lack in the ability of the viscous granulation liquid to penetrate and spread. This resulted in the powder to behave as a dry powder while given a bimodal size distribution.

However, in the presence of the kneading elements the materials within the granulator tend to behave as a highly concentrated suspension. This was concluded as the higher power required from the motor to convey materials forward, which subsequently gave an increase in both residence time and torque [33, 36, 79]. The granules formed using a viscous granulation liquid were able to withstand the shear stresses and frictions imparted upon them by screw rotation and granule collision, due to the increased strength of liquid bridges. As a result there was an observation of a growth of the agglomerates/granules within the granulator.

Dhenge et al [36] also found that increasing the viscosity of the granulation liquid, while keeping L/S consistent, shifts the size distribution from a bimodal to a mono-modal distribution. The granule growth was indicated by the increase of  $d_{50}$  as the viscosity increased at different L/S ratios as shown in Figure 2-15. Furthermore, the granules tend to obtain a more spherical shape while increasing in strength and decreasing porosity as more solid binder added to the granulation liquid (i.e. increasing the granulation liquid's viscosity). Although, their findings are informative for the effect of the screw configuration while changing the viscosity of the granulation liquid, the author did not consider different material.

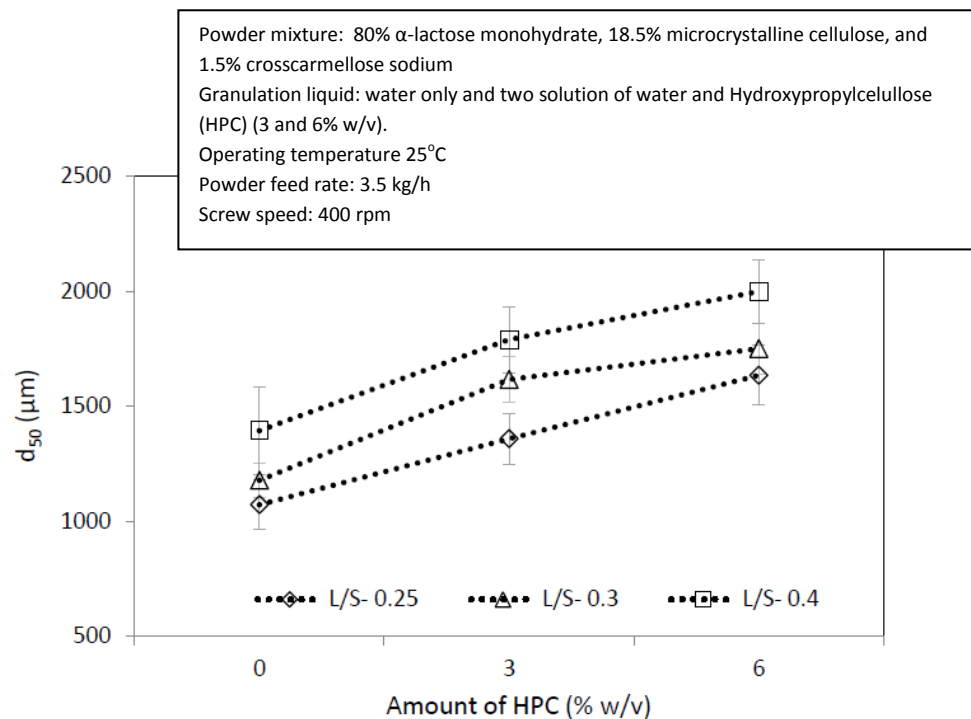


Figure 2-15 Median granule size with increasing amounts of HPC at different liquid to solid ratios [36].

#### 2.3.4.1.5 The effect of the Liquid/Solid (L/S) Ratio

The liquid/solid ratio refers to the mass flow-rate of the liquid media in ratio to the solid powder mass flow-rate. Change in the initial moisture content can result in a change of L/S ratio within the granulator, where L/S ratio can be increased by increasing the materials initial moisture [80].

One of the advantages the twin screw granulator offers over the conventional batch wet granulation (high shear mixer and fluidized bed), is the requirement of a lower L/S ratio [3, 81]. All the same, the L/S ratio still remains a vital parameter, as Keleb et al [75] has found that using a low L/S ratio, in twin screw granulation, could lead to many problems such as high power consumption, a high barrel temperature (generated from friction) as well as screw blocking. Conversely, a high L/S ratio will cause problems such as over-wetted. Therefore, the granule properties will change as the L/S ratio varies, as this will affect the strength of the material and its resistance to the stress imparted on it [3, 43, 75].

Increasing the L/S ratio will inevitably increase liquid molecule availability within the barrel. This will induce more particles to bind together as more liquid bridges form between the primary particles [43]. Increasing the number of liquid bridges will subsequently increase the strength of the agglomerate. As the number and strength of agglomerates increase, within the twin screw granulator, the resistance to conveyance will increase. Such a resistance will increase the residence time of the material according to Kleinebude and Lindne [2, 51]. This also increases the load on the screws and hence an increase in the torque produced by the shaft. The change in torque is in accordance to the material's resistance to flow. However, as L/S ratio continues to increase up to a certain level, further addition of liquid will start acting as lubricant and therefore, decreases the friction and hence the torque [2, 3, 78, 82, 83].

Different studies have also considered the effect of L/S ratio on size distribution [1-3]. El Hagrasy et al [1] investigated the effect of changing L/S ratio on a pharmaceutical formulation, (consisting of  $\alpha$ -lactose monohydrate, microcrystalline cellulose, crosscarmellose sodium and hydroxypropyl-methyl cellulose), using a twin screw granulator. Within the formulation, three different grades of lactose, (Supertab 30GR, Pharmatose 200M and lactose impalpable) were changed. The findings concluded that increasing L/S ratio caused a shift in the size distribution from the bimodal to monomodal, regardless of the grade of lactose. Dhenge et al [2], also observed a similar findings using similar formulation (while the lactose grade used was Pharmatose 200M) where they related this shift in size distribution to the increase in residence time and friction level in the granulator. They also found that increasing the L/S ratio increased the strength of the granules and shift from elongated to a more spherical shape, due to the increase in the number of liquid bridges [32, 36, 84]. Furthermore, increasing the L/S ratio showed to decrease the porosity of the granules when using the formulation [1, 36]. However, Lee et al. (2013) showed that changing increasing the L/S ratio, the granules porosity was not significantly affected.



## **2.4 Objectives**

The advantages offered by continuous twin screw granulation make it appealing for implementation for several manufacturing industries, which are looking to move away from batch operations. However, at present there is a lack of complete understanding of the mechanisms taking place during the process. In particular, the effect of changing formulation variables during the operation of the twin screw granulation on final granule products has not fully been investigated.

To date, the author is not aware of any research conducted on looking into the mechanistic understanding of the twin screw granulator and binder delivery during operation or how the liquid binder viscosity influence the process at varying shear stress and material properties. This research will involve investigating the role of the binder (and the form of the binder) as the stress applied by the process is varied. Also, the research will incorporate the behavior of different powders with differing properties.

Moreover, this research will be distinctive, as it will consider the role of binder not only on the mechanism, which results in different properties on the desired product (i.e. granules), but also look into how these variables cause the formation of undesired granulation (such as powder caking/sticking to barrel surface) during production. Such a phenomena has not been studied during the twin screw granulation and therefore, its causes are still unknown. This phenomenon may have a negative impact on the content uniformity of the granules. The study is schematically depicted in Figure 2-16.

Finally, to be able to enhance the understanding of the mechanisms taking place, online monitoring techniques will be deployed. This will be conducted using Particle Image Velocimetry. Such understanding will be used to relate to the outcome of the desired and undesired granulation.

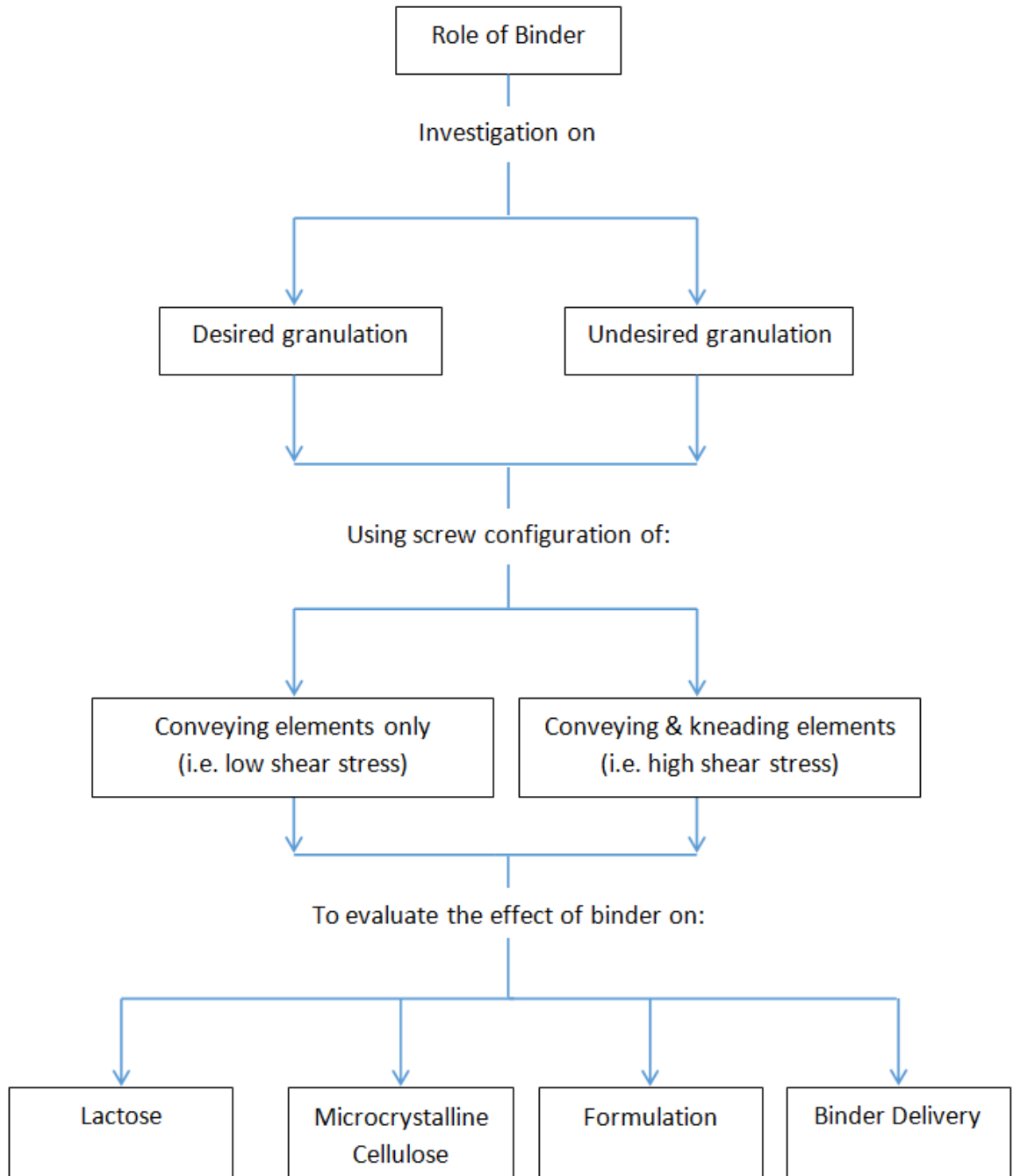


Figure 2-16 Schematic of research objective.

## **Chapter 3 Materials and Experimental methodology**

### **3.1 Material**

The materials used during this study are commonly used excipients and binder in the pharmaceutical industry [2, 33, 47, 76, 78, 81, 85-88]. Such excipients are used to improve the achieving the product with desired attribute. Typically a wet granulated formulation will contain one or more excipients for bulk or to aid processing

#### **3.1.1 Lactose**

$\alpha$ -Lactose monohydrate (Pharmatose 200M, EP & USP & JP, Bovine, Crystalline Powder) is a disaccharide which consists of two hexose sugars, glucose and galactose. In the solid state, lactose powder is found as odourless and white to off-white crystalline particles with a slightly sweet-tasting and soluble in water. Depending on the processing conditions, lactose can exist in different amorphous and crystalline forms with different properties in terms of solubility, mechanical properties and morphology. Due to the small size of the primary particles, it has good wettability owing to the high surface area, while providing an improved compaction property. On the contrary, it shows a poor flowability. The solubility of lactose in water is a useful property in granulation, as it will strengthen the granules after drying, due to re-crystallization of lactose. It is a common ingredient used in the pharmaceutical industry due to its stability and inert nature. It has, apart from some special cases, no significant tendency to react with the active pharmaceutical ingredients (API) or other components of a formulation where it is used as a filler in tablet production [85, 89].

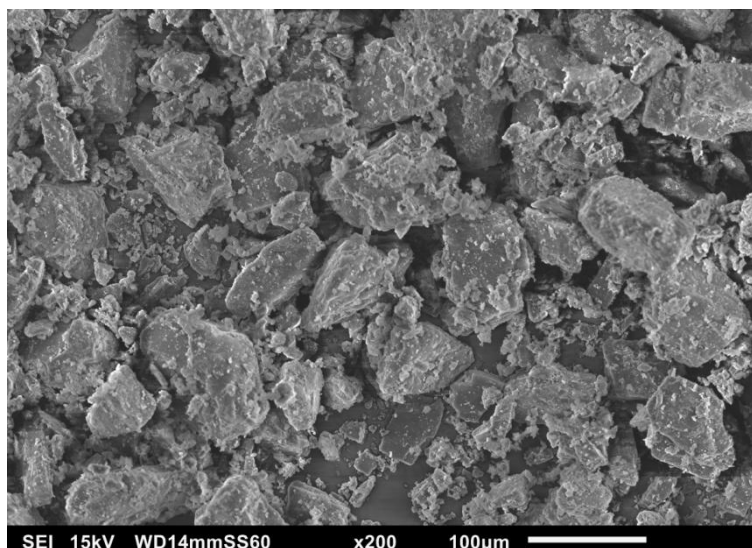


Figure 3-1 SEM image of primary particles of lactose monohydrate.

### **3.1.2 Microcrystalline cellulose (MCC)**

Microcrystalline cellulose (MCC) (Avicel PH 101, EP & USP & JP, Bovine) is another commonly used excipient in wet granulation. It is a white, odorless and free flowing powder. MCC is insoluble in water and free flowing, plastically deforming material. It is made of microcrystals that form pores. This gives the MCC properties such as water absorptive, swelling and dispersion. It is also compactable and its inclusion can add strength and robustness to a tablet. Furthermore, using MCC in a formulation makes it generally easy to disintegrate, i.e. giving a rapid drug dissolution for instant drug release products [85, 90].

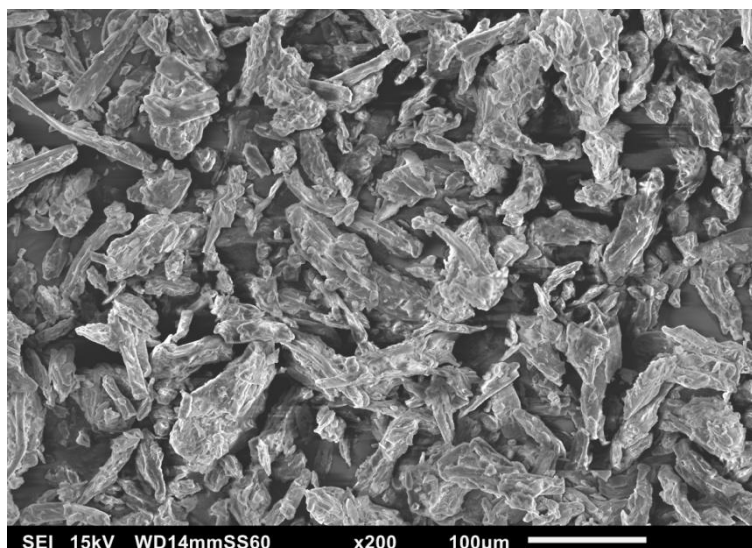


Figure 3-2 SEM image of primary particles of MCC.

### **3.1.3 Crosscarmellose sodium**

Crosscarmellose sodium (Ac-di-Sol, EP & USP & JP, Bovine) is white, free-flowing, odorless powder. It is a cross linked polymer of carboxymethyl cellulose sodium. This cross linking of fibers reduces its water solubility, while allowing the material to swell and absorb substantial amount of water. Crosscarmellose sodium provides superior drug dissolution and disintegration characteristics, thus improving bioavailability of formulations. It is used in pharmaceutical formulation as a disintegrant for tablets, capsules and granules [91, 92].

### **3.1.4 Hydroxypropyl methylcellulose (HPMC)**

Binders are used to facilitate granule growth and to aid compaction into hard tablets. Hypromellose 2910 (Pharmacoat 603, EP & USP & JP) is white odorless powder. It is a cellulose derivative (hydroxypropyl methylcellulose, HPMC) and it acts as binder, where it doesn't interact with drugs. It is available in different viscosity grades for granulation purposes. It is soluble in water and aqueous alcohols such as ethanol. The dissolution of large amount of HPMC in water may require a long time to dissolve as its introduction into water at once could form lumps [85, 91, 93].

### 3.1.5 First Intent formulation

During this study, a 'First Intent Formulation' is used, as shown in Table 3-1. This will be referred to as 'formulation' for simplicity. This formulation is commonly used in literature while also being suggested by glaxosmithkline (GSK) [2, 33, 78, 87, 88]. The formulation will be studied in two distinct ways. Firstly, the effect of increasing the liquid binder viscosity and the stress applied by the system. Secondly, the form of the HPMC binder within the formulation (i.e. the same amount of HPMC within the system at all times) while varying the stress on the material. This will be referred to as 'Binder delivery'.

Table 3-1 The first intent formulation.

Material	Activity	Composition (%w/w)	d <sub>50</sub> (µm)
Lactose	Filler	73.5	41
MCC	Filler	20	78
Crosscarmellose sodium	Disintegrant	1.5	59
HPMC	Binder	5	83

## 3.2 Granule production

### 3.2.1 Powder conditioning

Prior to the production of wet granules, the powder was firstly conditioned to the same humidity and temperature to avoid a change in the moisture of the powder. This was a necessity as the humidity of the storage varied throughout the year and this might result change in the product regardless of the condition used. The humidity was set at 40 %RH with temperature at 25°C for three days, using an environmental humidity chamber (Binder KMF 240 climatic chamber, Binder, UK). The powder was spread out on a tray to achieve a thin layer.

### 3.2.2 Liquid preparation

During this study the conditions will vary where the liquid granulation viscosity will change accordingly. This will be referred to as liquid binder viscosity (or binder viscosity). The liquid binder viscosity will vary as the amount of solid binder (i.e. hydroxypropylmethyl cellulose (HPMC)) used is adjusted.

The distilled water was heated up to 50-60 °C, before slowly adding the HPMC while ensuring the system is continuously agitated. This helped to prevent any formation of powder lump.

Table 3-2 change in liquid binder viscosity with increase in the mass percentage of HPMC in the granulation liquid.

Percentage of HPMC in the granulation liquid (w/w %)	Viscosity of the granulation liquid (Pa.s)
0%	0.001
3.75%	0.007
6.25%	0.022
7.5%	0.026
11.25%	0.081
12.5%	0.223
15%	0.258

The dynamic viscosity, presented in Table 3-2, was determined experimentally with a rheometer (Kinexus, Malvern Instruments, UK) using the cone and plate geometry (1°/50 mm) at shear rate of  $1 \text{ s}^{-1}$  and temperature of 25°C. All solutions displayed Newtonian behaviour at the given shear rate. From Table 3-2, it can be seen that increasing the dissolved HPMC amount results in an increase of the granulation liquid viscosity

### 3.2.3 Blending

In the case of a formulation, the materials were firstly dispensed accordingly and then transferred into the high shear Mixer (HSM) (Romaco Roto Junior). The HSM was operated at 300rpm for 5 minutes to improve the uniformity of the mixture.

### 3.2.4 Twin screw granulator and screw configuration

After conditioning the powder, the experiments were performed using a co-rotating twin screw granulator (TSG) (16 mm Prism Euro lab TSG, Thermo Fisher Scientific, Karlsruhe,

Germany). It is a laboratory scale granulator, which is specially built for pharmaceutical wet granulation. The barrel length is 400 mm and the diameter is 16 mm (length to diameter ratio (L/D) of 25:1). It is a co-rotating intermeshing self-cleaning twin screw granulator. This granulator is capable of producing a maximum of 1000 rpm for the screw speed and 12Nm of torque. The assembly of the parts for the twin screw granulation, as shown in Figure 3-3, is feeding hopper, feeding funnel, granulation liquid nozzle, twin screw barrel, control panel, peristaltic pump and cooling system. The feeding hopper used in this experiment is a gravimetric, loss-in-weight screw feeder (K-Tron Soder, Switzerland), which can give a powder feed rate up to 25 kg/h.

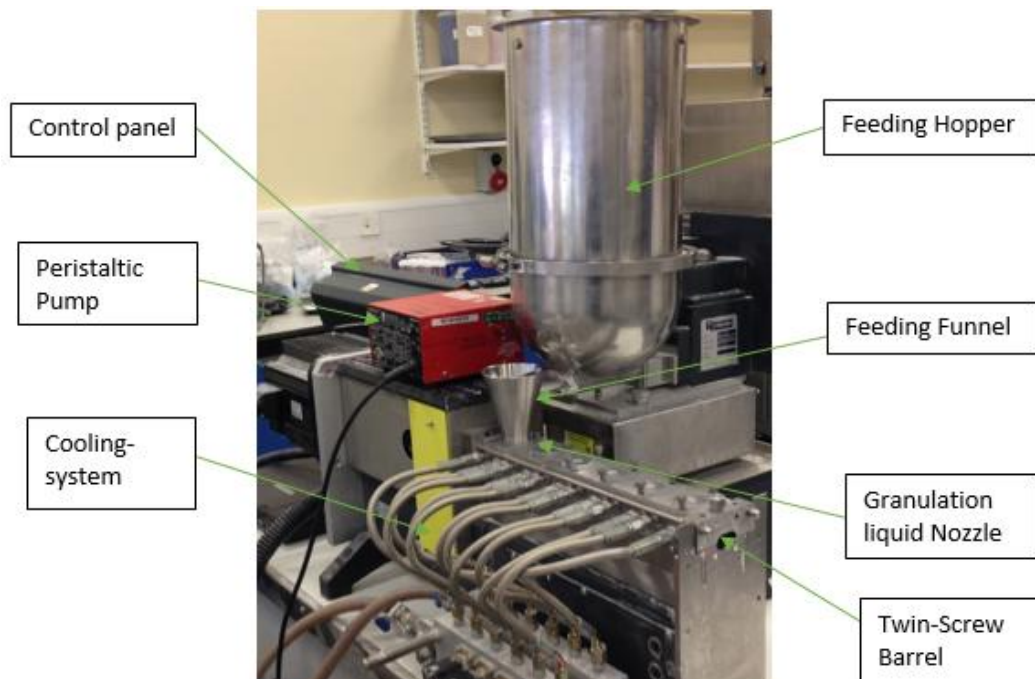

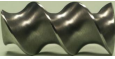



Figure 3-3 Image of the parts the the twin screw granulator used in the current-expermental set-up.

During this study the shear stress was altered by changing the screws configuration, where were accommodated in the TSG barrel. To produce low shear stress, the screw configuration consisted of conveying screws only as shown in Figure 3-4 (a) where the code for the elements used are described in Table 3-3. To produce a higher shear stress, a zone of four kneading elements, arranged at angle of 60°, was weaved into the shaft of the screws, as shown Figure 3-4 (b).



Table 3-3 the screw element coding.

Element Code	Element name	Length/Diameter ratio	Element image
SPCE	Short Pitch Conveying element	L=D	
LPCE	Long Pitch Conveying element	L=2D	
K60°	Kneading Element at 60° pitch	L=D/4	

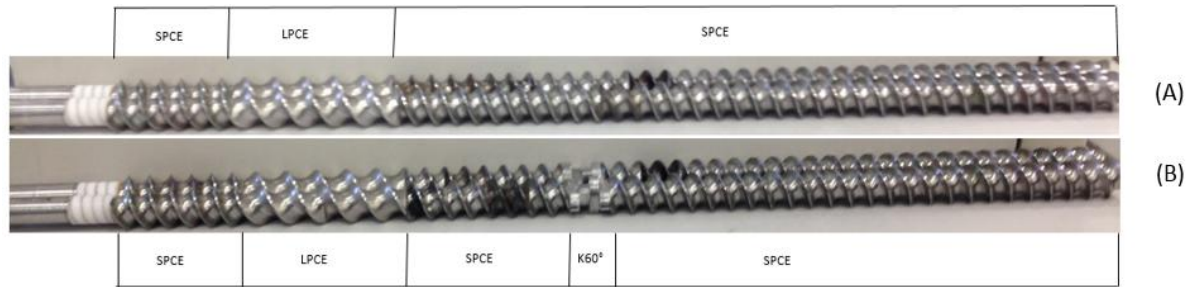


Figure 3-4 illustrating the configurations of screw used in throughout the experiments: (A) conveying elements only (i.e. low stress) and (B) conveying elements with one section of kneading elements (i.e. high stress).

### 3.2.5 Peristaltic pump

The liquid binder was added via a peristaltic pump (Watson Marlow, UK). Two peristaltic pumps were used during this study to cover a range of mass flow rate of liquid binder.

The number of revolutions per minute (rpm) of the rotating device can be controlled. These numbers do not reflect the mass flow-rate of liquid. The liquid binder mass flow rate, for a given revolutions per minute, will depend on the pipe (its elasticity or diameter) and the liquid viscosity. This resulted in calibration of the pump as the liquid viscosity changed, while ensuring the same pipe is used. Figure 3-5 shows an example for a

calibration performed for granulation liquid, in this case the granulation liquid consisted of water only.

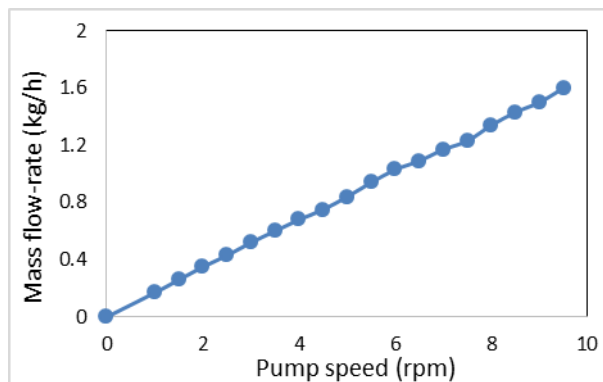


Figure 3-5 Calibration of peristaltic pump using water.

### 3.3 Granule analysis

After the drying process, the granules produced were analyzed to determine their size distribution, shape, surface topography and structural characterization.

#### 3.3.1 Drying

After the production of the granules from the twin-screw granulator, they were subjected to heat of 45°C while maintain the environment humidity at 15%RH for two days, using the environmental humidity chamber. To minimize any agglomeration/caking of the powder during the drying process, the wet granules were also spread out into thin layer in a tray.

#### 3.3.2 Size distribution

After the granulation process reached equilibrium, a representative sample was directly collected from the end of the barrel as they are produced. This was placed in adequate tray and after drying; the sample was transferred to the CAMSIZER (Retsch Technology GmbH, Germany) for the size distribution analysis.

The CAMSIZER apply the principle of digital image analysis (ISO 13322-2). The sample is fed into the measurement field via a vibratory feeder, as the particles fall between the planar light source and cameras; images are recorded. The vibration system of the chute

was adjusted to ensure a thin layer of granules fed. The images are binarised and the particle maximum and minimum lengths are measured.

Determining the size of real granule can be difficult as it is irregularly shaped and therefore, it does not have one defined diameter to measure the size. This led to many different approaches using 'equivalent diameters' to calculate the size in practice (such as Ferret's diameter, Stokes diameter, Martin's diameter, Particle sieve diameter etc.) [62, 94]. During this study the presented equivalent diameter used was particle sieve diameter, i.e. the shortest chord of the measured set of maximum chords of a particles projection. Such a diameter gives results closest to the screen/sieving. Size distribution was then presented as frequency distribution using a volume based.

### **3.3.3 Sieving**

Sieving was used to obtain granules of different size classes. The granules were separated into three different classes namely; small (<500  $\mu\text{m}$ ), medium (500-2000  $\mu\text{m}$ ) and big (>2000  $\mu\text{m}$ ). The sieve shaker (Retsch Technology, Germany) was used for 2 minutes at a low amplitude of 0.2 mm, to minimize any possible breakage of the granules during the process. 100 g of granules were used during sieving. A sample divider was used to ensure a representative sample was obtained.

### **3.3.4 Shape**

The granule shape was determined numerically using CAMSIZER, where it considers the aspect ratio of the granule. The aspect ratio is taken to be the ratio of the minor diameter of the irregular shape of the granule over the major diameter. A ratio of 1 assumed to give a spherical shape and closer to zero for more elongated shapes. In addition, a qualitative assessment of granules was conducted using a Zeiss stereo microscope (Zeiss UK).

### **3.3.5 Surface topography**

The granules, from the big class (>2000  $\mu\text{m}$ ), were randomly chosen, stabilised into a stub using carbon tape. As the granules have low conductivity, gold coating of the granules to create a conductive layer on the sample was necessary. This allowed the Scanning

Electron Microscopy (SEM) to examine the surface topography of the granules. SEM, JEOL JSM-6010LA was used to obtain electron micrographs, where it was operated at 15 kV under vacuum conditions. Minimum of three different granules from each sample were investigated.

### **3.3.6 Structural characterization**

X-ray computer tomography scans were conducted on granules (>2000  $\mu\text{m}$ ) and ribbon of powder cakes (undesired granulation). This allows materials of different densities to be resolved, allowing the visualisation of the internal structure. The sample is positioned between an X-ray source and detector, with images taken which are then reconstructed on the software of the machine to create a 3D volume.

Scans were conducted on the Scanco  $\mu\text{CT}$  35 (Scanco Medical, Switzerland). The scanning parameters were chosen after trial scans. Due to the low density of the material, the lowest energy setting was chosen, where a voltage of 45 kV, current of 177  $\mu\text{A}$  were used. The voxel size used was 3.5  $\mu\text{m}$ .

All images were analysed using Image J. The threshold of air was determined from scanning only air, which was then used to isolate the grey value of air from sample. The total number of pixels with the corresponding grey level of air was divided by the total number of pixels of the sample to give the porosity of the sample. Minimum of three different granules from each sample were investigated.

## **Chapter 4 Desired Granulation: Influence of binder viscosity**

This chapter explores the role of liquid binder viscosity on the granule properties. This investigation involves the use of different starting material namely; lactose, MCC and formulation.

Increasing the binder viscosity, while imparting low stress in the system (i.e. the use of conveying elements only) showed to give a wider size distribution and more elongated granules, while insignificant change in surface topography and porosity, regardless of the starting materials.

Increasing the stress produced by the system (i.e. incorporating kneading elements in screw configuration) resulted in a growth of the size distribution (shift toward the right) for lactose, while a narrower span for MCC and formulation, as the liquid binder viscosity increased. The aspect ratio and the porosity showed to increase, while resulting in more compacted surface topography for the different materials, as the binder viscosity increased.

### **4.1 Introduction**

In the pharmaceutical industries, products are developed to improve our wellbeing. Such a product, e.g. generic solid dosage forms (granules or tablets, capsules), are generated through a carefully planned product and process development [95]. The product development will involve targeting and identification of different excipients with desired physical and mechanical properties which considered necessary to achieve a product with targeted profile [96]. The process development will require a comprehensive understanding of the mechanisms taken place during raw material processing and the effect of process variables on the product quality. Such planning will extend to secondary manufacturing for oral solid dose forms such as granulation.

The emergence of the twin screw granulator as a continuous manufacturing of granules has encouraged the pharmaceutical companies to consider such a process for a future. Unfortunately, such a transition will require a substantial depth of understanding the effect of the process parameters on the mechanisms and hence, the final product attributes. Within an established quality system for a particular manufacturing process, one would expect an inverse relationship between the level of process understanding and the risk of producing a poor quality product [95, 96]. This is important when complying with regulatory agency to apply techniques such as Quality by Design (QbD), where the effect of critical process parameters on the critical quality attribute of the granules, must be determined [96, 97].

This has triggered various studies conducted in order to gain a better understanding on the mechanisms of the twin screw granulator. Most studies on twin screw granulation focused on the influence of process parameters on granule attributes [2, 32, 33, 52, 64, 65, 71, 81, 88, 98, 99]. This is in contrast with the formulation parameters, where it received limited attention [1, 100, 101]. Occasionally formulation parameters were investigated such as different lactose isomers [81], lactose grades with different size characteristics[1] and the hydrophobicity and solubility of excipients [17, 76]. Although, the role of binder with different formulation mixture has illustrated a noticeable effect on granule properties while using different wet granulation technique, the role of binder within twin screw is still largely unknown.

Therefore, the scope of this chapter will include the investigation of different materials while increasing the viscosity of the binder used. The stress applied will be also varied by the change of the screw configuration for each material. The material to be investigated will be lactose, MCC and formulation, where the binder viscosity will be increased from 0% (i.e. distilled water) to 15%w/w solution of dissolved HPMC. The effect of these variables on the granule properties (namely; size distribution, granular shape, surface topography and structural characterization) will be investigated.

## **4.2 Experimental and analysis methodology**

### **4.2.1 Droplet studies**

To understand the interaction of the primary material and the binder (while varying binder viscosity), a droplet of the liquid binder was placed on static compressed bed of the raw material. The droplet analysis will involve monitoring contact angle, the penetration time and maximum droplet spread on the surface of the compressed bed. 10 compressed beds for each powder were produced, using a Zwick/Roell 0.5 materials testing machine with a PC for real time data logging and analysis. The powder was carefully placed in a die of 10 mm diameter and 10 mm height. A maximum compression force of 500 N was applied, with 10 mm/min speed of the upper punch used.

The droplet volume was approximately  $3.4 \text{ mm}^3$  using a 30-gauge needle (the needle outer diameter of 0.31 mm). The tip of the needle was elevated to 4.5 mm above the surface of the compressed bed. This allowed the droplet to retain a spherical shape, as illustrated in Figure 4-1 (A). A high speed camera; (Photron Fastcam 1024 PCI, Itronx Imaging Technologies, CA) was used to capture the spreading and penetration of the droplet through the compressed bed while using a lighting, as schematically shown in Figure 4-1(B).

The high speed camera frame rate varied depending on the time taken for the droplet to complete the penetration through the compressed bed. The penetration time of the droplet was determined as the total of the number of frames taken from the instant the droplet lands on the surface until it is not distinguishable from the surface of the compressed bed. The captured images were then analyzed using First Ten Angstrom software (FTA32 version) to determine the contact angle and the maximum spreading of the droplet.

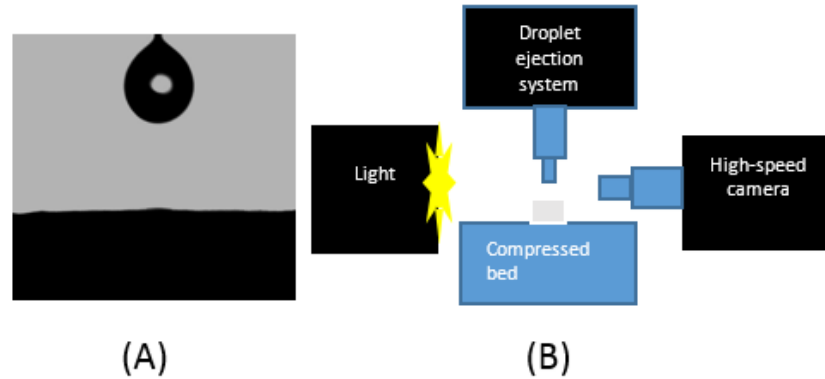


Figure 4-1 image of the droplet and surface bed (A), with the set-up used (B) used.

Choosing the contact angle value of droplet on the solid surface can be difficult. Many authors consider the apparent contact angle at the equilibrium state. The equilibrium will depend on the surface energy of the three phases (gas, liquid and solid) [21, 102], where the droplet starts spreading (Advancing) as it rests on the bed surface, and this gives an apparent contact angle that change with time (dynamic contact angle). It was assumed that the droplet reaches equilibrium at the instant the droplet stops spreading. This was taken to be as the 'static advancing contact angle' [103]. This is illustrated in Figure 4-2.

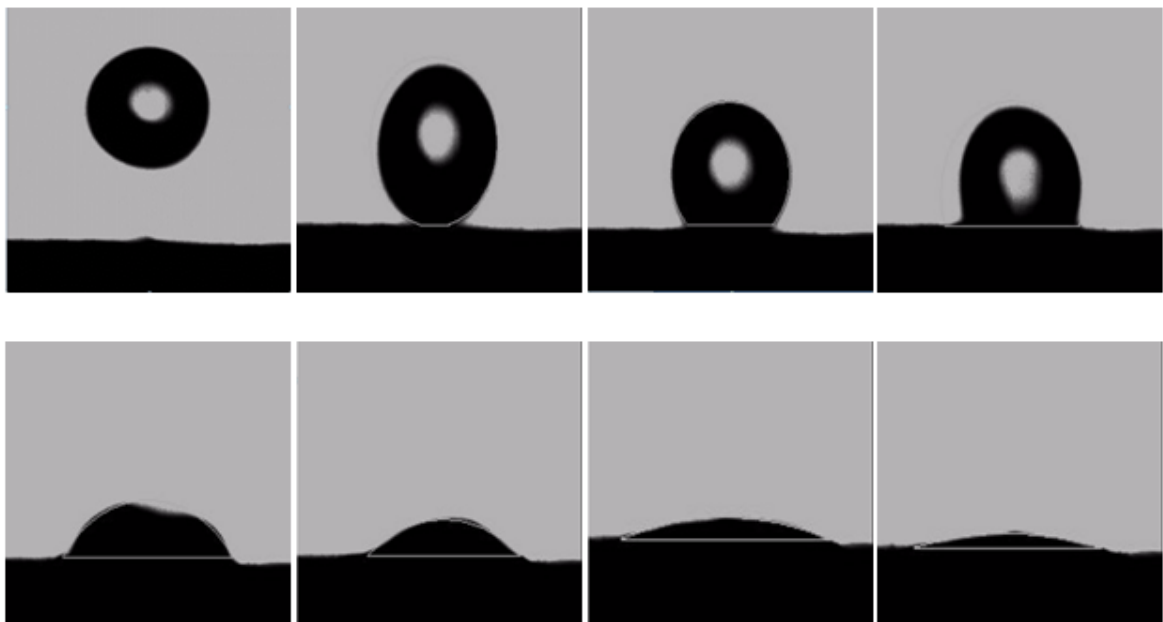


Figure 4-2 shows the spreading and penetration of the droplet once placed on a compact of powder.



The spreading of the droplet will be taking place on rough porous compacts. To account for the surface roughness, Wenzel's approach was applied to give the actual contact angle given in Equation 2-2 ( $\text{Cos } \theta_w = r_{RF} \text{ Cos } \theta_y$ ). During this thesis the actual contact angle will be referred to as 'contact angle'.

The variable  $r_{RF}$  (in Equation 2-2) accounts for the surface roughness by considering the actual area available on the surface over the projected area (smooth area), similar assumptions were made as described by Charles-Williams [103]. The assumptions they made were that the primary particles, on the surface of the compressed bed, can be approximated as spherical particles with a radius of  $r_p$ . As a result the actual available area of particle is equal to the area of a hemisphere, as shown in Figure 4-3B. The total surface area for  $n$  particles and projected area of the same number of particles are determined using Equation 4-1 [103].



Figure 4-3 Schematic drawing of (A) Projected area of the compressed bed (B) the actual (rough) area of the compress bed.

$$\begin{aligned} A_{\text{particle}} &= \sum^n 2\pi r^2 \\ A_{\text{projected}} &= \sum^n \pi r^2 \end{aligned} \quad \text{Equation 4-1}$$

While assuming that the porosity of both actual (B) and projected (A), in Figure 4-3, area is the same. The author concluded that  $r_{RF}$  would equal twice the projected area as shown in Equation 4-2.

$$r_{RF} = \frac{\sum^n 2\pi r^2}{\sum^n \pi r^2} \quad \text{Equation 4-2}$$

The maximum spread of a droplet was given as a dimensionless value. This was done by dividing the maximum spreading diameter of droplet on the powder bed surface ( $d_{\text{max}}$ ) over the original spherical diameter of the droplet ( $D_0$ ).

#### **4.2.2 Process and formulation parameters**

To solely investigate the role of binder, the process parameters were fixed to a feed rate of 1 kg/h and a screw speed of 100 rpm (to minimize the stress applied on the material) and a barrel temperature of 25 °C. Two different screw configuration were used to impart low shear stress on the material (i.e. using conveying elements only as shown in Figure 3-4 (a)) and high shear stress (i.e. conveying element and one zone consisting of four kneading elements Figure 3-4 (b)). The L/S ratio was not changing during granulation, but the different L/S ratio was used for different material where L/S ratio of 0.14 for lactose, 1 for MCC and 0.4 for formulation. The mass of HPMC dissolved varied from 0-15% w/w to give three different liquid binder viscosities. Further information on the process and formulation parameters (i.e. screw speed, powder feeder rate and Liquid/Solid ratio) on lactose and MCC, as well as information can be related to this chapter, is found in Appendix A.

#### **4.2.3 Granule analysis**

The granule size distribution, shape, surface topography and porosity; were analyzed as described in section 3.3.

### **4.3 Results and discussion**

#### **4.3.1 The influence of binder viscosity on lactose powder**

##### ***Droplet analysis***

The droplet analysis was carried out as described in section 4.2.1. Table 4-1 shows how the contact angle value varies as binder viscosity adjusted. Such a value can be used as a way to determine to the degree of wettability between liquid binder and particles of the powder, which will influence the structure and binding ability of the produced granules [19-21, 23, 104]. The contact angle value showed to increase as the binder viscosity increased. Such an increase indicates a reduction in the affinity between the liquid binder and solid particles [18]. This increase in contact angle, will give a reduction in the maximum spread of the droplet over the surface area, as shown in Figure 4-4. This shows that increasing the binder viscosity will act against spreading, as the molecules will show

more resistance to flow under shear stress, resulting in a decrease of the rate of spreading of the droplet over the compressed bed. The droplet will then tend to approach its maximum spread over short period of time [105-107]. As a result it will cover a short area and will have less capillary channels to penetrate through.

Table 4-1 Contact angle using the Wenzel approach ( $\theta_w$ ) on compressed bed of lactose at 500N.

<b>%HPMC</b>	<b>binder viscosity (Pa.s)</b>	<b>contact angle</b>
<b>0%</b>	0.001	64°
<b>7.5%</b>	0.026	78°
<b>15%</b>	0.258	82°

Furthermore, from Figure 4-4 increasing the liquid binder viscosity resulted in a slower penetration of liquid through the compressed bed.

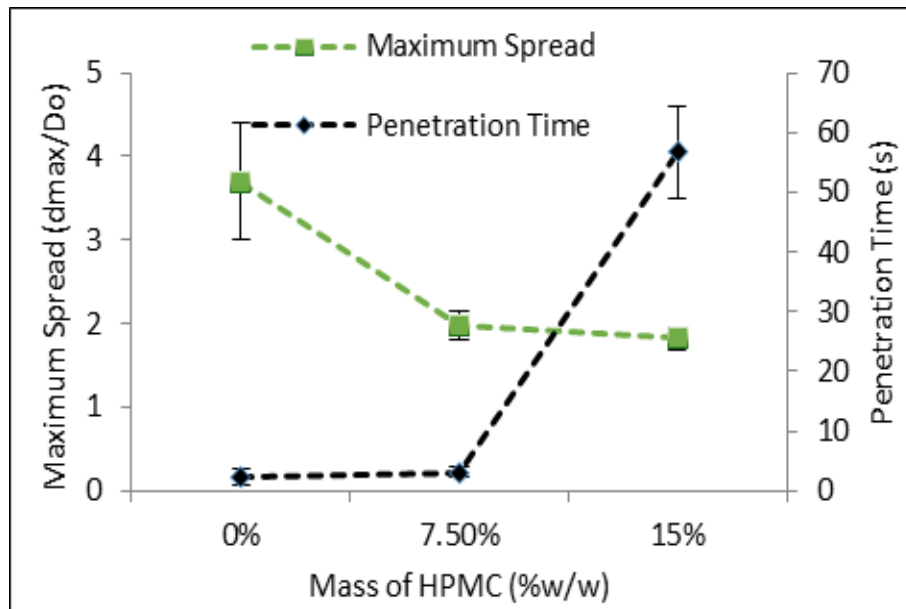


Figure 4-4 Effect of binder viscosity on maximum spread and penetration time on a static bed of lactose.

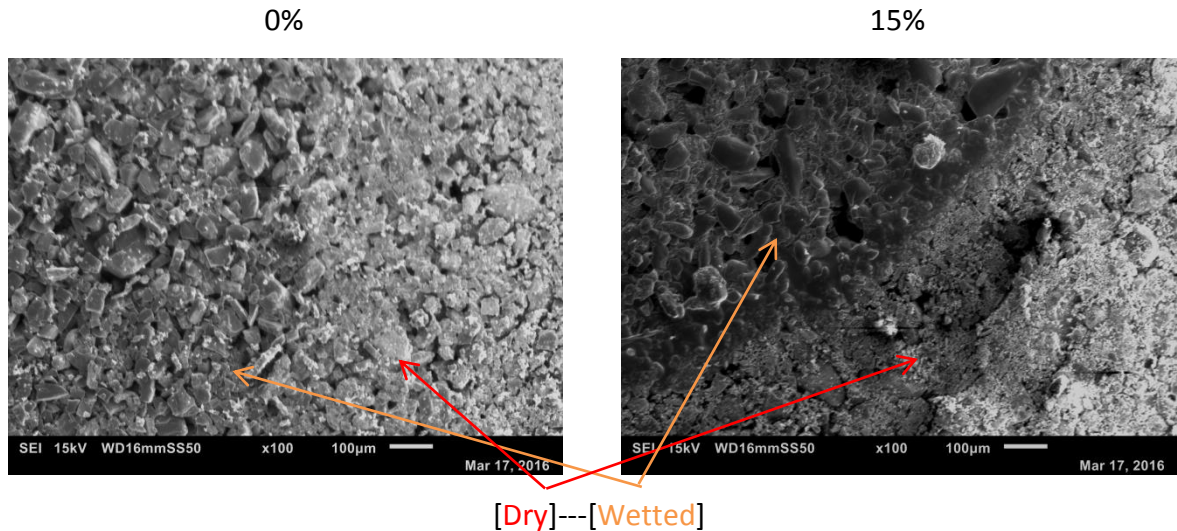


Figure 4-5 Shows the tablet's surface topography of compressed bed for the low (0%w/w HPMC) and high (15w/w HPMC) liquid binder viscosity.

Figure 4-5 shows a SEM images of surface of the lactose compressed bed after the droplet penetration (1 day after penetration) for the two extreme binder viscosity (i.e. 0% and 15%). In each image two regions defined as 'Dry' and 'Wetted'. The 'Dry' region represents the surface area of the bed for which the droplet did not come into contact with. The 'Wetted' region shows the region in which the droplet came into contact with.

In the case of the low liquid binder viscosity (i.e. 0% HPMC), the wetted region showed to be more porous than the dry region. This could be due to the ability of lactose to dissolve the smaller particles as it penetrated through [104]. For the more viscous liquid binder, the wetted region shows to be at a lower level than the dry region while sign of thin layer covering the surface area. It is more evident when considering the edge of the wet region. This could be due to the increase in weight of the viscous binder which caused the surface of the bed to be more compacted, as well as the inability for the binder to penetrate through.

#### ***Size distribution***

Figure 4-6 shows the effect of increasing the liquid binder viscosity on the size distribution of granules produced as the shear stress imparted on the material varied (i.e. changing the screw configuration). Firstly, increasing the binder viscosity, while imparting low shear

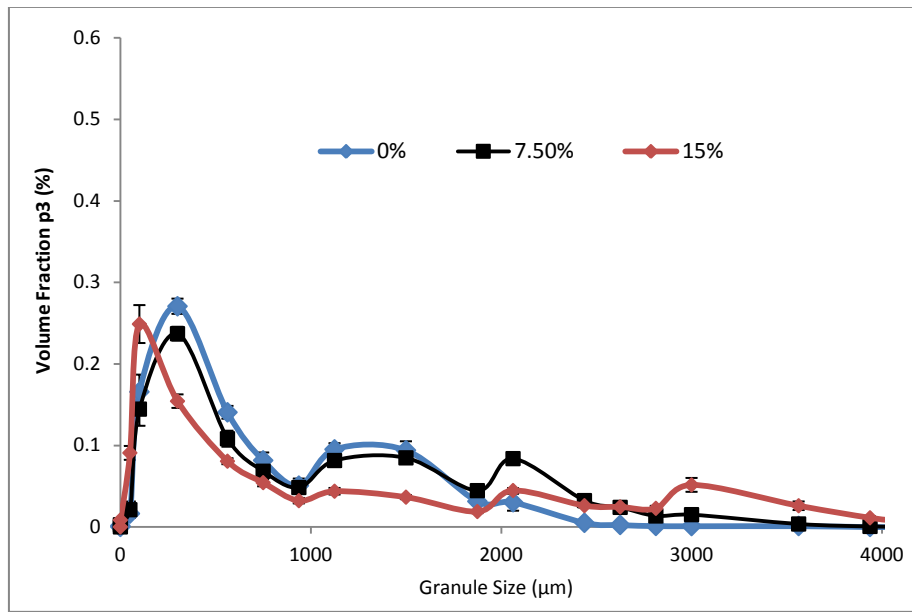
stress on the material (i.e. using conveying elements only), the range of the size distribution was bigger in comparison to that of low binder viscosity, as shown in Figure 4-6a. This was seen as it produced more of small sized granules (<300  $\mu\text{m}$ ) and the large sized granules (>3000  $\mu\text{m}$ ). This is supported by the increase in span of the size distribution as the granulation liquid viscosity increased, as illustrated in Figure 4-7.

The mechanical dispersion of the liquid is vital to ensure a uniform liquid binder distribution, in particular for the viscous liquid binder [52]. Due to the low shear stress on the material, the granulation mechanism will largely depend on the ability of the liquid binder to spread and penetrate through to create nuclei and subsequently granules. From the droplet analysis section, it was seen that increasing the binder viscosity reduced the ability of the liquid binder to spread and penetrate, while resulting in a lower affinity with the lactose powder (i.e. higher contact angle). The absence of the mechanical dispersion and liquid binder's inability to spread may have led to localisation of the liquid binder [33]. This means mainly the patch on which the liquid binder landed on formed agglomerate, leaving the rest of the powder mixture to remain un-granulated/poorly granulated. This can be illustrated as shown in Figure 4-8.

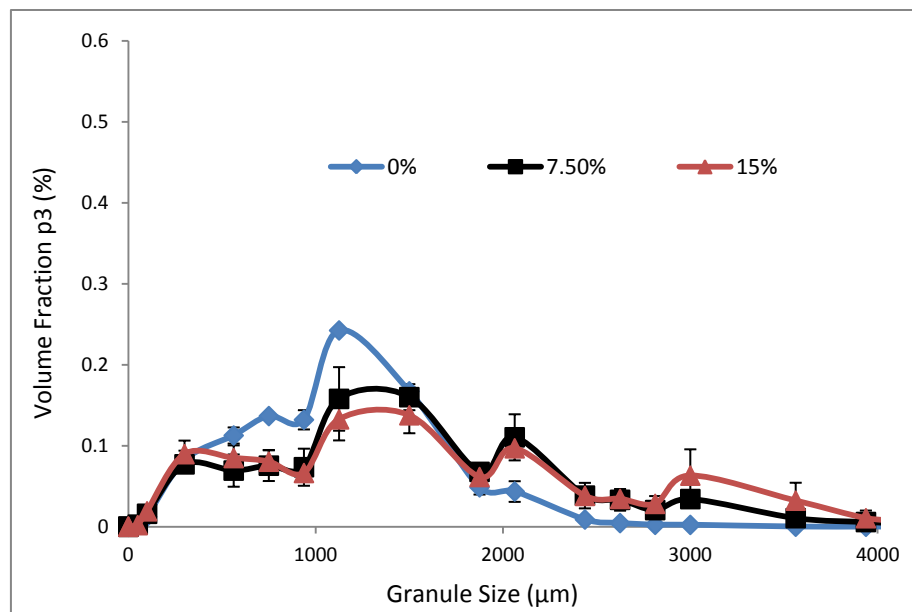
In the case of higher shear stress (i.e. using kneading elements), the granule size distribution resulted in a shift toward the bigger granules size, as shown in Figure 4-6b. This is clear when considering the highest volume fraction (%) of granules at a size around 1000-1500 $\mu\text{m}$  in Figure 4-6b, compared to their corresponding results, in Figure 4-6a, where highest volume fraction (%) was at a size around 300-500 $\mu\text{m}$ . This is due to the property of lactose, i.e. partially dissolves, and the enhanced the mixing between the liquid binder and lactose powder due to the higher shear stress imparted on the material by the granulator. The material will be more compressed and deformed forming 'crumb' as it enters the kneading element zone. This will help to distribute the liquid binder more uniformly [32, 52, 81]. This can be schematically depicted as illustrated in Figure 4-9. The

introduction of additional shear stress, gave a similar span in size distribution, indicating similar uniformity in liquid and powder mixing, as can be seen in Figure 4-7.

Furthermore, increasing the binder viscosity resulted in a noticeable shift toward the right (i.e. bigger granule size) in comparison with that of low binder viscosity. This is due to ability of the granules to resist the breakage upon collision as higher binder viscosity results in a stronger bonding [81].



(a)



(b)

Screw speed 100 rpm, Feed rate 1kg/h, L/S 0.14, 25 °C

Figure 4-6 Effect of liquid binder viscosity on size distribution; (a) low stress and (b) high stress.

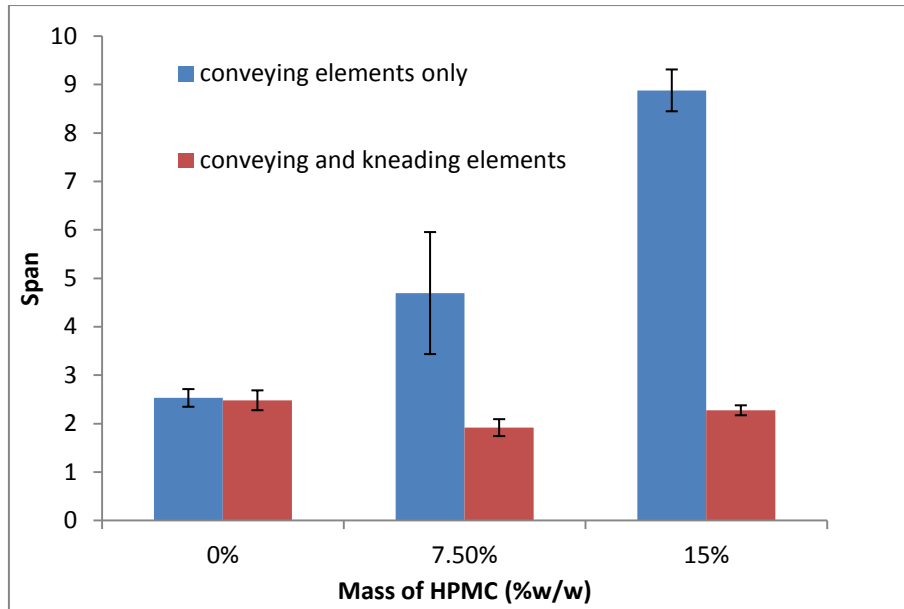


Figure 4-7 shows the span of size distribution as the liquid binder viscosity changed during low and high shear stress.

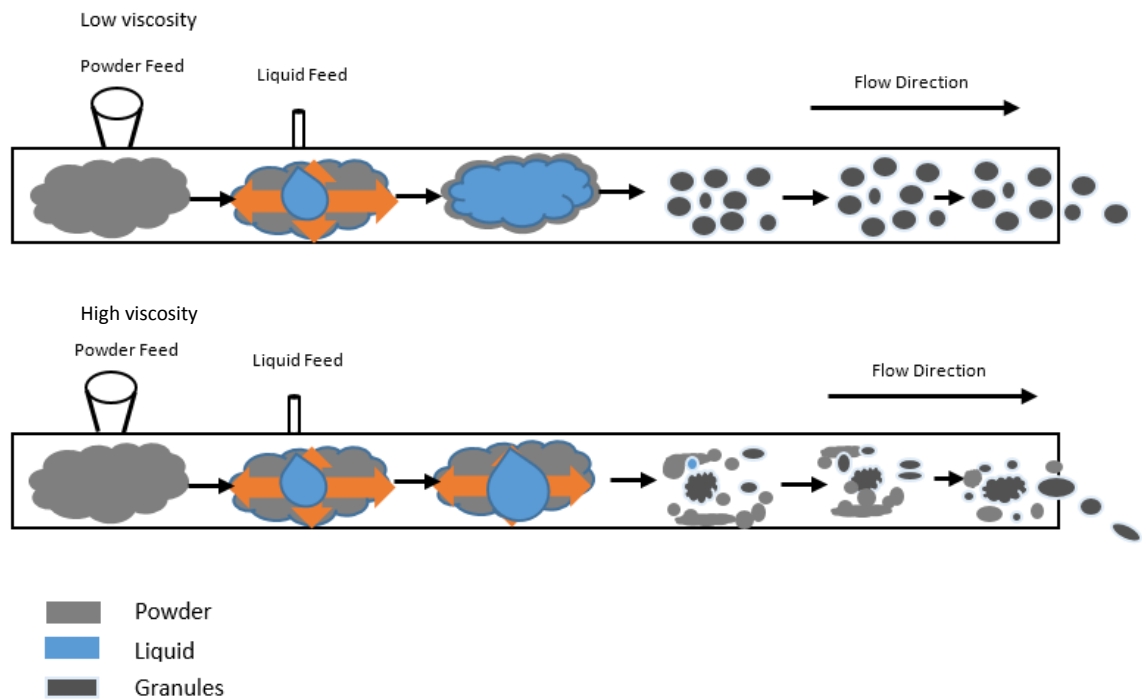


Figure 4-8 schematic explanation of the spreading of binder of varying viscosity at a low shear stress.



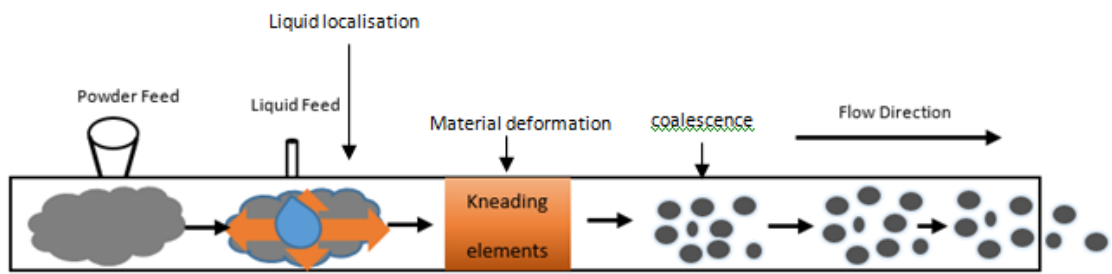


Figure 4-9 schematically describes the function of the kneading elements

### ***Granular shape***

Figure 4-10 shows the influence of binder viscosity, at different shear stresses, on the aspect ratio of lactose granules ( $\geq 2000 \mu\text{m}$ ). For low stress, the aspect ratio of granules decreased with increasing the liquid binder viscosity. This also seen by the images presented in Figure 4-11 (a-c). Varying the liquid binder viscosity resulted in a change in size distribution as seen Figure 4-6 (a). This change may have led to a change of material flow within the barrel of the granulator, where an increase in the binder viscosity will reduce the mobility of the liquid causing localization of liquid producing large granules. This may have resulted in the big granules being trapped between the intermeshing regions of the screw, and causing the material to flow perpendicular to the flow of the screw rotation, which may have caused the granules to be stretched as it resists breakage (further information on the granules flow will be studied in Chapter 7). In the case of low viscosity, the liquid binder will spread more forming granules of a narrower size distribution, where the granules will flow parallel to the rotation of the screws. The granules will experience rolling and rounding as the flow in the channel of the conveying elements and hence forming more spherical shaped granules. This different material flow behavior is illustrated in Figure 4-12.

Increasing the shear stress produced by the system on the material, has enhanced the liquid distribution, particularly for the more viscous liquid binder. This resulted in a reduction to the aspect ratio, where similar findings were found in literature [108]. The increase in the shear stress induced further consolidation and forcing the liquid binder to migrate to the surface of the granules which allows for more coalescence. As the binder viscosity increased the strength to bind to other granules/powder increases, where the final shape attained tends to be more irregular in Figure 4-11 (e & f).

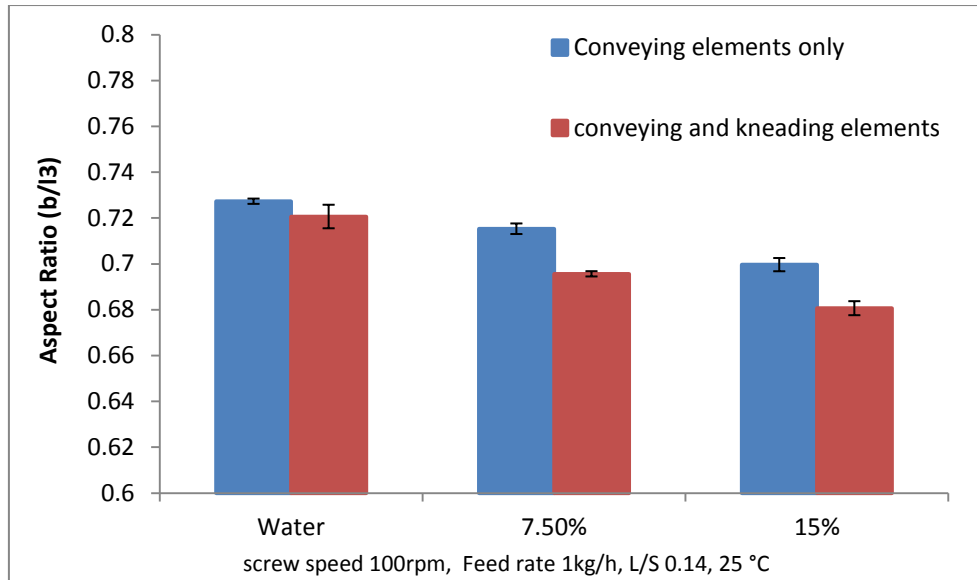


Figure 4-10 Effect of liquid binder viscosity on the aspect ratio of lactose granules as the stress varied.

% HPMC

Conveying elements only

Conveying and kneading elements

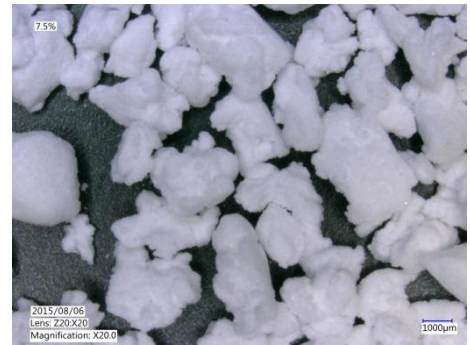
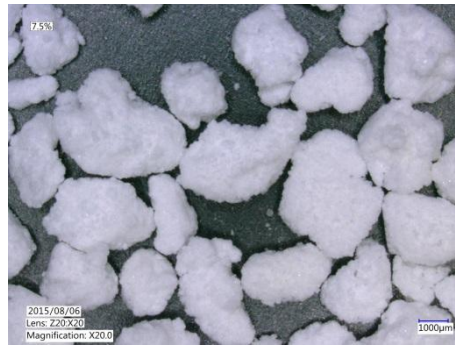
0%



(a)

(d)

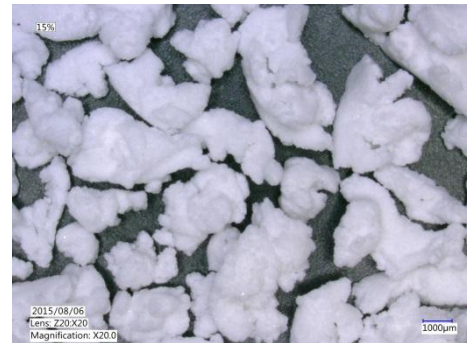
7.5%



(b)

(e)

15%



(c)

(f)

Figure 4-11 Effect liquid binder viscosity on the shape of lactose granules as the stress varied.

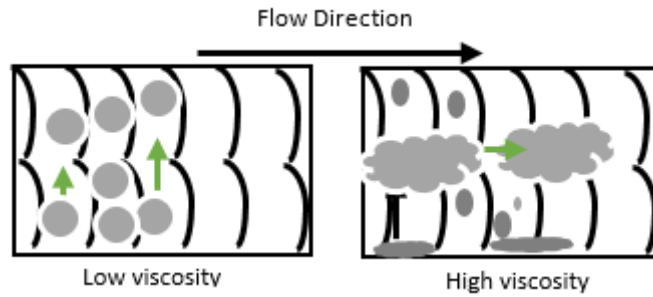


Figure 4-12 schematic diagram showing the flow of the material during low stress.

***Surface topography***

Figure 4-13 shows the surface topography of the granules ( $\geq 2000 \mu\text{m}$ ) at different shear stress as the liquid binder viscosity increases. The use of low shear stress had a minimum effect on the granular's surface topography, as the primary particle of lactose remained unaffected as shown in Figure 4-13 (a & b). On the contrary, the use of kneading element increased the shear stress imparted on material. This caused the material to undergo deformation and more densified surface topography, as shown in Figure 4-13(c & d).

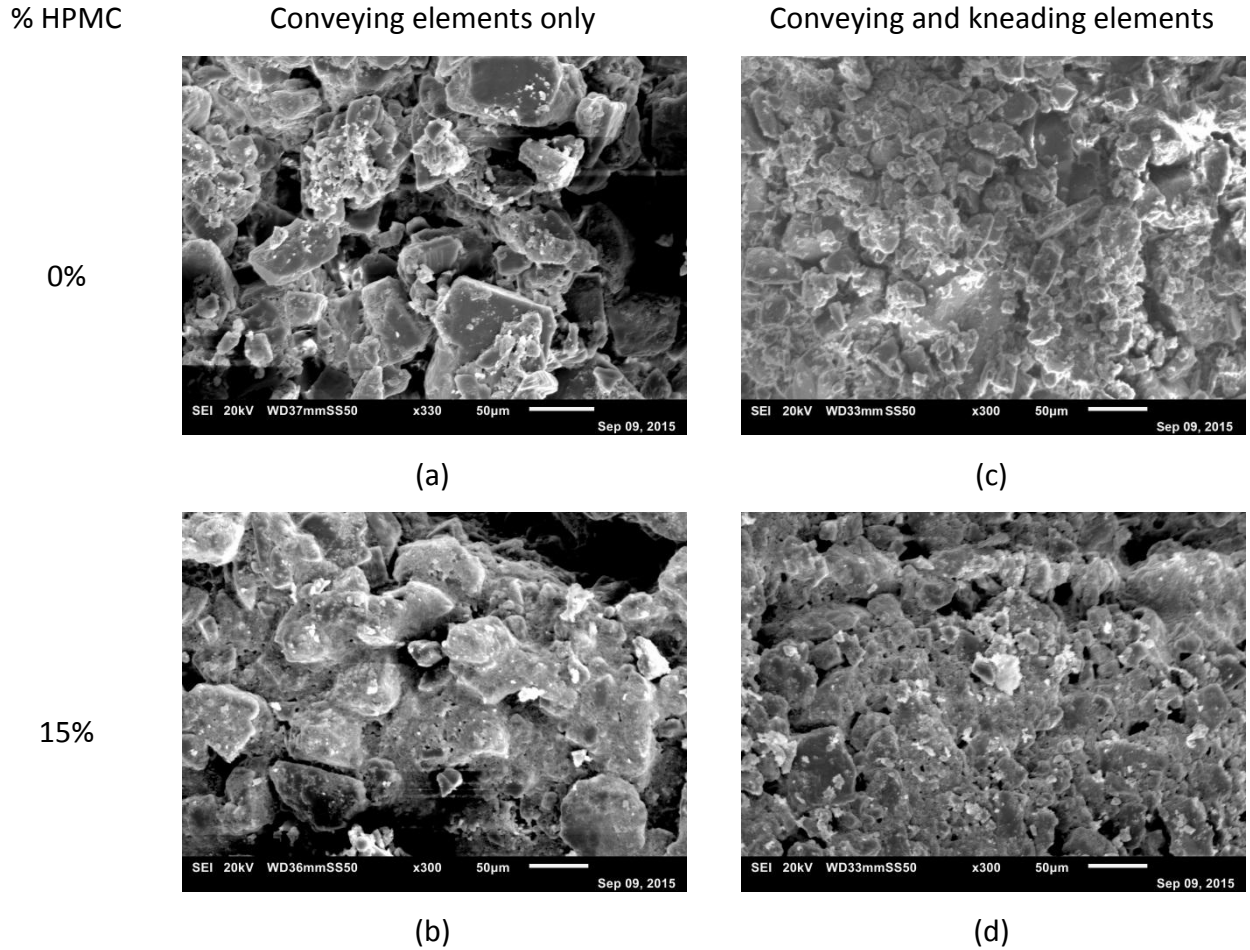


Figure 4-13 Effect of low (0%) and high (15%) liquid binder viscosity on surface topography of lactose granules, as the stress varied.

**Structural characterization**

Figure 4-14 shows the change in porosity of the granules as the binder viscosity changes, while varying the shear stress imparted on the material. The x-ray images of the granules are also presented in Figure 4-15. The granule porosity values ranged from 16-30% depending on the stress and the binder viscosity used.

Generally, at low shear stress the granules tend to form a more porous granule, while the change as the binder viscosity increases was insignificant. This is because the granules tend to be loosely attached to each other [108]. This can be seen in the images presented in Figure 4-15 (a-c).

Increasing the shear stress on the material decreased the porosity, in particular for the low binder viscosity. This could be due to the property of the lactose as it dissolves in water. This made the material softer and easier to be consolidated and hence reduce the voids within the internal structure. In the case of high binder viscosity, although the granules showed localized consolidation, as shown in Figure 4-15 (f), the granules undergo splitting/breakage and coalescence where they create voids in the internal structure, hence increase the porosity [108].

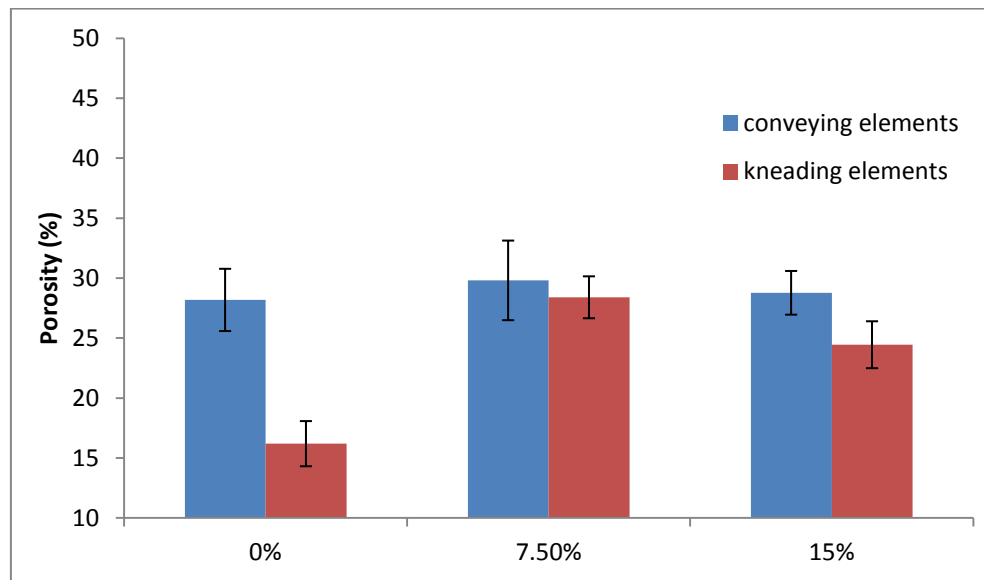


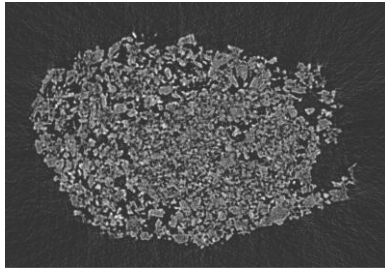
Figure 4-14 Effect of liquid binder viscosity on the porosity of lactose granules, as the stress varied.

% HPMC

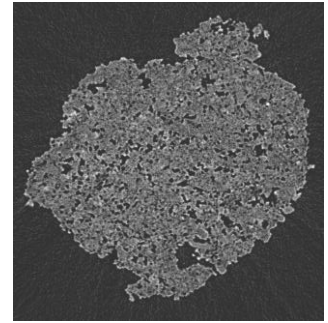
Conveying elements only

Conveying and kneading elements

0%

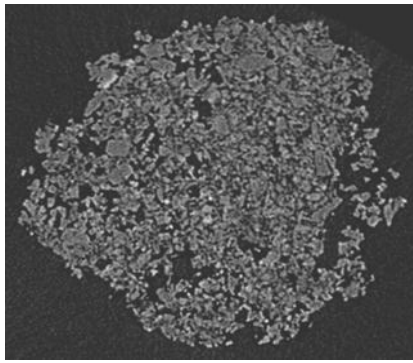


(a)

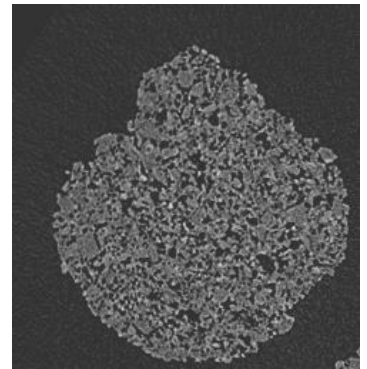


(d)

7.5%

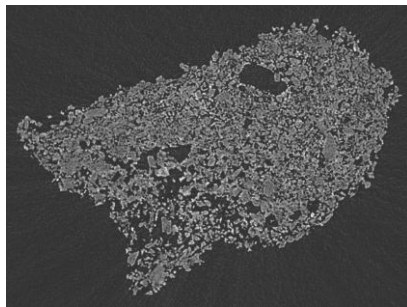


(b)

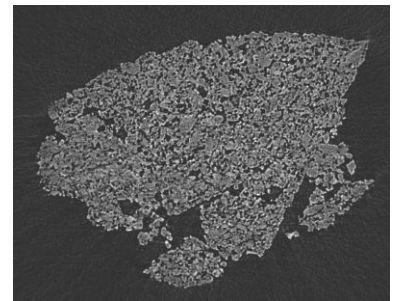


(e)

15%



(c)



(f)

Figure 4-15 Shows X-ray of lactose granules produced as the liquid binder viscosity and the stress changed.



### 4.3.2 The influence of binder viscosity on MCC powder

#### *Droplet analysis*

Table 4-2 shows the change in contact angle as the viscosity of the droplet increases. Increasing the binder viscosity increased the contact angle of the droplet with the compressed bed, i.e. decreasing the powder-binder affinity. This was similar to that seen for lactose.

Table 4-2 Contact angle using the Wenzel approach ( $\theta_w$ ) on compressed bed of MCC at 500N.

<b>%HPMC</b>	<b>binder viscosity (Pa.s)</b>	<b>contact angle</b>
<b>0%</b>	0.001	67°
<b>Set 2</b>	0.026	81°
<b>Set 3</b>	0.258	87°

Figure 4-16 shows the penetration time and the maximum spread of the droplet, as the binder viscosity increases, on the compressed bed. Again, the observation is similar to that seen in lactose. Increasing the binder viscosity increased the penetration time and decreased the maximum spread. Though, the trends were similar, the low viscosity showed to penetrate much faster than it did with lactose, while the higher viscous binder took long time (shown in Figure 4-4). This is due to the characteristic difference of the MCC, which has the ability to retain the water and swell in size [109, 110], and hence explains the penetration time of low viscosity. In the lactose, the droplet tends to dissolve material as it penetrates through the available channel.

In the case of higher viscosity, where HPMC is dissolved in the liquid and this reduces the MCC ability to take the water from the solution, as HPMC tends to be adsorbed onto the surface of the MCC particles [111]. This also shown in Figure 4-17, which illustrates SEM images for the surface of the bed after the droplet penetrated through, for different binder viscosity. The Image for viscous liquid binder shows the powder bed has to have a layer of HPMC remaining on its surface.

Figure 4-17 shows that placing a droplet of liquid binder viscosity (i.e. 0%) on the surface of compressed bed, though it shows a crack, has not shown a significant difference between primary particles or porosity of the bed in the 'dry' and 'wetted' section of the surface. This is because after drying the MCC particles retain their shape. The crack is due to MCC elevating as a result of swelling during water uptake.

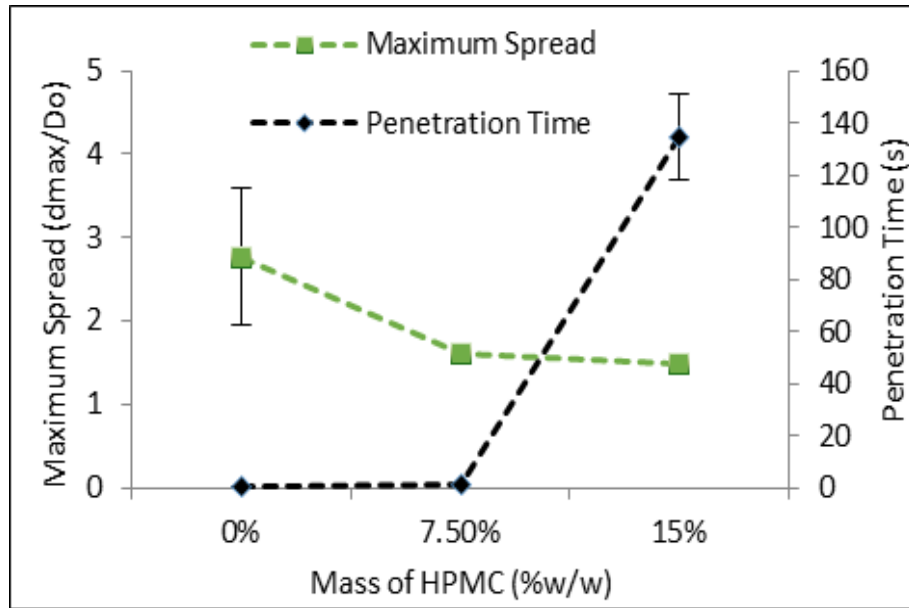


Figure 4-16 effect of binder viscosity on maximum spread and penetration time on a static bed of MCC.

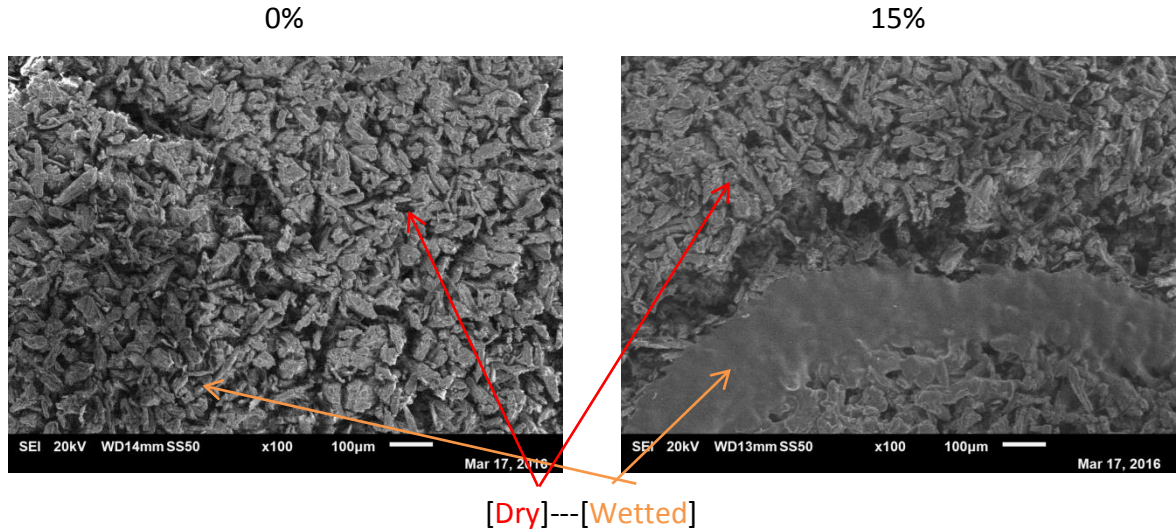
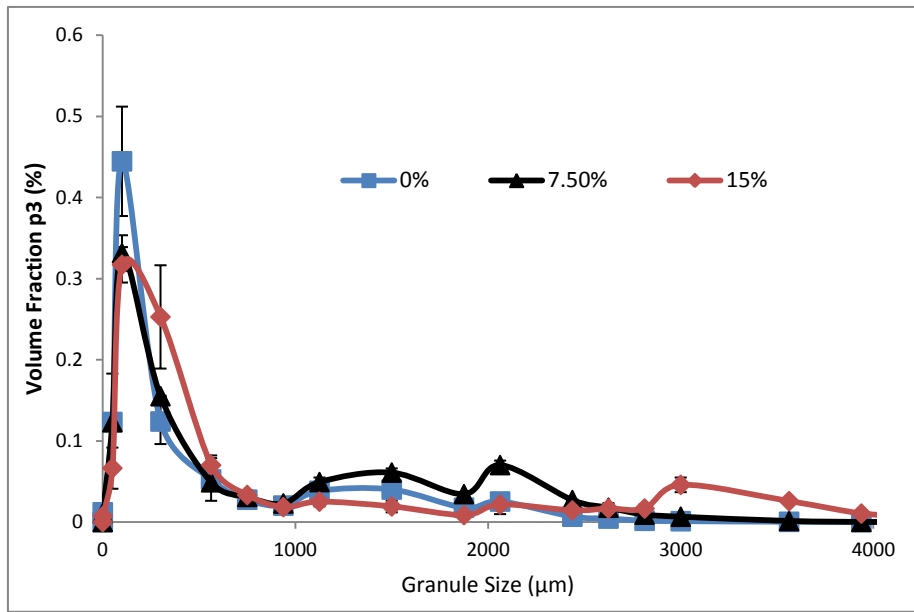


Figure 4-17 Shows the tablet's surface topography of compressed bed for the low (0%w/w HPMC) and high (15w/w HPMC) liquid binder viscosity.

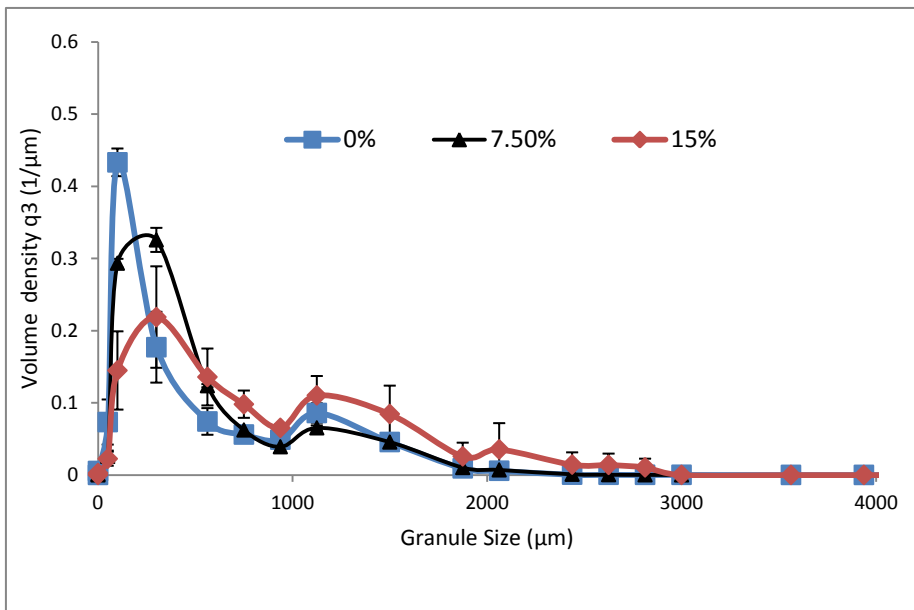
#### ***Size distribution***

Figure 4-18 shows the size distribution of MCC as the liquid binder viscosity changed, at different shear stress. During the low shear stress, shown in Figure 4-18 (a), increasing the binder viscosity increases the range of the size distribution, where the span also increased as shown in Figure 4-19. This is similar observation seen for the lactose. This is due to the inability of the liquid binder to penetrate and spread the viscosity increases and hence, cause of liquid binder localization.

Increasing the shear stress, the size distribution of granule becomes a narrower as illustrated in Figure 4-18 (b), where the change in span did not show any significant difference, as shown in Figure 4-19. This is more pronounced for the higher viscosity. This observation is different to that seen for the lactose, where a shift toward the bigger size was seen. This difference is related to the difference in the characteristic of the MCC (retaining water) and lactose (dissolving). The increase in shear stress helped to distribute the adsorbed HPMC (in the high viscous binder) within the big granules more uniformly.



(a)



(b)

Screw speed 100 rpm, Feed rate 1kg/h, L/S 1, 25 °C  
 Figure 4-18 Effect of liquid binder viscosity on size distribution; (a) low stress and (b) high stress.

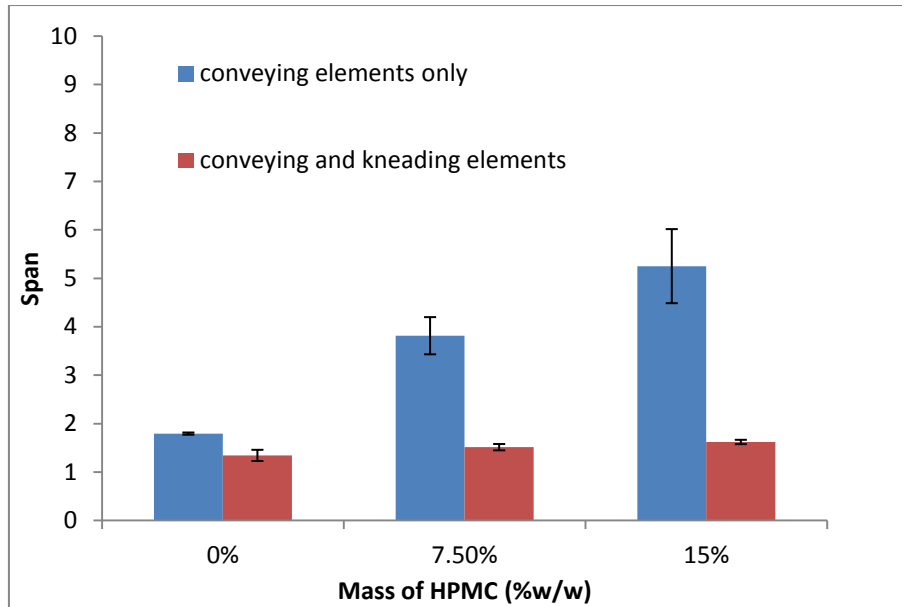


Figure 4-19 shows the span of size distribution as the liquid binder viscosity changed during low and high shear stress.

### ***Granular shape***

Figure 4-20 shows the influence of increasing binder viscosity on the aspect ratio of MCC granules ( $\geq 2000 \mu\text{m}$ ), at different shear stress. In the case of low shear stress, increasing the binder viscosity produced more elongated granules, as shown in Figure 4-21 (a-c). This is similar to that observed for the lactose, shown in Figure 4-11, which is related to the flow of material within the barrel.

Producing higher shear stress on the material resulted in a higher aspect ratio in particular for the higher binder viscosity. This was the opposite observation for lactose. Due to the characteristic of MCC of retaining the water, increased its plasticity during the consolidation and crumbing in the kneading element zone. The adsorbed HPMC allowed for the small granules to coalesce together, as shown in Figure 4-21 (f), as they continue to roll forward in the conveying elements. This is also supported by the reduction in the big granule production shown in Figure 4-18 (b). In the case of the lactose, where the material is partially dissolved, i.e. the binder liquid remains on the surface, allowed for big granules to coalesce giving it a more irregular shape.

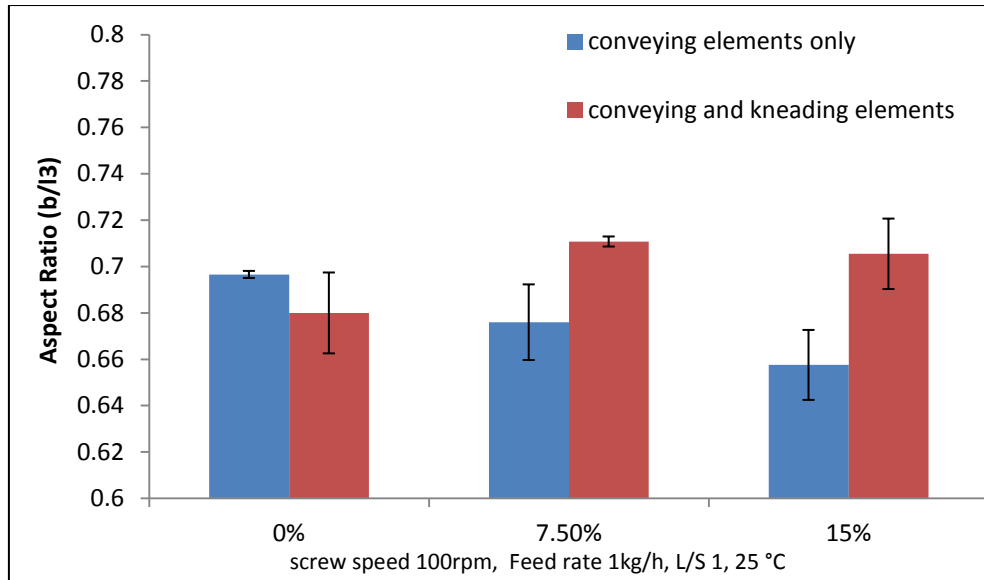


Figure 4-20 Effect of liquid binder viscosity on the aspect ratio of lactose granules as the stress varied.

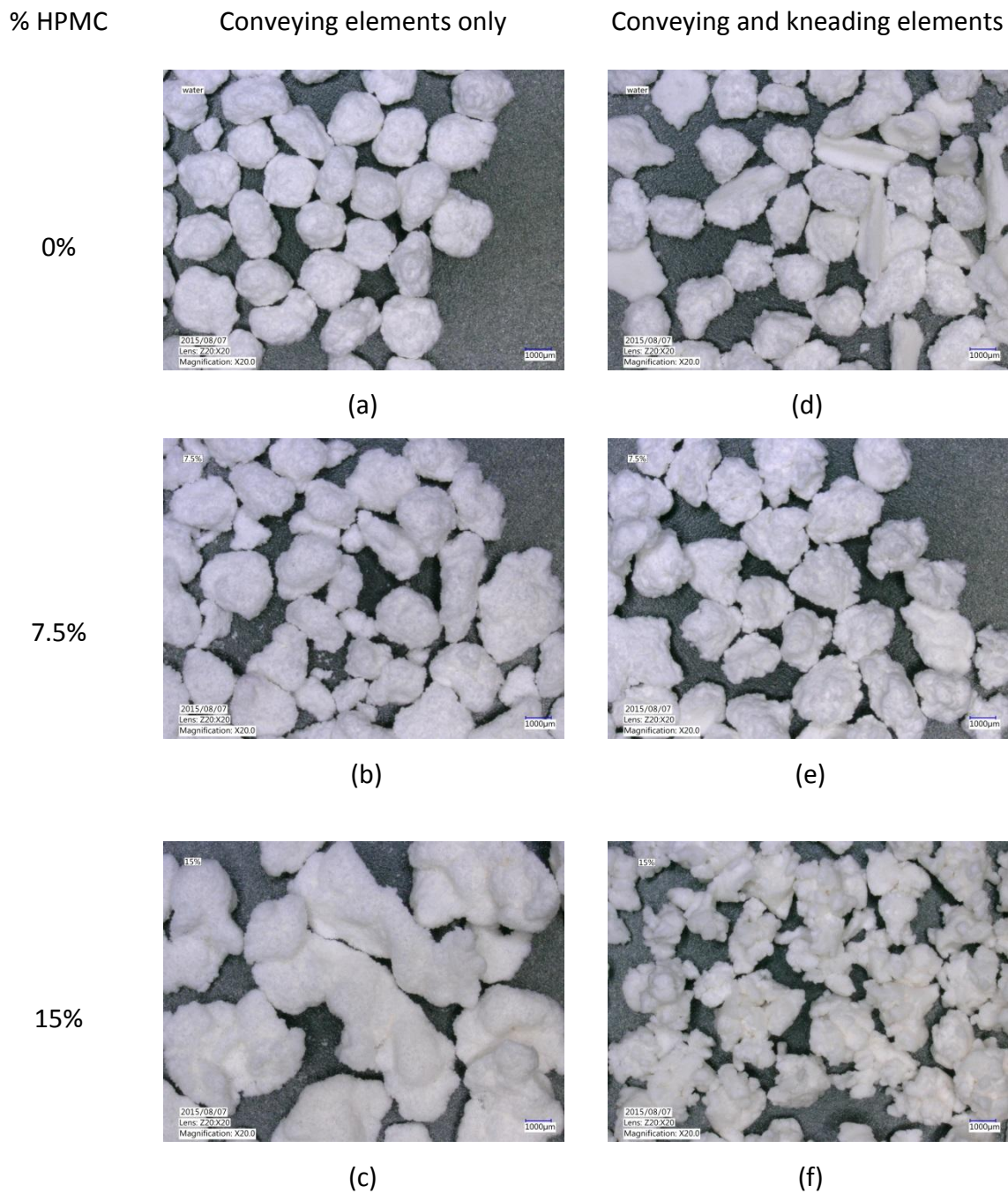


Figure 4-21 Effect liquid binder viscosity on the shape of lactose granules as the stress varied.

**Surface topography**

Figure 4-22 shows the surface topography of MCC granules ( $\geq 2000 \mu\text{m}$ ) as the binder viscosity and shear stress varied. The SEM images show similar behavior as seen for

lactose, where the low shear stress did not show significant effect on the primary particles of the MCC. More deformation to the primary particles were seen as the high shear stress was imparted on the material. This effect is more pronounced for the more viscous granulation liquid. This could be due to the inability of the MCC to absorb the HPMC, where it tends to adsorb on the surface as shown by the images in Figure 4-17, where it helped for bind more particles and smear on the top surface.

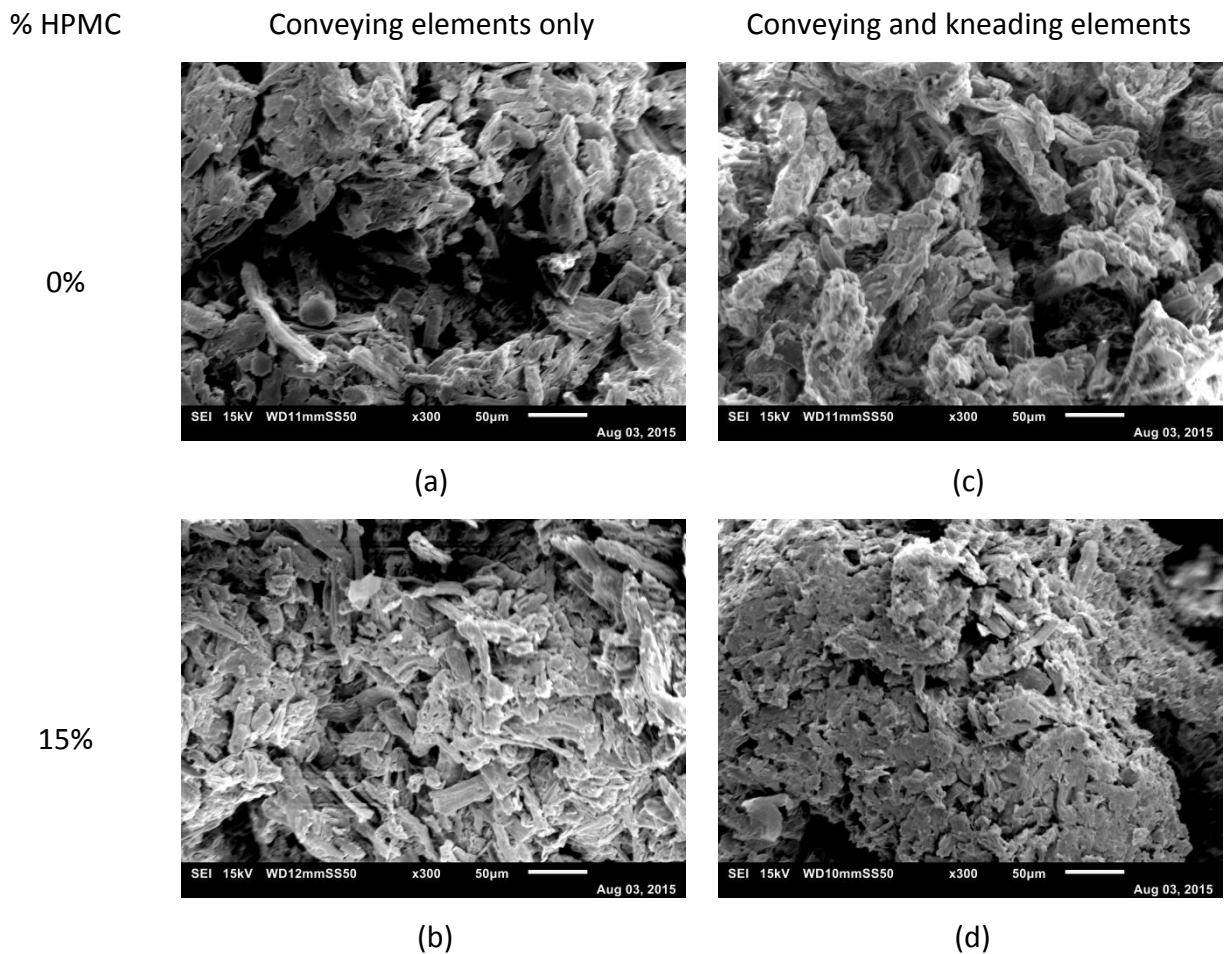


Figure 4-22 Effect of low (0%) and high (15%) liquid binder viscosity on surface topography of MCC granules, as the stress varied.

**Structural characterization**

Figure 4-23 shows the change of the porosity of the MCC granules, as the liquid binder viscosity and shear stress applied varied. Increasing the liquid binder viscosity, at low



shear stress, the granules tend to be loosely packed and as result the porosity showed to be insignificant, as it can be seen in Figure 4-24(a-c).

The granules tend to become more compacted as higher shear stress is applied on the material, regardless of the binder viscosity. Also, increasing the binder viscosity showed to decrease the porosity (during higher stress). This is the opposite of that seen in the lactose. The MCC loses its retained water during drying where the primary particles tend to shrink in size and hence creating voids. This is not expected for excess viscous binder which is present on the surface, due to adsorbing of HPMC, causing the particles to be held closely reducing the voids. The difference can be seen in the images presented in Figure 4-24 (d-f).

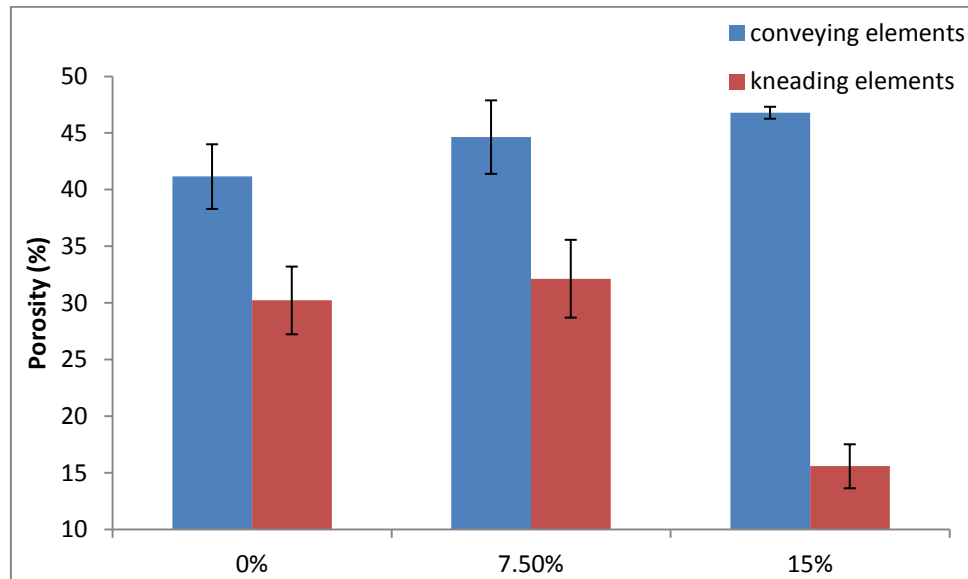


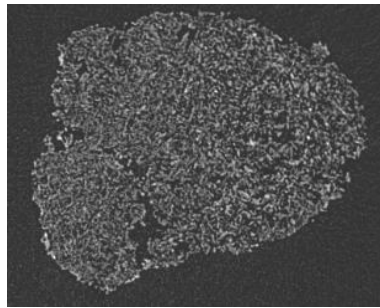
Figure 4-23 Effect of liquid binder viscosity on the porosity of MCC granules, as the stress varied.

% HPMC

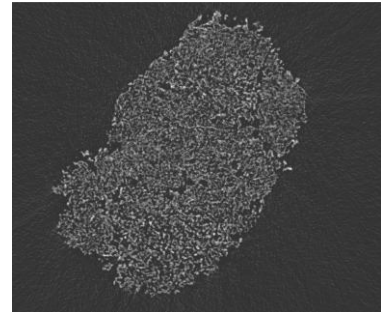
Conveying elements only

Conveying and kneading elements

0%

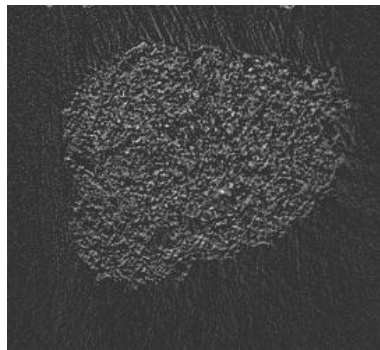


(a)

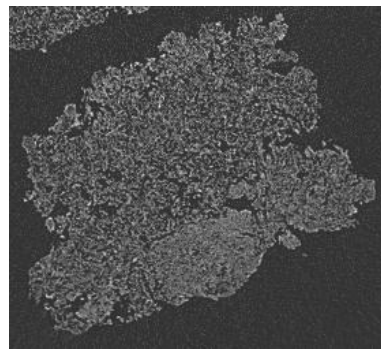


(d)

7.5%

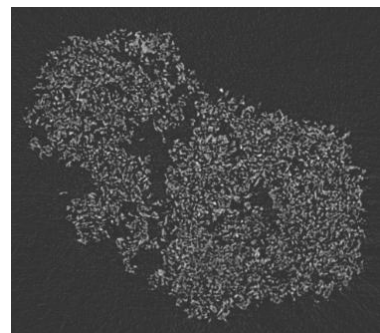


(b)

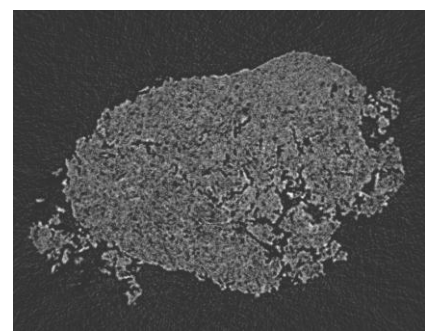


(e)

15%



(c)



(f)

Figure 4-24 Shows X-ray of MCC granules produced as the liquid binder viscosity and the stress changed.

### 4.3.3 The influence of binder viscosity on formulation

#### *Droplet analysis*

The results shown Table 4-3 were generated as a droplet with different binder viscosity were placed on the compressed bed. Increasing the viscosity of the droplet binder increases the contact angle. This increase also resulted in an increase of penetration time and decrease of maximum spread, as show in Figure 4-25. This is in accordance with result presented by Dhenge et al [19, 33].

Table 4-3 Contact angle using the Wenzel approach ( $\phi_w$ ) on compressed bed of formulation at 500N.

<b>%HPMC</b>	<b>binder viscosity (Pa.s)</b>	<b>contact angle</b>
<b>0%</b>	0.001	66°
<b>7.5%</b>	0.026	80°
<b>15%</b>	0.258	84°

Although the trends remained the same as that seen for the lactose and MCC, the absolute values have changed. The penetration time for the most viscous binder was much longer, when compared with a lactose or MCC individually. This is due to a combination of slower movement of the droplet (due to viscosity), the reduction of the porosity (packed material with different size/density) and the water retaining by the MCC may have been limited. Furthermore, during penetration process the water may have evaporated from the droplet, increasing the viscosity of the binder. This can be seen by viewing the SEM image presented in Figure 4-26. For the 15% a layer of HPMC is fully covering the 'wetted' region.

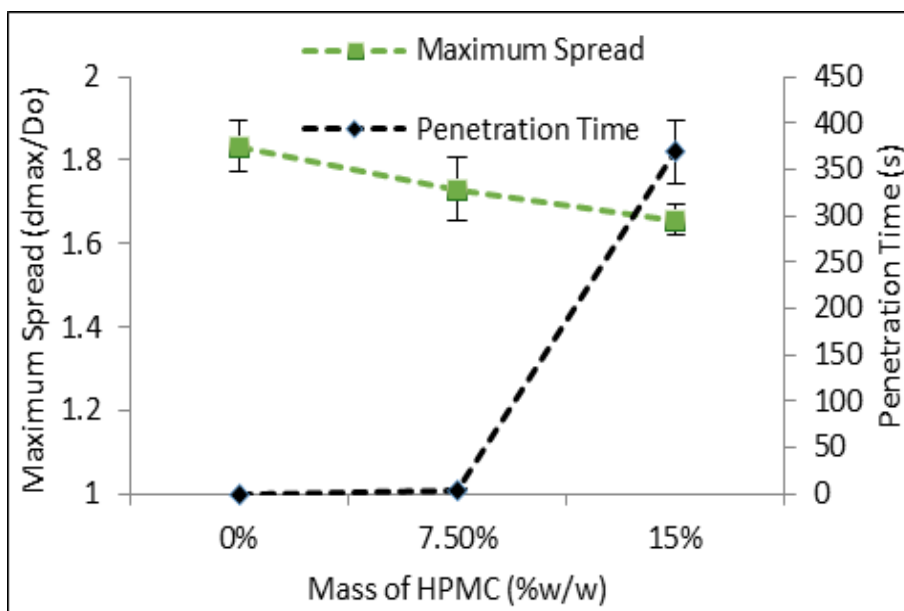


Figure 4-25 effect of binder on maximum spread and penetration time on a static bed of formulation.

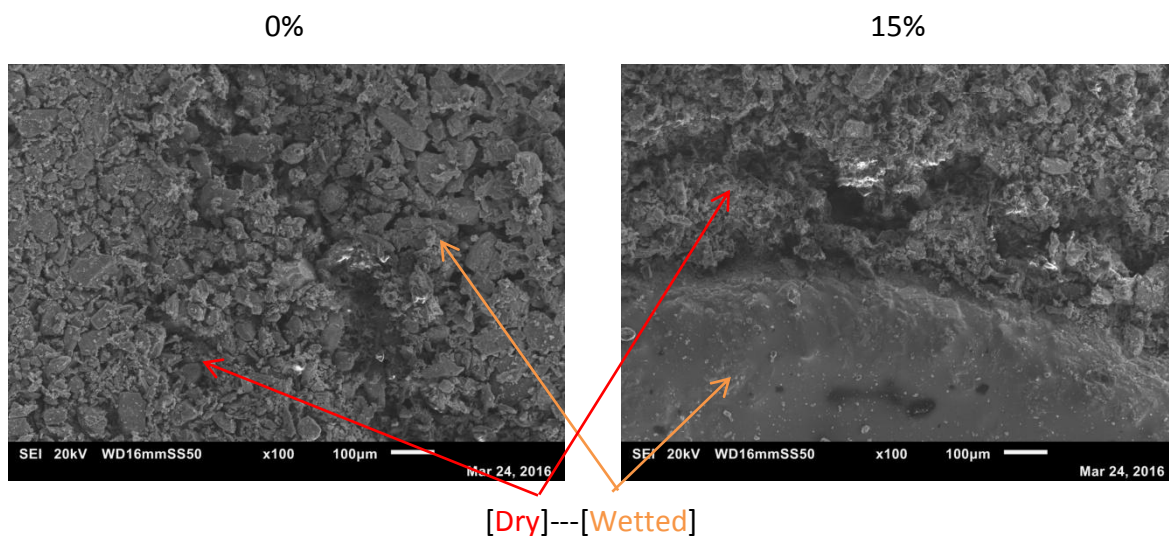
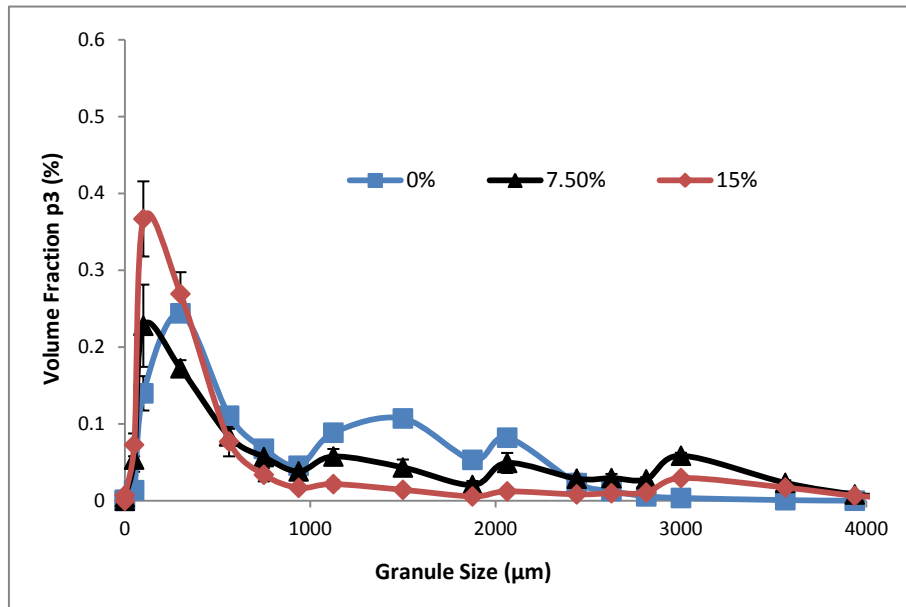


Figure 4-26 Shows the tablet's surface topography of compressed bed for the low (0%w/w HPMC) and high (15w/w HPMC) liquid binder viscosity.

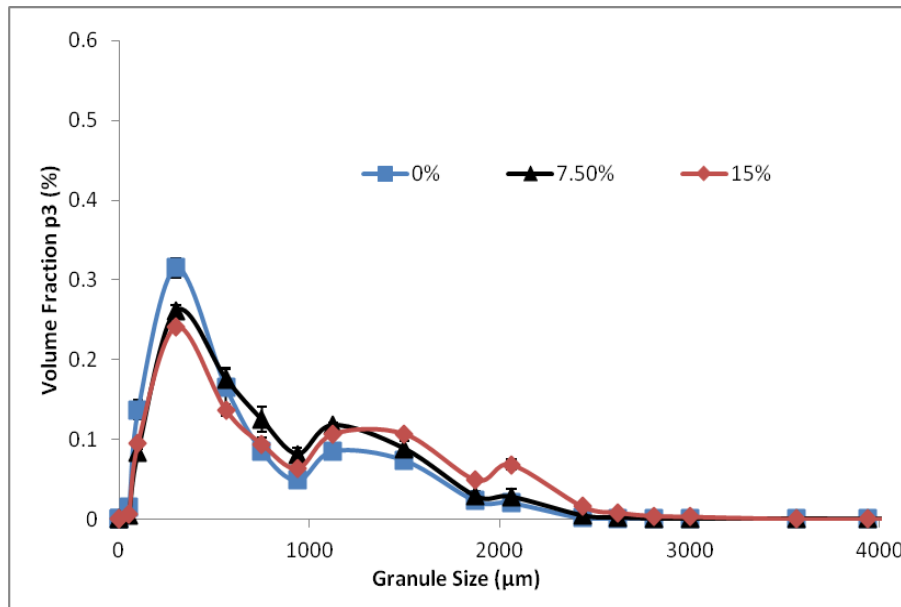
**Size distribution**

Figure 4-27 shows how the liquid binder viscosity influences the size distribution as the shear stress varied. Applying low shear stress on the material resulted in a broader size distribution as the liquid binder viscosity increased, where the span showed to increase as illustrated in Figure 4-28. This is due the liquid inability to spread and penetrate (localization), which was seen for the lactose and MCC too.

Although, at higher shear stress; increasing the binder viscosity showed to give more big granules than the low viscosity, the range of size distribution was reduced than that for the low shear stress as seen in Figure 4-28. This is similar to the MCC trends shown in Figure 4-18. As the formulation contained MCC, more water will be retained due to the better distribution of liquid binder. Therefore, the less liquid binder will be available on the surface which will be distributed more evenly, producing granules of similar size and limiting their growth.



(a)



(b)

Screw speed 100 rpm, Feed rate 1kg/h, L/S 0.4, 25 °C  
 Figure 4-27 Effect of liquid binder viscosity on size distribution; (a) low stress and (b) high stress.

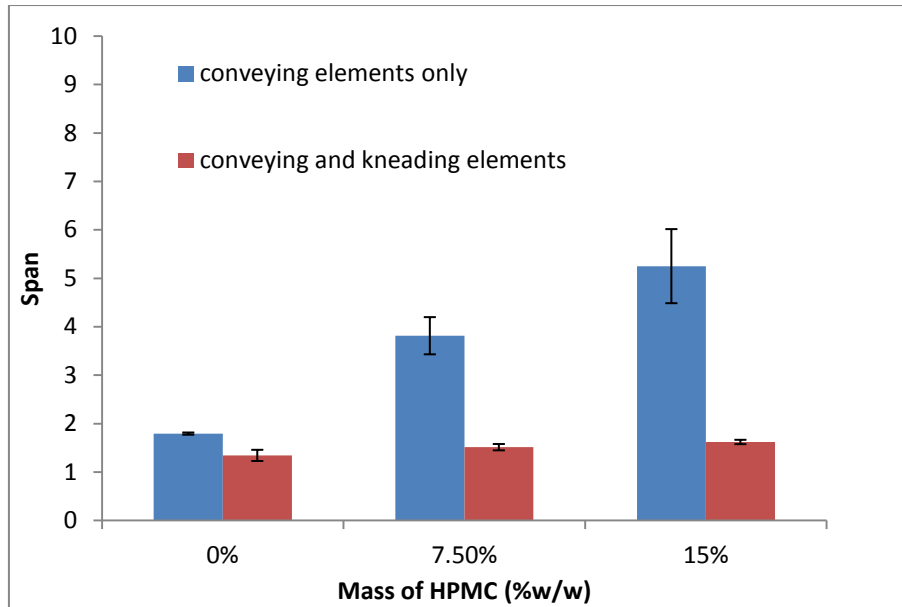


Figure 4-28 shows the span of size distribution as the liquid binder viscosity changed during low and high shear stress

### **Granular shape**

Figure 4-29 shows the influence of binder viscosity on the aspect ratio for the formulation granules ( $\geq 2000 \mu\text{m}$ ), as shear stress applied on the material varied. At low shear stress, the aspect ratio of the granules tends to decrease as the liquid binder viscosity increased, where they attain elongated shape, as shown in Figure 4-30 (a-c). This was seen for the both lactose and MCC, which illustrates the importance of liquid binder's ability to spread in the absence of higher shear stress.

Increasing the shear stress, showed to give a higher aspect ratio, which was more prominent for the higher binder viscosity. This is similar behavior seen for the MCC. As the size distribution showed a reduction in big granules, while applying a high shear stress, which indicates the imparted stress caused the crumbing of small granules where they coalesce together attaining a more spherical shape, as shown in Figure 4-30 (d-f). Using lactose alone showed to give more irregular shapes, which was related to the increase in size as big granules coalesce.

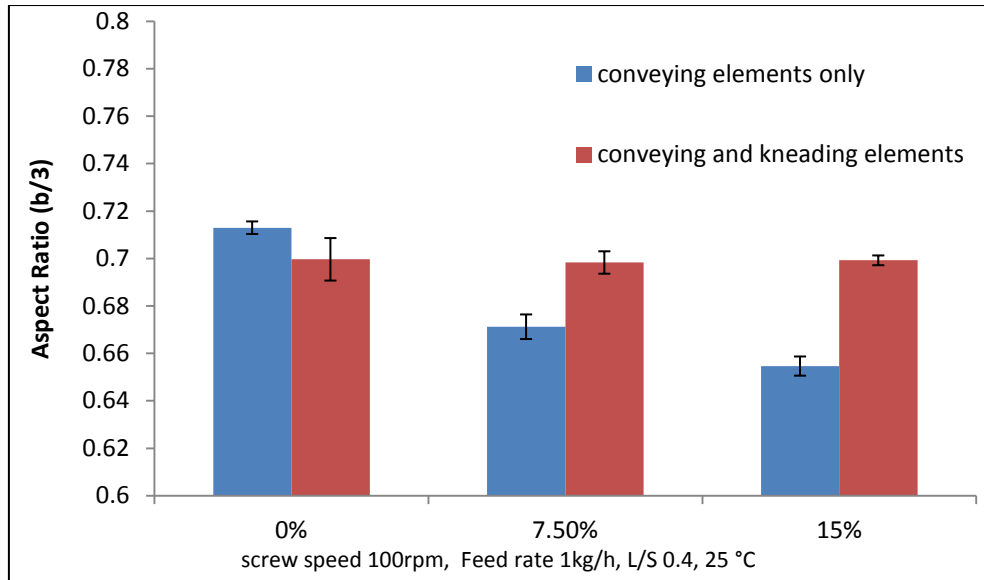


Figure 4-29 Effect of liquid binder viscosity on the aspect ratio of lactose granules as the stress varied.



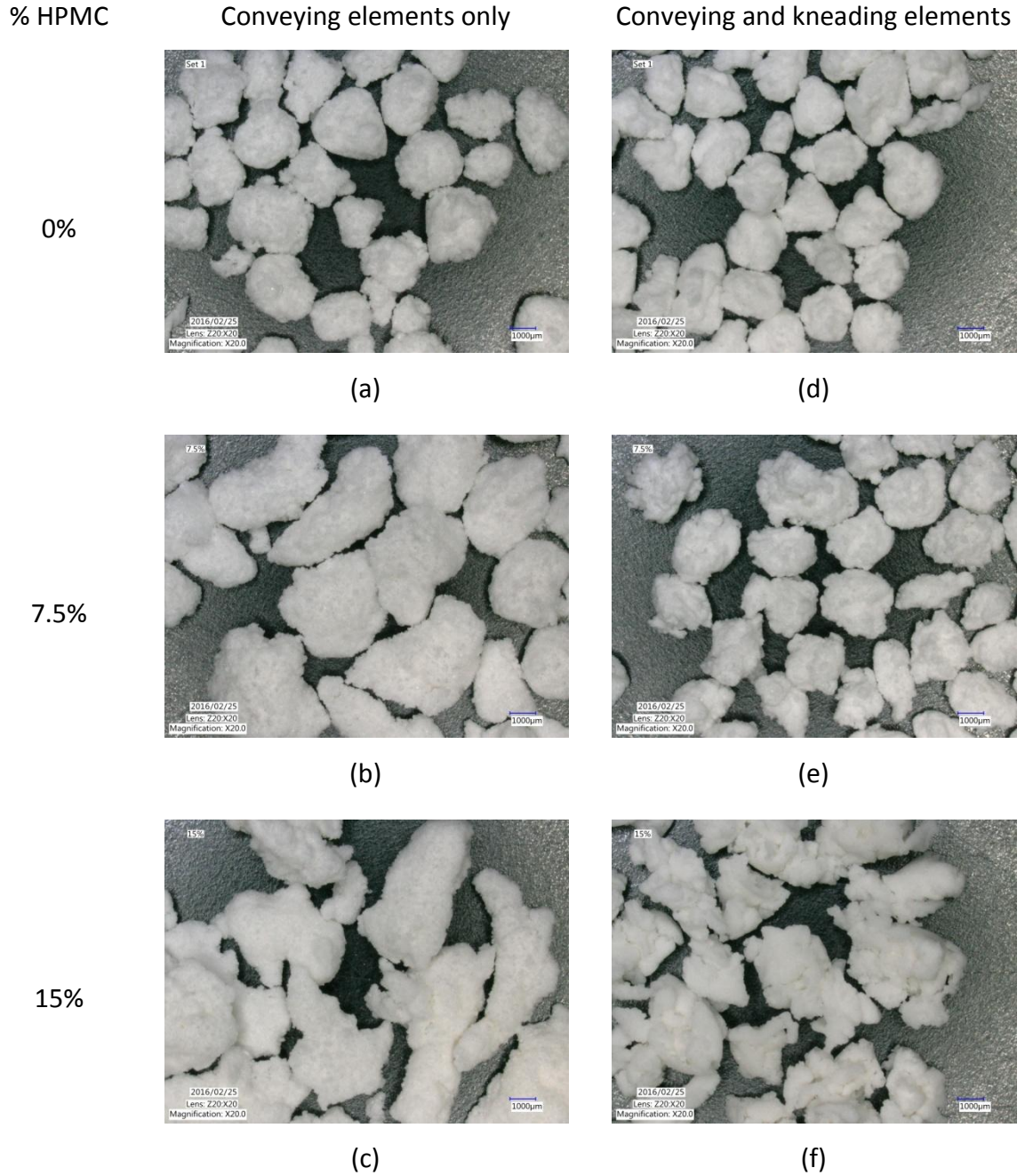


Figure 4-30 Effect liquid binder viscosity on the shape of lactose granules as the stress varied.

As seen previously for lactose and MCC; the increase in elongation with an increase in HPMC amount indicated that the initial wet agglomerates formed in the liquid addition port had some elongation or stretching during granulation along the screw.

**Surface topography**

Figure 4-31 shows the surface topography of the granules ( $\geq 2000 \mu\text{m}$ ) at different binder viscosity as the shear stress changes. At low shear stress, the primary particles shows to undergone minimal change. This can be seen in Figure 4-31 (a & b). This was similar for the lactose and MCC.

The granule's surface showed to be more compacted and deformed as higher shear stress is applied on the material, which can be seen in Figure 4-31 (c & d). The higher viscosity showed to be more deformed, as the primary particle can no longer be distinguished. This could be due to the presence of thick layer of viscous binder.

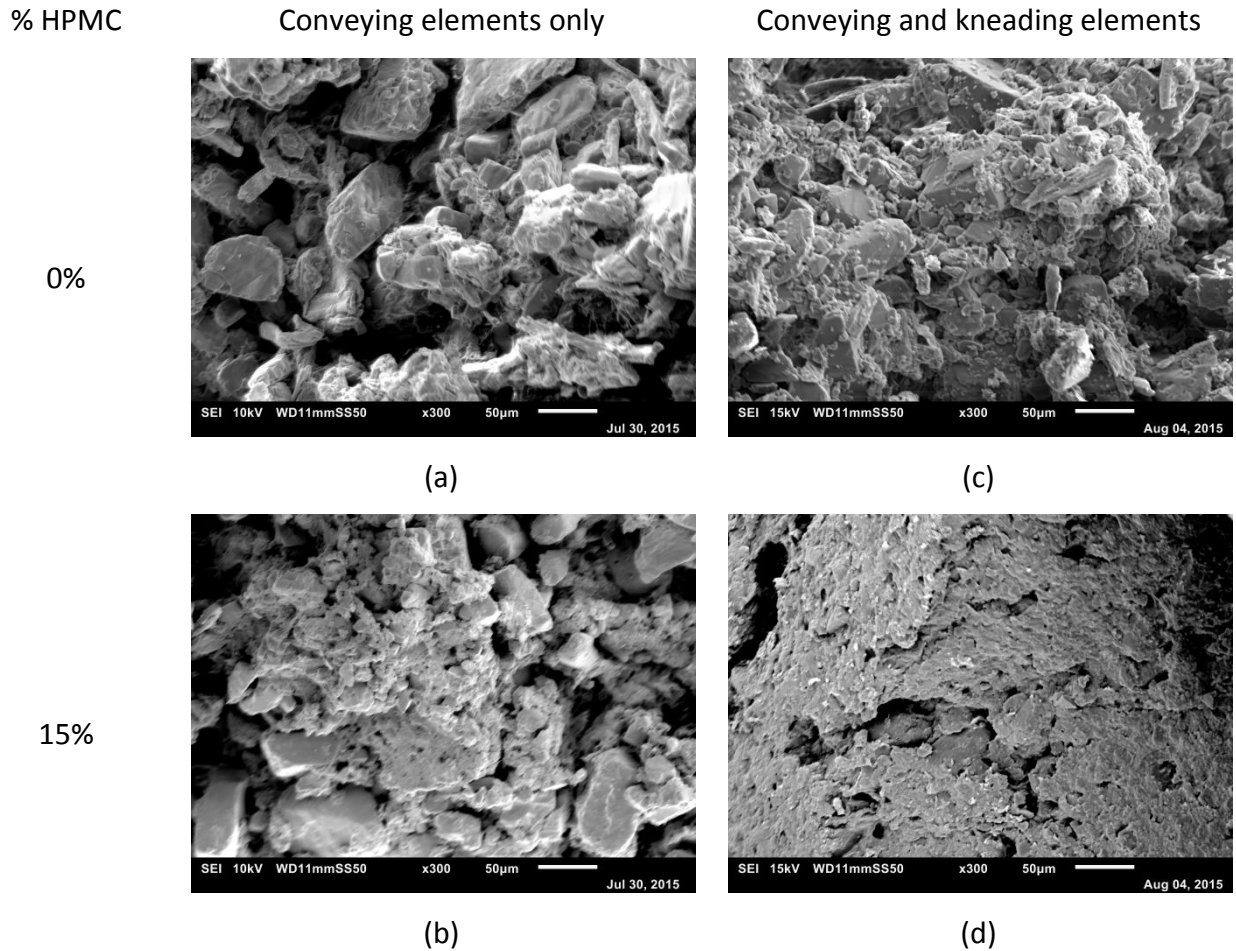


Figure 4-31 Effect of low (0%) and high (15%) liquid binder viscosity on surface topography of lactose granules, as the stress varied.

**Structural characterization**

Figure 4-32 shows the effect of increasing binder viscosity on the internal structure of the granules, produced at varying shear stress. The granules showed to be loosely packed, with considerable voids present within the structure, as the shear stress applied on the material was low. This can be seen in Figure 4-33 (a-c), where similar outcome was seen for the lactose and MCC.

The granules become more compacted and as a result lower porosity is present as higher shear stress was imparted on the material. This is also seen when comparing the images presented in Figure 4-33 (e & f). In addition, increasing the liquid binder viscosity resulted in a reduction of the porosity. This is due to presence of adsorbed HPMC on the surface of the particles, which allowed the particles to be held more closely reducing the air voids.

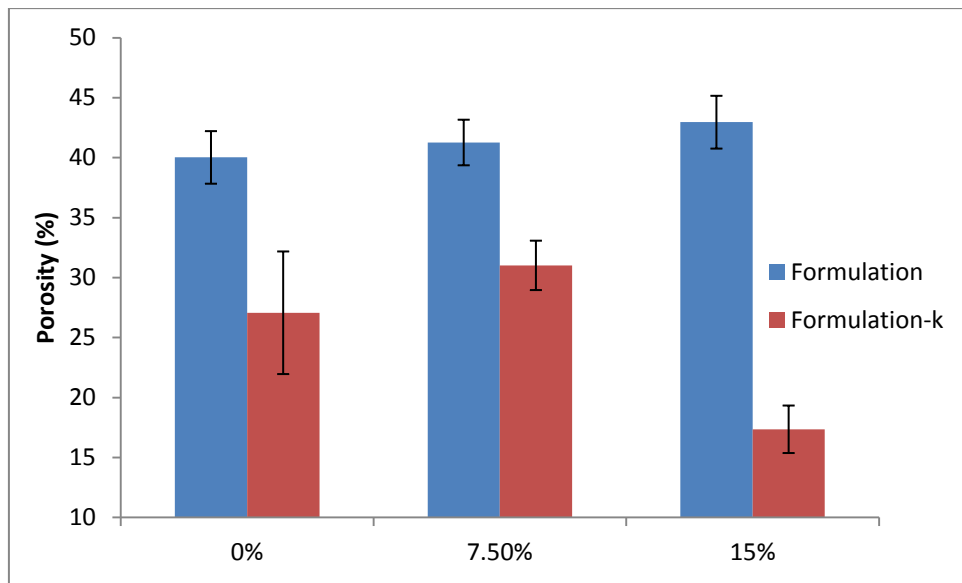


Figure 4-32 Effect of liquid binder viscosity on the porosity of formulation granules, as the stress varied.

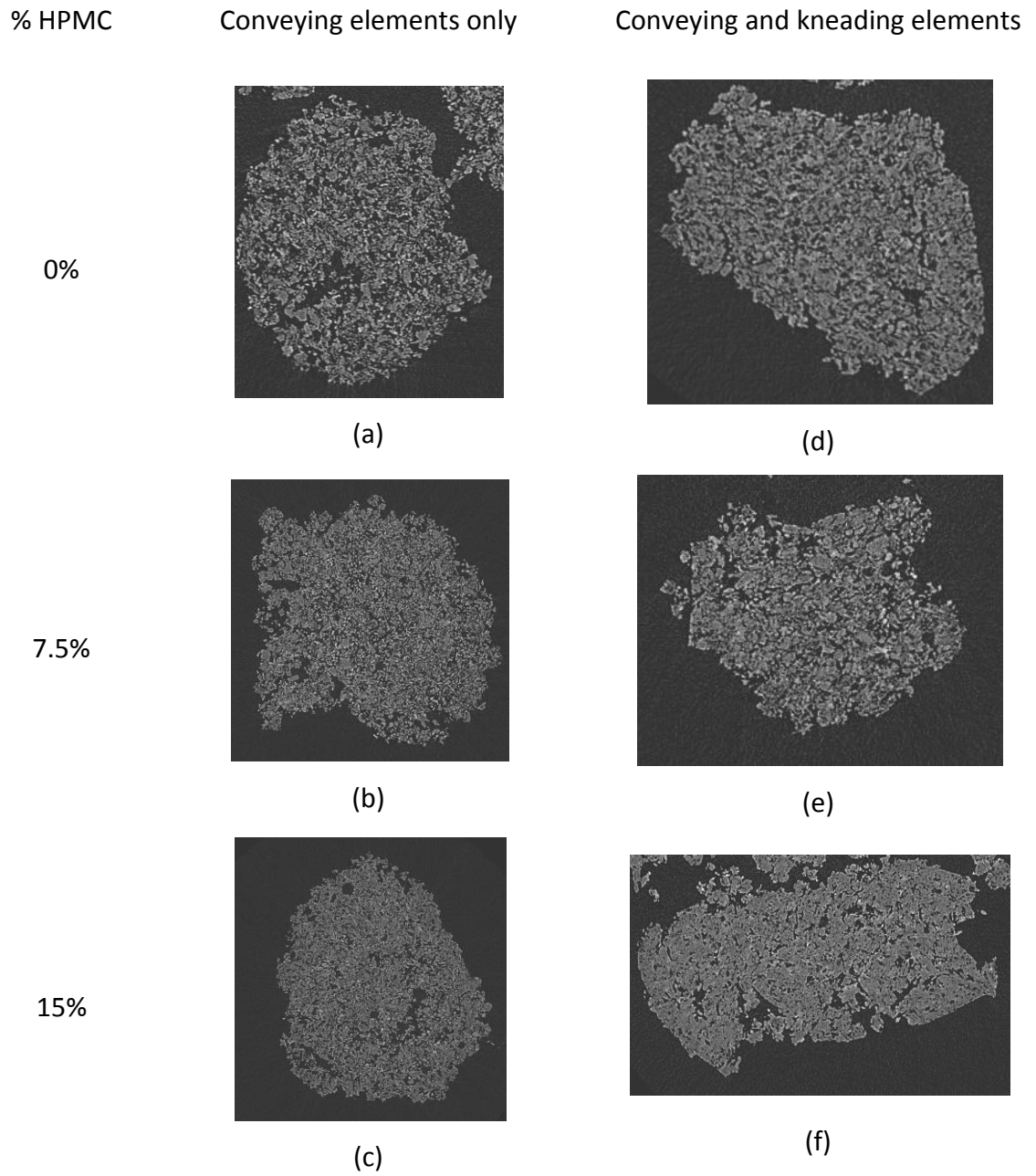


Figure 4-33 Shows X-ray of formulation granules produced as the liquid binder viscosity and the stress changed.

#### **4.4 Conclusion**

The change in the liquid binder viscosity showed to affect the granules properties differently depending on the shear stress applied and the material used. Generally, applying low shear stress (i.e. conveying elements only), the material properties showed to have limited effect on the outcome trends. As the granulation was depending largely on the ability of liquid binder to spread and penetrate. Generally, the size distribution tends to be broader as the binder viscosity increases. In addition, the granules attain a more elongated shape and the primary particles on the surface showed minimal change while giving loosely packed granules.

The influence of increasing the liquid binder viscosity on the granule properties, during high shear stress (i.e. use of kneading elements), showed to depend on the material. The size distribution showed to give higher growth for lactose, while a reduction for MCC and formulation. The granules shape tend to be more irregular for lactose, while more spherical for MCC and formulation as the liquid binder viscosity increased, though, the surface showed to be more rough due to coalescence. Furthermore, the primary particles showed to be more compacted and deformed, where the structure showed to be held more closely, regardless of the material used.

## **Chapter 5 Desired Granulation: Binder Delivery**

During this chapter, the effect of binder delivery upon the granule properties is investigated, whilst changing the shear stress applied on the material. For this study the formulation, as described in section 3.1.5, was used. The amount of solid binder (i.e. HPMC) was kept the same at all times, where only the form (i.e. solid and liquid) was varied. The HPMC binder was delivered in three different ways, namely; Set 1 (all solid binder incorporated with powder mixture where the liquid binder used is distilled water only), Set 2 (50% of solid binder mixed with powder mixture and 50% mixed with water), and Set 3 (all the solid binder dissolved in water). The droplet analysis was conducted on the three possible delivery of HPMC binder. The granules analysis, included the size distribution, granule shape, surface topography and structural characterization were also considered.

During a low stress, the form of the binder has largely affected the granule attributes. Introducing the HPMC in solid form (i.e. Set 1) had the narrowest size distribution, while producing more spherical shape and having a better liquid binder distribution, although, the surface topography and porosity showed to be insignificant as the binder delivery varied. The granule properties showed less sensitivity to the binder delivery during higher shear stress being imparted on the material. Imparting higher shear stress also showed to give a narrower size distribution and more spherical shape (in particular for the wet delivery of HPMC, i.e. Set 3), while showing a more deformed and compacted structure.

### **5.1 Introduction**

The pharmaceutical product and process development may vary from one industry to another. Such a variation may involve the form of the binder in which it is delivered during wet granulation. The binder delivery in the conventional wet granulation has been studied, e.g. in high shear granulator (HSG) and Fluidised bed granulator (FBG) [112-114]. Osborne et al [112] examined the effect of binder delivery using a 'wet' (dissolved in the granulation liquid) and 'dry' (incorporated within the powder) during high shear

granulation (HSG) and Fluidised bed granulation (FBG). They found that the binder delivery brought an effect on the granule properties, regardless of the granulator used. In HSG the dry binder addition method generated slightly larger granule size than wet binder addition method. However, in FBG the wet binder addition method generated significantly larger granules than the dry binder addition method. In FBG the granulation liquid is introduced as droplets, where the size of the droplet in the case of the wet binder addition was assumed to be bigger as the viscosity of the droplet was higher than in the case of the dry binder addition method (water). And as it was explained by Hapgood, Litster [27], in the case of high viscosity granulation liquid the growth of the nuclei is more likely to increase by coalescence mechanisms. The difference in observation between the two granulators might be due to the difference in mixing ability between the powder and liquid binder [112].

Despite the studies of the binder delivery in other granulation techniques, its effect during continuous twin screw wet granulation has received limited attention. El Hagrasy, et al. [1] was the first and only group to consider the binder delivery within the twin screw granulation. They studied the influence of different ways of binder addition into the granulator on the size distribution. They added the solid binder as 'dry' (blended with powder mixture), 'wet' (dissolved in a solution with distilled water) and in both phases in ratio of 50:50. In the study they used the GSK formulation, while varying the grade of lactose within the formulation (three different grades). It was suggested that the binder delivery did not show a significant effect on the size distribution using three different grade of lactose as seen in Figure 5-1. In the three figures (A, B and C), representing the three different grades, the three trends were similar for the three binder addition methods.

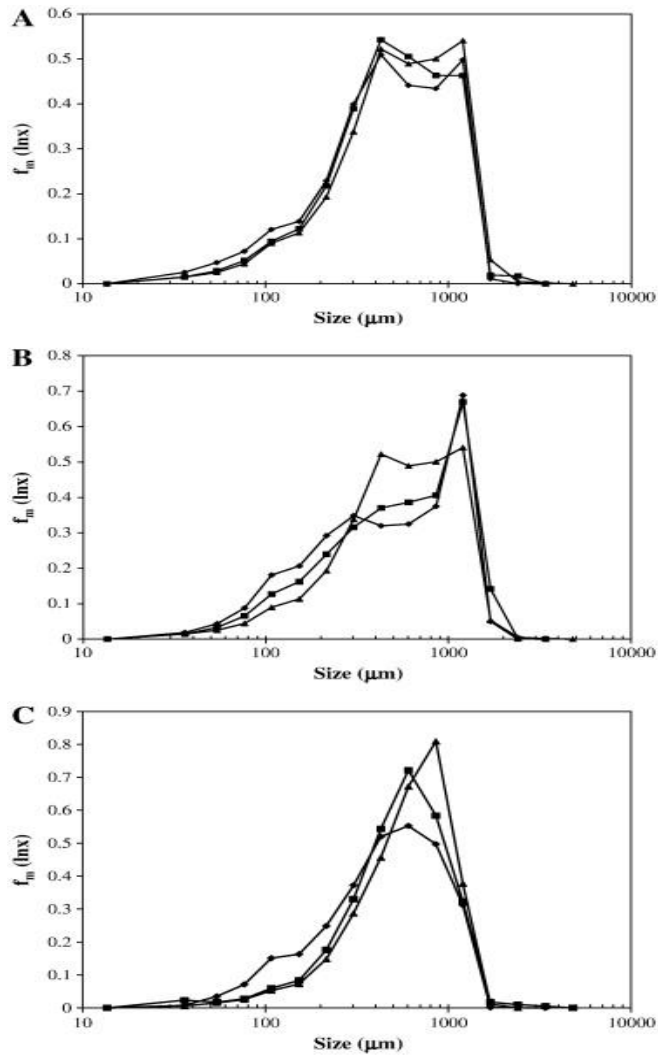


Figure 5-1 The change in granule size distribution for formulations containing pharmatose 200 M (A), impalpable (B), and supertab 30GR (C) as the lactose grade using dry binder ( $\blacklozenge$ ), 1:1 liquid:dry binder ( $\blacksquare$ ) and liquid binder ( $\blacktriangle$ ) at  $L/S = 0.3$  [78].

Although, such a parameter showed to influence granule properties using different granulators, the study within the twin screw granulator was carried out at very higher shear stress (two zones of four kneading elements, high screw speed and feed rate). They neglected the effect of binder delivery may have on the other granule attributes. The study also failed to give more insight/explanation to why no significant effect was seen.



Therefore, in this chapter a more detailed study was conducted to investigate the effect of binder delivery within the TSG, using the GSK formulation. This included online monitoring of the binder distribution along the barrel length using a specially built transparent barrel. This is aimed to further the understanding of the effect of binder delivery and gain a greater insight of the process taken place inside the granulator. The effect of the binder delivery as the shear stress varied was also considered. Furthermore, the effect of binder delivery on the granule properties (size distribution, shape, topography and structural characterization) and droplet analysis were considered. The HPMC binder was delivered in three ways (Set 1(dry), Set 2 (1:1) and Set 3 (wet)).

## 5.2 Experimental and analysis methodology

### 5.2.1 Experimental plan

The effect of three ways of solid binder delivery on the granule properties (size, shape, surface topography and porosity) and binder distribution were investigated using the following approach;

**Set 1** - All solid binder is mixed with the powder mixture.

**Set 2** - 50% of the solid binder in powder mixture and 50% in the granulation liquid media (water)

**Set 3** - All solid binder in granulation liquid (water).

Formulations composition and process conditions used in the three sets are shown in Table 5-1.

Table 5-1 Formulation composition and process conditions used in three sets

Binder delivery	Powder (kg/h)	%Lactose	%MCC	%Crosscarmellose sodium	L/S ratio	%dry HPMC	%wet HPMC
Set 1	1	73.5	20	1.5	0.4	5	0
Set 2	1	75.43	20.53	1.54	0.4	2.5	6.25
Set 3	1	77.37	21.05	1.58	0.4	0	12.5

The granulation liquid viscosity can be found in Table 3-2. Furthermore, more work is presented in Appendix B, which takes into consideration the slight variation in material composition and amount of water in each set. The result showed that such variation was less significant in comparison to the form of binder on the size distribution.

### 5.2.2 Droplet studies and process and formulation parameters

The study of the droplet analysis and preparation of granules for the binder delivery was conducted as mentioned in section 4.2.1 & 4.2.2 (for the formulation), respectively.

### 5.2.3 Binder spreading in Twin Screw Granulator (TSG)

To monitor the liquid spreading within the granulator, the steel barrel was replaced with a transparent barrel. Within the transparent barrel, three sections were monitored as shown in Figure 5-2. The sections were named; 'Start section', 'Middle section' and 'End section'. Each section covered an area of three flights of the screw (16 mm).

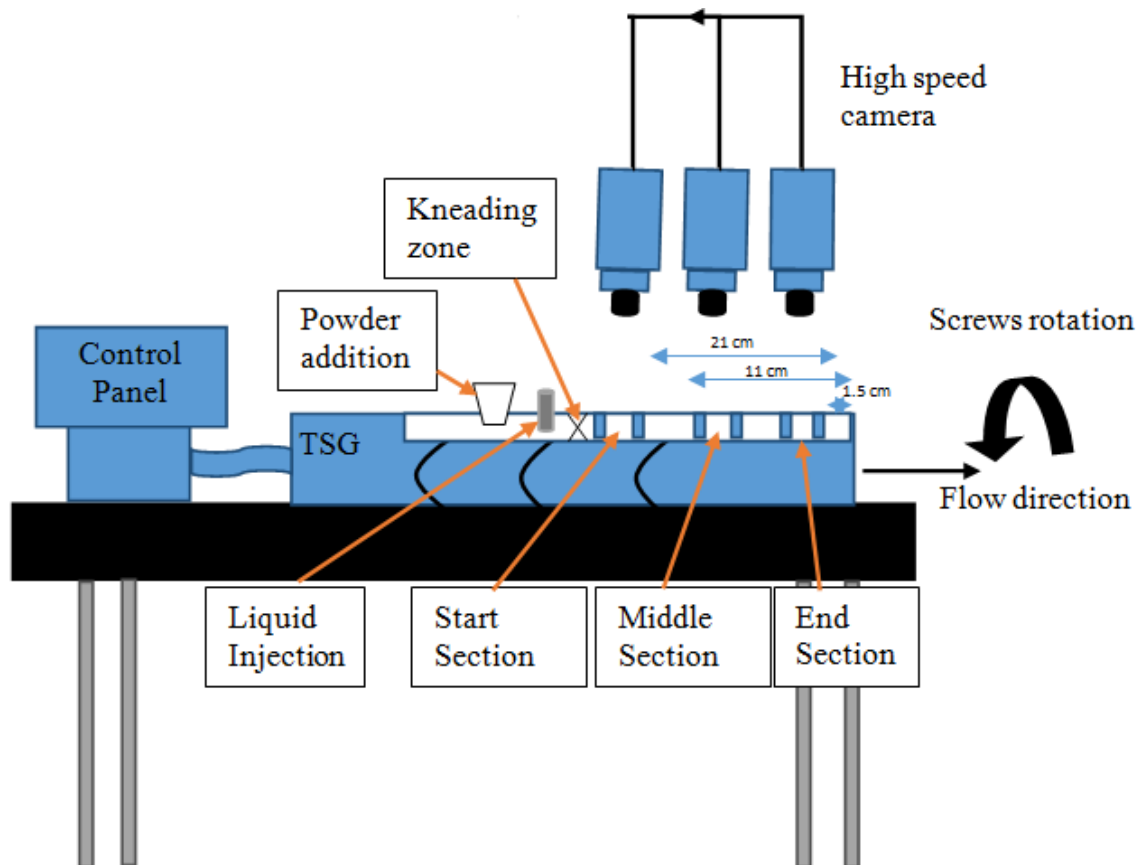


Figure 5-2 Illustration of the set-up to determine binder distribution over a moving bed.

The powder was firstly fed until it reached the end of the barrel. Then the liquid binder, which was coloured with the red dye (Erythrosine B), is added until it was visible on the surface of the moving powder. A high speed colour cameras (Photron Fastcam (1024 PCI, Itronx Imaging Technologies, Inc. Westlake Village, CA, US) and Dino-Lite digital microscopes (Premier, AM-4013, Taiwan) were used to capture the spreading of coloured liquid binder at frame rate of 60 fps. The video from each section was transferred into Image-J software for analysis. The images considered for this analysis were taken at two different times for each of the three sections. The time within this scope was referred to as 'spreading time' ( $T_s$ ). The  $T_s$  of 0 s was for the first image before the red colour comes into the field of view and after this, the images at  $T_s$  of 4.17 s and 8.33 s were considered. This was repeated a minimum of three times for each set.

#### **5.2.4 Granule analysis**

The granule analysis for size distribution, shape, surface topography and structural characterization; were performed as described in section 3.3.

### **5.3 Results and Discussion**

#### **5.3.1 Droplet analysis on static bed**

The liquid binder viscosity varied as the binder delivery changed. The liquid binder viscosity in Set 3 was the most viscous and in Set 1, it was the least viscous, i.e. distilled water only. To account for this change, firstly a replicate of each set was carried out on a static bed.

Table 5-2 shows the influence of binder delivery on the contact angle. As more HPMC is delivered in the liquid form, the observed contact angle showed to increase, i.e. in Set 2 & 3. This is due to the increase of liquid binder viscosity and hence resulted in a reduction in the maximum spread and increase penetration time as seen in Figure 5-3.

Table 5-2 Contact angle using the Wenzel approach ( $\theta_w$ ) on compressed bed at 500N.

Binder delivery	Binder viscosity (Pa.s)	contact angle
Set 1	0.001	66°
Set 2	0.022	69°
Set 3	0.228	76°

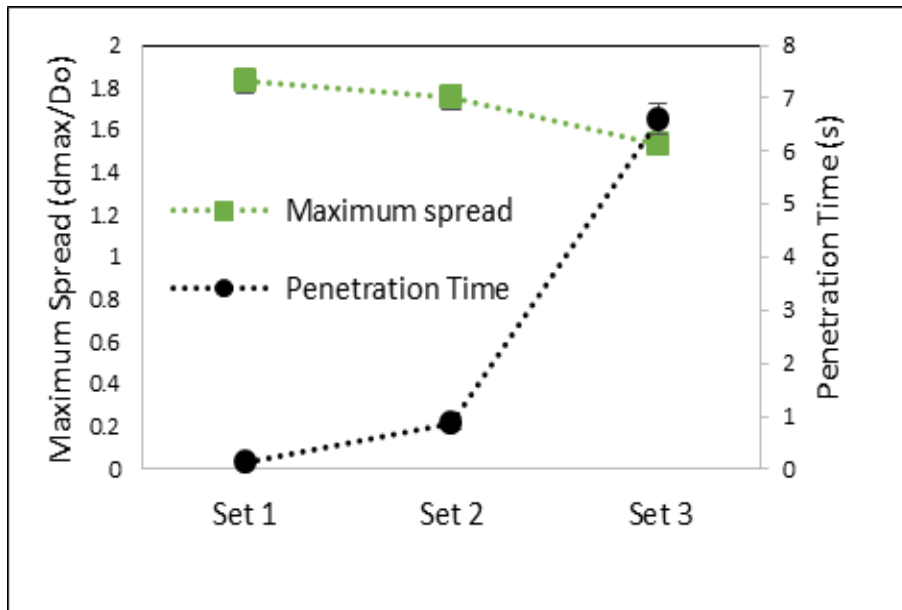


Figure 5-3 Effect of binder delivery on maximum spread and penetration time on a static bed.

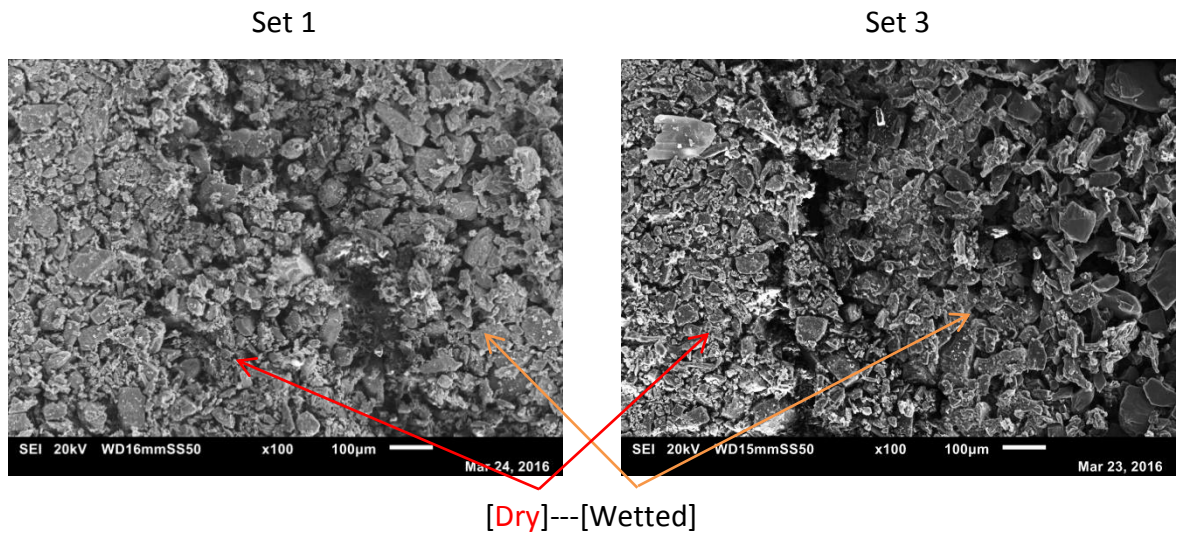


Figure 5-4 Shows surface topography for compressed bed from Set 1 and Set 3.

Figure 5-4 shows the boundaries on the compressed bed surface between the 'Dry' and wetted' regions for Set 1 and Set 3. The distinctive feature shown by the images that the dry section shows to be more compacted than the wetted region. This is may be due to the fact that the liquid was able to dissolve the smaller sized primary particles (i.e. lactose), which tends to fit between the voids. Furthermore, the compressed bed of Set 3 shows regions that are more compacted than that in Set 1. This could be a sign of the inability to fully penetrate through the compressed bed, and therefore dissolved solid binder within the granulation liquid tends to form a thin layer.

### **5.3.2 Liquid spreading on a moving bed**

During this section the spreading of liquid binder on a moving powder bed, was optically monitored (as described in 5.2.3). This was done to gain a qualitative understanding of how liquid binder and powder interact as the binder delivery changed.

Figure 5-5 shows the spreading of the liquid binder on a moving bed as the binder delivery changes at low shear stress. Due to the low shear stress, the liquid binder viscosity dominates as it relies on the ability of liquid binder to spread and wet more powder in order to form a 'nuclei'. Generally, regardless of the binder delivery; the liquid binder tends to spread more with time and along the screw (i.e. through 'start section' to 'end section'). However, delivering more HPMC in the wet form (e.g. Set 3) showed more uncolored powder (indicating less spreading of liquid binder), as shown in Figure 5-5 (g-i) & (p-r) when compared with their corresponding results of Set 1 (i.e. dry form of HPMC).

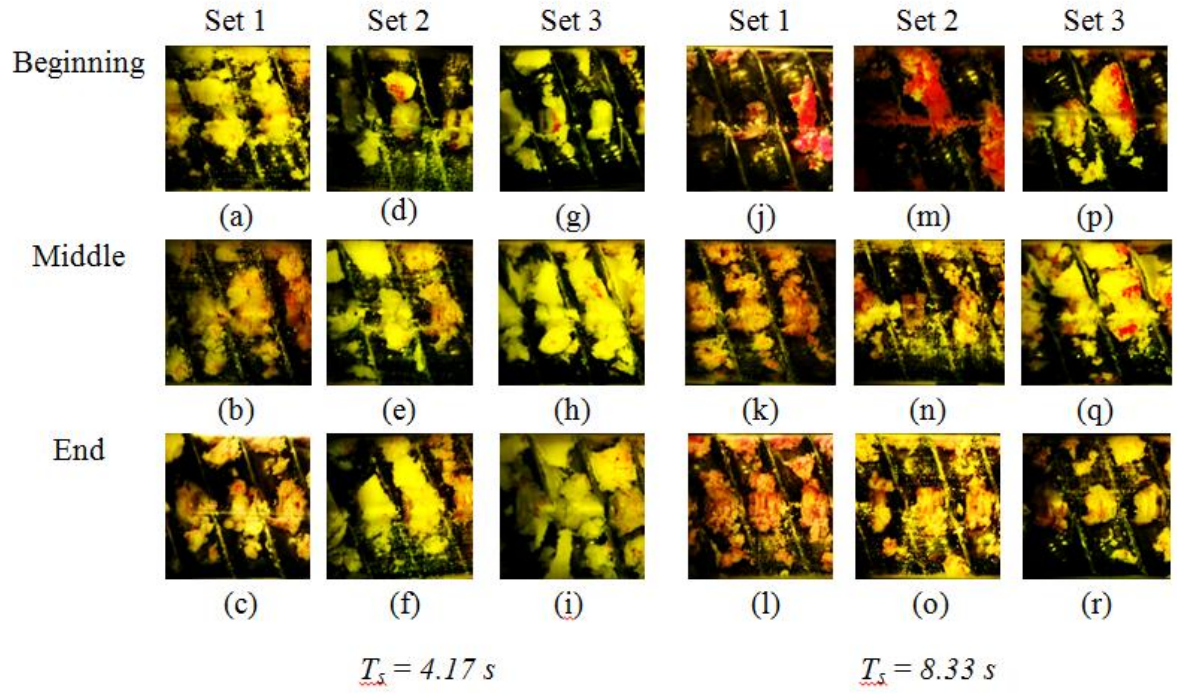


Figure 5-5 Images taken at  $T_s$  of 4.17s (left) and 8.33s (right) for the three sections of the barrel (Beginning, Middle and End) for each set at low shear stress.

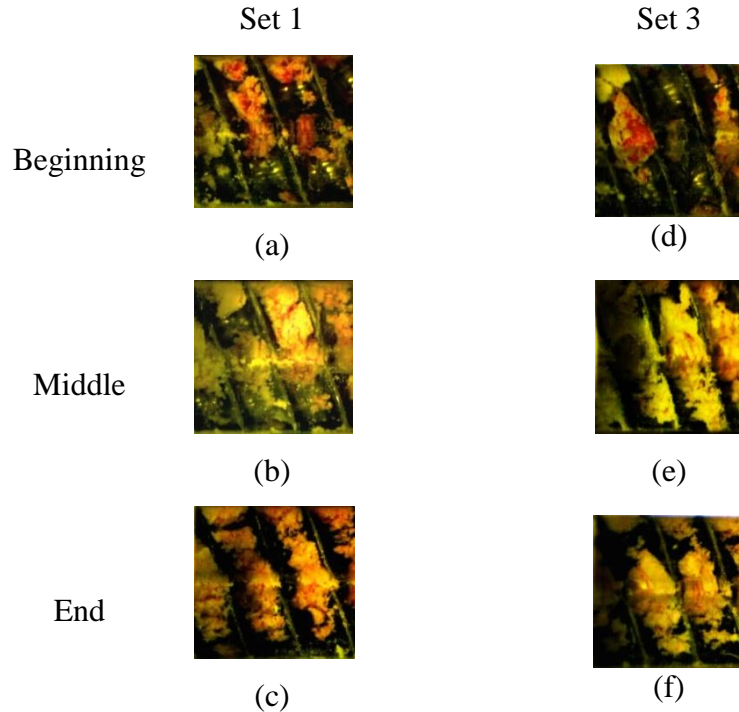


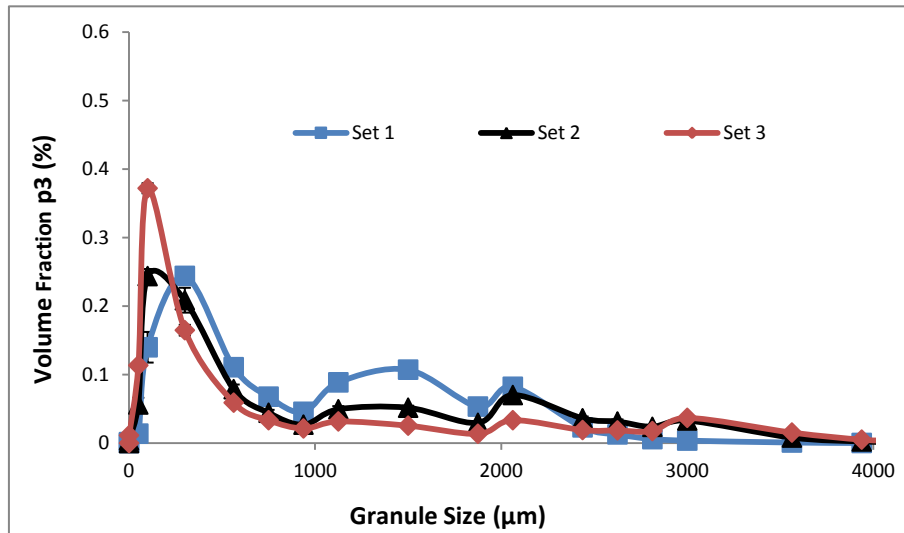
Figure 5-6 Images taken at  $T_s$  of 8.33s for the three sections of the barrel (Beginning, Middle and End) for two extreme sets (Set 1&3) at high shear stress.

Figure 5-6 shows the effect of binder delivery (for Set 1 & 3 only) on the liquid binder ability to spread and wet the material at higher shear stress. The mixing between the liquid binder and powder was more uniform for both Set 1 and Set 3 when compared with their corresponding results shown in Figure 5-5 ( $T_s$  8.33 s). This is due to the use of kneading elements zone which helps to hold the material (due to low conveyance ability) and h improves the mixing.

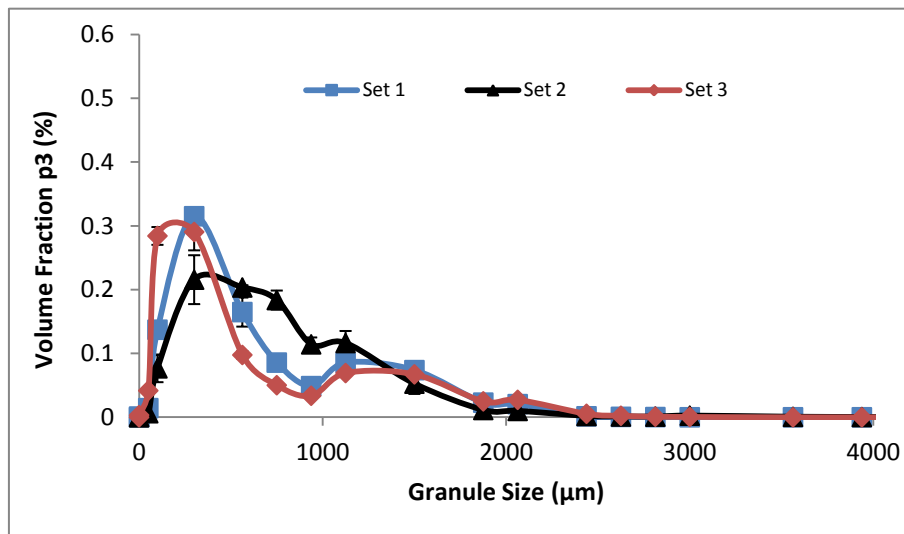
### 5.3.3 Size distribution

Figure 5-7 shows the effect of the binder delivery on the size distribution as the shear stress imparted on material varied. During a low stress, delivering the HPMC binder in the liquid form (i.e. Set 3) limited the spreading of liquid binder (localization) resulting in a wider range of size distribution, as shown Figure 5-7 (a) (also shown by the span illustrated in Figure 5-8). Increasing the shear stress, helped to distribute the liquid binder (regardless of viscosity) and, resulted in minimal difference in size distribution as the binder delivery

varied, as shown in Figure 5-7 (b). The difference within the span showed to flatten out as seen in Figure 5-8. The trends shown are similar to those found in Figure 4-27, where the formulation was kept the same while increasing the HPMC in the liquid binder. This indicates that the liquid binder ability to spread is more dominant than the form of the HPMC binder on the size distribution.



(a)



(b)

Screw speed 100 rpm, Feed rate 1kg/h, L/S 0.4, 25 °C

Figure 5-7 Effect of binder delivery on size distribution: (a) low stress, (b) high stress.



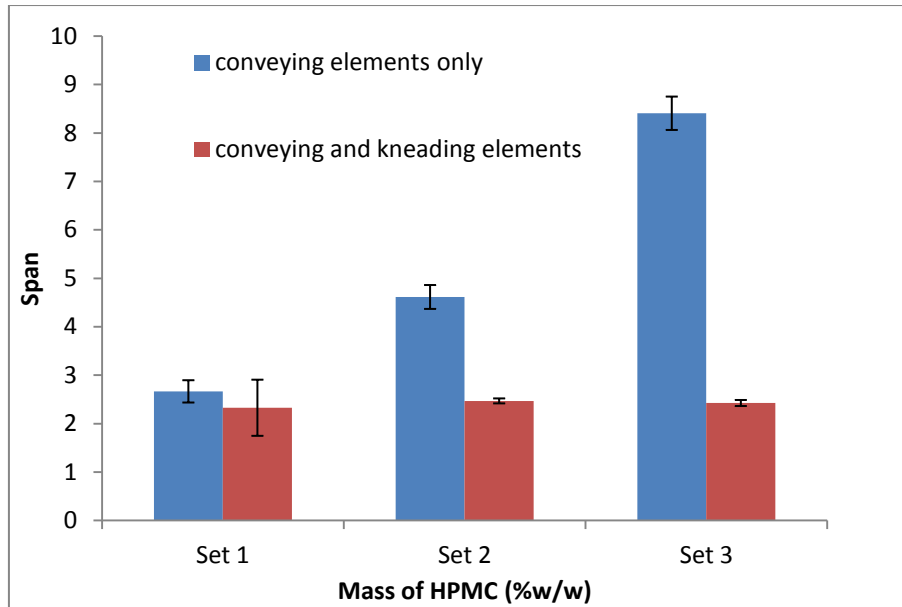


Figure 5-8 shows the span of size distribution as the binder delivery changed during low and high. shear stress

### 5.3.4 Granular shape

Figure 5-9 shows the influence of binder delivery on the aspect ratio of the granules ( $\geq 2000 \mu\text{m}$ ) as shear stresses imparted on the material varied. During low stress, the particles are loosely compacted and as more HPMC is delivered in the wet form, (e.g. Set 3), due to localization of the liquid binder resulting in the formation of the big granules. This resulted in the big granules being trapped and hence attaining a more elongated shapes as shown in Figure 5-10 (b & c).

Increasing the shear stress, showed to give a higher aspect ratio as more HPMC delivered in the wet form (i.e. Set 3) while showing insignificant difference for dry delivery of HPMC binder (i.e. Set 1). Introducing kneading zone to impart higher stress showed to give a reduction in big granules for Set 3, as shown Figure 5-7. This may have caused the crumbing of big granules into smaller where they coalesce together as they roll in the channel of the conveying elements resulting in more rounding as they leave the kneading zone, resulting in a more spherical shape (shown in Figure 5-10 (f)).

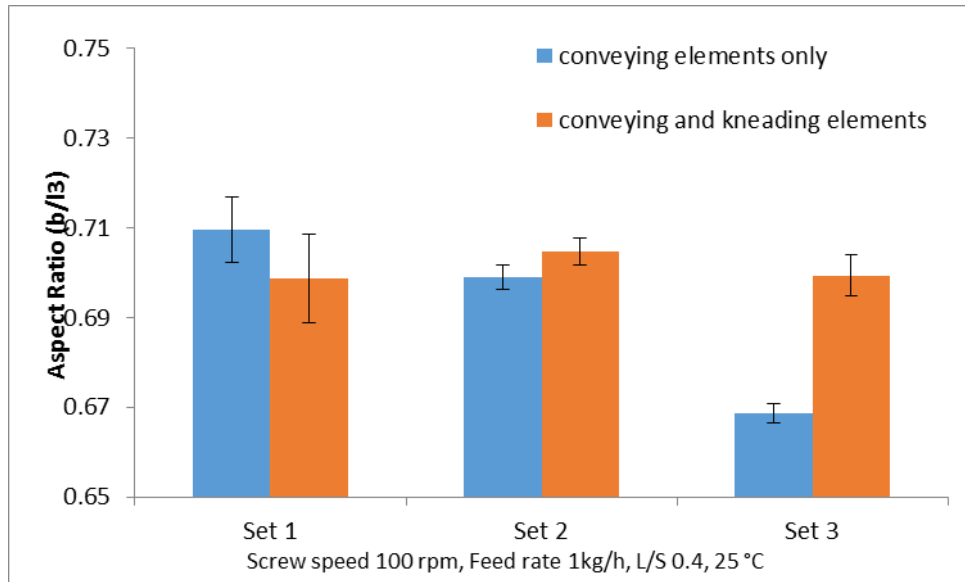


Figure 5-9 Effect of binder delivery on the aspect ratio as stress varied.

Binder  
delivery

Conveying elements only

Conveying and kneading elements

Set 1



(a)



(d)

Set 2



(b)



(e)

Set 3



(c)



(f)

Figure 5-10 Effect of binder delivery on granules' shape ( $\geq 2000\mu\text{m}$ ) as stress changed.

### 5.3.5 Surface topography

Figure 5-11 shows the surface topography of the granules ( $\geq 2000\mu\text{m}$ ) as the binder delivery and shear stress changed. At low shear stress, the primary particles shows to

remain unaffected. This can be seen in Figure 5-11 (a-c). Increasing the shear stress however show to produce granule's surface which is more compacted and deformed, as in Figure 5-11 (d-f). The delivering the HPMC in wet form (i.e. Set 3) showed to be more deformed, as the primary particle can no longer be distinguished. This could be due to the presence of layer of viscous binder. Generally the findings of binder delivery show similar for that of the formulation as liquid binder viscosity increased (i.e. more HPMC) shown in Figure 4-31.

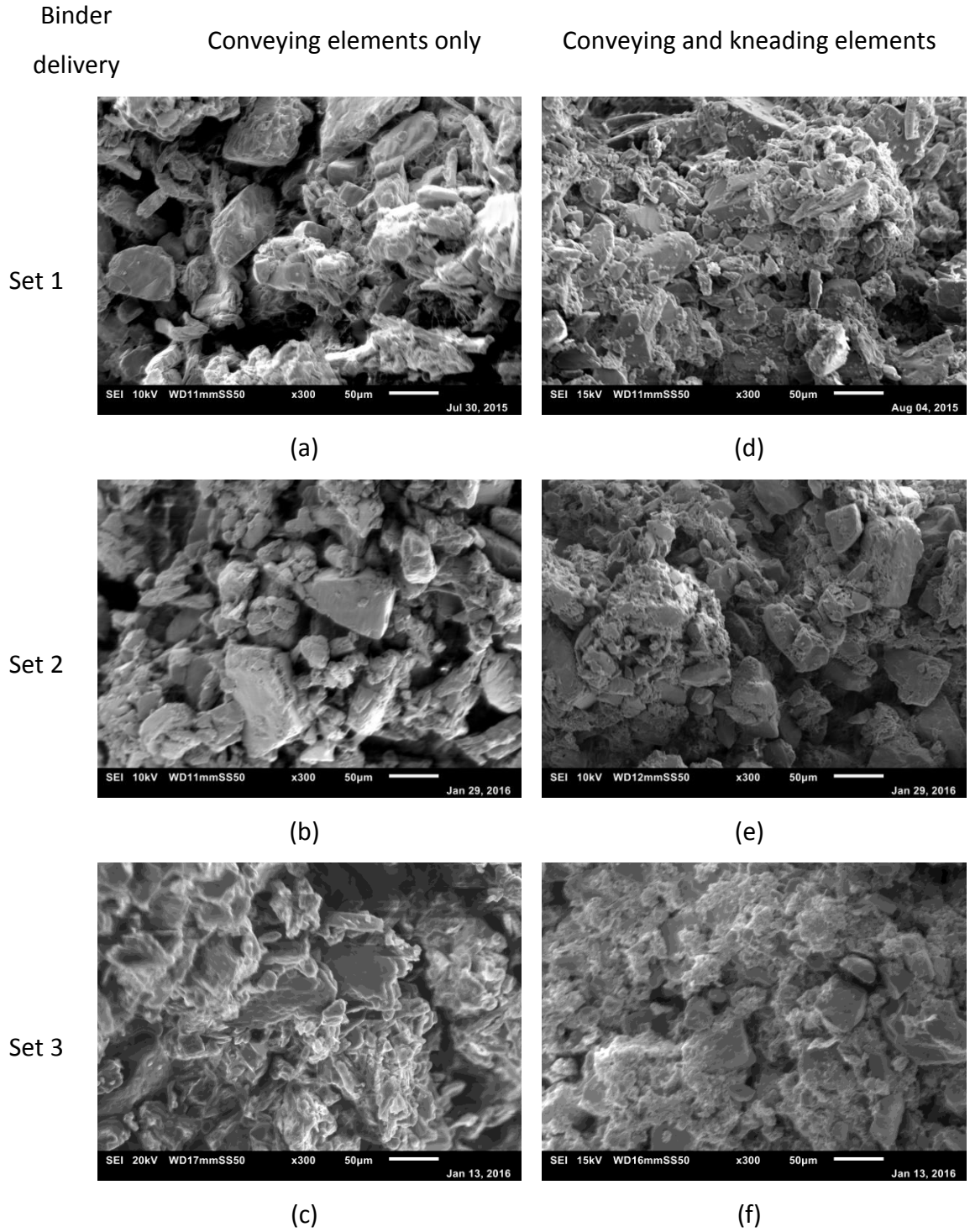


Figure 5-11 Effect of binder delivery on granular surface tomography, as the stress varied.

### 5.3.6 Structural characterization

Figure 5-12 shows the effect of binder delivery on the internal structure of the granules produced at varying shear stress. The granules showed to be loosely packed, with considerable voids present within the structure while imparting low shear stress on the material, as shown in Figure 5-13 (a-c). Regardless of binder delivery, increasing the shear stress resulted in the granules becomes more compacted and as a result lower porosity is present. This is also seen when comparing the images presented in Figure 5-13 (e-f).

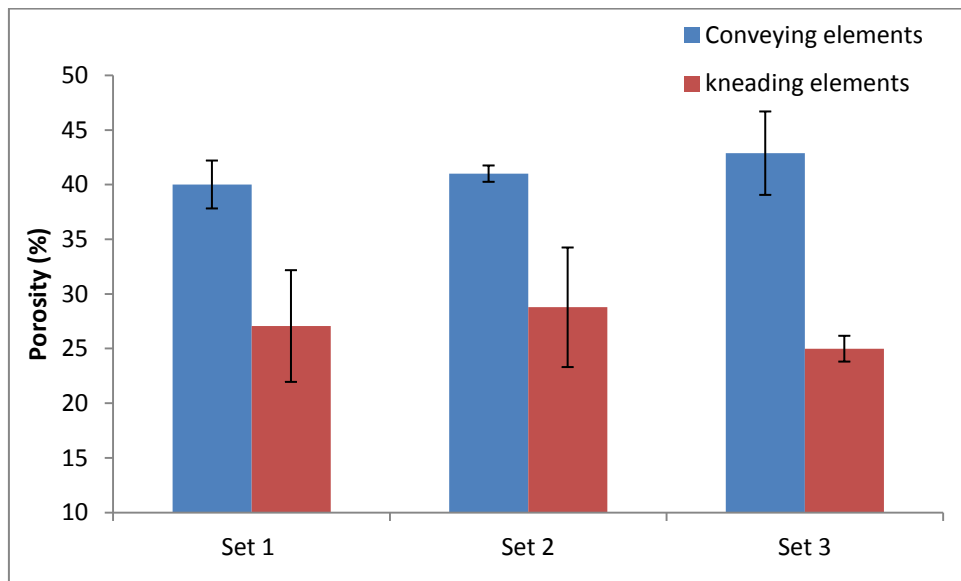


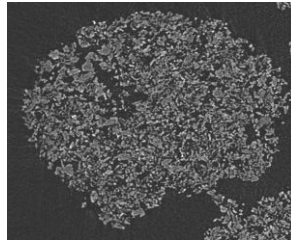
Figure 5-12 Effect of binder delivery on the porosity of granules, as the stress varied.

Binder delivery

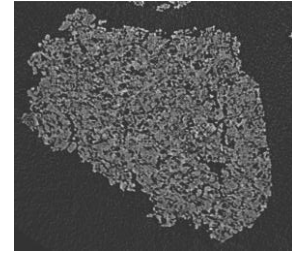
Conveying elements only

Conveying and kneading elements

Set 1

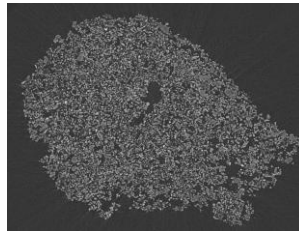


(a)

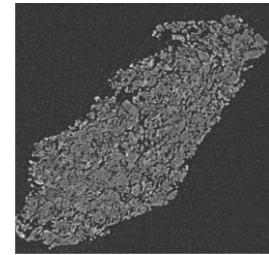


(d)

Set 2

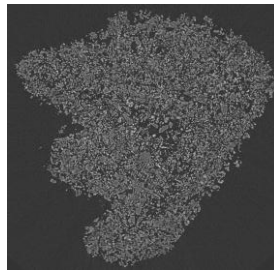


(b)

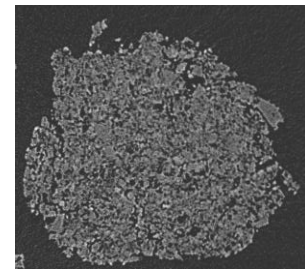


(e)

Set 3



(c)



(f)

Figure 5-13 Shows X-ray of granules produced while varying the binder delivery and the stress.

## 5.4 Conclusion

The binder delivery showed to have significant influence on the liquid binder and powder mixing uniformity during a low shear stress system. This in turn affected the granules properties. Although, the surface topography and structural characterization showed to be insignificant to the binder delivery, delivering the HPMC in the wet form (i.e. Set 3) resulted in a wider range of size distribution and more elongated granules shapes.

Increasing the shear stress, has improved the liquid binder and powder mixing uniformity, as result the effect of binder delivery on the granule properties was minimal. Furthermore, the granules showed a narrower size distribution while more spherical shape, in particular when delivering the HPMC in wet form (i.e. Set 3). The surface topography and granular's porosity showed to be more compacted and less air voids regardless of the binder deliver.

Finally, the findings for binder delivery and formulation (in Chapter 4) showed a degree of similarity. This indicating the liquid binder ability to spread is more dominant on the granules properties rather than binder delivery or the amount of HPMC.



## **Chapter 6 Undesired Granulation: Powder Caking/Sticking**

This chapter considers the undesired granulation as the liquid binder and shear stress imparted on the material varies. The behavior of powder caking onto the upper barrel was optically monitored, while recording the mass. The collected sample of powder caking (which is referred to as a ribbon) is analysed for the surface topography and structural characterization. The barrel of the granulator was interchanged between the steel and transparent barrel. The process and formulation parameters used within this chapter were same as that in Chapter 4 and Chapter 5 (i.e. for lactose, MCC, formulation and binder delivery). Further study, using mixture of powder (90% w/w of lactose and 10% w/w of salt) at higher shear stress while using low liquid binder viscosity (i.e. distilled water), was conducted to determine the uniformity of mixture within the ribbons using conductivity measurement.

At low shear stress, the behavior of powder caking showed to change as the liquid binder viscosity increases, regardless of the material used, where the mass of powder caking to the barrel showed to reduce. Although, generally the primary particles within the ribbons showed to remain unaffected and loosely packed, in exception for MCC as it showed plastic deformation under low shear stress. Increasing the shear stress, resulted in more consistent powder caking behavior in terms of location in which the powder started to cake, regardless of powder or liquid binder viscosity. The tendency of powder adhering on the surface was dependent on both powder property and liquid binder viscosity changed. The surface topography and internal structure showed to be more deformed and compacted, regardless of the material and liquid binder viscosity used. The conductivity of salt within the ribbon showed to decrease with time as lactose tends to cake more than salt.

### **6.1 Introduction**

The development of powder caking during processing, transportation and storage, may vary with a change in powder, material composition, particle size, particle shape, moisture

content, pressure, and variation in temperature and humidity. Such dependence on large number of factors indicates the difficulty in defining the mechanisms of powder caking in a given powder system [39-41]. Generally, different inter-particle forces can give rise to the powder caking, such as Van der Waals forces in the case of dry caking, capillary and viscous forces for wet caking, material bridge formation for solid caking and more occasionally, electrostatic, magnetic or interlocking forces are also involved [115]. The dominance of one inter-particle force in a given system, will depend on various factors. For example the size of the particle will give rise to different type of inter-particle forces, as shown in Figure 6-1, where Van der Waals will be significant as the primary particles get smaller. For the case of capillary forces; there is a necessity of liquid to be mobile and present, unlike the Van der Waals forces, to form the liquid bridges.

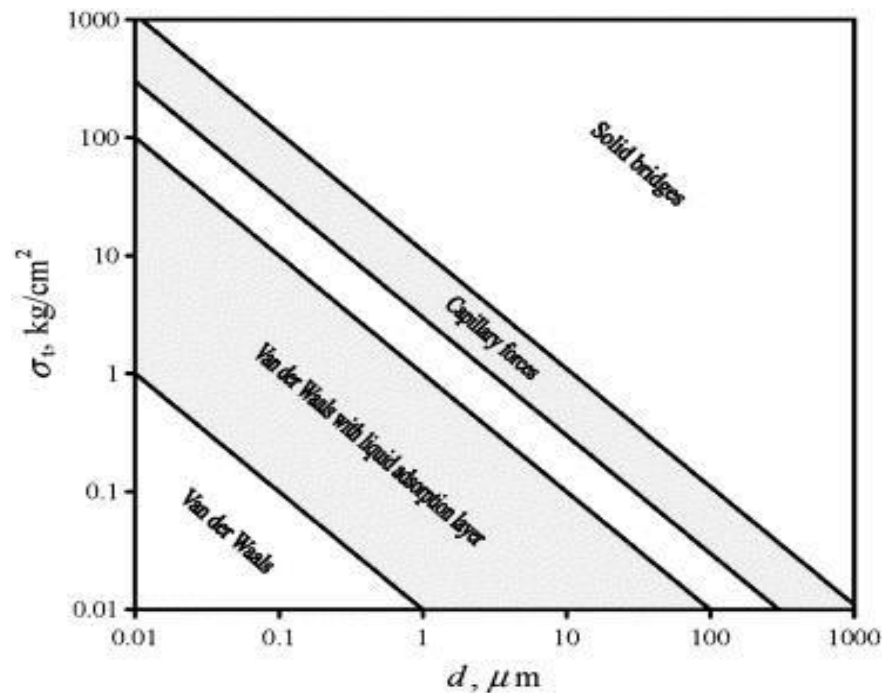


Figure 6-1 Magnitude of the inter-particle forces as the primary particle size changes [116].

Although, currently there is limited studies concerning the powder caking within a granulation process equipment, it has been observed within various granulation equipment as the process and formulation variables changed [117-122]. Briens and Logan [118] observed accumulation of powder caking as the change of centrifugal forces with a

change in the impeller speed. This limited the function of the chopper as the layer powder caking grew around the chopper, and resulting in a change of the pattern flow of the material within the bowl of the high shear mixer. Smith and Nienow [121] found that the position in which the liquid binder is atomized, in a fluidized bed granulator, relative to the powder bed is major factor on encouraging powder caking. Powder caking has shown proneness in dry granulation as Hamdan, Reklaitis [122] exploited this phenomena in roller compaction as the oscillation in the roller's gap varied. They concluded such an occurrence of undesired problem would influence the integrity of the product and continuity of the process. However, as the twin screw granulator remains relatively new equipment within the pharmaceutical field and hence such an issue has yet to be addressed and investigating the effect of the process and formulation variables on powder caking.

Therefore, within this chapter, the study endeavors to explore the effects of liquid binder viscosity at varying shear stress on the powder caking. This will involve the process and formulation variables used in Chapter 4 and Chapter 5 (i.e. using lactose, MCC, formulation and binder delivery). The study will be split into three different parts, explained as follow:

Part 1: This part of the study will focus on optically monitoring the behavior of powder caking on the upper part of the barrel. In order to do that, in-house made acrylic transparent barrel was used. The mass of powder caking was also recorded.

Part 2: This part of the study will focus on characterizing the ribbon of powder caking to the steel barrel. The two extreme conditions for each material used in Part 1 were considered for the study. The ribbon of powder caked was analyzed for powder behavior, surface tomography and structure characterization.

Part 3: This part of the study will focus on investigating the powder caking phenomena using a blend of lactose and salt. The blend will be granulated at high shear stress with low liquid binder viscosity (i.e. distilled water). The size distribution and mass of powder caking was considered with time as well as the salt content within the granules.

## 6.2 Experimental and analysis methodology

### 6.2.1 Process and formulation parameters

The process and formulation variables were kept the same as that presented in Chapter 4 and Chapter 5. This allows the investigation on how liquid binder viscosity at varying shear stress effects the desired as well as the undesired granulation. For the optical monitoring of powder caking behaviour (i.e. Part 1), the number of liquid binder viscosity studied between 0-15%w/w of PHMC is increased to five different viscosity (instead of three only which was done for the previous chapters). The liquid binder viscosity values are presented in Table 3-2.

### 6.2.2 Caking on Transparent Barrel

The default stainless steel barrel was removed and replaced with a transparent barrel to allow for powder caking to be optically monitored. The length of the barrel was split into two sections, which were labelled, 'Start section' and 'End section', as shown in Figure 6-2. Two Dino-Lite digital microscopes (Premier, AM-4013, Taiwan) were positioned perpendicularly above the barrel.

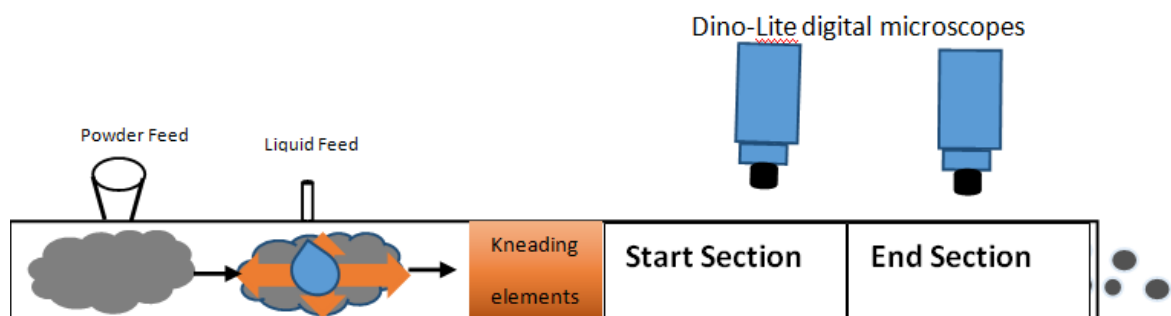


Figure 6-2 Illustration an overhead view of the transparent barrel. The kneading zone is the location where the kneading elements will fit in the case of high shear stress.

The powder was fed and the liquid binder was injected 5 s later. This was done to minimize the liquid binder wetting of the barrel surface without powder. The cameras started recording upon the granules production, at speed of 0.5 frame/second for duration of 6 minutes. For each run, three images are presented for the beginning and end sections. The images considered for this work were extracted at 2 minutes, 4 minutes and 6 minutes.

After 6 minutes, the amount of powder caked to the upper surface of the barrel was removed carefully and accounted for its mass (g). Each run was repeated minimum of five times. The size distribution of granules, produced using transparent barrel, is presented in Appendix C.

### **6.2.3 Caking on Stainless Steel barrel**

The steel barrel is used for this study, where the lowest and highest liquid binder viscosity for each material (used in transparent barrel) at varying shear stress were considered. After 6 minutes of granule production, the system was stopped and an images of the upper barrel was taken. The powder cakes were carefully removed to obtain undamaged ribbon (an image shown in Figure 6-3) while measuring its mass. The ribbons were also analyzed for surface topography and structure characterization as described in section 3.3.5 and 3.3.6, respectively. Each run was repeated minimum of 5 times.

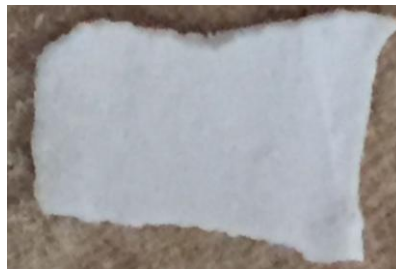


Figure 6-3 Imaged of undamaged ribbon of powder caking.

### **6.2.4 Conductivity**

The experimental condition is illustrated in Table 6-1, where the blend was mixed in according to section 3.2.3. Prior to blending the salt was milled using a Ballmill to produce fine particles (<250  $\mu\text{m}$ ). The reduction of size was necessary to reduce the disparity of

raw materials when mixed with the powder mixture. For the study of conductivity, three sample locations were considered, as illustrated in Figure 6-4. The sample collected from the blender (i.e. high shear granulator, 1<sup>st</sup> point) was selected from various regions of the granulator to obtain 2g. This was assumed to be the baseline of the conductivity; which is expected to be produced from the feeding hopper (2<sup>nd</sup> point). The 3<sup>rd</sup> point was the powder caking on the upper surface of the barrel.

Table 6-1 Experiment conditions for the conductivity of ribbon adhered to steel surface.

Starting material	Granulation liquid	Operation conditions	Screw configuration
Lactose (90%w/w) and salt (10%w/w)	Distilled water only	Screw speed: 100rpm Feed rate: 1kg/h L/S ratio: 0.14 Barrel Temp: 25°C	Conveying and kneading elements (as shown in Figure 3-4b), i.e. high shear stress

To consider the change in uniformity with time, the conductivity of the salt within the sample collected (for 2<sup>nd</sup> and 3<sup>rd</sup> points) was taken at 6 different times; after the system reached equilibrium. The time considered in this section was at 2, 4, 6, 15 and 20 minutes, i.e the granulator will be stopped after 2 minutes to collect the sample and then start again for 4 minutes and so on. Each given time was repeated minimum of three times. The calibration of the conductivity was also determined, by dissolving a known amount of salt in a fixed volume of distilled water. The calibration curve can be seen in Figure 6-5.

The samples were dissolved in 50 ml of distilled water, where the conductivity was measured using Jenway (provided by Bibby Scientific). The probe of the conductor was removed cleaned and placed in a distilled water to record the starting conductivity before each reading of the actual sample is taken. Although, the conductivity showed slight variance for the baseline, the average is considered as the baseline (where the error bar is not presented in the line). The samples collected from 2<sup>nd</sup> and 3<sup>rd</sup> points were plotted against the baseline.

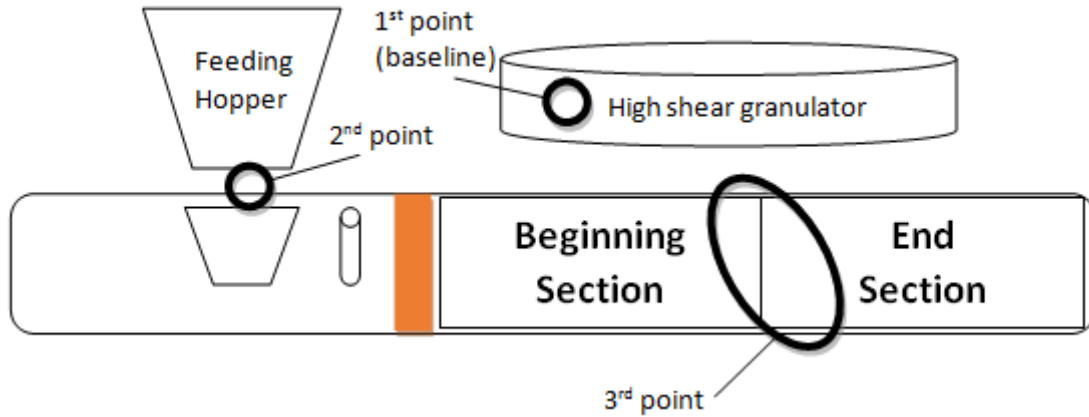


Figure 6-4 schematically indicating the three points of collecting the sample for conductivity.

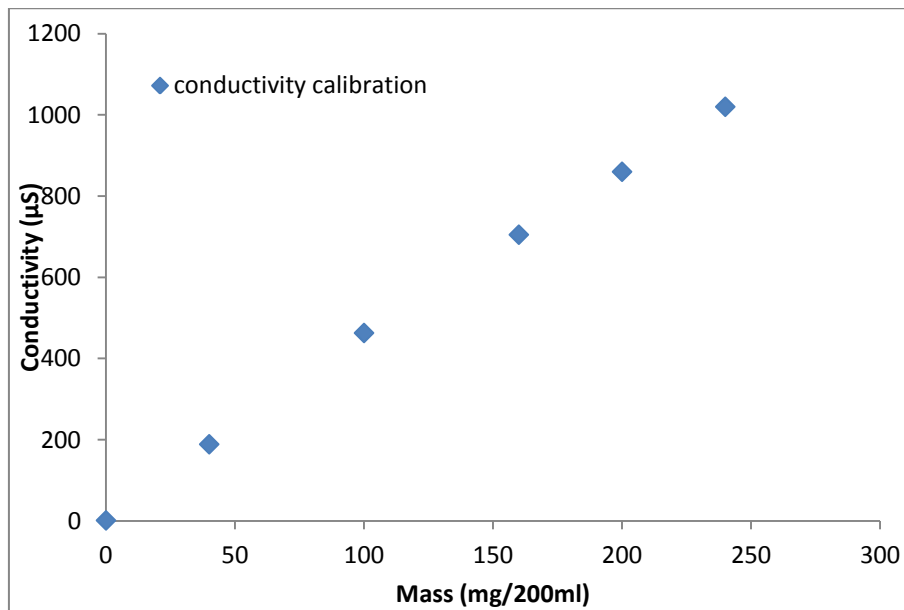


Figure 6-5 shows the calibration of salt conductivity.

### 6.3 Results and discussion- Part 1: Powder caking on the transparent barrel

During this section of the chapter, the results considered for the different materials were obtained while using an in-house made acrylic transparent barrel, where it enables the monitoring of rate and pattern/behaviour of powder caking with time. The size distribution of the granules, produced using this set-up, will be analyzed and compared for trends with their corresponding results presented in Chapter 4 and Chapter 5 whilst using the steel barrel. Finally the mass built up on the top surface of the barrel will be accounted for.

### 6.3.1 Lactose

#### *Powder caking on the top barrel*

Figure 6-6 shows how the liquid binder viscosity, at different shear stress affects the mass (g) of powder caking after 6 minutes. Increasing binder viscosity resulted in a reduction in mass (g) of powder caking, while increasing the shear stress gave a higher mass of powder caking.

In general, during wet granulation; the agglomerates are formed by usage of liquid binder to bring the primary particles together as a combination of capillary forces, surface tension and viscous forces [123]. Thus, increasing the liquid binder viscosity causes an increase in the viscous forces which leads to strong granules [32]. These stronger granules are expected to resist attrition more and may have resulted in a less tendency of powder caking to the surface of the barrel when coming into impact with it. Furthermore, as lactose tend to dissolve when in contact with water, lowering the liquid binder viscosity will allow for more lactose to dissolve and making it soft and hence easily attrite and adheres to the surface. Lowering the binder viscosity also increases the liquid ability to spread and penetrate through the capillary channels, as seen in Figure 4-4. Such mobility of liquid may also encouraged further powder caking as more liquid binder will be available on the surface of powder when the granules/particles come into contact with the surface of the barrel. This could also explain the increase in powder caking as higher shear stress was imparted on the material by using kneading elements. The kneading elements increase the dispersive and distributive mixing of the liquid binder with the powder [17]. This will result in more liquid binder present on the surface of the powder, which could wet the surface of the barrel. The presence of liquid may increase the adhesive forces between the powder and surface of barrel.

Such findings can also be observed in Figure 6-8, which present the images, of powder caking onto the upper barrel, taken at different times (2, 4 and 6 minutes). From the images, it can be seen that regardless binder viscosity or shear stress applied on the



material, caking tends to increase with time. This is more apparent when comparing powder caking presented in images taken after 6 minutes, which covers a larger area of the barrel, compared to the images taken after 2 minutes, as shown Figure 6-8 (a & b). Comparing the images presented in Figure 6-8 (a) with their corresponding results in Figure 6-8 (b) (after 6 minutes) showed that increasing the shear stress resulted in more areas of the barrel covered with powder caking. This is more pronouncedly for the low liquid binder viscosity.

Figure 6-8 (a) shows that changing liquid binder viscosity gave a different behavior of the powder caking onto the surface of the barrel, during low shear stress. Using very high liquid binder viscosity forced powder caking to propagate from the centre and then to progress in both upstream and downstream of the screw rotation directions, i.e. start from the intermeshing region as illustrated in Figure 6-7. This may be due to the resistance of the big granules, which are associated with increase of liquid binder viscosity during low shear stress (as seen in Figure 4-6 (a)), to flow from the intermeshing into compartment 2 (shown in Figure 6-7) . Using low liquid binder viscosity produced narrower size distribution and the granules showed less tendency to reside within the intermeshing region. As a result compartment 2 tends to be covered with more of powder caking relative to compartment 1. This could be due to the increase of velocity that granules tend to gain as they leave the intermeshing area, where they experience obstruction [36]. This increase of velocity may have stemmed in a higher impact force causing the powder/granule to deform more easily and stick to the surface more quickly. From Figure 6-8 (b) using high shear stress uniformed the powder behavior, regardless of liquid binder viscosity. This could be due to the narrower size distribution (shown in Figure 4-6 (b)) which results in less resistance of granules to reside within the intermeshing region.

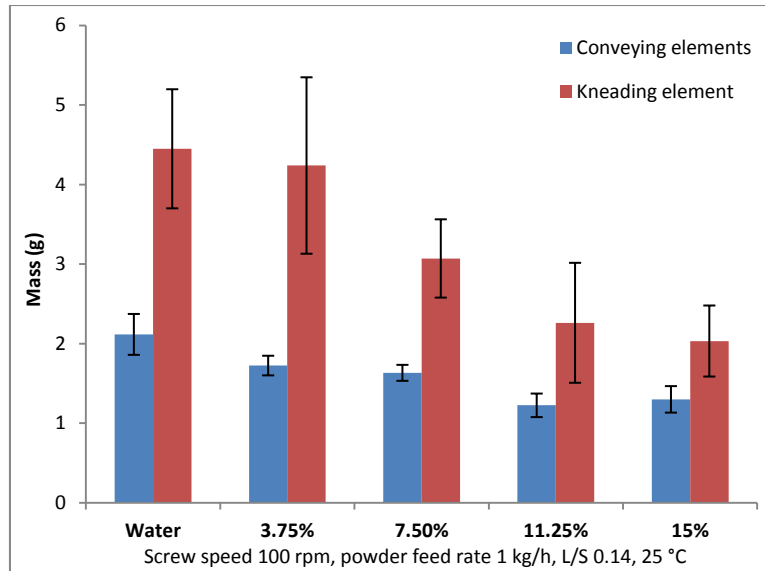


Figure 6-6 Effect of liquid binder viscosity on the mass (g) of lactose powder caking: low stress (■) and high stress (■).

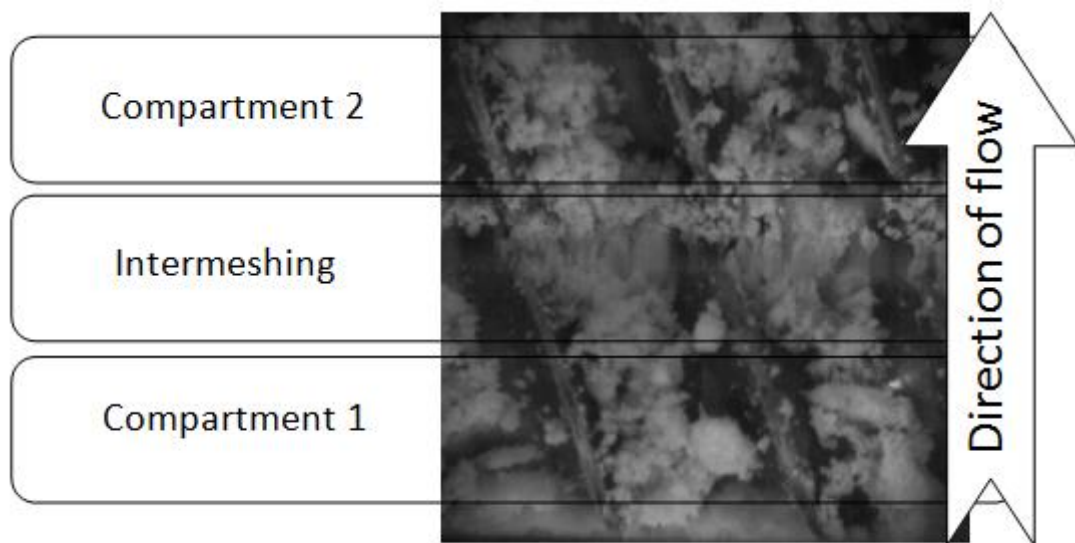
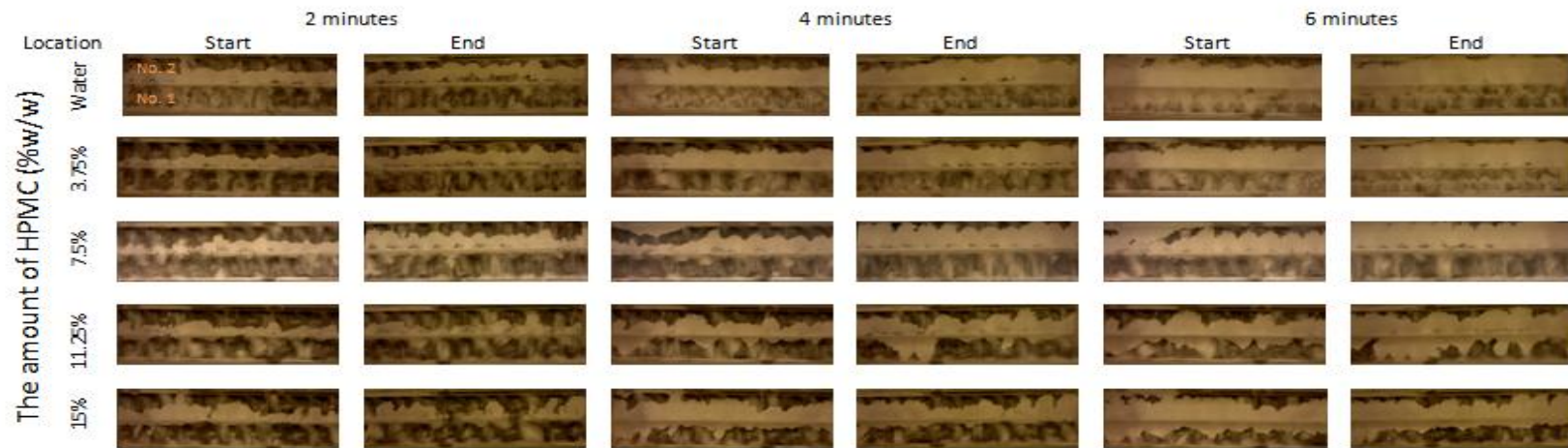
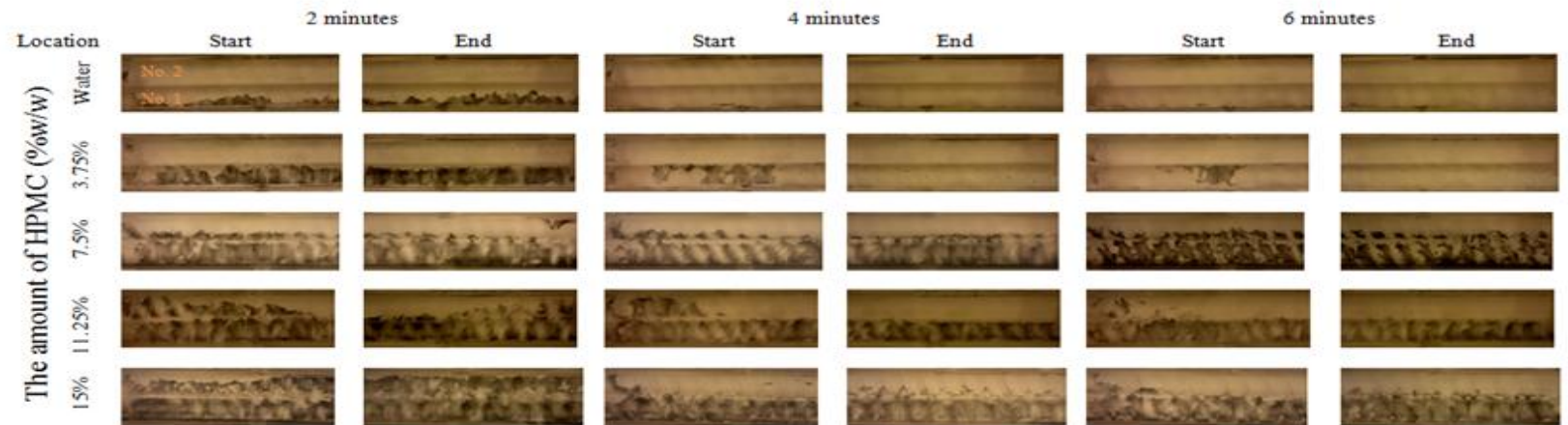


Figure 6-7 show the flow direction of the material within the granulator.



(a)



(b)

Figure 6-8 Effect of liquid binder viscosity on the behavior of powder caking: (a) low stress (b) high stress. The material flows from screw No. 1 to screw No. 2.

### 6.3.2 MCC

#### *Powder caking on the top barrel*

Figure 6-9 shows how the liquid binder viscosity, at different shear stress affects the mass (g) of powder caking after 6 minutes. Increasing the liquid binder viscosity, at low shear stress, results in a reduction in mass of powder caking. This emphasizes the importance of liquid binder ability to spread and penetrate through to surface of the bed. A combination of reduction in liquid binder mobility and rise to viscous forces, as the liquid binder viscosity increases, shows that the trend of powder caking during low stress is unaffected by the powder (i.e. lactose or MCC). Although, the trends (i.e. reduction of caking as viscosity goes up) for both lactose and MCC are similar, MCC powder shows far less tendency to cake onto the surface of the barrel. This could be due to the characteristics of MCC, which tends to retain water within its internal structure [33, 109, 110]. This will limit the water availability on the surface of powder bed and hence reduce the adhesive forces, by liquid bridges, with the transparent barrel surface.

Increasing the shear stress gave inconsistent trends, in mass of powder caking, as the liquid binder viscosity increased. The lower the liquid binder viscosity is, the less sensitive the powder caking becomes to the change in shear stress, as the most of the water remains within the internal structure. This was seen for the size distribution for the low viscosity (e.g. distilled water) shown in Figure 4-18, where changing the shear stress did not show a significant change.

The further increase in liquid binder viscosity showed to result in an increase of powder caking to its corresponding findings at low shear, but trends showed to first reduce then increase significantly. This could be due to the inability of MCC to absorb HPMC binder instead it adsorbs onto the surface of the particles [111], where also images in Figure 4-17 shows a layer of HPMC remains on the top surface of the compressed tablet. The increase in adsorbed binder may have been distributed more uniformly to allow more primary particles of the powder to agglomerate (which was observed in Figure 4-18 (b)) and hence

limits its contact with surface of the barrel. Further increase in liquid binder viscosity resulted in further reduction of water retaining by the MCC, as seen in Figure 4-16. This along with the excess of adsorbed HPMC binder may have allowed more liquid binder to migrate to the surface of the powder, and hence adhering more particles onto the upper surface of the barrel.

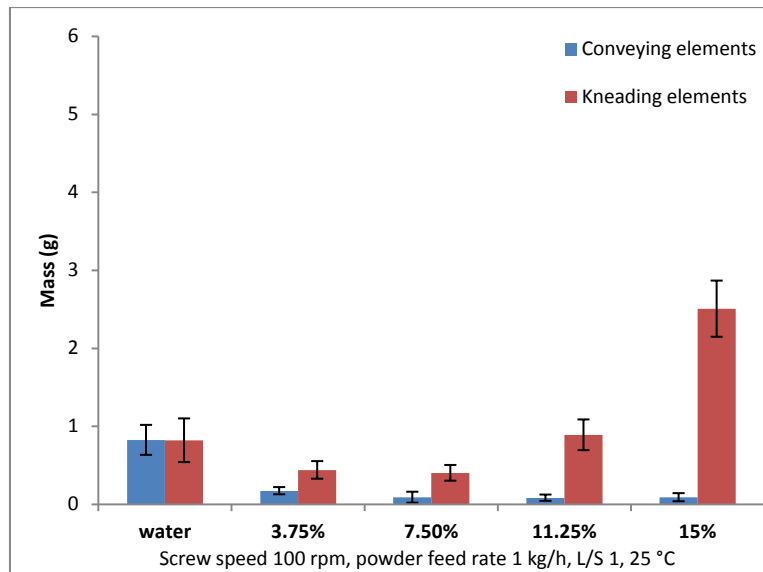
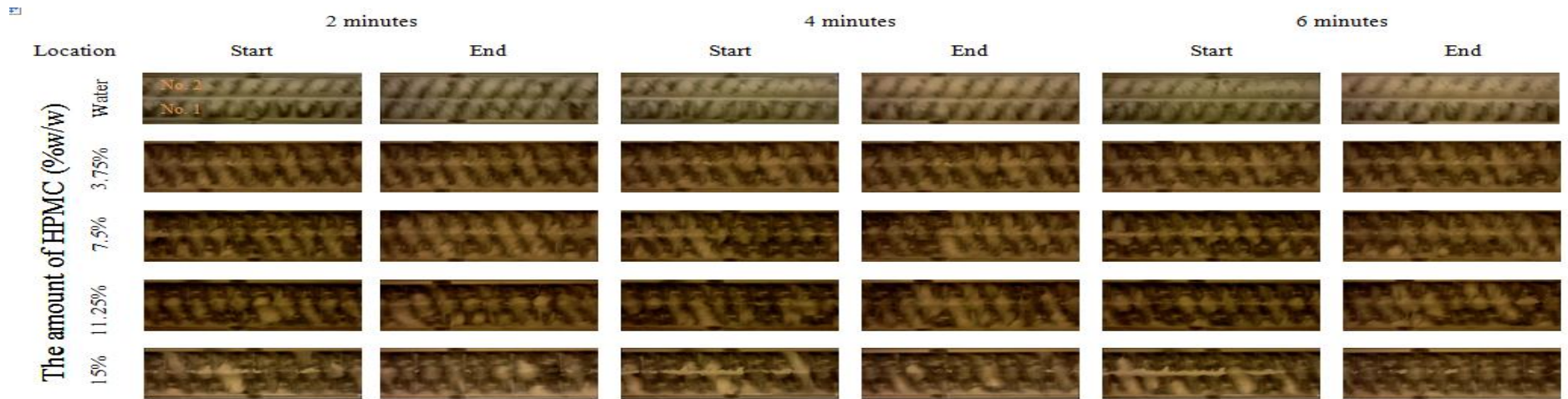
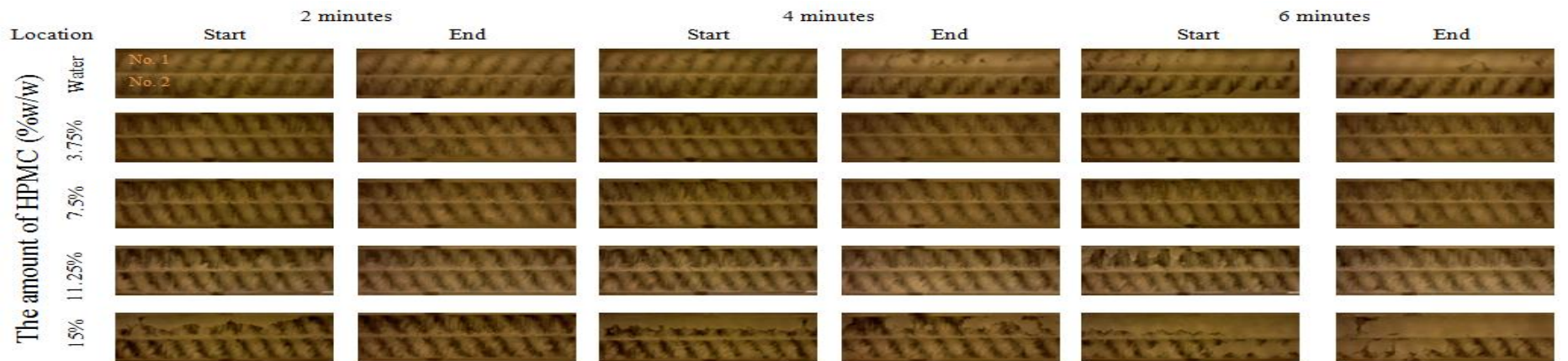


Figure 6-9 Effect of liquid binder viscosity on the mass (g) of MCC powder caking: low stress (■) and high stress (■).

Figure 6-10 shows the behaviours of the powder caking with time, as the liquid binder and shear stress varied. As the MCC showed low tendency to cake, in particularly during low stress, it is difficult to monitor it, though, it shows signs of similar behaviour as that seen in lactose. Increasing the shear stress gave a uniform behaviour of powder caking in that it start from one side and progress to to the next. This is similar behaviour as that seen in lactose Figure 6-8 (b), which is reflectant of the powder flow within the granulator.



(a)



(b)

Figure 6-10 Effect of liquid binder viscosity on the behavior of powder caking: (a) low stress (b) high stress.

### 6.3.3 Formulation

#### *Powder caking on the top barrel*

Figure 6-11 shows how the liquid binder viscosity, at different shear stress affects the mass (g) of powder caking after 6 minutes. During low shear stress, increasing the liquid binder viscosity, gave inconsistent trends of mass of powder caking. This could be due to the different mechanisms of lactose and MCC as the formulation contains different components. The main two mechanisms understood so far, it is the ability of MCC to retain the water (showing in Figure 4-16) and lactose will tend to dissolve when coming into contact the remaining liquid binder. As the liquid binder viscosity increase, there is initial reduction in powder caking. This could be due to reduced amount of water present on the surface of the power, where the remaining adsorbed HPMC binder on the surface helps to bind the particles together. Further increase in liquid binder viscosity showed an increase in mass of powder caking, which could be related the reduction in ability of MCC to retain the water, which may have resulted in excess liquid binder present on the surface. Increasing the shear stress, shown in an increase in mass of powder caking generally, but no trend is observed the binder viscosity is increased.

Figure 6-12 shows how the powder caking behavior changed as the liquid binder viscosity and shear stress varied. At low shear stress, as the liquid binder viscosity increase the powder caking shift from the sides to propagate from the centre, as shown in Figure 6-12 (a). Increasing the shear stress uniform the powder caking behavior as it starts from the side, as seen in Figure 6-12 (b). This is similar to that observed for lactose and MCC, which indicates that the flow of the material is more responsible for such an observation.

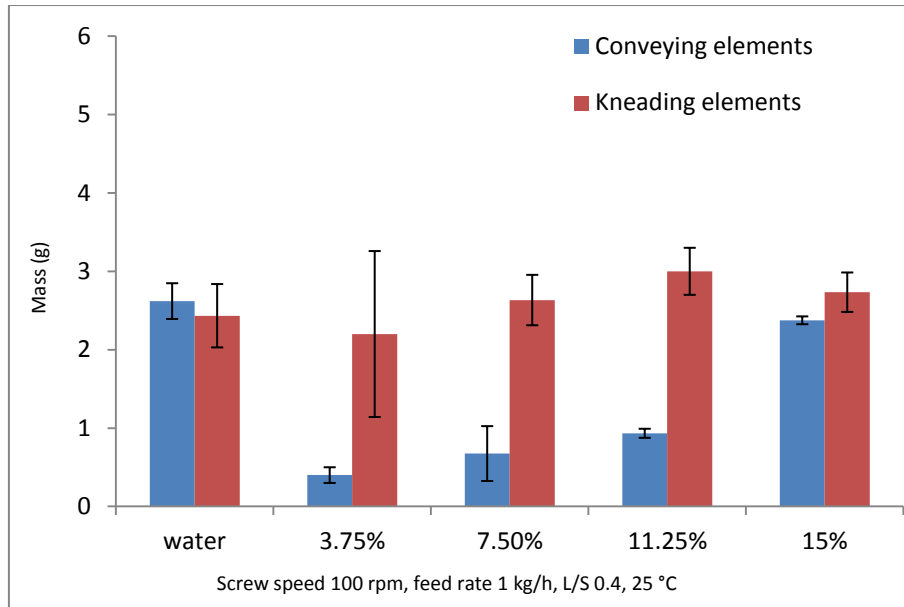
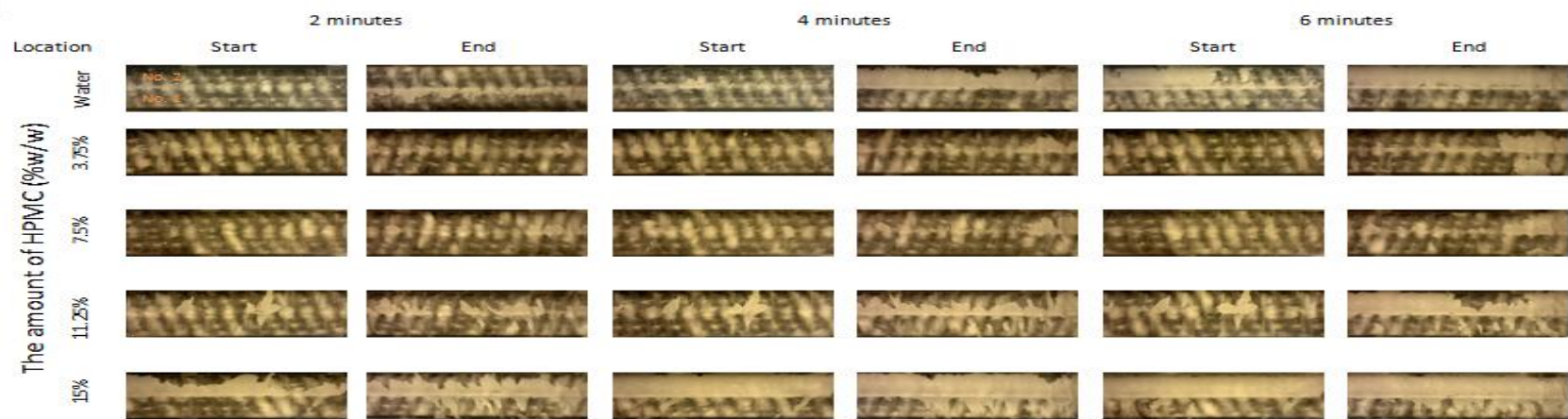
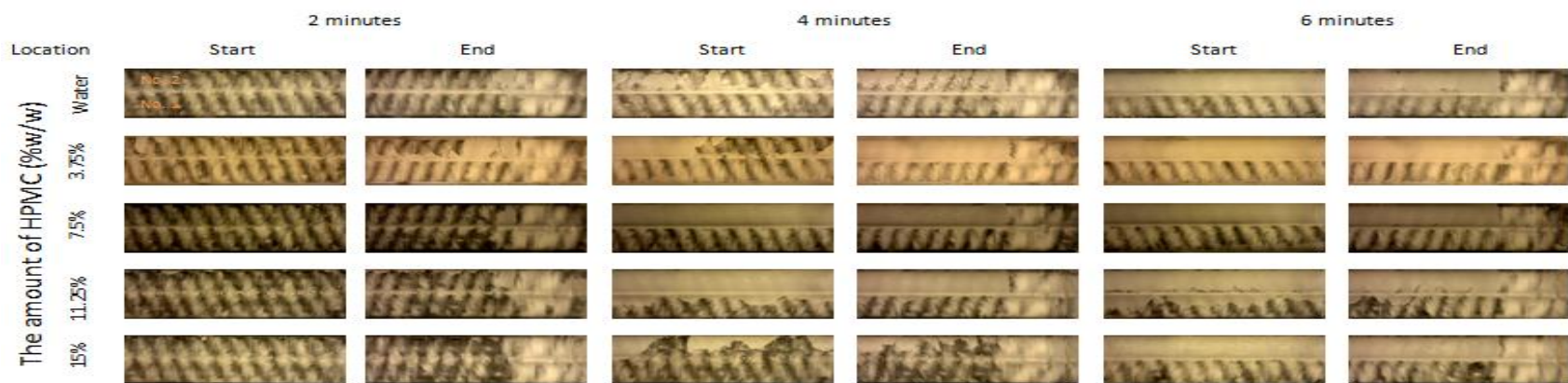


Figure 6-11 Effect of liquid binder viscosity on the mass (g) of formulation powder caking: low stress (■) and high stress (■).





(a)



(b)

Figure 6-12 Effect of liquid binder viscosity on the behavior of powder caking: (a) low stress (b) high stress.

### 6.3.4 Binder delivery

#### *Powder caking on the top barrel*

Figure 6-13 shows how the binder delivery, at different shear stress affects the mass (g) of powder caking after 6 minutes. At low shear stress, it shows a reduction in powder caking as the more HPMC binder delivered in the liquid form, which is similar to that seen in Figure 6-11 for the early stage (of increase liquid binder viscosity) in the formulation. The slight difference could be related to the amount of HPMC present in the liquid binder and the composition within the powder. At higher shear stress, delivering the binder in different forms did not show to affect the mass of powder caking. This is similar to the findings of the formulation.

Figure 6-14 shows how the powder caking behavior changed as the binder delivery and shear stress varied. The behavior for low and high shear is same as seen previously.

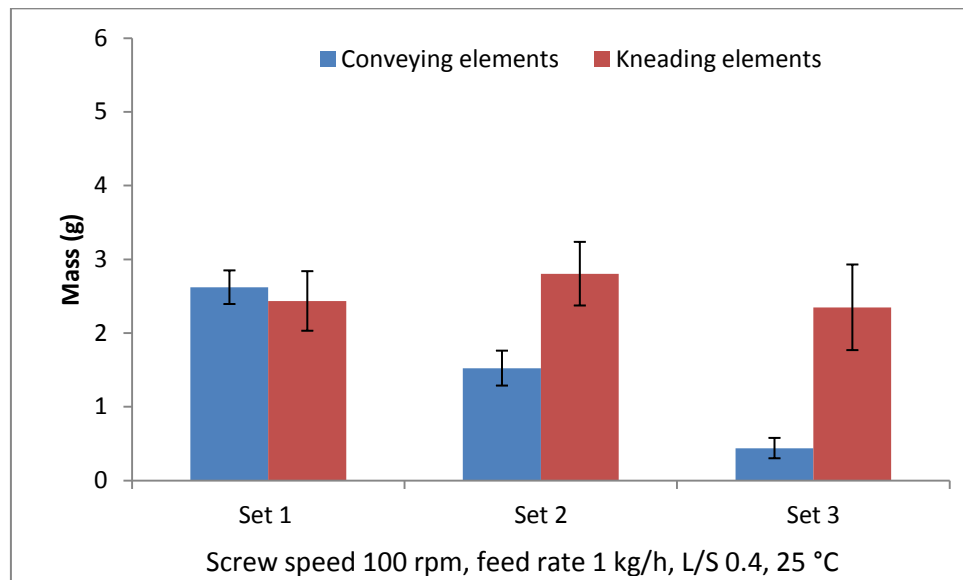
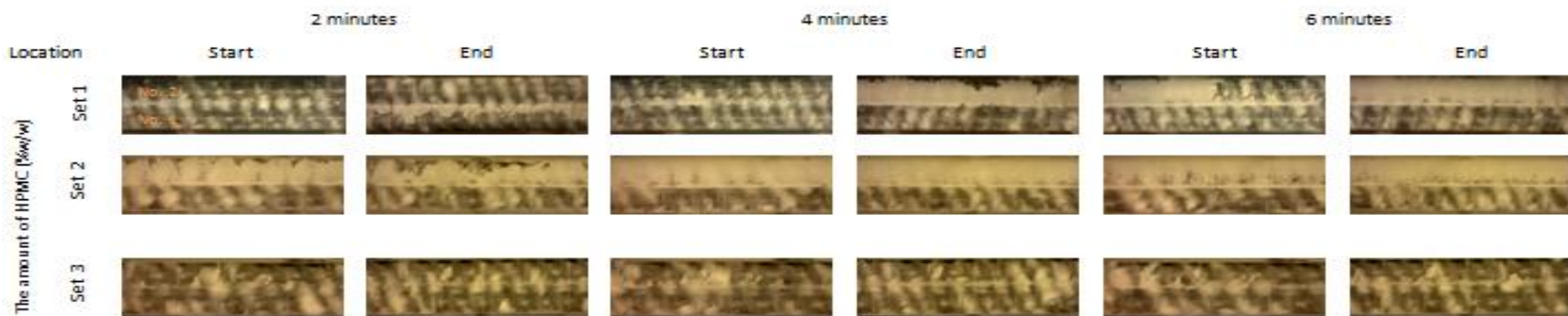
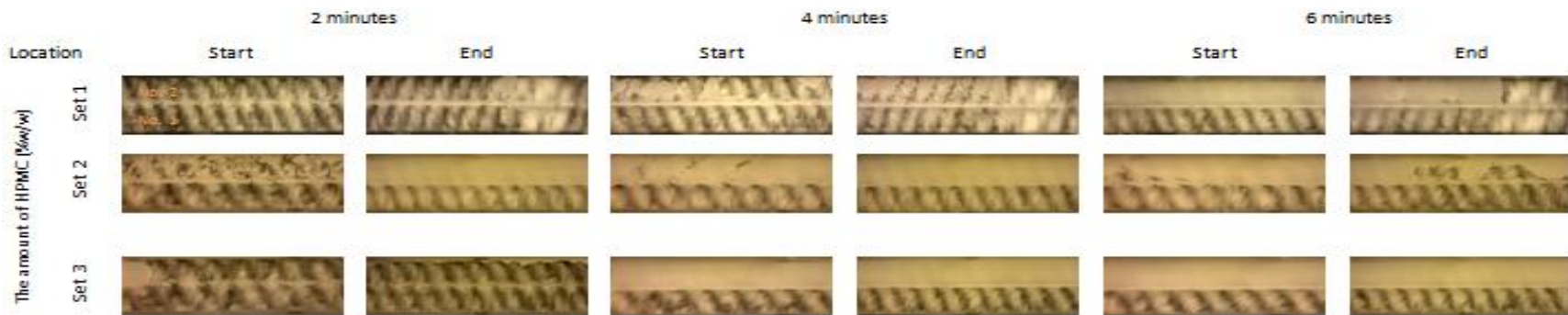


Figure 6-13 Effect of binder delivery on the mass (g) of formulation powder caking: low stress (■) and high stress (■).



(a)



(b)

Figure 6-14 Effect of binder delivery on the behavior of powder caking: (a) low stress (b) high stress.

## 6.4 Results and discussion- Part 2: Powder caking on the stainless steel barrel

This section of the chapter will consider the use of the steel barrel. The lowest and highest liquid binder viscosity (Set 1 and Set 3 for the binder delivery) in Part 1 will be considered for this part. The results for the mass (g) and images of powder caking were taken after 6 minutes, as described in section 6.2.3. In addition to the results presented during this investigation, Figure 6-15 shows some extrudate of caked powder coming at the end of the barrel, when running at higher conditions (which were not included in this study). This phenomenon may be observed during operation and hence should be avoided as it could affect the quality of the product. Also, during this study, only the upper part of barrel is considered. There is some powder caking which adheres to the bottom portion of the barrel, which will not be considered during this study (although some results are presented in Appendix C).

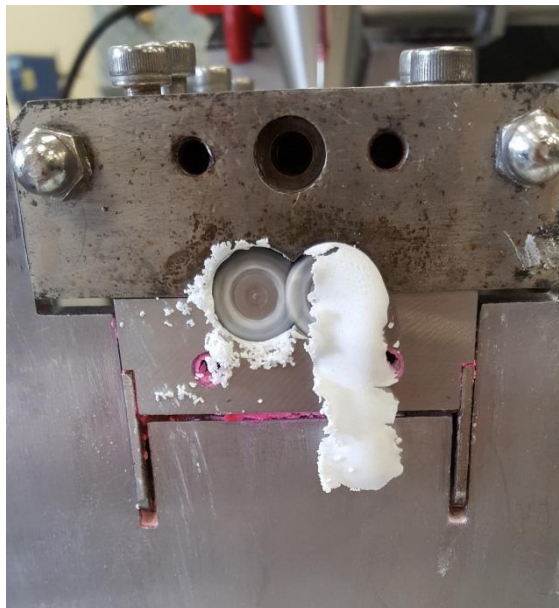


Figure 6-15 extrude coming out at the end of the barrel at extreme conditions.

### 6.4.1 Lactose

#### *Powder caking/stickiness onto steel barrel*

Figure 6-16 shows the mass (g) of powder caking onto the barrel, as the liquid binder viscosity and shear stress changed. The results correspond well with those presented in Figure 6-6. Furthermore, the change of the barrel property (i.e. acrylic and steel) did not

show to affect the powder caking behaviours, as the findings in Figure 6-17 shows similar to the corresponding results seen in Figure 6-8.

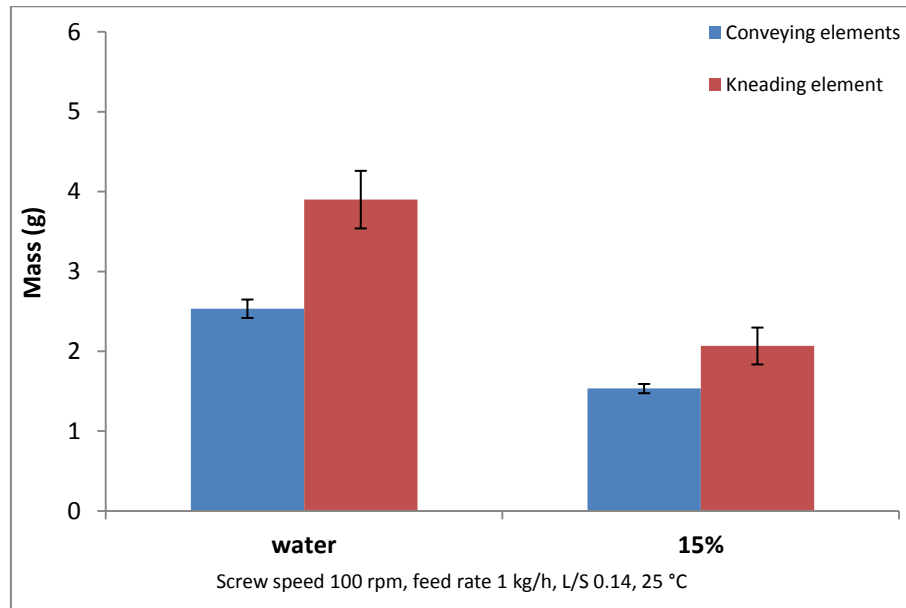


Figure 6-16 Effect of the low (0%) and high (15%) liquid binder viscosity on the mass (g) of lactose powder caking: low stress (■) and high stress (■)..

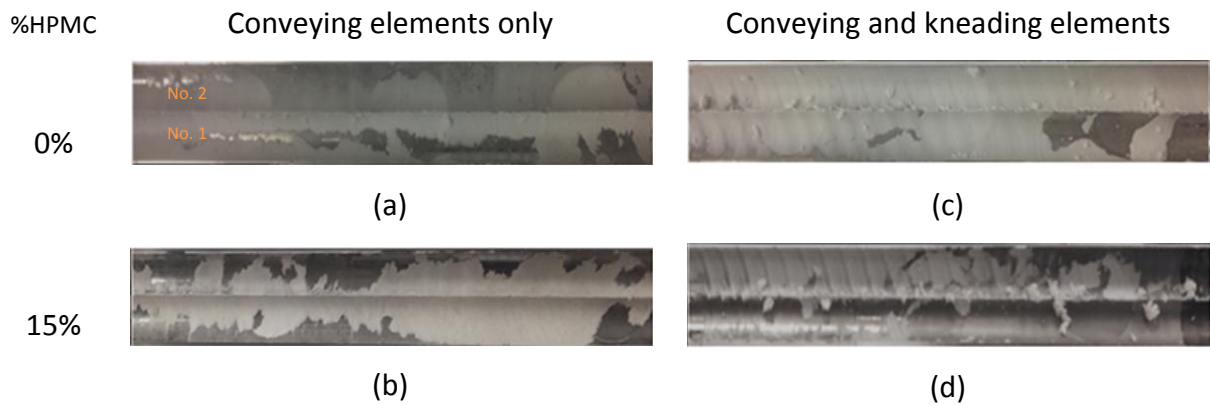


Figure 6-17 Effect of low (0%) and high (15%) liquid binder viscosity on the behavior of powder caking: (a) low stress (b) high stress. The material flows from screw No. 1 to screw No. 2.

### Surface topography

Figure 6-18 shows the change in surface topography of the lactose powder caking to the surface of the steel barrel, as the liquid binder (lowest and highest) and shear stress varied. The surfaces topography was visualized using scanning electron microscopy.

The primary particles showed to remain unaffected when using low shear stress. This could be due to the ungranulated particles and small fragment of granules (as result of attrition when they collide with the barrel) forming an adhesive forces with surface of barrel which is largely driven by the availability of liquid binder on the surface of the powder. Increasing the shear stress on the material gave more compacted surface. Increasing the shear stress may have increased the hardening work on the powder causing it to compact and fragment more.

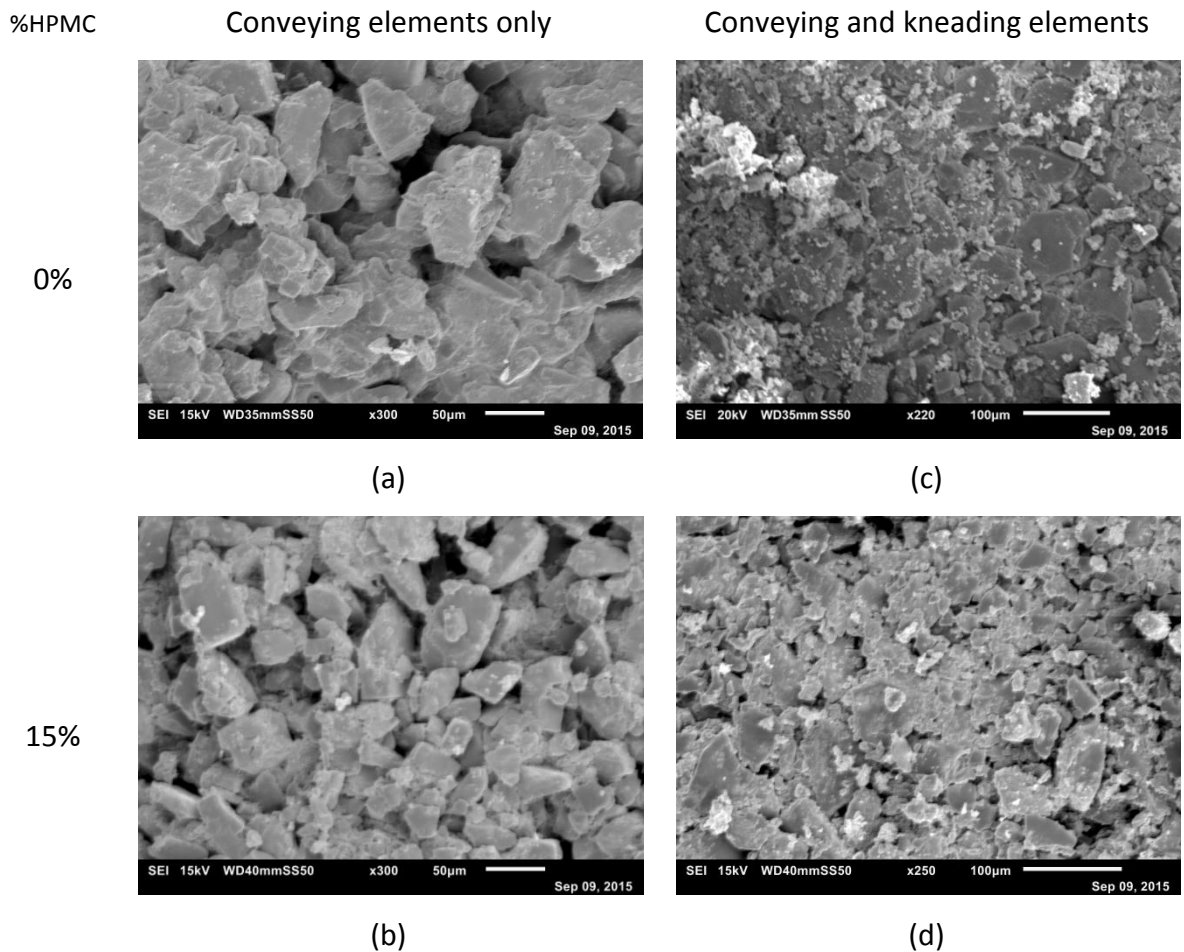


Figure 6-18 6-19 Effect of low (0%) and high (15%) liquid binder viscosity on surface topography of lactose ribbon of cake, as the stress varied.

**Structural characterization**

Figure 6-20 shows the change in the porosity of ribbons as liquid binder viscosity and shear stress varied. Applying the low shear stress, the particles within the ribbon were loosely packed, which allowed for more air voids to reside within structure. This can be visualized in the images presented in Figure 6-21 (a & b). Increasing the shear stress increased the number of granules produced (as shown in Figure 4-6 (b)). This may have caused the ribbon of powder caking, on the surface of the barrel, to undergo higher shearing as the granules flow through. Hence, the consolidation of the particle helped to reduce the air voids within the structure, which can be visualized as shown in Figure 6-21 (c & d).

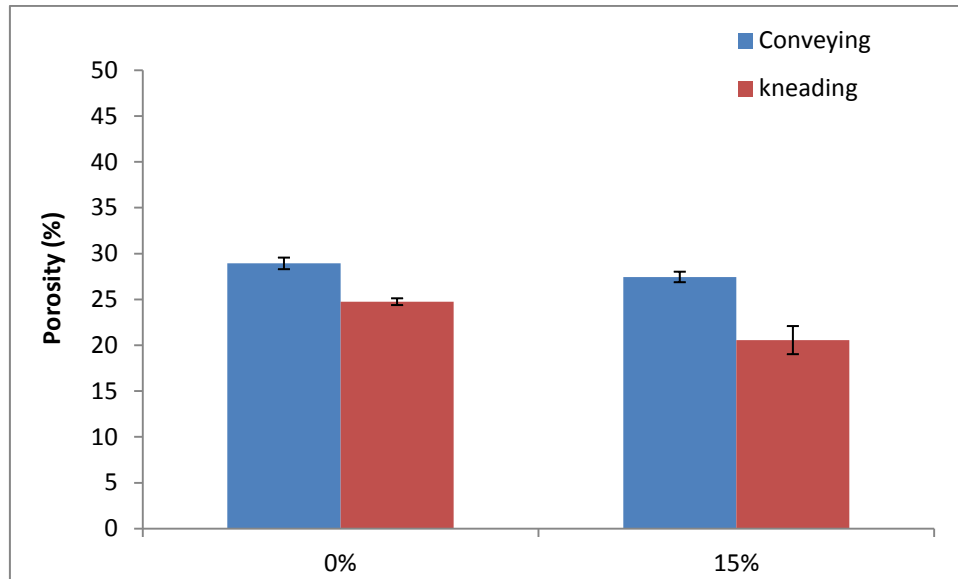


Figure 6-20 Effect of low (0%) and high (15%) liquid binder viscosity on porosity of lactose ribbon of cake, as the stress varied.

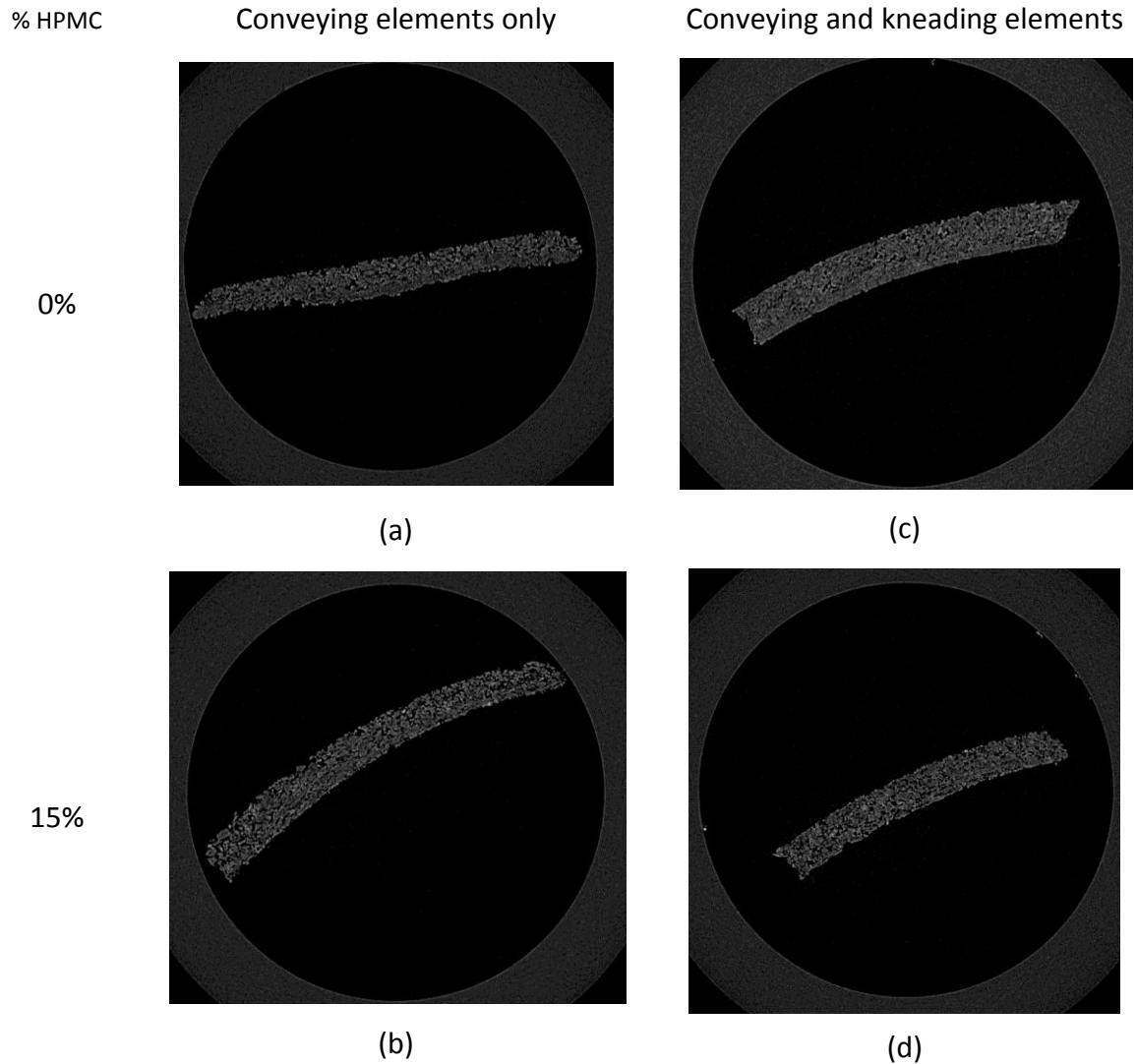


Figure 6-21 X-ray images of lactose ribbon as liquid binder viscosity and stress varied.

## 6.4.2 MCC

### ***Powder caking/stickiness onto steel barrel***

Figure 6-22 shows the mass (g) of powder caking into the barrel, as the liquid binder viscosity and shear stress changed. The results correspond well with those presented in Figure 6-9. Furthermore, the change of the barrel property (i.e. acrylic and steel) did not show to affect the powder caking behaviours, as the findings in Figure 6-23 shows similar to the corresponding results seen in Figure 6-10.



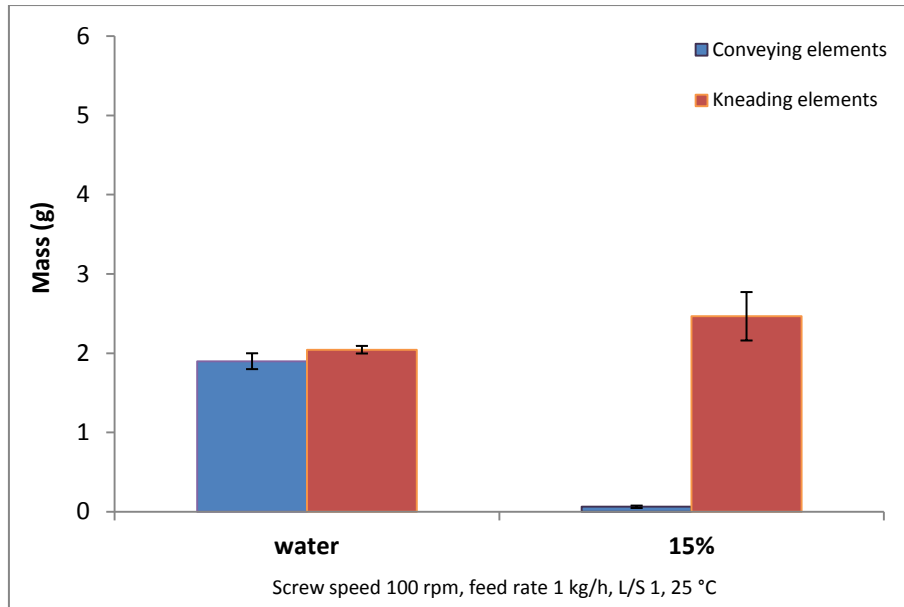


Figure 6-22 Effect of the low (0%) and high (15%) liquid binder viscosity on the mass (g) of MCC powder caking: low stress (■) and high stress (■).

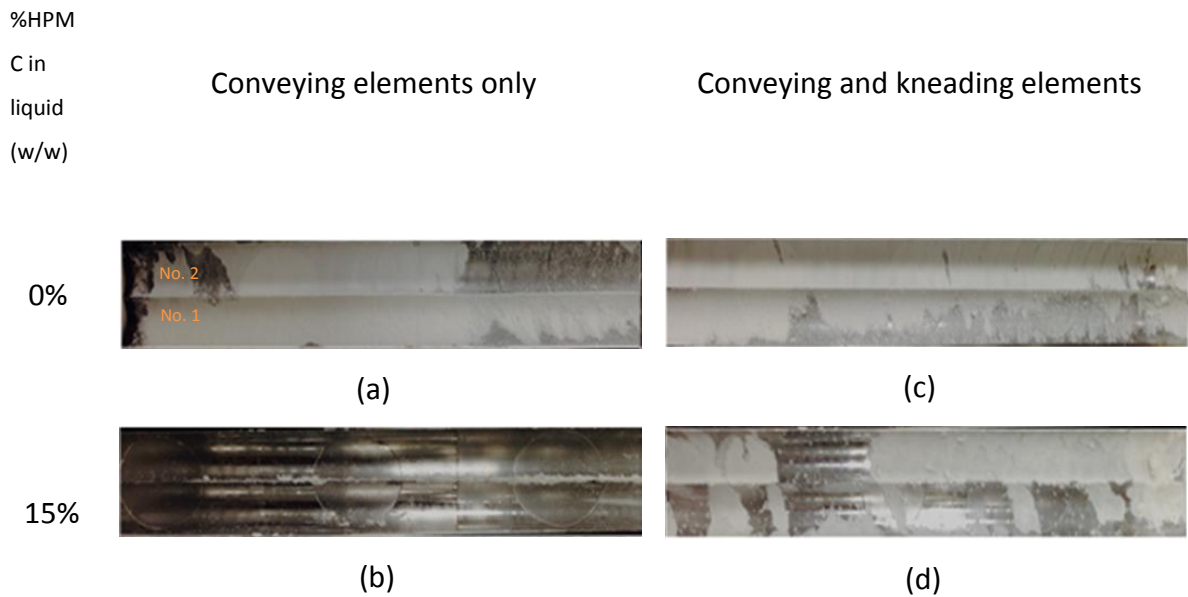


Figure 6-23 Effect of low (0%) and high (15%) liquid binder viscosity on the behavior of powder caking: (a) low stress (b) high stress.

### Surface topography

Figure 6-24 shows the change in the surface topography of the MCC powder caking to the surface of the steel barrel, as the liquid binder viscosity (lowest and highest) and shear stress varied. At low shear stress, there was no adequate powder caking to retrieve for high liquid binder viscosity, as shown in Figure 6-23 (b). Although, the shear stress was

low, the surface of the ribbon showed to have undergone plastic deformation when using low liquid binder viscosity, as shown in Figure 6-24 (a). The water-retaining characteristic of the MCC may have acted as a plasticizer causing such deformation. The driven force for this kind adhesion to the surface of the barrel may have been due to the increase of contact area. Increasing the shear stress, the powder tends to deform regardless of the material (i.e. lactose and MCC).

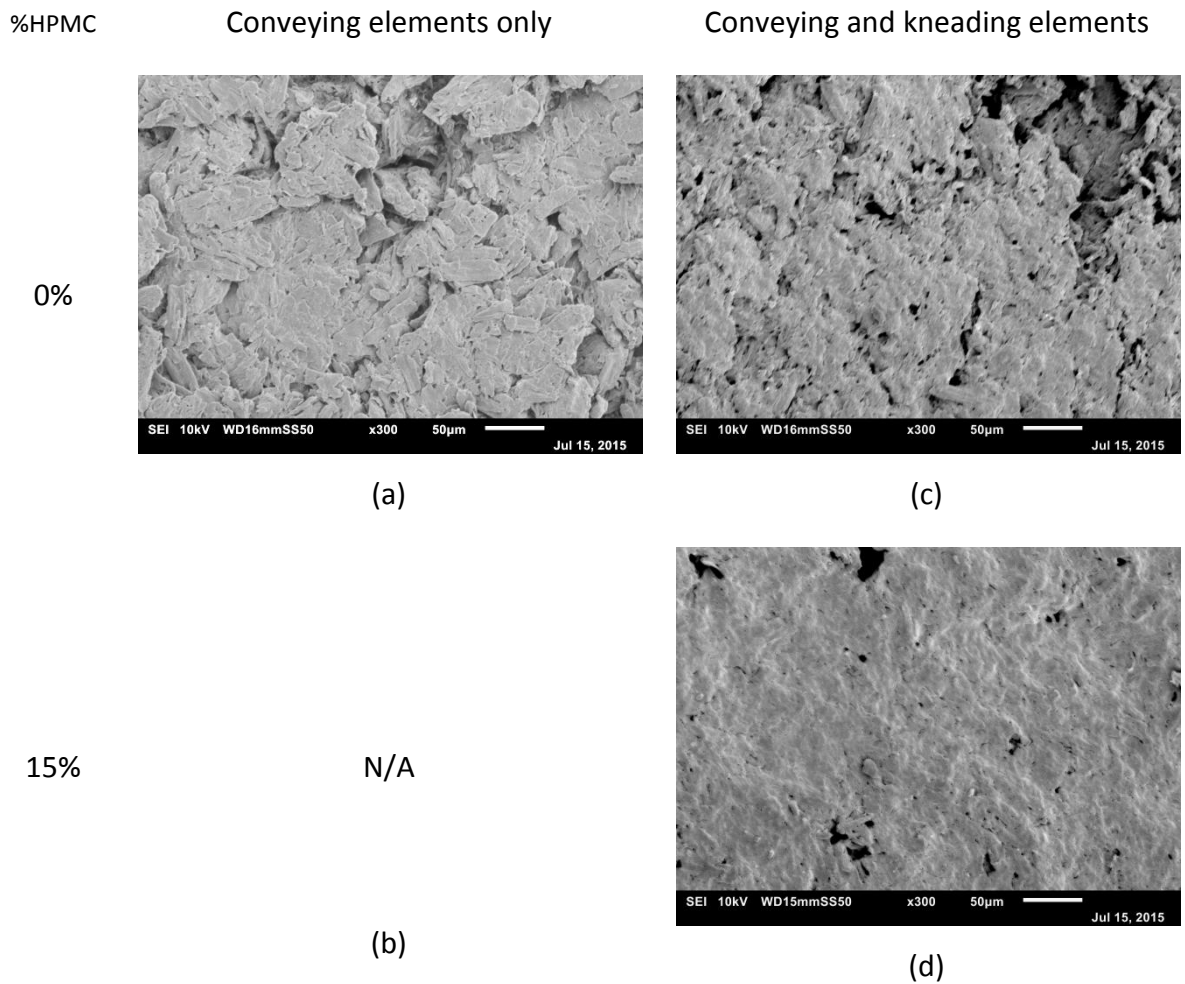


Figure 6-24 Effect of low (0%) and high (15%) liquid binder viscosity on surface topography of MCC ribbon of cake, as the stress varied.

**Structural characterization**

Figure 6-25 shows the change in the porosity of ribbons as liquid binder viscosity and shear stress varied. Increasing the shear stress gave a lower porosity as particles within the ribbons compacted further, reducing the air voids. This can be visualized in particular for the low liquid binder viscosity, as shown in Figure 6-26 (a & c).

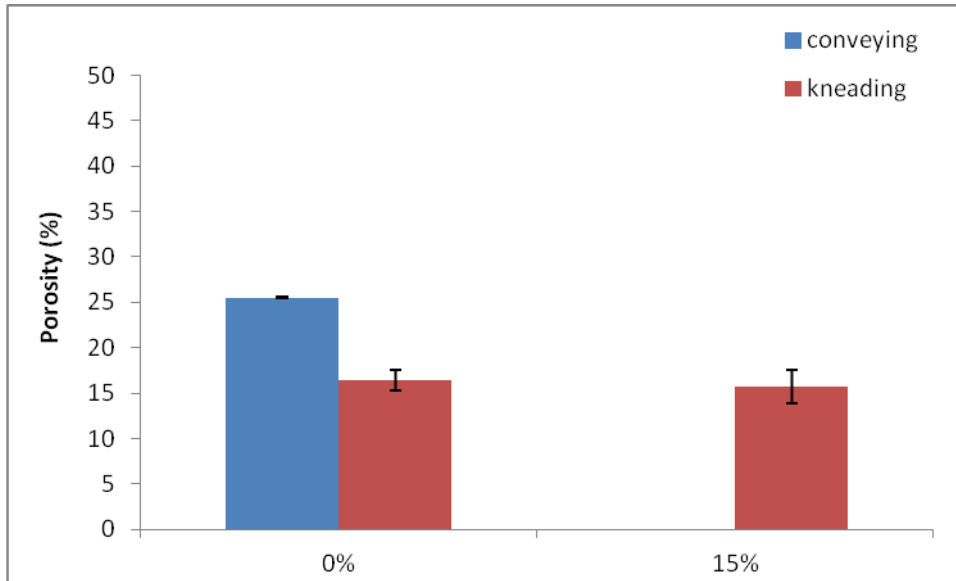


Figure 6-25 Effect of low (0%) and high (15%) liquid binder viscosity on porosity of MCC ribbon of cake, as the stress varied.

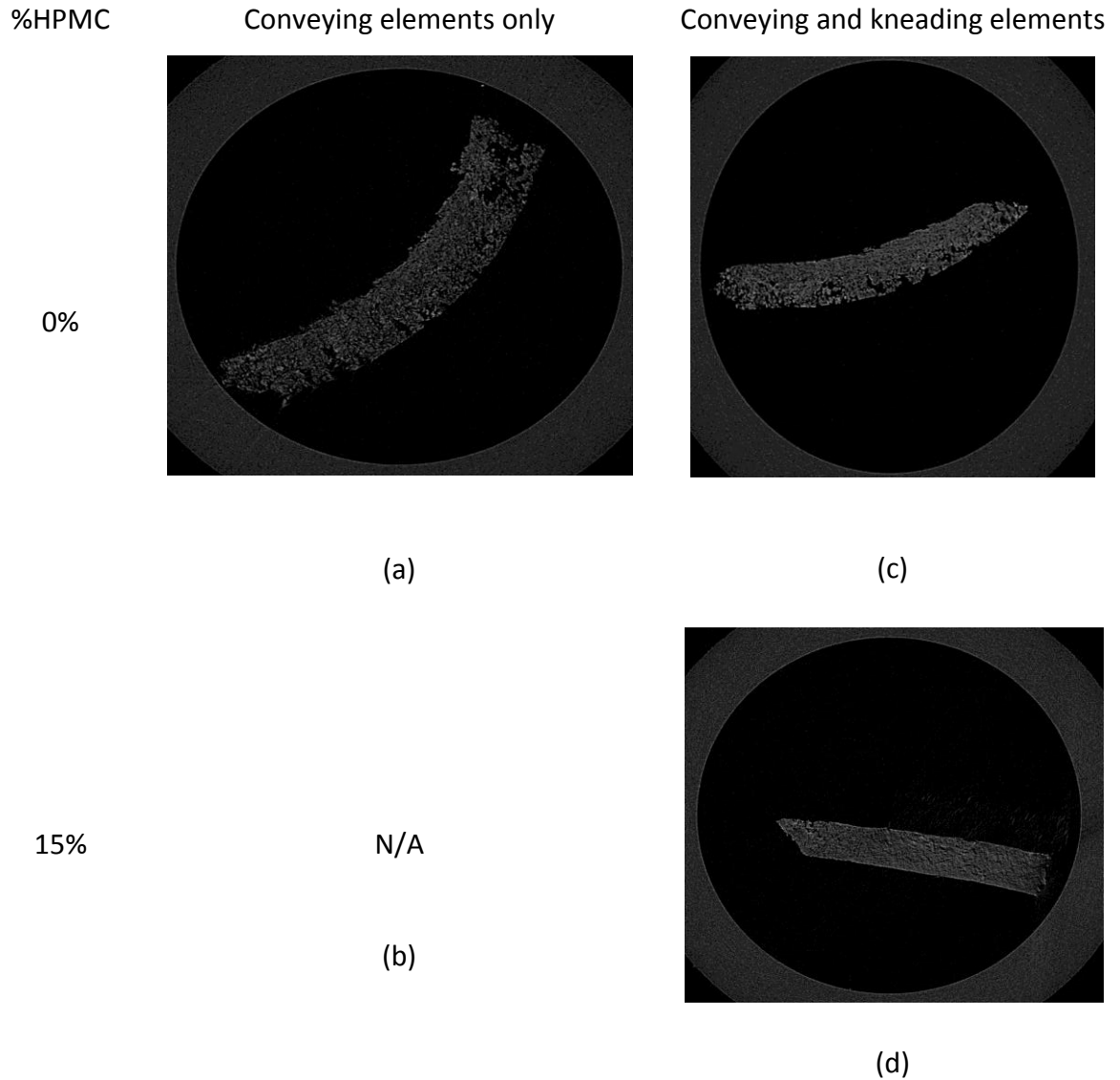


Figure 6-26 X-ray images of MCC ribbon as liquid binder viscosity and stress varied.

### 6.4.3 Formulation

#### ***Powder caking/stickiness onto steel barrel***

Figure 6-27 shows the mass (g) of powder caking into the barrel, as the liquid binder viscosity and shear stress changed. The results correspond well with those presented in Figure 6-11. Furthermore, the change of the barrel property (i.e. acrylic and steel) did not show to affect the powder caking behaviours, as the findings in Figure 6-28 shows similar to the corresponding results seen in Figure 6-12.

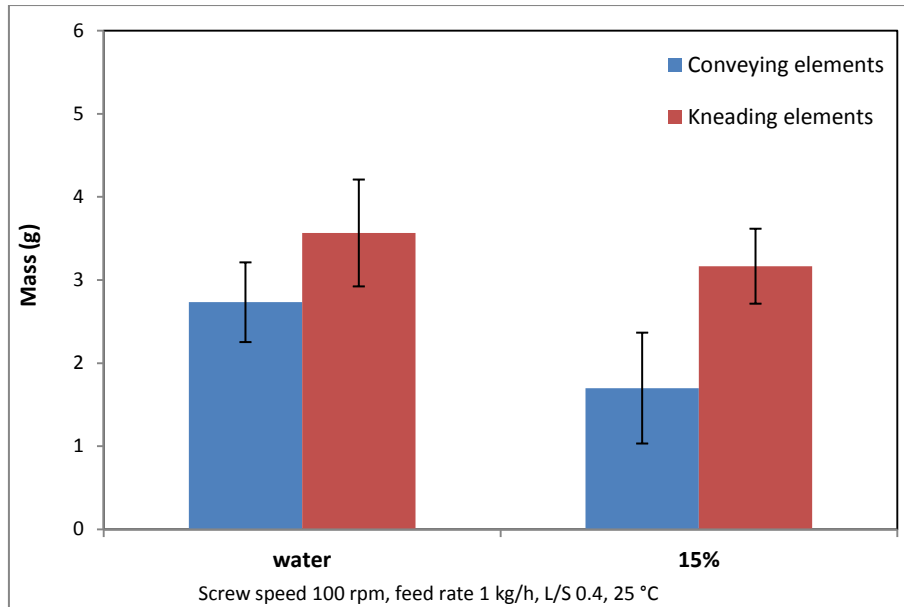


Figure 6-27 Effect of the low (0%) and high (15%) liquid binder viscosity on the mass (g) of formulation powder caking: low stress (■) and high stress (■).

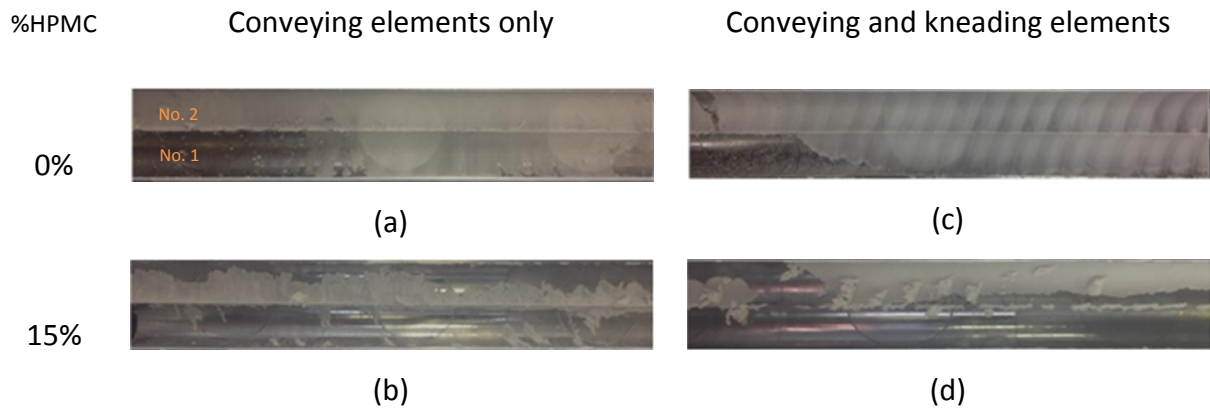


Figure 6-28 Effect of low (0%) and high (15%) liquid binder viscosity on the behavior of powder caking: (a) low stress (b) high stress.

### Surface topography

Figure 6-29 shows the change in surface topography of the powder caking to the surface of the steel barrel, as the liquid binder (lowest and highest) and shear stress varied. During the low shear stress, as we have two materials within the formulation that exhibited different topography (lactose unaffected and MCC plastically deformed), this has reflected

on the surface which shows some deformation and some unaffected particles, as shown Figure 6-29 (a & b). Increasing the stress increased the shearing of the ribbon resulting in more compacted and deformation, as seen in Figure 6-29 (c & d).

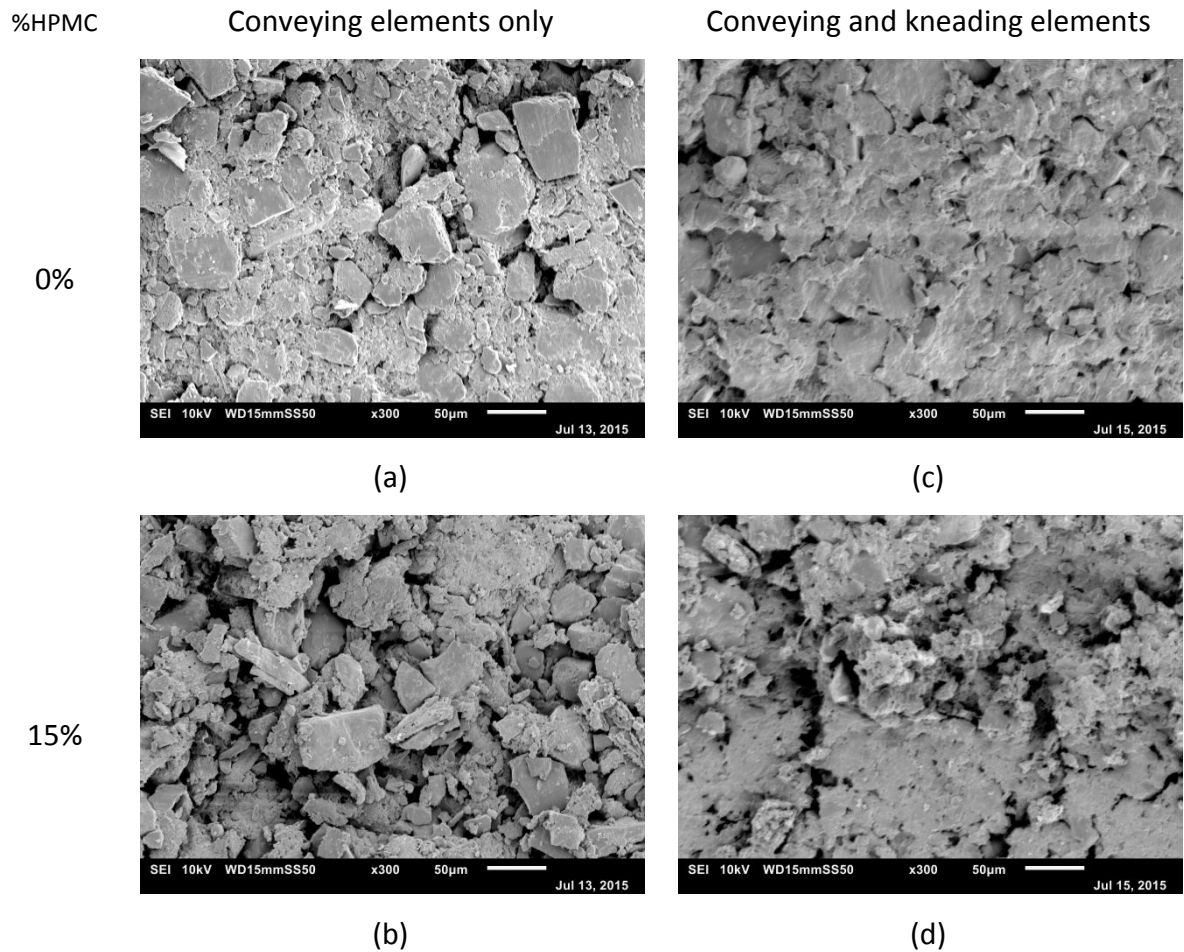


Figure 6-29 Effect of low (0%) and high (15%) liquid binder viscosity on surface topography of formulation ribbon of cake, as the stress varied.

### ***Structural characterization***

Figure 6-30 shows the change in the porosity of ribbons as liquid binder viscosity and shear stress varied. As seen with lactose and MCC, increasing the shear stress on the material produced more shear and consolidation of the ribbon on the surface of the barrel. This resulted in a reduction of air voids and the particles are brought closer. This

can be visualized by comparing images in Figure 6-31 (a & b) with their corresponding results in Figure 6-31 (c & d).

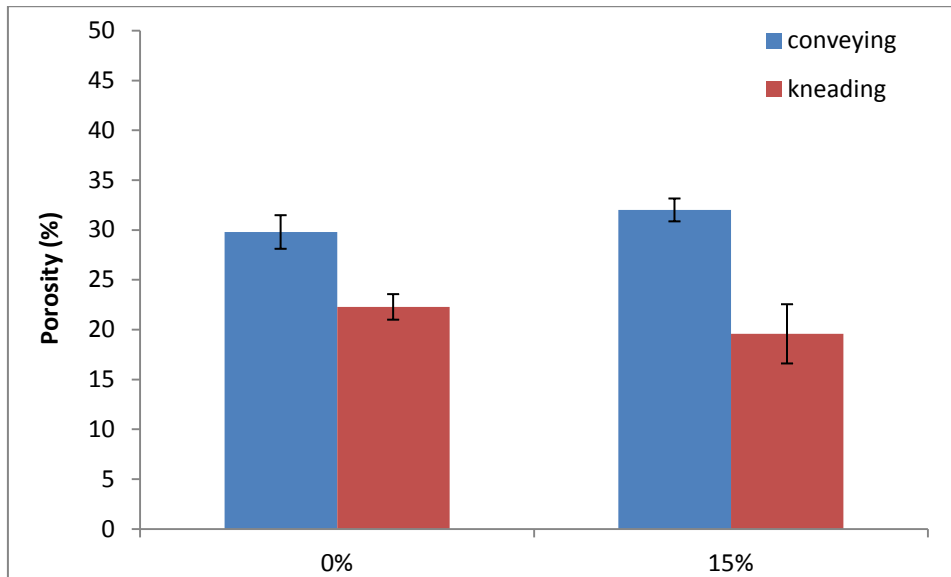


Figure 6-30 Effect of low (0%) and high (15%) liquid binder viscosity on porosity of formulation ribbon of cake, as the stress varied.

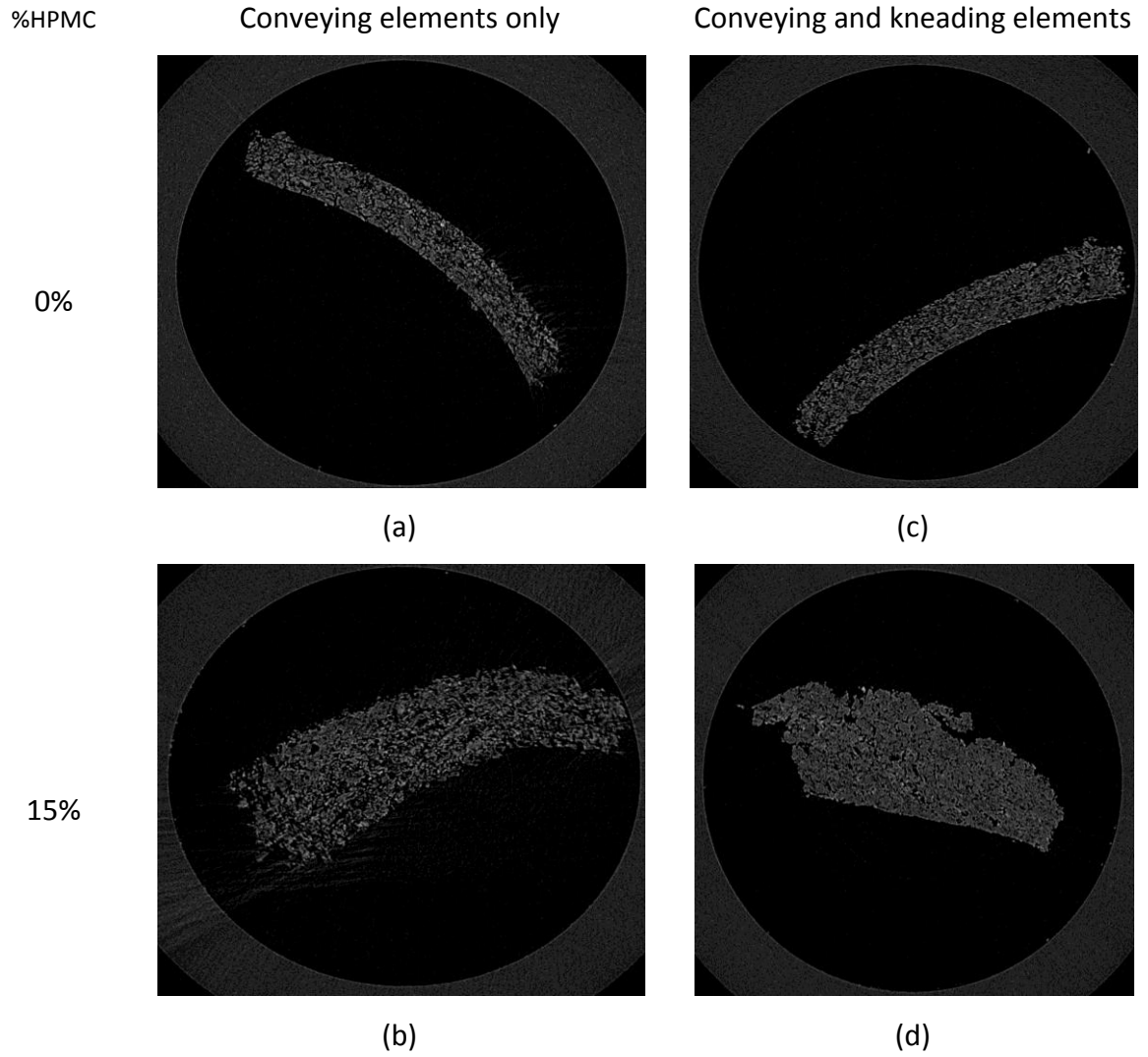


Figure 6-31 X-ray images of formulation ribbon as liquid binder viscosity and stress varied.



#### 6.4.4 Binder delivery

##### *Powder caking/stickiness onto steel barrel*

This section is comparing the results presented in Figure 6-32 and Figure 6-33, with their corresponding results shown in Figure 6-13 and Figure 6-14. They correspond well which emphasize the minimal effect the material of the barrel has on the outcome.

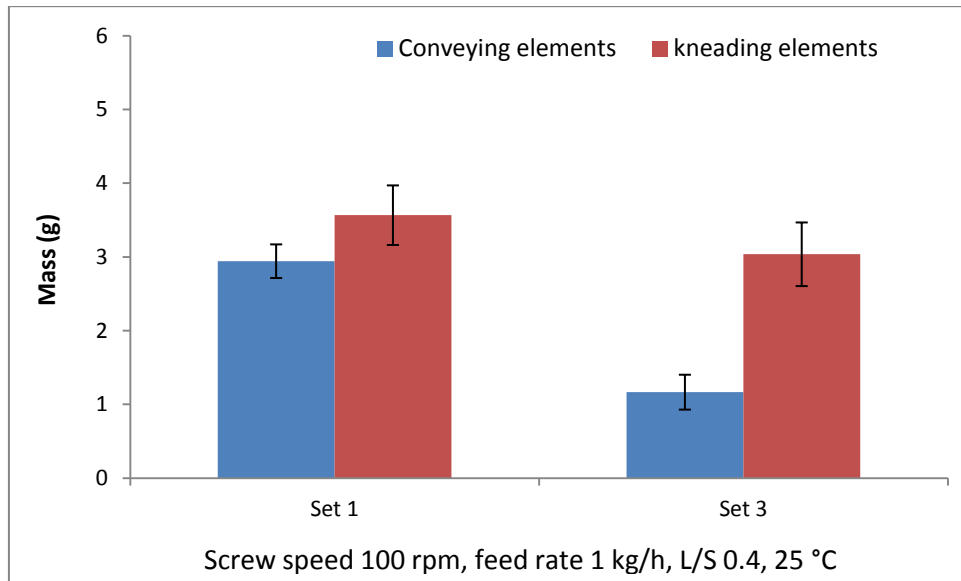


Figure 6-32 Effect of binder delivery (Set 1 & 3) on the mass (g) of powder caking: low stress (■) and high stress (■).

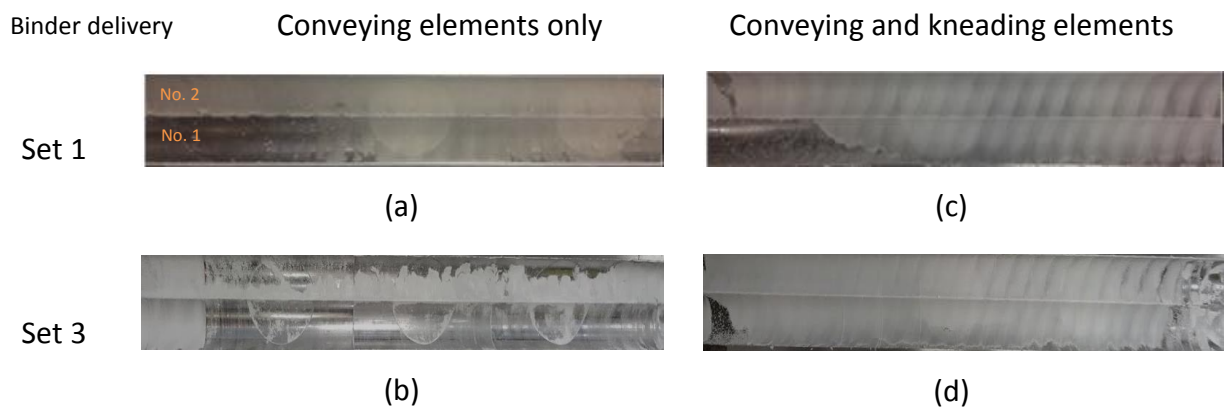


Figure 6-33 Effect of binder delivery (Set 1 & 3) on the behavior of powder caking: (a) low stress (b) high stress.

The results on granule properties (such as size) and powder caking up to this point (throughout Chapter 4-6) are evidence for further improvement to the regime map presented in Figure 2-5. Although, some aspects still remain true such that one would expect the powder caking to appear in the Overwetted regime, the effect of screw configuration along with powder properties suggest a possible drastic change to the regime boundaries. This will require comprehensive work to understand such changes that could be inflicted once these variables are incorporated.

### ***Surface topography***

Figure 6-34 shows the change in surface topography of the powder caking to the surface of the steel barrel, as binder delivery (Set 1 & 3) and shear stress varied. Although, there is a change within the composition of the blend and the liquid binder viscosity during binder delivery, the findings are similar to that seen in Figure 6-29 for the formulation. Increasing the shear stress resulted in further deformation and compaction of surface of the ribbon.

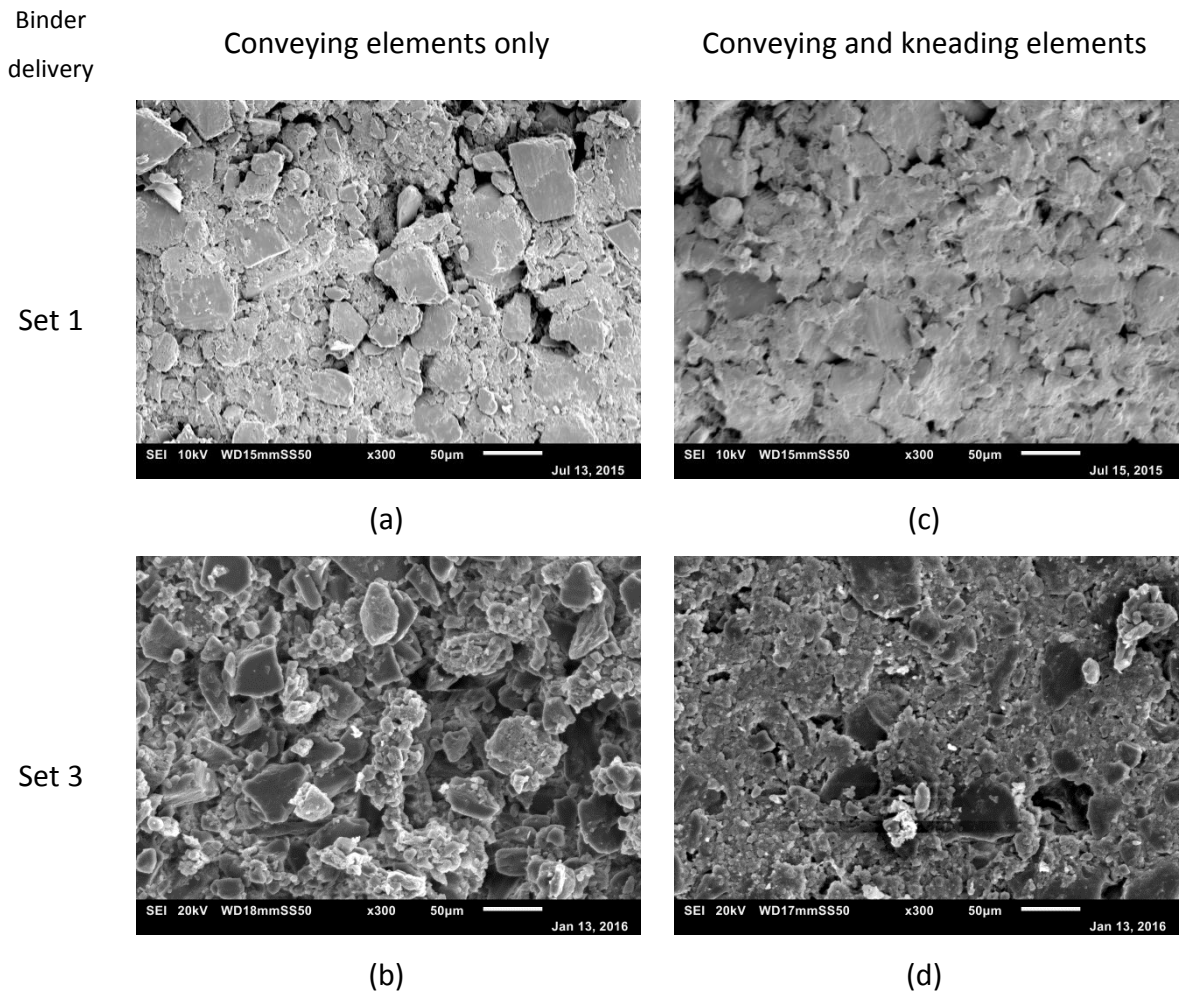


Figure 6-34 Effect of binder delivery (Set 1 & 3) on surface topography of ribbon, as the stress varied.

***Structural characterization***

Figure 6-35 shows the change in the porosity of ribbons as binder delivery and shear stress varied. The trends are similar to that seen in Figure 6-30. The images in Figure 6-31 shows the structure as the shear stress increased while varying the binder deliver. Though, the changes in composition of the blend to that of the formulation, the observation is similar. This shows that the shear stress is more dominant when the change of composition is minimal.

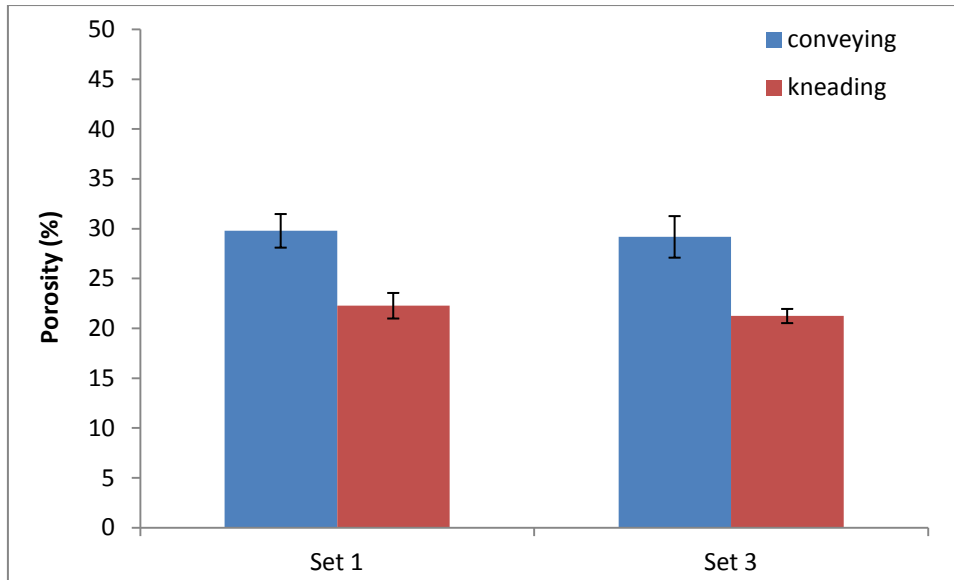


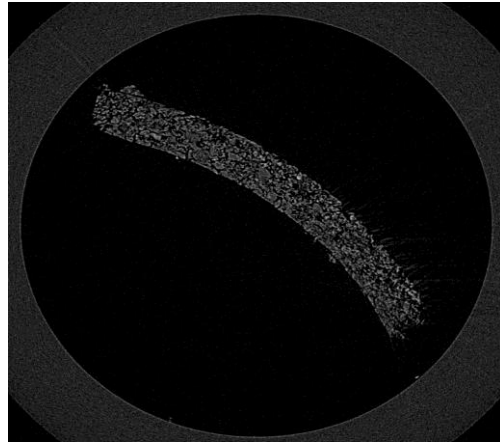
Figure 6-35 Effect of binder delivery (Set 1 & 3) on porosity of ribbons, as the stress varied.

Binder  
delivery

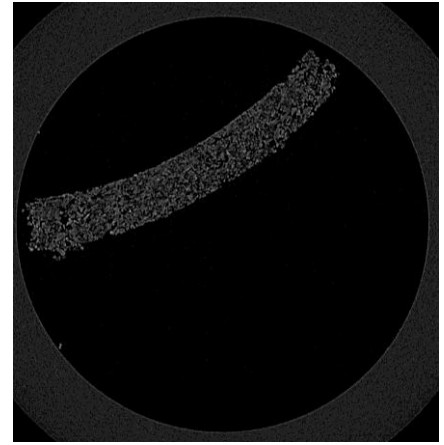
Conveying elements only

Conveying and kneading elements

Set 1

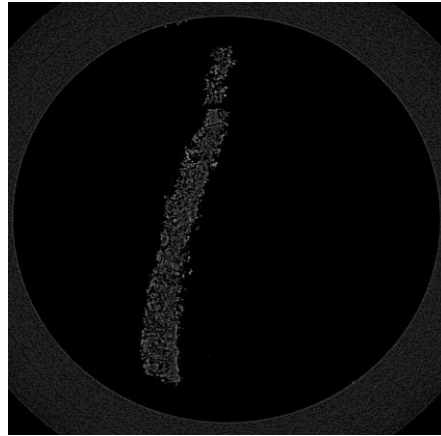


(a)



(c)

Set 3



(b)



(d)

Figure 6-36 X-ray images of ribbon as binder delivery (Set 1 & 3) and stress varied.

### 6.5 Results and discussion- Part 3: The effect of caking on granule content

During this section the influence of powder caking on the content uniformity will be investigated. The granules will be made from a blend of 90% w/w of lactose and 10% w/w of salt. The lowest liquid binder viscosity (i.e. distilled water) and a high shear stress (i.e. kneading element zone) in combination were used to produce granules. The size distribution, the mass of powder caking and the conductivity from three different locations (as described in section 6.2.4) are considered to assess the extent effect of powder caking.

Figure 6-37 shows how the size distribution of granules varies as it is collected after certain point of time (i.e. 2 min, 4 min, 6 min, 10 min, 15 min and 20 min). As expected there is minimal change in the size distribution as the operating conditions are expected to reach steady state after short time (e.g. 30 seconds). Any settle change (e.g. powder caking) within the system does not show to be reflected on the size, since a range of size are produced.

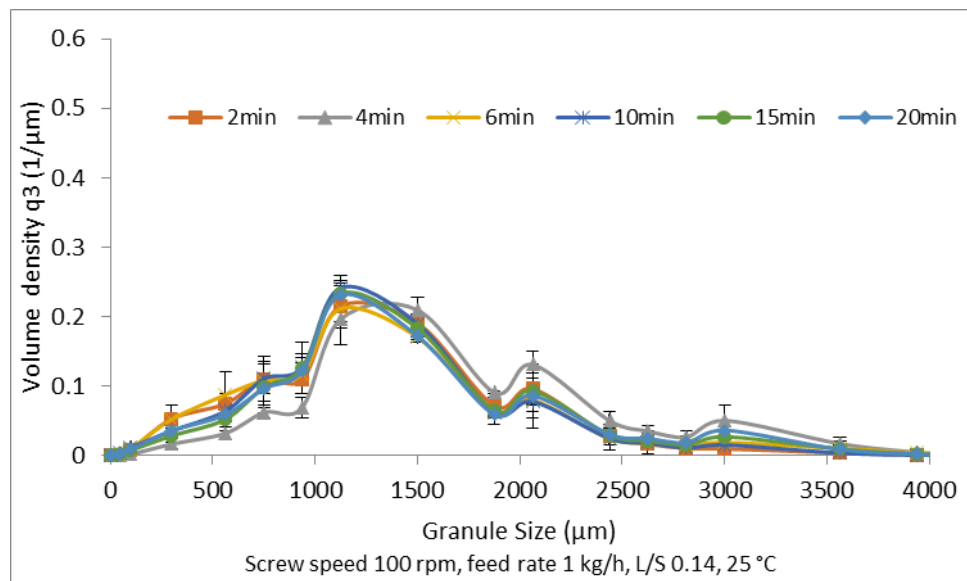


Figure 6-37 Size distribution granules with time produced with low liquid binder viscosity and high stress.

Figure 6-38 shows the mass of powder caking with time. The mass of powder caking show a significant increase at the early stages of granulation (i.e. up to 10 min), and as more time is allowed the mass change tend to plateau out (i.e. 10 – 20 min). This could be due to the available surface area in the early stages, which allows particles to adhere to the surface. As the time goes on less surface available given the clearance between the screw and the barrel is fixed at 0.5 mm.

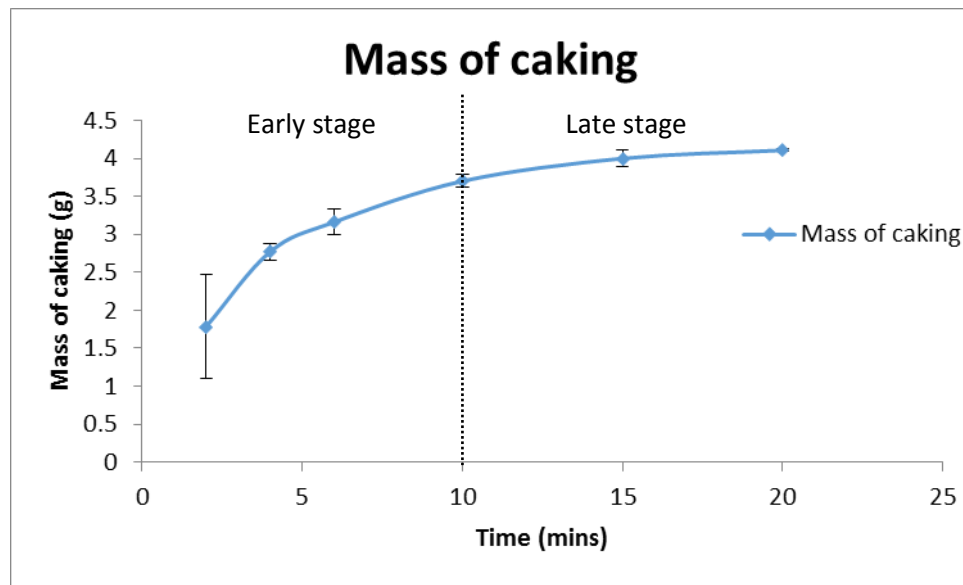


Figure 6-38 Mass (g) of powder caking with time.

Figure 6-39 shows how the conductivity of the salt within the blend, which is fed into the granulator (i.e. 2<sup>nd</sup> position in Figure 6-4). The salt conductivity shows slight variation at the early stage. This is not significant, as it is plotted against the average of the baseline.

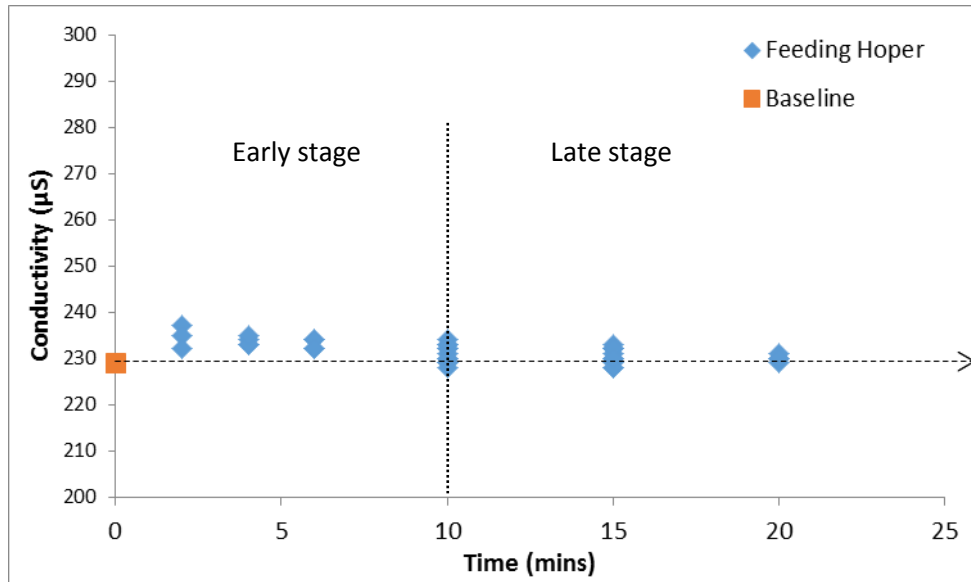


Figure 6-39 Conductivity of salt coming from the feeding hopper with time (min).

Figure 6-40 shows the variation in salt conductivity in the powder caking (i.e. 3<sup>rd</sup> position) with time. Although, the mass powder caking showed to increase with time, the salt conductivity showed to decrease with time. This could indicate that lactose tends to cake more than the salt. Such a variation could influence the integrity of content uniformity within the product.

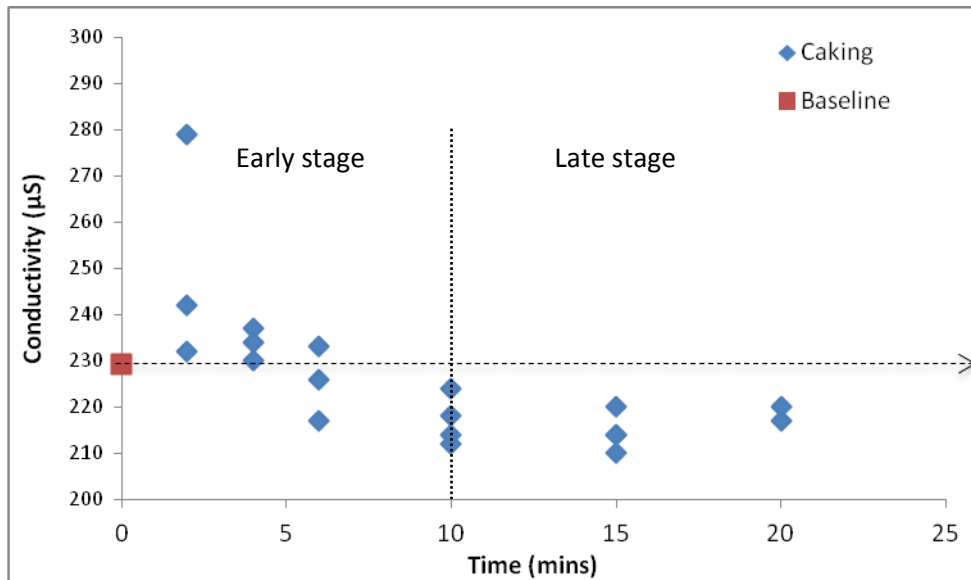


Figure 6-40 Conductivity of salt from the ribbon with time.



Table 6-2 shows the average mass (mg) of salt present in the powder cake as time varied.

<b>Time (min)</b>	<b>Salt in powder caking (mg)</b>	<b>Theoretical salt processed (mg)</b>	<b>Loss of salt within product (%)</b>
<b>2</b>	1186.06	6666.67	17.79
<b>4</b>	1085.59	13333.33	8.14
<b>6</b>	1061.23	20000.00	5.31
<b>10</b>	996.16	33333.33	2.99
<b>15</b>	990.45	50000.00	1.98
<b>20</b>	997.30	66666.67	1.50

Table 6-2 shows the average mass of salt (mg) within the powder caking for the top part of the barrel (the bottom part is not considered during this study). These results are considered against a theoretical amount of salt to be processed at a given time, with the assumption of 100% uniformity within the lactose and salt mixture. It shows a significant loss of salt at the start, however, as time increases the loss of salt due to powder caking is reduced. Although, such a loss may not seem significant, during a low drug loading, ensuring 100% uniformity of mixture and avoiding any API loss to either the upper/lower barrel-powder adhesion, will be of paramount importance to achieve consistent product quality.

## 6.6 Conclusion

The influence of liquid binder viscosity showed to be dominant during the low shear stress. Generally, increasing the liquid binder viscosity reduced the mass of powder caking while forcing powder caking to propagate from the centre of the barrel due to the localization. The tendency for powder to cake was also largely dependent on the powder used (e.g. lactose highest and MCC lowest) due to different mechanisms. The effect of liquid binder viscosity on the surface topography during low stress was also dependent on the powder used (e.g. lactose unaffected and MCC plastically deformed). Regardless of the liquid binder viscosity the ribbons of powder caking were loosely pack forming air voids within the structure, due to the low shear stress applied on the material.

Increase the shear stress, showed different trends of powder caking as liquid binder viscosity changed depending on the powder used. Despite the different trends increasing the liquid binder viscosity gave generally higher mass powder caking, while showing a uniform behavior of the caking (i.e. start from one end and to the other of barrel). The increase of shear stress also showed to give a more compacted surface with less porosity.

The powder caking phenomena showed possibility of influencing the content uniformity of drug product, as the content could change due to different tendency of the component within the blend to cake. Finally, the powder caking phenomena showed insignificant difference in trends as the material of the barrel changed.

## **Chapter 7 Mechanistic understanding twin screw granulation**

This chapter studies the material flow within the barrel, where the conditions involved the use of the same combination of starting material and granulation liquid as that described for lactose and MCC (in Chapter 3) and Binder delivery in (in Chapter 4). The process was scaled down where screw speed and feed rate have been lowered to 10 rpm, and 100 g/h, respectively. This was done to reduce the powder caking to the surface of the transparent barrel, which enables the material flow to be optically monitored.

The Particle Image Velocimetry (PIV) technique gave valuable insight to the understanding of the mechanism of the twin screw granulation. It showed a variation in the surface velocity of granules from one screw to another, during low shear. This was related to the material obstruction between the screws (intermeshing area) either by big granule entrapment (during high liquid binder viscosity) or increase in fill level (MCC swelling). Furthermore, applying high shear stress showed to minimise the difference between the two screws while giving a lower surface velocity overall. The indifference of the surface velocity of granules between the screws was seen to be related to the size distribution. The overall reduction in surface velocity was related to the material build up prior to the kneading elements zone and the higher probability of liquid binder availability on the surface. This helped to dissipate energy and lower the surface velocity.

### **7.1 Introduction**

The twin screw granulation remains within the launching stages in pharmaceutical field. This is due to the limitation in mechanistic understanding of the process. Such an understanding includes the flow pattern of the dense granules as process and formulation parameters vary. Studying the flow of the material could be challenging due to difficulties in performing representative measurement. This led to a number of studies considering other options such as tracking a tracer [17, 124-127]. Positron Emission Particle Tracking (PEPT) [17] is an example, which is frequently used within the twin screw granulator.

Although, such a technique provides useful information, it is limited to a single radioactive particle which is not presentative of the bulk flow of granules.

Furthermore, imaging technique such as Particle Image Velocimetry (PIV) provided insightful information in process such as high shear mixer [128], the spheronization process [129] as well as a two-dimensional spouted bed (2DSB) [130]. Dhenge et al [33] has taken the initiatives to apply such a technique to optically monitor the flow of the material in TSG. It was found that the flow of the material varies from one screw to another, which was related to the accumulation of powder between the two screws. While the information generated mark a step toward improving the mechanistic understanding of twin screw granulation, the influence of process (e.g. screw configuration) and formulation parameters (e.g. material and liquid binder viscosity) on the flow of material are yet to be explored. Their study consisted of the formulation while operating under 'dry' conditions, as the liquid binder used was not adequate to produce granules (L/S 0.06), where the screw consisted of only conveying element. Such conditions may have not been representative of the granular's flow.

Therefore, the study within this chapter aims to apply such a non-intrusive technique, on the twin screw granulation. This will be done by operating under condition which is capable of producing granules rather than just dry operation conditions. The change of the screw configuration will also be considered while varying the material type and liquid binder viscosity. The operating conditions will be a scale down from those for lactose and MCC (in Chapter 3) and binder delivery (in Chapter 4).

## **7.2 Particle Image Velocimetry (PIV) background**

PIV involves the use of a camera to capture the bulk of powder in motion. The captured images are transferred and analyzed within Matlab program (MPIV toolbox). MPIV provides different algorithms (Cross-correlation or MQD (Minimum Quadratic Difference)) to translate the images into surface velocity. This technique was firstly used to measure the flow of transparent fluid phases that contained a low fraction of solids or gas tracer. This was possible by considering two consecutive images that shows a small movement of

the particle (distance); with the knowledge of the time difference between the two images, the velocity (mm/s) is calculated. However, this was not as simple when measuring the flow of granular materials, as most of the particles have a similar look. Therefore the movement of a bulk of particles is considered rather than singular ones.

### 7.3 Experimental and analysis methodology

#### 7.3.1 Experiment Condition

This investigation involved using the same combination of starting powder and liquid binder as that described for lactose and MCC (In Chapter 3) and Binder deliver in (in Chapter 4). However, the screw speed and feed rate were lowered to 10 rpm, and 100 g/h, respectively. These conditions were chosen after trials under several conditions to minimize the possibility of powder caking during operation. Scaling down such a process could be done via various considerations. Examples of possible routes are; the channel fill, tip speed or Specific Mechanical Energy (SME, J/kg).

The choice of operation conditions, for this study, were reasoned by the theory related with the dimensionless group as scaling factor proposed by Juan G. Osorio and Lamprou3 [131], which considers the channel fill. This was referred to as powder feed number (PFN) and it tends to govern the flow of the material within the barrel given. PFN is a theoretical volumetric fraction of channel fill of powder at given powder feed rate,  $\dot{m}$ , and screw speed,  $N$  with a mean bulk density of  $\bar{\rho}_B$  within the channels of the screw as shown in Equation 7-1 [131].

$$\text{PFN} = \frac{\dot{m}}{\bar{\rho}_B \left( V_F \frac{S_L}{L} \right) N} \quad \text{Equation 7-1}$$

The bracketed terms in the denominator equate to the theoretical volume displaced per rotation of the screw. The conveyer free volume  $V_F$ , is the volume of the channels available for material. The value of  $67.75 \text{ cm}^3$  was determined using ScrewConfig software from ThermoFisher for the 16 mm Prism Euro Lab Twin Screw Granulator with a 25:1 L/D

(length to diameter ratio).  $S_L$  is the lead length of the screw which is axial advancement of the screw during one complete turn ( $360^\circ$ ). Since the volume displaced per rotation kept consistent, changing the screw speed ( $N$ ) and the powder feed rate ( $\dot{m}$ ), by the same factor (i.e. 10), to obtain the same PFN which could theoretically result in similar granule properties in comparison with higher scale.

### 7.3.2 PIV system Set-Up

The experiments were carried out using specially built transparent acrylic barrel. A high speed camera (Photron Fastcam 1024 PCI, Itronx Imaging Technologies, Inc. Westlake Village, CA, US), was set at a frame rate of 60 fps, which was considered to be high enough to account for a small motion of the powder from one image to the consecutive one. The resolution of the images was 512x512 (pixels x pixels). The camera was positioned perpendicular to the barrel at 1.5 cm from the end of the barrel, as it is shown in Figure 7-1 (a). A typical images captured from this set-up is shown Figure 7-1 (b).

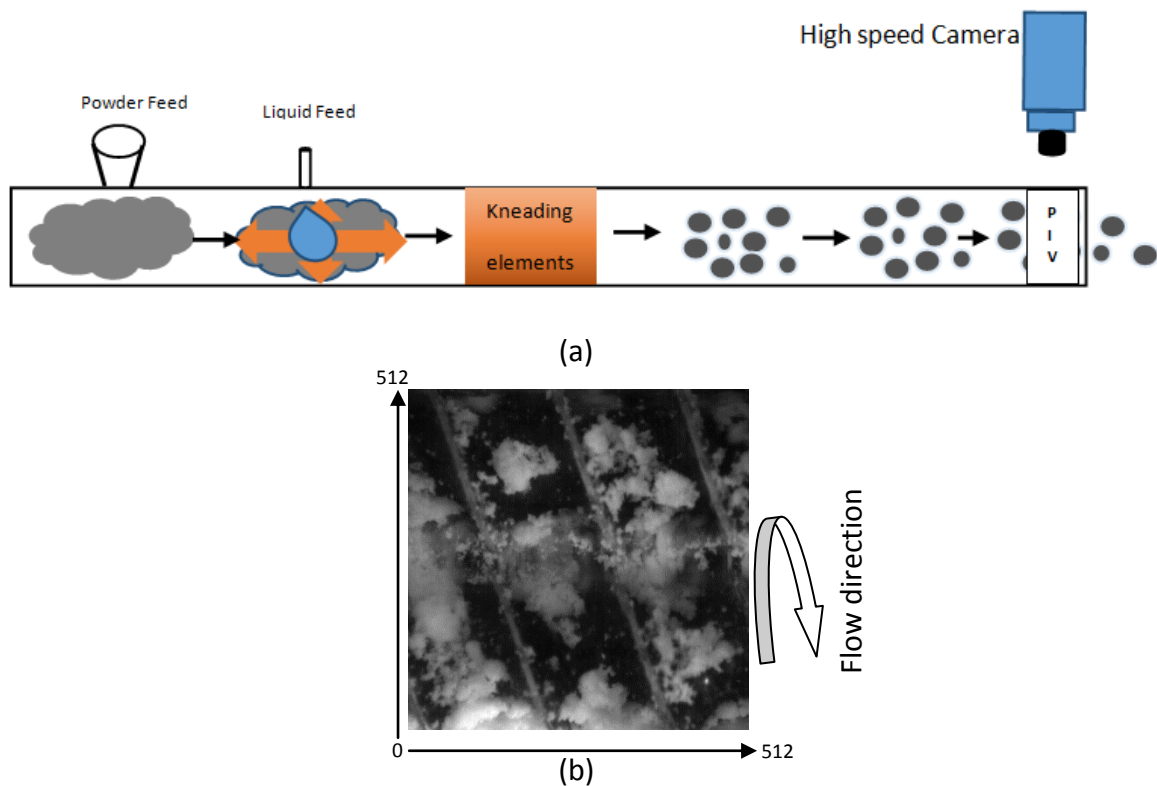


Figure 7-1 shows PIV set up (a) and an example of images taken (axis shown) (b).

### 7.3.3 PIV analysis

The images were firstly calibrated in Image-J software against a known distance (distance of the two flights of the screw). This was carried out in order to account for the actual distance (in mm) shifted by the powder from one image to the consecutive image (i.e. mm/pixels). The images were then analysed in MPIV toolbox, which is written in MATLAB 7.1 software (MATLAB R2008a, MathWorks) [132]. The MPIV toolbox contains two programs; one is used for image processing and the other for post-processing.

The image processing toolbox analyzes the images to give the average resultant surface velocity of the bulk powder,  $U_{aver}$ . The average resultant surface velocity (which will be referred to as 'surface velocity' in this study) is determined by considering the velocities in the X and Y components (as shown in Figure 7-1 (b)) as the flight movement will give a rise to the velocity in axial and transaxial direction. The X component gives the velocity,  $U_x$ , of the bulk powder moving in the horizontal plane perpendicular to the direction of the rotation of the screw. The Y component gives the velocity,  $U_y$ , of the bulk powder moving along the direction of the screws rotation.

The analysis was done using the Minimum Quadratic Differences; MQD algorithm. This algorithm gives smaller error during the calculation of the displacement than Cross Correlation Algorithm (COR) [132]. The MQD algorithm divides the image into small areas called 'interrogations'. Each interrogation area consisted of 32 x 32 (pixel x pixel), which the programme assigns it with a central grey value. The MQD then calculates the spatial shift of each interrogation area in the consecutive image, by considering the difference in grey value between the two images. This is referred to as the 'grey level difference accumulation'. To calculate the velocity, by which the spatial shift (i.e the number of pixels in which the bulk of powder has shifted) is converted into distance (in mm) from the calibration and then dividing by the time (s) between the two consecutive images (i.e. 0.0167 s). This algorithm applies the same principle for each interrogation area, where it

gives velocity vectors over the image, as shown in Figure 7-2. Further details of two algorithms are reviewed by Dhenge [33].

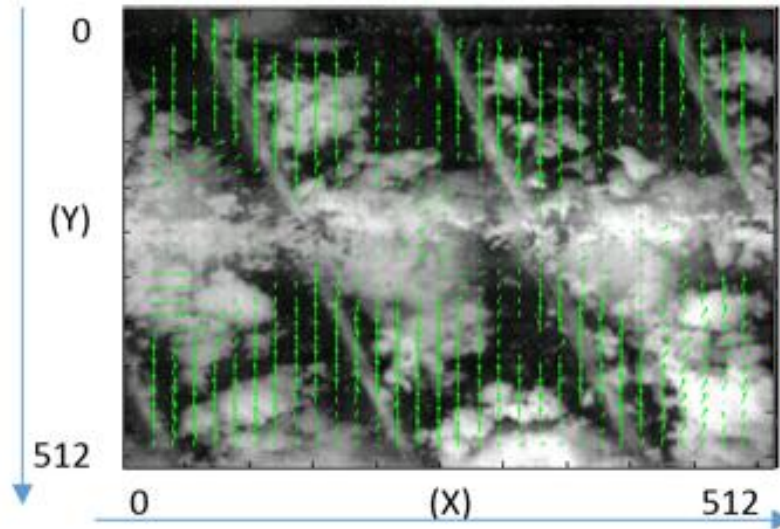


Figure 7-2 Velocity in each integration area.

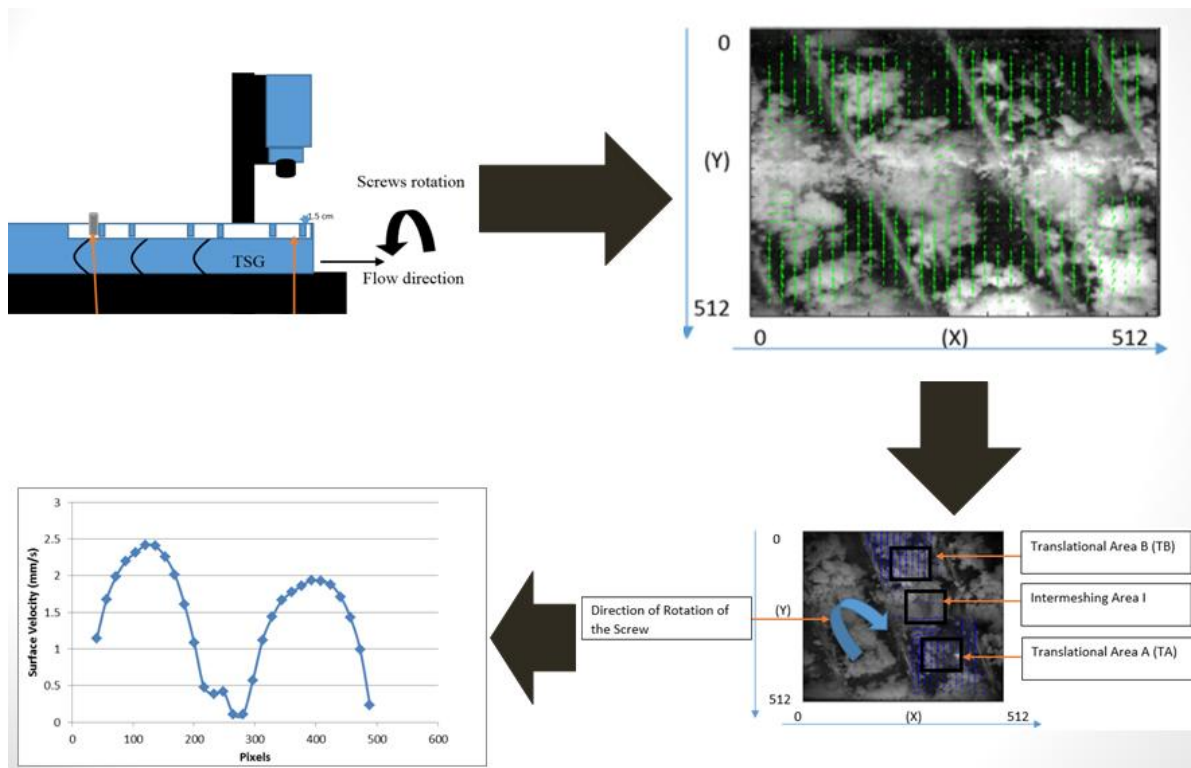
The velocity of the vector is extracted using FORTRAN program, which is then further processed using the post-processing in mpiv toolbox to filter the vectors, so only the velocity within a chosen channel is considered. This is the channel between two screw flights in one full screw revolution during this test, and it is indicated by the blue vectors in Figure 7-3 (a).

Due to the limits of 2D images, it is difficult to monitor the velocity of the vectors towards the intermeshing and sides regions of the barrel. Therefore, the screw channel was divided into three areas; Intermeshing Area, I (area between the two screws), Translational Area A (TA) (taking the material into the intermeshing) and Translational Area B (TB) (taking material away from the intermeshing) as shown in Figure 7-3 (b). These areas were considered to be the apex of the screw where the flow of the powder is perpendicular to the camera. This eased the monitoring and hence quantifying the surface velocity, which can be seen from Figure 7-2 that the vectors show one direction. However, the intermeshing area was not considered as it was difficult to account for the velocity because of the protruding edge of the barrel at that particular point. Also, as the powder



moves upwards and downwards the camera cannot capture the true movement, and this is illustrated by the inconsistent vectors shown in Figure 7-2 around the middle of the screws.

To get one single value to make the comparison easier, an average resultant surface velocity,  $U_{aver}$ , was considered (it will be called surface velocity during this section). This was calculated by averaging the velocity of vectors over the both translational areas (TA and TB) in given area of each translational area in the Y-direction, as shown in Table 7-1.



(a)

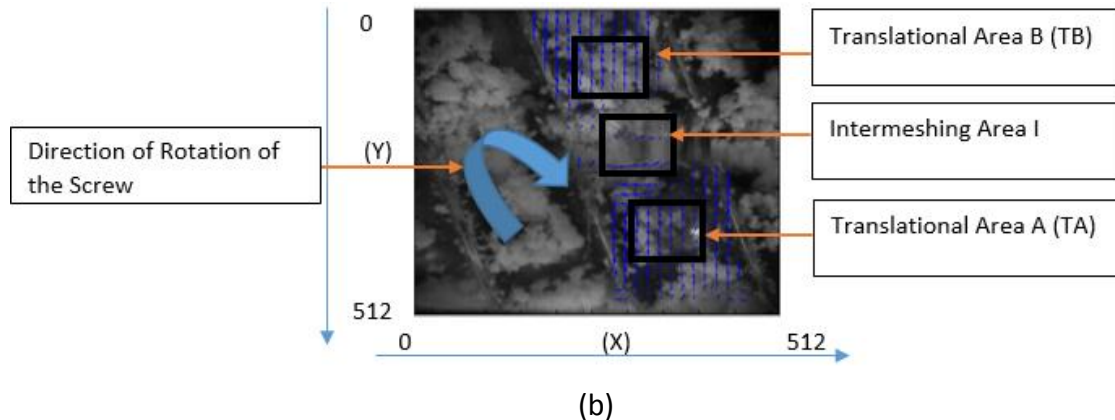


Figure 7-3 Steps of analyzing images for surface velocity (a) and the three areas of each image (b).

Table 7-1 Position of the translational areas in the Y-direction.

Translational area	Pixels (Y-direction)
TB	100-150
TA	350-400

## 7.4 Results and discussion

### 7.4.1 Lactose

#### **Surface velocity**

Figure 7-4 shows the change in average resultant surface velocity,  $U_{aver}$ , of the granules in TA and TB as the liquid binder and shear stress varied. At low shear stress (in Figure 7-4 (a)), increasing the liquid binder viscosity showed to increase the difference in the surface velocity of the granules between TA and TB. TB shows to have a higher surface velocity than TA for the high liquid binder viscosity. This is could be due to the reduction of possible flow obstruction as the granules are conveyed away from the intermeshing area in to TB. Increasing the liquid binder viscosity reduced the liquid spreading causing more localization of the big granules within the intermeshing area. This acts as an obstruction resulting in more collision of the granules conveyed from TA to the intermeshing area. Increasing the collision increases the energy dissipation and hence lowers the surface velocity [129]. In the case of low liquid binder viscosity, the liquid is expected to be distributed more resulting in a narrower size distribution and dissolving more powder of lactose. As result, the incoming

granules (from TA) will be able to displace the granules already present within the intermeshing. This limits the accumulation of granules within the intermeshing area. Since the fill level within the two screws is expected to be similar, the granules within TA and TB may have experienced similar energy dissipation. The fill level in TA and TB as the liquid binder viscosity varied can be visualized as shown in Figure 7-5 (a & b).

Increasing the shear stress, in Figure 7-5 (B), showed to reduce the surface velocity of the granules regardless of the liquid binder viscosity. Furthermore, increasing the liquid binder does not show significant effect in the surface velocity of the granules in TA and TB as there is no difference. The reduction in surface velocity of the granules could be attributed to the material build up prior to the kneading element zone, as illustrated in Figure 7-6, and presence of more liquid on the surface of the powder. The kneading elements zone shows minimal conveyance ability, and as result the material tends to build up prior to the kneading to generate enough pressure to cross zone. This build up will tend to bring the granules' velocity to zero and hence reduces its overall surface velocity before it reach exist. Additionally, the kneading elements will consolidate the granules forcing the liquid binder to migrate to the surface of the granules. The presence of liquid will help to dissipate the energy more upon collision causing the surface velocity to go down.

The insignificant difference of surface velocity of granules between in TA and TB may be due the narrower size distribution as higher sheer stress applied. This means no oversized granules will be entrapped within the intermeshing as granule of similar size will have the capability to displace each other. This ensures the smooth flow of granules in the intermeshing forming similar fill level in both TA and TB (regardless of liquid binder viscosity), which shown in Figure 7-5 (c & d). The granules will experience similar collision and hence similar energy dissipation.

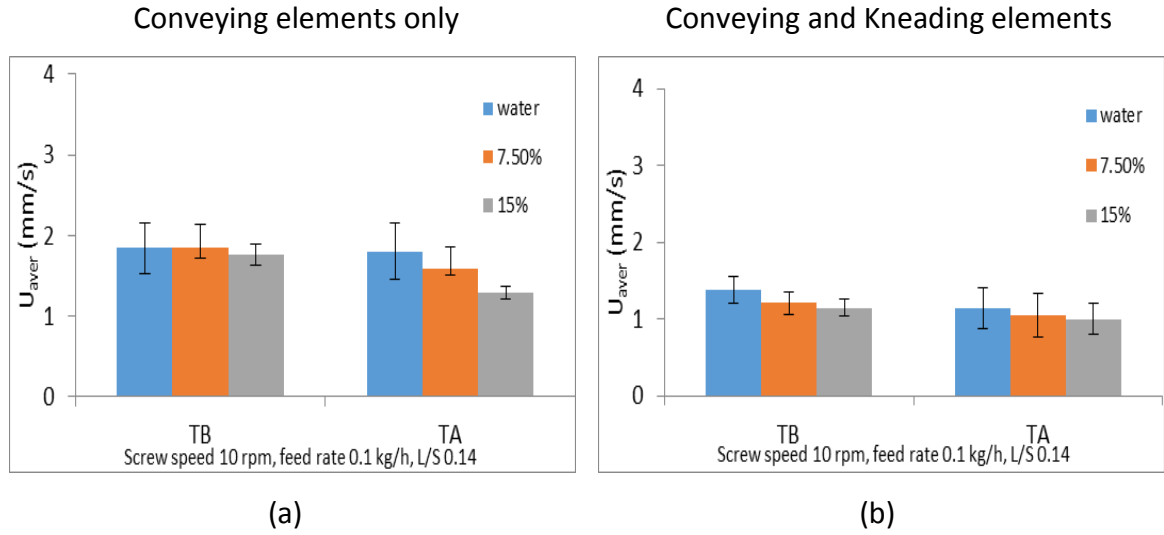


Figure 7-4 Effect of liquid binder viscosity on the surface velocity of lactose granules in the translational areas (TB and TA): (a) low stress and (b) high stress.

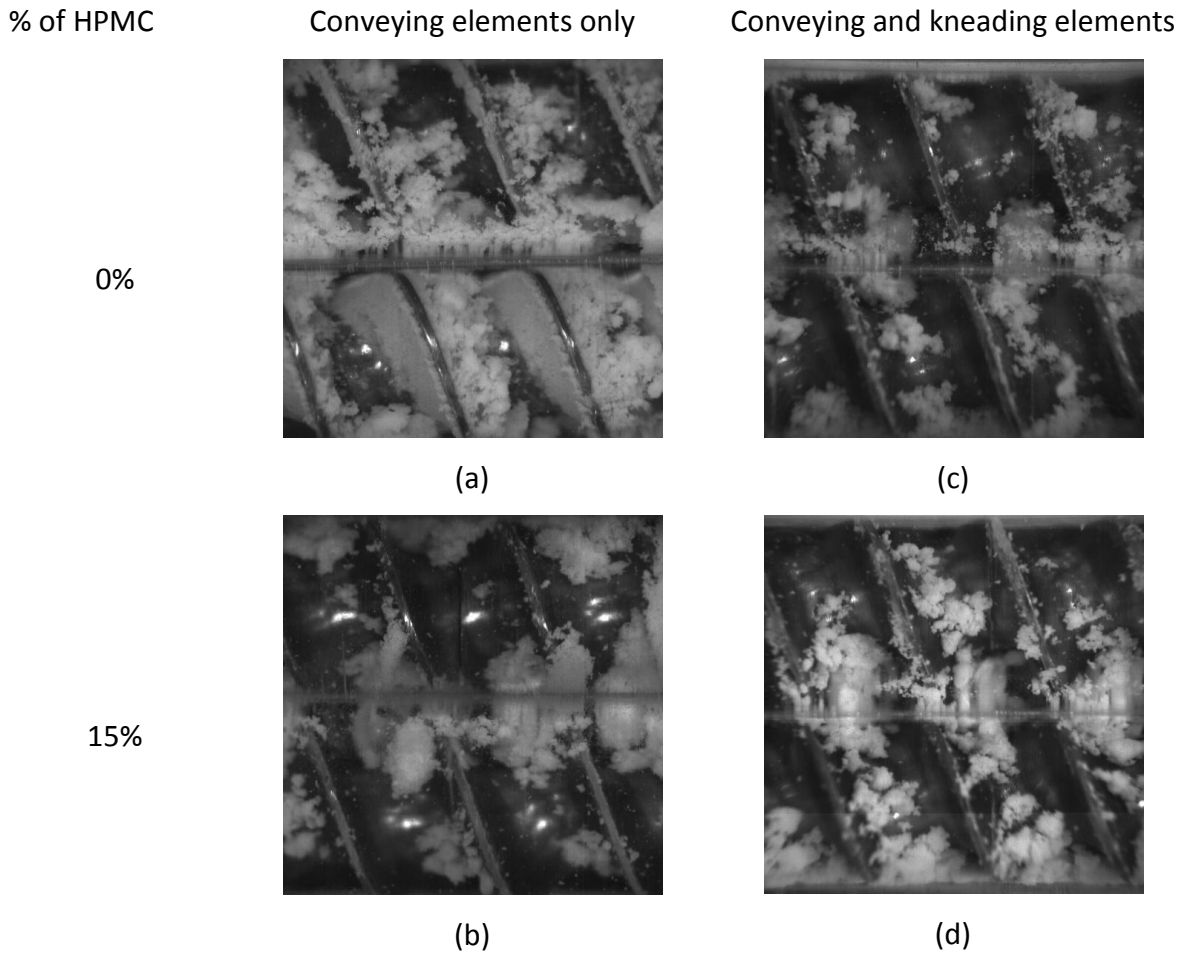


Figure 7-5 Effect of liquid binder viscosity on the channel fill as stress varied.

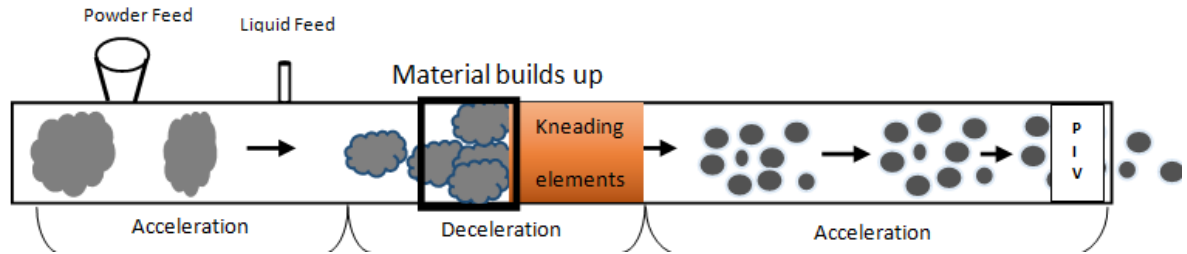
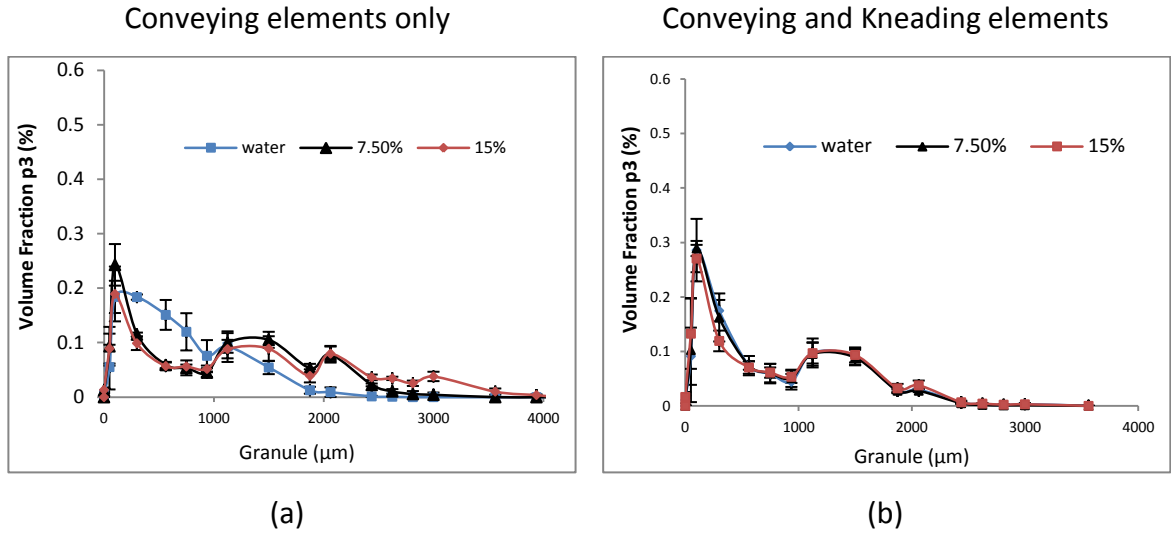


Figure 7-6 Describes the phenomena of the material build up prior to the kneading elements schematically.

### ***Granule size distribution and shape***

Figure 7-7 shows the size distribution and Figure 7-8 shows the shape of lactose granule as the liquid binder viscosity and shear stress varied. This is done to account for the granule's difference when compared with their corresponding findings seen in Figure 4-6 and Figure 4-10, respectively. At low shear stress, it shows that scaling down of the process (while keeping same PFN value) did not affect the size distribution (as shown in Figure 7-6 (a)) or the granules shape (as seen in Figure 7-7 (a-c)). Increasing the liquid binder viscosity gave a wider size distribution and more elongated granule shape. This show the conveying elements do not affect the granule's properties as much as the ability of the liquid binder to spread.

At higher shear stress, the size distribution (as shown in Figure 7-6 (b)) and granule shape (seen in Figure 7-7 (d-f)) showed to change as the process is scaled down. Changing the liquid binder viscosity did not result any change of the size distribution or granule property. This could be due to the kneading elements which show minimal conveyance ability, where the material will build up and as it enters the zone it will undergo consolidation and change in density of agglomerates. As the agglomerate leave the zone they will be smears and crumbled and as result the agglomerate will experience minimal agglomeration, where granules shows to have the kneading element signature (indicated by the flat surface) as seen in Figure 7-7 (d-f).



Screw speed 10rpm, powder feed rate 100g kg/h, L/S ratio 0.14, 25°C

Figure 7-7 Effect of liquid binder viscosity on size distribution of lactose granules: (a) low stress and (b) high stress.

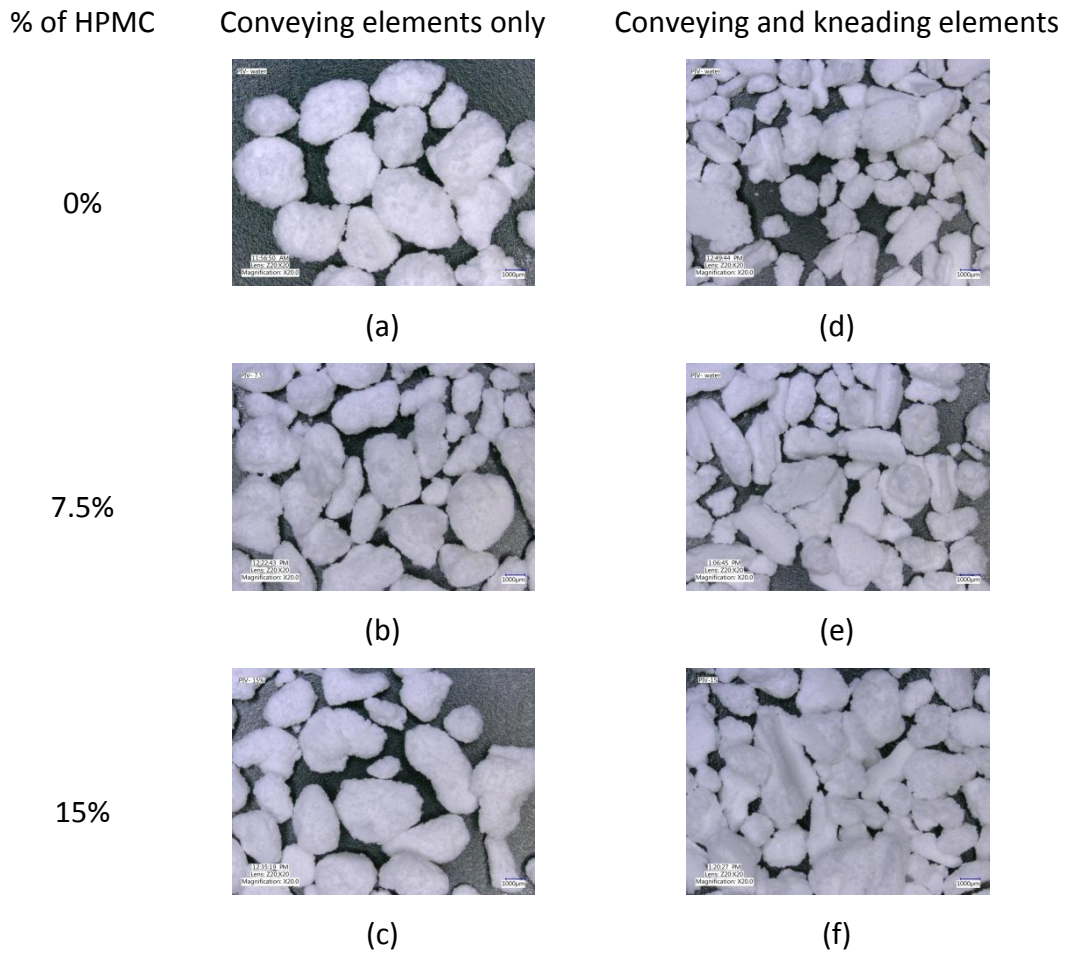


Figure 7-8 Effect of liquid binder viscosity on the shape of lactose granules as the stress varied.

## 7.4.2 MCC

### **Surface velocity**

Figure 7-9 shows the change in surface velocity,  $U_{aver}$ , of the granules in TA and TB as the liquid binder viscosity and shear stress varied. At low shear stress, the observation varies in comparison to that seen lactose, in Figure 7-4 (a). The surface velocity of the granules shows to be lower in TA than TB, regardless of the liquid binder viscosity (i.e. even for low liquid binder viscosity). For low binder viscosity the fill level of MCC granules within the barrel as seen Figure 7-10 (a) shows to be higher when compared with that seen in Figure 7-5 (a) for lactose. This could be related to the difference in material's property. The MCC has the ability to retain the water and swell in size [109, 110]. The lactose granule fill level showed to be significantly lower, which could be due to ability of low liquid binder viscosity to partially dissolve the lactose and form lumps and hence reducing the channel fill. The increase in fill level for the MCC may have caused the obstruction in the intermeshing area, where the material leaving the intermeshing into TB experienced less collision and hence, less energy dissipation and therefore, higher surface velocity. For the case of high liquid binder viscosity, the obstruction the granule's flow from TA may have been caused by the entrapment of big granules (due to liquid binder localization) as seen in Figure 7-10 (b).

At higher shear stress, the difference in surface velocity in TA and TB is minimized while showing a reduction in comparison with low shear stress. This is similar to what have been observed with lactose. Therefore, the reduction could be associated with the ability of kneading elements to give a narrow size distribution (as seen in Figure 4-18 (b)) and the deceleration caused by the material build up prior to the zone.

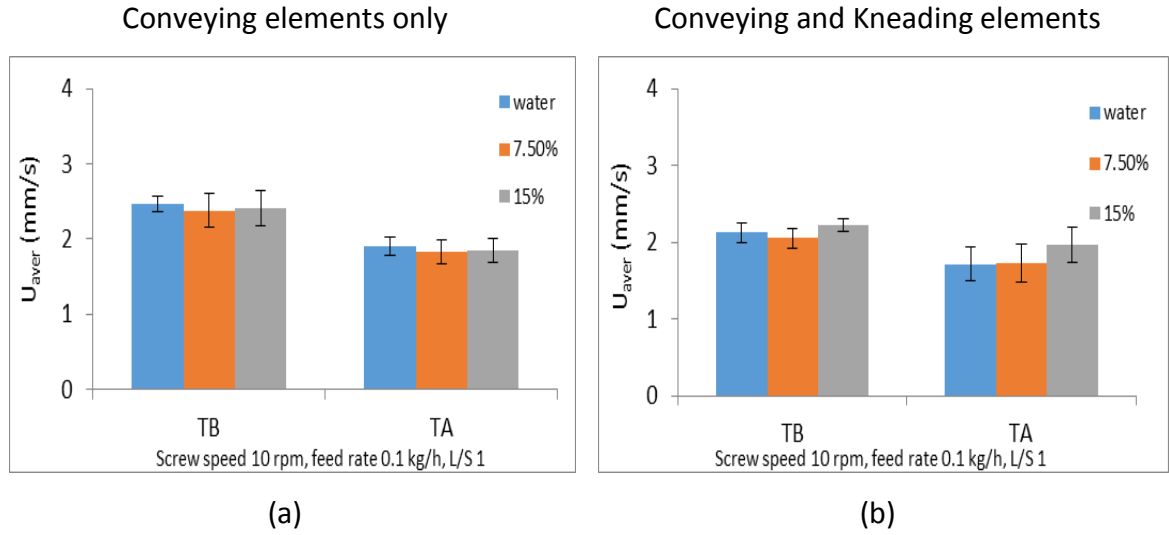


Figure 7-9 Effect of liquid binder viscosity on the surface velocity of MCC granules in the translational areas (TB and TA): (a) low stress and (b) high stress.

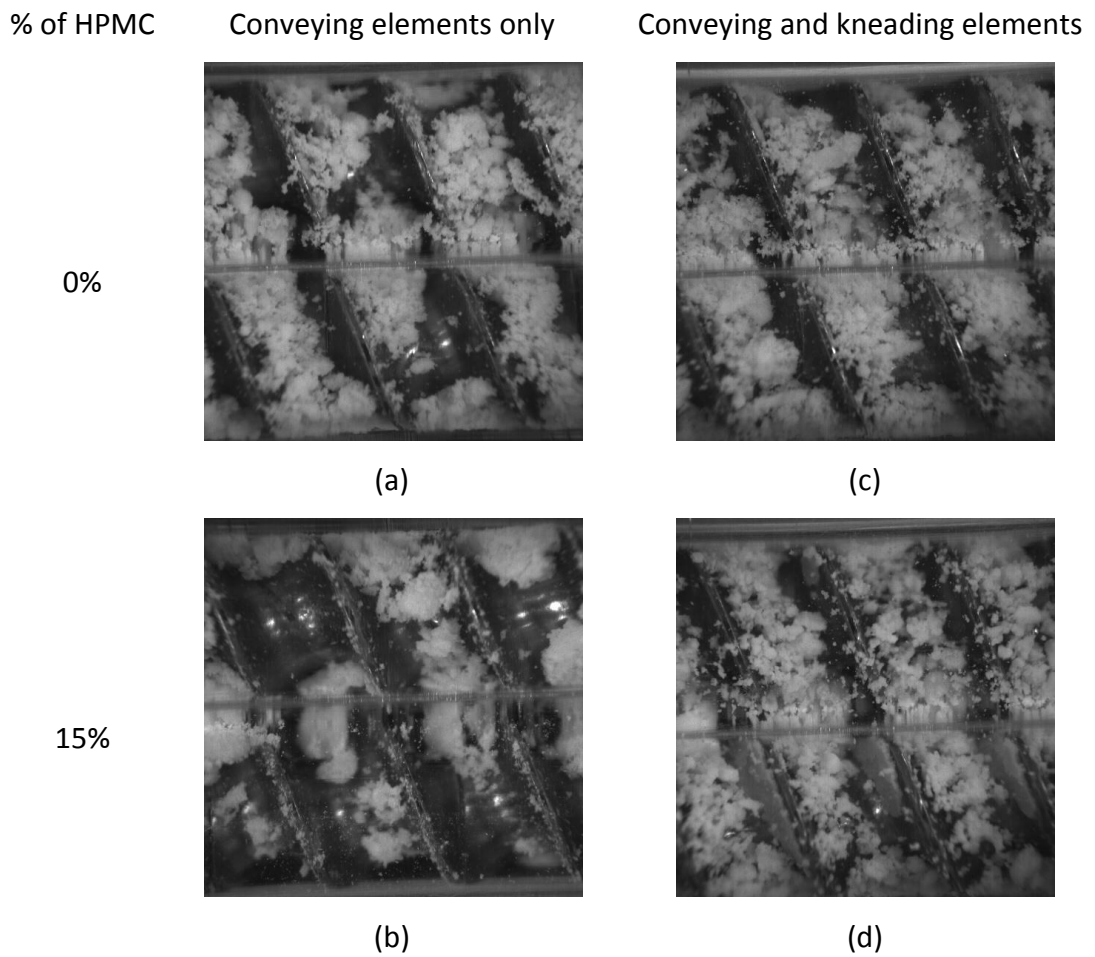
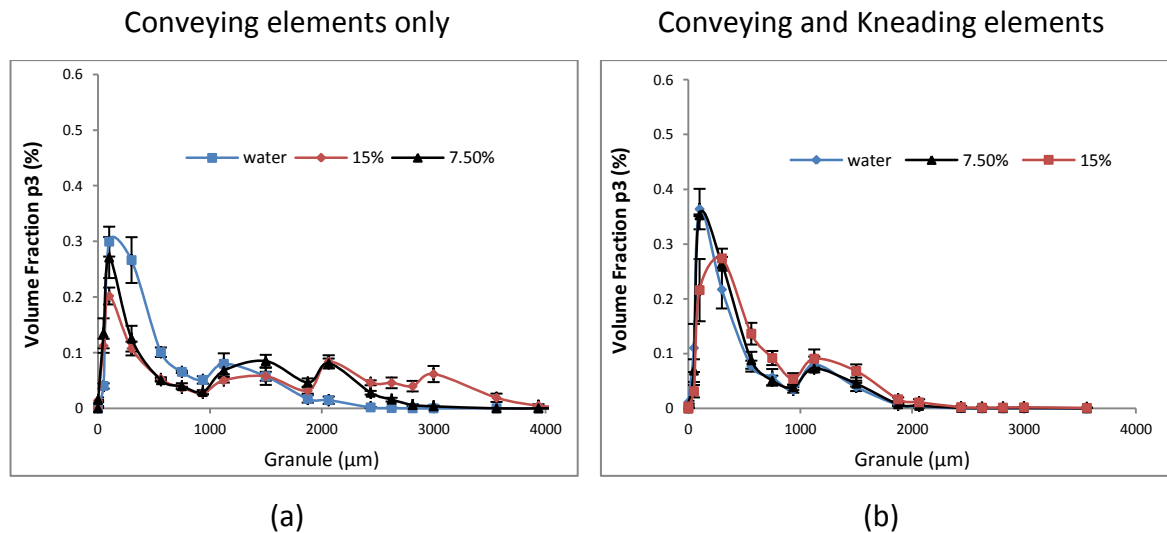


Figure 7-10 Effect of liquid binder viscosity on the channel fill as stress varied.



### Granule size distribution and shape

Figure 7-11 shows the size distribution and Figure 7-12 shows the shape of MCC granule as liquid binder viscosity and shear stress varied. These findings are compared with those found in Figure 4-18 and Figure 4-21, respectively for the higher process scale. Applying low shear stress produced similar findings in shape and granules, emphasising the importance liquid binder ability to spread, regardless of material. Increasing the shear stress, showed to give similar granule properties (i.e. size distribution and shape), regardless of the liquid binder viscosity. This is similar to the observation seen in lactose, which indicate the change of the granules density after passing the kneading element zone.



Screw speed 10 rpm, powder feed rate 100 kg/h, L/S ratio 1, 25°C  
Figure 7-11 Effect of liquid binder viscosity on size distribution of MCC granules: (a) low stress and (b) high stress.

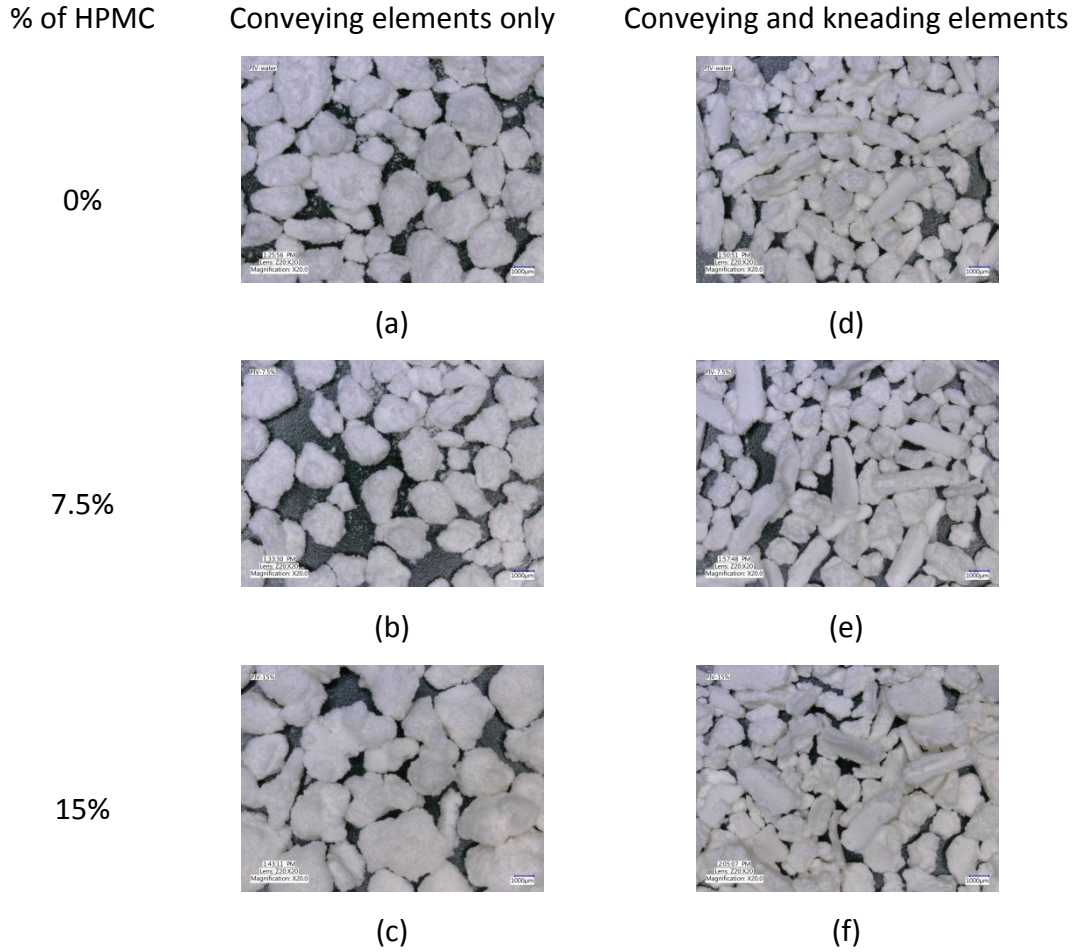


Figure 7-12 Effect of liquid binder viscosity on the shape of MCC granules as the stress varied.

### 7.4.3 Binder Delivery

#### **Surface velocity**

Figure 7-13 shows the change in surface velocity,  $U_{aver}$ , of the granules in TA and TB as the binder delivery and shear stress varied. At low shear stress, the difference in momentum generated by granules in TA and TB as showed to increase, as more HPMC is delivered in the liquid form (e.g. Set 3). As more of the HPMC binder is delivered in the liquid form, the liquid binder viscosity increases. This causes more obstruction within the intermeshing area, due to liquid binder localisation. This can be seen in Figure 7-14 (a & b) where the fill level of granules shows to be similar in both screw during Set 1 while shown a big granules entrapped in the intermeshing area for Set 3. Hence, the granules conveyed from TA into the intermeshing will experience more collision for Set 3 and therefore reduction in surface velocity of the granules.

Although, increasing the shear stress did not show a difference between surface velocity in TA and TB for both Set 1 and Set 3, the overall surface velocity has been lowered in comparison with the low shear stress. The insignificant difference between TA and TB could be related to the narrower size distribution, where the reduction is related to the deceleration and liquid binder presence on the surface of the granules. The channel fill also shows to be similar in both screws, as seen in Figure 7-14 (c & d).

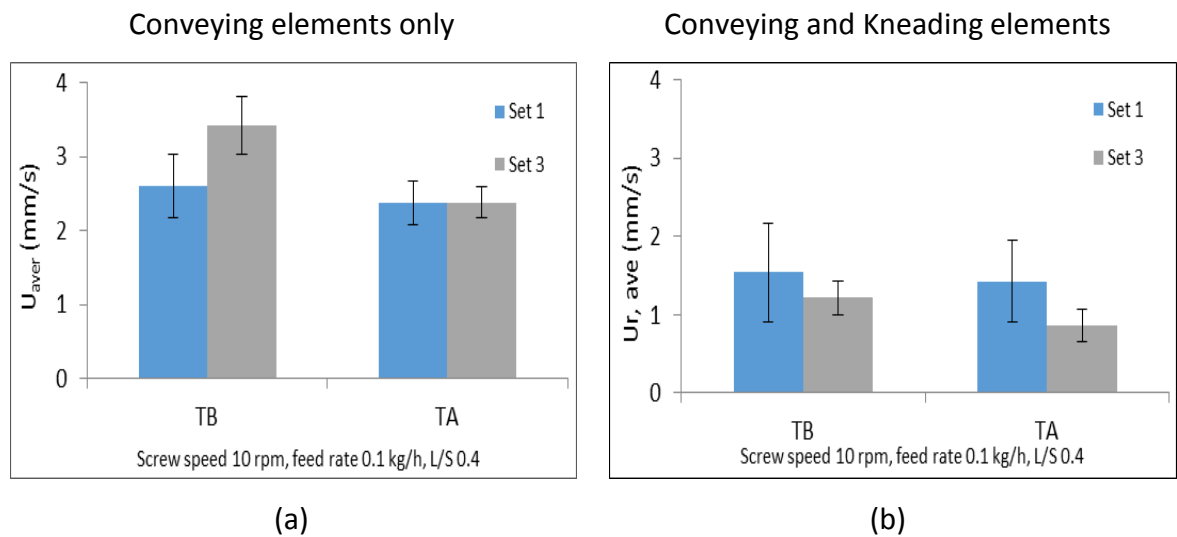


Figure 7-13 Effect of binder delivery on the surface velocity of granules in the translational areas (TB and TA): (a) low stress and (b) high stress.

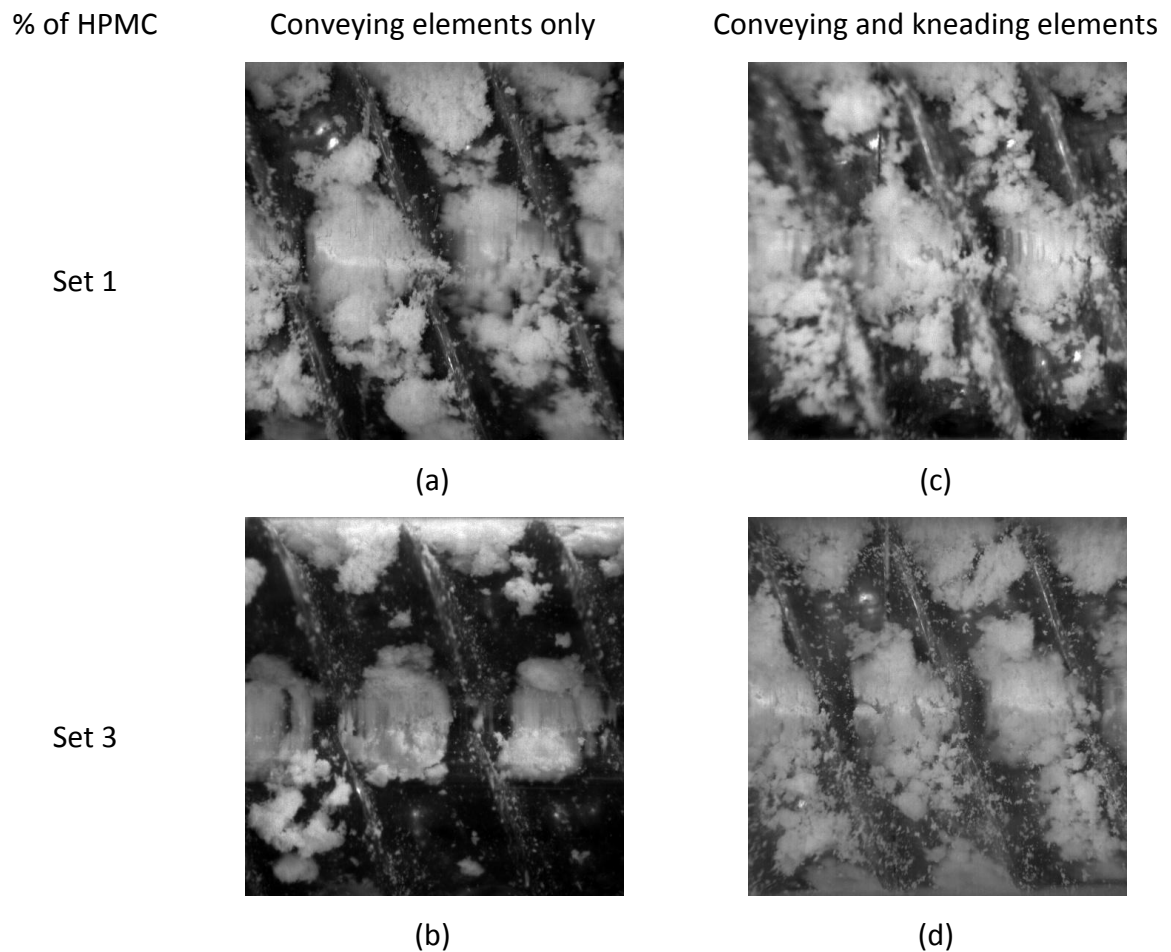
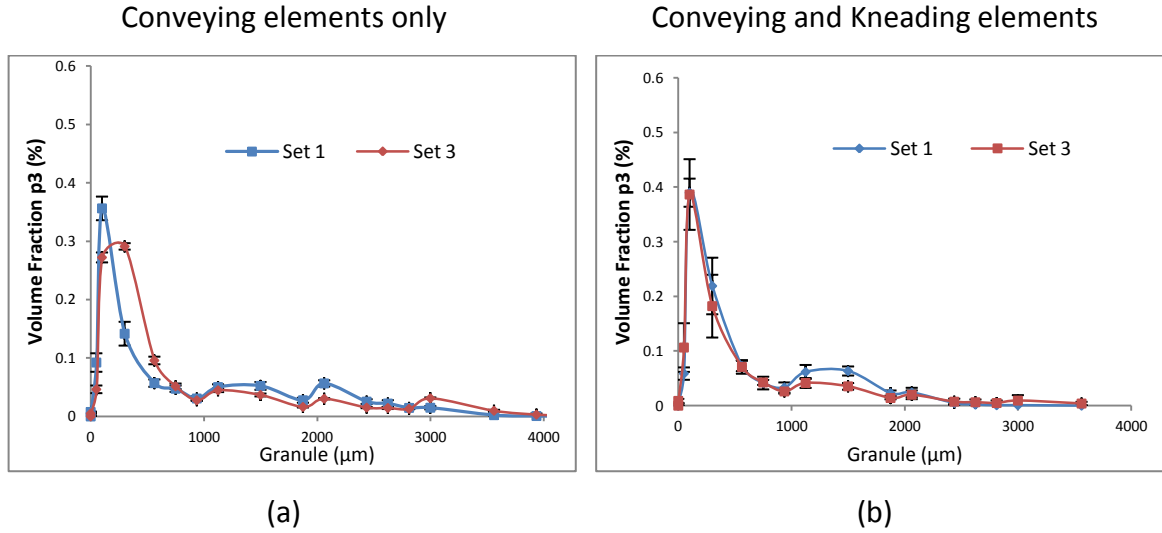


Figure 7-14 Effect of binder delivery on the channel fill as stress varied.

***Granule size distribution and shape***

Figure 7-15 shows the size distribution and Figure 7-16 shows the granules shape as the binder delivery and shear stress varied. These findings are compared with that seen in Figure 5-7 and Figure 5-10, respectively, at higher process scale. The granules size distribution and shape (as seen with lactose and MCC) shows to align well with findings at higher scale as well as the shape during low shear stress. This is further indication of the importance in the liquid binder ability to spread at low shear stress. Increasing the shear stress, showed different findings in that at higher process scale as the granules size distribution and granules shape showed to be similar regardless of the binder delivery. This is related to higher densification of material within the kneading element zone and

hence minimal impact on granules beyond the zone (i.e. in the consecutive conveying elements) at low process scale.



Screw speed 10 rpm, powder feed rate 100 kg/h, L/S ratio 0.4, 25 °C  
 Figure 7-15 Effect of binder delivery on the granules size distribution: (a) low stress and (b) high stress.

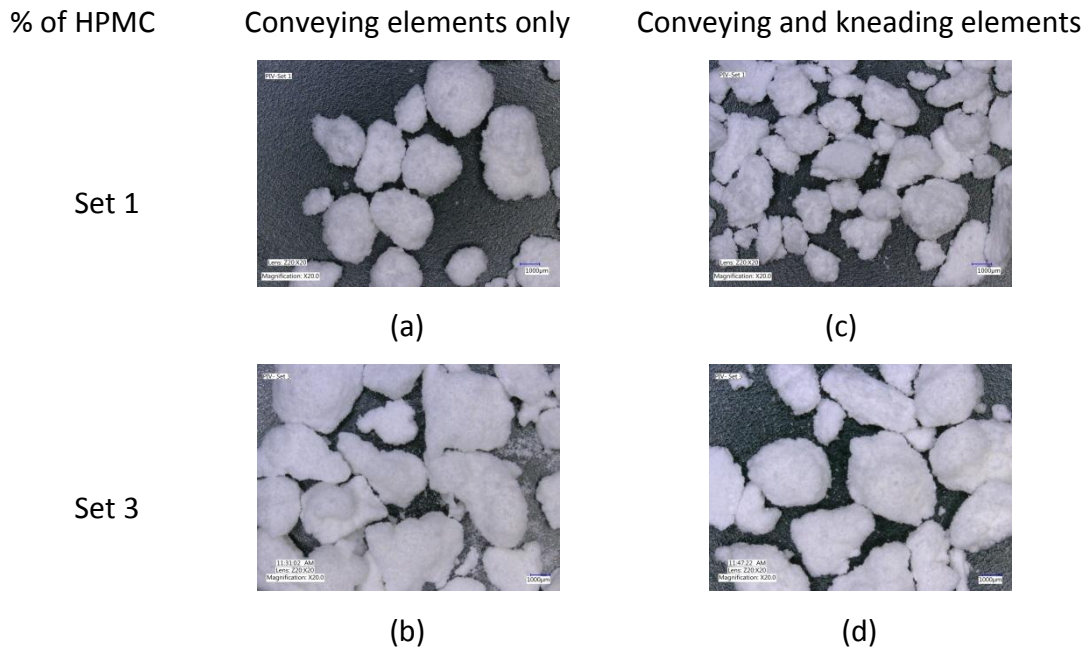


Figure 7-16 Effect of binder delivery on granules' shape as the stress varied.

## 7.5 Conclusion

The measurement of surface velocity using the PIV technique gave valuable insight to the understanding the mechanism of the twin screw granulation. It showed the difference in surface velocity between the two screws as the liquid binder viscosity varied, particularly during low shear stress. The surface velocity of granules in the screw which conveys the material into the intermeshing area (i.e. TA) showed to be the lowest. This was associated with the obstruction to granule flow which cause further energy dissipation as the granules experience more collision. The obstruction showed to be triggered by the entrapment of big granules (in the high liquid binder viscosity) due to localization or the increase of fill level.

At higher shear stress, the overall surface velocity of granules on either screw showed to decrease (regardless liquid binder viscosity). This was related to the deceleration and liquid availability on the surface. The deceleration of the granules was caused by the material build up prior to the kneading elements zone. The liquid availability on the surface of granule was caused by the consolidation of granules. Furthermore, the surface velocity of granules in TA and TB showed little difference. This was related to the narrower size distribution of granules, which minimised the entrapment for granules within the intermeshing area.

## Chapter 8 Conclusions

The influence of liquid binder viscosity (and binder delivery), on desired and undesired granulation, showed to depend largely on the shear stress being applied on the material during granulation. The property of the powder also showed to influence both desired and undesired granulation. Increasing the liquid binder viscosity (or delivering more HPMC in wet form during binder delivery) limited the ability of the liquid to spread. The process therefore, showed to depend largely on the stress applied on the material.

Increasing the viscosity of the liquid binder for low stresses (i.e. conveying elements only) on the desired granulation was similar for all powders. While for undesired granulation this was not the case as the property of the powder showed to influence the results. For desired granulation, the granules size distribution tends to widen in its range, while producing more elongated granules with increasing the liquid viscosity. The primary particles on the granule's surface remained unaffected while loosely bonded creating considerable voids within its internal structure. For undesired granulation, the adhering of powder caking onto the surface of the barrel was a function of liquid binder viscosity, regardless of the powder property. The caked powder started to adhere to the surface of the barrel from the side and advancing into the centre whilst using low liquid binder viscosity. This was the opposite behavior as the liquid binder viscosity increase, regardless of the powder. However, the mass of powder caking showed to be significantly affected by the powder properties. Lactose showed the highest tendency to cake on surface of the barrel in comparison to MCC and formulation. Furthermore, increasing the liquid binder viscosity showed to decrease the mass of powder caking for lactose and MCC, while initial decrease and a significant increase of mass of caked powder when using the formulation. The particles on the surface of the ribbons of powder caking showed, to generally remain unaffected for lactose however, were plastically deformed for MCC.

The effect of increasing the viscosity of liquid binder while applying high stresses (i.e. conveying and kneading elements) on the desired and undesired granulation was

dependent on the powder property. For desired granulation, lactose showed a shift toward larger granules ( $\geq 3000 \mu\text{m}$ ), while the MCC and formulation showed a reduction in big granules as the liquid binder viscosity was increased. The increase in shear stress also resulted in granules with rougher surface (in particular for the high liquid viscosity) regardless of the powder used. The particles on the surface of the granules showed to give a more compacted topography and less voids within the internal structure, regardless of liquid binder viscosity or material used. These changes were influenced by the increase in the shear stress.

For the undesired granulation, the powder caking showed a similar behavior, i.e. initiating from the sides of the barrel regardless of the liquid binder viscosity and the powder property. The mass of the powder caking was dependent on the powder property as well as the liquid binder viscosity. Increasing the liquid binder viscosity resulted in a reduction in mass of the powder caking for lactose and inconsistent trend (i.e. initial decrease followed by significant increase) for MCC while showing no trend for the formulation. The surface topography showed to be more compacted, while less air voids within the internal structure of the ribbon of powder caking. Furthermore, the powder caking phenomena showed possibility of deteriorating the drug product uniformity, as the content could change due to different tendency of the component within the blend to adhere to the surface of the equipment. Although, the barrel was changed, the main driving force for the powder caking phenomena was the process and formulation parameters.

Optical measurements of monitoring the powder flow using Particle Image Velocimetry (PIV) gave a valuable insight into the understanding of the mechanism of the twin screw granulation. During low shear stress, the momentum of granules showed to increase as the powder conveyed from the driving screw (i.e. conveying material into the intermeshing area) into the receding screw (conveying the material away from the intermeshing). This increase was caused by the reduction in flow obstruction as the granules moved away from the intermeshing area. The flow obstruction within the



intermeshing was caused by either increasing of liquid binder viscosity (i.e. giving a rise to entrapment of granules as they grew in size) or the increase in fill level (i.e. swelling of MCC powder).

At higher shear stress, the overall surface velocity of granules on either screw showed to decrease (regardless liquid binder viscosity). This was related to the deceleration and liquid availability on the surface. The deceleration of the granules was caused by the material build up prior to the kneading elements zone. The liquid availability on the surface of granule was caused by the consolidation of granules where the energy dissipation is expected to be higher. Furthermore, the surface velocity of granules in TA and TB showed little difference. This was related to the narrower size distribution of granules, which minimised the entrapment for granules within the intermeshing area.

## **Chapter 9 Future work**

Although, the twin screw granulator's popularity is rapidly growing owing to the variety of parameters which can be altered to achieve the desired product properties, a complete understanding of the mechanisms taking place is still not fully comprehended. This research has contributed to the understanding the role of binder, while exploring undesired by-product; however, there is a need to build upon this knowledge. Such knowledge could be enhanced by exploring the following areas:

### **9.1 Impact of change in screw configuration:**

The alteration of the screw configuration is expected to impart different stresses on the material. Such a change in a stress showed to significantly affect both the desired and undesired granulation. Therefore, there is yet a need to relate and understand the stress change on the twin screw granulation mechanisms. The screw configuration can be designed by the use of various elements, such as conveying element, kneading elements (which can be staggered at different angles), screw mixing element and tooth-mixing elements. This leads to a numerous possible ways of configuring the screws to give different designs. However, the variation of screw configuration was kept to two elements (i.e. conveying and 4 kneading elements staggered at 60°). Despite, the minimal change in screw configuration, this research has showed the influence it has on the material flow and hence the desired and undesired granulation.

### **9.2 Binder Activation**

During this study, it was observed that using low liquid binder viscosity (i.e. distilled water) gave a narrower size distribution such as in Set 1 during the binder delivery investigation (where the HPMC binder was delivered in the solid form). This was due to the ability of the liquid spread over shorter period of time. However, the strength of the granules will depend on the strength of the bridges created between them, where distilled water would naturally form weak granules in comparison to those which use HPMC to gel the particles

together. Delivering the HPMC in the liquid form would ensure uniform distribution of the HPMC binder. However, delivering the HPMC in the solid form would require an adequate amount of water to activate the binder. Therefore, it would add more value to understand the extent of HPMC which gets activated upon coming into contact with liquid within the barrel and how far along the barrel would this be achieved. This can be quantified by coloring HPMC particles with a dye where the concentration of the dye can be measured using UV spectrometer. Then granules which are produced can be collected from different regions of the barrel and analysed.

### **9.3 Powder caking/stickiness:**

This research focused on the undesired granulation as well as the desired granulation. It was noticed that different powder showed different tendency to adhere to the equipment surface. This could lead to serious problems as it could result in content non-uniformity within the drug product (e.g. Tablets). However, the significance of the effect on the drug product integrity caused by such phenomena is yet to be fully explored as this research set the platform for further investigation. Future work could focus in relating the properties of powder and its interaction with liquid binder. This could focus on determining the difference between the work of adhesion and cohesion as the property of the material and liquid binder varied.

Such information could be used to determining the optimal conditions in which the powder caking during twin screw granulation can be mitigated. Also, consider using pharmaceutical excipients which can act as anti-caking agent, such as Colloidal silicon Dioxide [133] (either as part of the formulation or coating). The internal surface of the barrel could also be coated with anti-caking agent which are in compliance with FDA regulation such as Teflon [134].

#### **9.4 Surface velocity/material flow:**

During this research, the surface velocity of granules was measured for different granulation conditions. However, due to the material stickiness on the internal surface and the optical limitation, the conditions were lowered and the velocities in the intermeshing could not be measured. Furthermore, the surface velocity was only considered near the exit, where the granules are assumed to be fully formed. Therefore, there is a need to consider monitoring earlier stages of the barrel. Such information could be very essential to the understanding of twin screw granulation mechanisms. There is a need to account of the change in agglomerate bulk density due to the kneading, which could be incorporated during the scaling down of the process scale.

## References

1. El Hagrasy, A. S., Hennenkamp, J. R., Burke, M. D., Cartwright, J. J., and Litster, J. D., *Twin screw wet granulation: Influence of formulation parameters on granule properties and growth behavior*. Powder Technology, 2013. **238**: p. 108-115.
2. Dhenge, R. M., Fyles, R. S., Cartwright, J. J., Doughty, D. G., Hounslow, M. J., and Salman, A. D., *Twin screw wet granulation: Granule properties*. Chemical Engineering Journal, 2010. **164**(2-3): p. 322-329.
3. Lee, K. T. Ingram, A. Rowson, N. A., *Comparison of granule properties produced using Twin Screw Extruder and High Shear Mixer: A step towards understanding the mechanism of twin screw wet granulation*. Powder Technology, 2013. **238**: p. 91-98.
4. Chen, Y. H., Yang, J., Dave, R. N., and Pfeffer, R., *Granulation of cohesive Geldart group C powders in a Mini-Glatt fluidized bed by pre-coating with nanoparticles*. Powder Technology, 2009. **191**(1-2): p. 206-217.
5. Kleinebudde, P., *Roll compaction/dry granulation: pharmaceutical applications*. Eur J Pharm Biopharm, 2004. **58**(2): p. 317-26.
6. Agrawal, Rajesh, *Pharmaceutical Processing – A Review on Wet Granulation Technology*. International Journal of Pharmaceutics Frontier Research, 2011. **1**(1): p. 65-83.
7. Keleb, Eseldin Ibrahim, *CONTINUOUS AGGLOMERATION PROCESSES USING A TWIN SCREW EXTRUDER*, in *Faculty of Pharmacy*. 2003-2004, Ghent University: Belgium. p. 188.
8. Cai, L., Farber, L., Zhang, D., Li, F., and Farabaugh, J., *A new methodology for high drug loading wet granulation formulation development*. Int J Pharm, 2013. **441**(1-2): p. 790-800.
9. Narang, Ajit S., *Addressing Excipient Variability in Formulation Design and Drug Development*, in *Excipient Applications in Formulation Design and Drug Delivery*, A.S. Narang and S.H.S. Boddu, Editors. 2015, Springer International Publishing. p. 541-567.
10. Roy, P., Khanna, R., and Subbarao, D., *Granulation time in fluidized bed granulators*. Powder Technology, 2010. **199**(1): p. 95-99.
11. Nakamura, H., Fujii, H., and Watano, S., *Scale-up of high shear mixer-granulator based on discrete element analysis*. Powder Technology, 2013. **236**(0): p. 149-156.
12. Vervaet, Chris and Remon, Jean Paul, *Continuous granulation in the pharmaceutical industry*. Chemical Engineering Science, 2005. **60**(14): p. 3949-3957.
13. Leuenberger, Hans, *New trends in the production of pharmaceutical granules: batch versus continuous processing*. European Journal of Pharmaceutics and Biopharmaceutics, 2001. **52**(3): p. 289-296.
14. Edwards, M. F. and Instone, T., *Particulate products - their manufacture and use*. Powder Technology, 2001. **119**(1): p. 9-13.

15. Kumar, A., Gernaey, K. V., De Beer, T., and Nopens, I., *Model-based analysis of high shear wet granulation from batch to continuous processes in pharmaceutical production--a critical review*. Eur J Pharm Biopharm, 2013. **85**(3 Pt B): p. 814-32.
16. Van Melkebeke, B., Vervaet, C., and Remon, J. P., *Validation of a continuous granulation process using a twin-screw extruder*. Int J Pharm, 2008. **356**(1-2): p. 224-30.
17. Lee, K. T., Ingram, A., and Rowson, N. A., *Twin screw wet granulation: the study of a continuous twin screw granulator using Positron Emission Particle Tracking (PEPT) technique*. Eur J Pharm Biopharm, 2012. **81**(3): p. 666-73.
18. Iveson, S. M., Litster, J. D., Hapgood, K., and Ennis, B. J., *Nucleation, growth and breakage phenomena in agitated wet granulation processes: a review*. Powder Technology, 2001. **117**(1-2): p. 3-39.
19. Charles-Williams, Heledd R., Wengeler, Robert, Flore, Karin, Feise, Herman, Hounslow, Michael J., and Salman, Agba D., *Granule nucleation and growth: Competing drop spreading and infiltration processes*. Powder Technology, 2011. **206**(1-2): p. 63-71.
20. Tadmor, R., *Line energy and the relation between advancing, receding, and young contact angles*. Langmuir, 2004. **20**(18): p. 7659-7664.
21. Wenzel, R. N., *Resistance of solid surfaces to wetting by water*. Industrial and Engineering Chemistry, 1936. **28**: p. 988-994.
22. Sefiane, K., Skilling, J., and MacGillivray, J., *Contact line motion and dynamic wetting of nanofluid solutions*. Adv Colloid Interface Sci, 2008. **138**(2): p. 101-20.
23. Wolansky, G. and Marmur, A., *Apparent contact angles on rough surfaces: the Wenzel equation revisited*. Colloids and Surfaces a-Physicochemical and Engineering Aspects, 1999. **156**(1-3): p. 381-388.
24. Chau, T. T., Bruckard, W. J., Koh, P. T., and Nguyen, A. V., *A review of factors that affect contact angle and implications for flotation practice*. Adv Colloid Interface Sci, 2009. **150**(2): p. 106-15.
25. Schæfer, Torben and Mathiesen, Christina, *Melt pelletization in a high shear mixer. IX. Effects of binder particle size*. International Journal of Pharmaceutics, 1996. **139**(1-2): p. 139-148.
26. Hapgood, K. P., Litster, J. D., Biggs, S. R., and Howes, T., *Drop penetration into porous powder beds*. J Colloid Interface Sci, 2002. **253**(2): p. 353-66.
27. Hapgood, Karen P., Litster, James D., and Smith, Rachel, *Nucleation regime map for liquid bound granules*. AIChE Journal, 2003. **49**(2): p. 350-361.
28. Kapur, P. C. and Fuersten.Dw, *A Coalescence Model for Granulation*. Industrial & Engineering Chemistry Process Design and Development, 1969. **8**(1): p. 56-&.
29. Pohlman, D. A. and Litster, J. D., *Coalescence model for induction growth behavior in high shear granulation*. Powder Technology, 2015. **270**: p. 435-444.

30. Ennis, Bryan J., Tardos, Gabriel, and Pfeffer, Robert, *A microlevel-based characterization of granulation phenomena*. Powder Technology, 1991. **65**(1-3): p. 257-272.
31. Iveson, S. M., Wauters, P. A. L., Forrest, S., Litster, J. D., Meesters, G. M. H., and Scarlett, B., *Growth regime map for liquid-bound granules: further development and experimental validation*. Powder Technology, 2001. **117**(1-2): p. 83-97.
32. Dhenge, R. M., Cartwright, J. J., Hounslow, M. J., and Salman, A. D., *Twin screw granulation: steps in granule growth*. Int J Pharm, 2012. **438**(1-2): p. 20-32.
33. Dhenge, R. M., Washino, K., Cartwright, J. J., Hounslow, M. J., and Salman, A. D., *Twin screw granulation using conveying screws: Effects of viscosity of granulation liquids and flow of powders*. Powder Technology, 2013. **238**: p. 77-90.
34. Rahmanian, Nejat, Naji, Ayman, and Ghadiri, Mojtaba, *Effects of process parameters on granules properties produced in a high shear granulator*. Chemical Engineering Research and Design, 2011. **89**(5): p. 512-518.
35. Veliz Moraga, Sussy, Villa, Marta P., Bertín, Diego E., Cotabarren, Ivana M., Piña, Juliana, Pedernera, Marisa, and Bucalá, Verónica, *Fluidized-bed melt granulation: The effect of operating variables on process performance and granule properties*. Powder Technology, 2015. **286**: p. 654-667.
36. Dhenge, R. M., Cartwright, J. J., Hounslow, M. J., and Salman, A. D., *Twin screw wet granulation: Effects of properties of granulation liquid*. Powder Technology, 2012. **229**(0): p. 126-136.
37. Pietsch, W., *Agglomeration in Industry: Occurrence and Applications*. Vol. 1. 2005, Weinheim: Wiley-VCH. 719.
38. Papadakis, S. E. and Bahu, R. E., *The Sticky Issues of Drying*. Drying Technology, 1992. **10**(4): p. 817-837.
39. Calvert, G., Curcic, N., Redhead, C., Ahmadian, H., Owen, C., Beckett, D., and Ghadiri, M., *A new environmental bulk powder caking tester*. Powder Technology, 2013. **249**(0): p. 323-329.
40. Cleaver, J. A. S., Karatzas, G., Louis, S., and Hayati, I., *Moisture-induced caking of boric acid powder*. Powder Technology, 2004. **146**(1-2): p. 93-101.
41. Ortega-Rivas, Enrique, Juliano, Pablo, and Yan, Hong, *Food powders: physical properties, processing, and functionality*. 2006, New York: Springer Science & Business Media.
42. Muzaffar, Khalid, *Stickiness Problem Associated with Spray Drying of Sugar and Acid Rich Foods: A Mini Review*. Journal of Nutrition & Food Sciences, 2015.
43. A.D Salman, M.J. Hounslow, J.P.K. Seville, *Granulation*. 1 ed. Vol. 11 (Handbook of Powder Technology). 2006: Elsevier Science.
44. Rauwendaal, Chris J, *Polymer Extrusion*. 4th ed. 2011, Carl Hanser Verlag, Munich. 759.

45. Thiele, William, *Twin-screw extrusion and screw design*, in *Pharmaceutical Extrusion Technology*, C.M. Isaac Ghebre-Selassie, Editor. 2003, Marcel Dekker, INC: New York. Basel.
46. Breitenbach, J., *Melt extrusion: from process to drug delivery technology*. Eur J Pharm Biopharm, 2002. **54**(2): p. 107-17.
47. Keleb, E. I., Vermeire, A., Vervaet, C., and Remon, J. P., *Cold extrusion as a continuous single-step granulation and tableting process*. European Journal of Pharmaceutics and Biopharmaceutics, 2001. **52**(3): p. 359-368.
48. Rina Chokshi, Hossein Zia, *Hot-Melt Extrusion Technique: A Review*. Iranian Journal of Pharmaceutical Research, 2004: p. 3-16.
49. Gamlen, M., Eardley, C. (1986), *Continuous granulation using a Baker Perkins MP50 (multipurpose) extruder*. Drug Dev. Ind. Pharm, 1986. **12**: p. 1710–1713.
50. Boyaci, B. B., Han, J. Y., Masatcioglu, M. T., Yalcin, E., Celik, S., Ryu, G. H., and Koksel, H., *Effects of cold extrusion process on thiamine and riboflavin contents of fortified corn extrudates*. Food Chemistry, 2012. **132**(4): p. 2165-2170.
51. Kleinebudde, P. and Lindner, H., *Experiments with an Instrumented Twin-Screw Extruder Using a Single-Step Granulation Extrusion Process*. International Journal of Pharmaceutics, 1993. **94**(1-3): p. 49-58.
52. Vercruyse, J., Córdoba Díaz, D., Peeters, E., Fonteyne, M., Delaet, U., Van Assche, I., De Beer, T., Remon, J. P., and Vervaet, C., *Continuous twin screw granulation: Influence of process variables on granule and tablet quality*. European Journal of Pharmaceutics and Biopharmaceutics, 2012. **82**(1): p. 205-211.
53. Lindberg, N. O., Tufvesson, C., Holm, P., Olbjer, L., *Extrusion of an Effervescent Granulation with a Twin Screw Extruder, Baker Perkins MPF 50 D. Influence on Intragranular Porosity and Liquid Saturation*. Drug Development and Industrial Pharmacy, 1988. **14**(13): p. 1791-1798.
54. Kleinebudde, P. and H. Lindner, *Experiments with an instrumented twin-screw extruder using a single-step granulation/extrusion process*. International Journal of Pharmaceutics, 1993. **1-3**(94): p. 49-58.
55. K.Kolyter, M.Karl, A.Gryczke, *Hot-Melt Extrusion with BASF Pharma Polymers*. 2nd ed. 2012: BASF The Chemical Company.
56. White, James Lindsay, *Science and Technology (Progress in Polymer Processing)*. . 1st Edition ed. 2003: Hanser Gardner Pubns.
57. Rudolf, Reiner, *General Overview of the Compounding Process: Tasks, Selected Applications, and Process Zones*, in *Co-rotating Twin-screw Extruder*, K. Kohlgrüber, Editor. 2008, Hanser. p. 57-89.
58. Kirchhoff, Jörg, *Mixing and Dispersing: Principles*, in *Co-rotating Twin-screw Extruder*, K. Kohlgrüber, Editor. 2008, Hanser. p. 159-179.



59. Mollan, Mayur Lodaya and Matthew, *Twin-Screw Wet Granulation*, in *PHARMACEUTICAL EXTRUSION TECHNOLOGY*, C.M. Isaac Ghebre-Selassie, Editor. 2003, Marcel Dekker: New York.
60. Fonteyne, M., Soares, S., Vercruyssen, J., Peeters, E., Burggraef, A., Vervaet, C., Remon, J. P., Sandler, N., and De Beer, T., *Prediction of quality attributes of continuously produced granules using complementary pat tools*. *Eur J Pharm Biopharm*, 2012. **82**(2): p. 429-36.
61. Knight, P. C., *Structuring agglomerated products for improved performance*. *Powder Technology*, 2001. **119**(1): p. 14-25.
62. Jim Listster, Bryan Ennis, *The Science and Engineering of Granulation Processes*. 2004: Kluwer Academic Publishers
63. Gogoi, B. K., Choudhury, G. S., and Oswalt, A. J., *Effects of location and spacing of reverse screw and kneading element combination during twin-screw extrusion of starchy and proteinaceous blends*. *Food Research International*, 1996. **29**(5-6): p. 505-512.
64. Djuric, Dejan, *Continuous Granulation with a Twin-Screw Extruder*. 2008, Zug; Dusseldorf university: Heinrich-Heine. p. 100.
65. A. S. El Hagrasy<sup>1</sup>, J. D. Litster<sup>1</sup>, *Granulation rate processes in the kneading elements of a twin screw granulator*. *AIChE Journal*, 2013.
66. van Zuilichem, D. J., Kuiper, E., Stolp, W., and Jager, T., *Mixing effects of constituting elements of mixing screws in single and twin screw extruders*. *Powder Technology*, 1999. **106**(3): p. 147-159.
67. Ainsworth, P., Ibanoglu, S., and Hayes, G. D., *Influence of process variables on residence time distribution and flow patterns of tarhana in a twin-screw extruder*. *Journal of Food Engineering*, 1997. **32**(1): p. 101-108.
68. Unlu, E. and Faller, J. F., *RTD in twin-screw food extrusion*. *Journal of Food Engineering*, 2002. **53**(2): p. 115-131.
69. Siew-Yoong Lee, Kathryn L. McCarthy, *Effect of Screw Configuration and Speed on RTD and Expansion of Rice Extrudate*. *Journal of Food Process Engineering* 1996.
70. Baron, R., Vauchel, P., Kaas, R., Arhaliass, A., and Legrand, J., *Dynamical modelling of a reactive extrusion process: Focus on residence time distribution in a fully intermeshing co-rotating twin-screw extruder and application to an alginate extraction process*. *Chemical Engineering Science*, 2010. **65**(10): p. 3313-3321.
71. Guha, M., Ali, S. Z., and Bhattacharya, S., *Twin-screw extrusion of rice flour without a die: Effect of barrel temperature and screw speed on extrusion and extrudate characteristics*. *Journal of Food Engineering*, 1997. **32**(3): p. 251-267.
72. Reitz, E., Vervaet, C., Neubert, R. H., and Thommes, M., *Solid crystal suspensions containing griseofulvin--preparation and bioavailability testing*. *Eur J Pharm Biopharm*, 2013. **83**(2): p. 193-202.

73. Ziegler, G. R. and Aguilar, C. A., *Residence time distribution in a co-rotating, twin-screw continuous mixer by the step change method*. Journal of Food Engineering, 2003. **59**(2-3): p. 161-167.
74. Keleb, E. I., Vermeire, A., Vervaet, C., Remon, J. P., *Continuous twin screw extrusion for the wet granulation of lactose*. International Journal of Pharmaceutics, 2002. **239**(1-2): p. 69-80.
75. Keleb, E. I., Vermeire, A., Vervaet, C., Remon, J. P., *Twin screw granulation as a simple and efficient tool for continuous wet granulation*. International Journal of Pharmaceutics, 2004. **273**(1-2): p. 183-194.
76. Djuric, D., Van Melkebeke, B., Kleinebudde, P., Remon, J. P., and Vervaet, C., *Comparison of two twin-screw extruders for continuous granulation*. European Journal of Pharmaceutics and Biopharmaceutics, 2009. **71**(1): p. 155-160.
77. Chitu, T. M., Oulahna, D., and Hemati, M., *Rheology, granule growth and granule strength: Application to the wet granulation of lactose-MCC mixtures*. Powder Technology, 2011. **208**(2): p. 441-453.
78. El Hagrasy, A. S., Hennenkamp, J. R., Burke, M. D., Cartwright, J. J., and Litster, J. D., *Twin screw wet granulation: Influence of formulation parameters on granule properties and growth behavior*. Powder Technology, (0).
79. Tu, Wei-Da, Ingram, Andy, and Seville, Jonathan, *Regime map development for continuous twin screw granulation*. Chemical Engineering Science, 2013. **87**(0): p. 315-326.
80. Ding, Q. B., Ainsworth, P., Tucker, G., and Marson, H., *The effect of extrusion conditions on the physicochemical properties and sensory characteristics of rice-based expanded snacks*. Journal of Food Engineering, 2005. **66**(3): p. 283-289.
81. Keleb, E. I., Vermeire, A., Vervaet, C., and Remon, J. P., *Twin screw granulation as a simple and efficient tool for continuous wet granulation*. Int J Pharm, 2004. **273**(1-2): p. 183-94.
82. Riyadh B. Al-Asady, Michael J. Hounslow & Agba D. Salman, *TWIN SCREW GRANULATOR: EFFECT OF PRIMARY PARTICLE SIZE*, in *6th International granulation Workshop*. 2013: University of Sheffield.
83. Jr, Harold F. Giles, *Extrusion: The Definitive Processing Guide and Handbook (Plastics Design Library)*. . 1 Edition ed. 2007: William Andrew.
84. Kumar, A., Vercruyssen, J., Bellandi, G., Gernaey, K. V., Vervaet, C., Remon, J. P., De Beer, T., and Nopens, I., *Experimental investigation of granule size and shape dynamics in twin-screw granulation*. Int J Pharm, 2014. **475**(1-2): p. 485-95.
85. pharma, DFE. *Introduction to tableting by wet granulation*. [cited 2014 Jan]; Available from: [www.dfepharma.com](http://www.dfepharma.com).

86. Schmidt, Christian and Kleinebudde, Peter, *Comparison between a twin-screw extruder and a rotary ring die press. Part II: influence of process variables*. European Journal of Pharmaceutics and Biopharmaceutics, 1998. **45**(2): p. 173-179.
87. Cartwright, J. J., Robertson, J., D'Haene, D., Burke, M. D., and Hennenkamp, J. R., *Twin screw wet granulation: Loss in weight feeding of a poorly flowing active pharmaceutical ingredient*. Powder Technology, 2013. **238**(0): p. 116-121.
88. Dhenge, R. M., Cartwright, J. J., Doughty, D. G., Hounslow, M. J., and Salman, A. D., *Twin screw wet granulation: Effect of powder feed rate*. Advanced Powder Technology, 2011. **22**(2): p. 162-166.
89. pharma, DFE. *Directly compressible lactose*. [cited 2014 Jan]; Available from: [www.dfepharma.com](http://www.dfepharma.com).
90. BioPolymer, FMC. *MATERIAL SAFETY DATA SHEET, Avicel PH Microcrystalline Cellulose*. 2008 [cited 2013 May]; Available from: <http://www.fmcbiopolymer.com/Portals/Pharm/Content/Docs/avicelphmsds>.
91. Corporation, American Polymer Standards. *Material Safety Data Sheet*. 2011 [cited 2013 May]; Available from: <http://www.ampolymer.com/MSDS/HPMC.pdf>.
92. NB. *Croscarmellose sodium (Disintegrant, Dissolution aid)*. 2008 [cited 2013 May]; Available from: <http://www.nbent.com/croscarmellose.htm>.
93. ShineEtsu. *Hypromellose, PHARMACOAT*. 2004 [cited 2013 May]; Available from: <http://www.elementoorganika.ru/files/pharmacoat.pdf>.
94. Merkus, Henk G., *Particle Size Measurements*. 2009: Springer.
95. Administration, U.S. Department of Health and Human Services Food and Drug, *Guidance for Industry, in Q8(R2) Pharmaceutical Development* November 2009, Center for Drug Evaluation and Research (CDER) U.S. p. 30.
96. Yu, L. X., *Pharmaceutical quality by design: product and process development, understanding, and control*. Pharm Res, 2008. **25**(4): p. 781-91.
97. Charoo, Naseem Ahmad and Ali, Areeg Anwer, *Quality risk management in pharmaceutical development*. Drug Development and Industrial Pharmacy, 2013. **39**(7): p. 947-960.
98. Vercruyse, J., Burggraeve, A., Fonteyne, M., Cappuyns, P., Delaet, U., Van Assche, I., De Beer, T., Remon, J. P., and Vervaeet, C., *Impact of screw configuration on the particle size distribution of granules produced by twin screw granulation*. Int J Pharm, 2015. **479**(1): p. 171-80.
99. Thompson, M. R. and Sun, J., *Wet granulation in a twin-screw extruder: Implications of screw design*. Journal of Pharmaceutical Sciences, 2010. **99**(4): p. 2090-2103.
100. Thompson, M. R., Mu, B., and Sheskey, P. J., *Aspects of foam stability influencing foam granulation in a twin screw extruder*. Powder Technology, 2012. **228**(0): p. 339-348.

101. Yu, S., Reynolds, G. K., Huang, Z., de Matas, M., and Salman, A. D., *Granulation of increasingly hydrophobic formulations using a twin screw granulator*. Int J Pharm, 2014. **475**(1-2): p. 82-96.
102. Marmur, Abraham, *EQUILIBRIUM AND SPREADING OF LIQUIDS ON SOLID SURFACES*. elsevier Science Publishers, 1983.
103. Charles-Williams, *GRANULATION: A STUDY OF INITIAL LIQUID-POWDER INTERACTION*, in *Department of Chemical and Process Engineering*. 2010, University of Sheffield University of Sheffield p. 216.
104. Ai, Q., Dhenge, R. M., Hounslow, M. J., and Salman, A. D., *Developing a miniaturized approach for formulation development using twin screw granulation*. Powder Technology, 2016. **300**: p. 83-91.
105. Vadillo, D. C., Soucemarianadin, A., Delattre, C., and Roux, D. C. D., *Dynamic contact angle effects onto the maximum drop impact spreading on solid surfaces*. Physics of Fluids, 2009. **21**(12): p. 122002.
106. Keller, A. A., Broje, V., and Setty, K., *Effect of advancing velocity and fluid viscosity on the dynamic contact angle of petroleum hydrocarbons*. Journal of Petroleum Science and Engineering, 2007. **58**(1-2): p. 201-206.
107. Šikalo, Š, Marengo, M., Tropea, C., and Ganić, E. N., *Analysis of impact of droplets on horizontal surfaces*. Experimental Thermal and Fluid Science, 2002. **25**(7): p. 503-510.
108. Lute, Sushma V., Dhenge, Ranjit M., Hounslow, Michael J., and Salman, Agba D., *Twin screw granulation: Understanding the mechanism of granule formation along the barrel length*. Chemical Engineering Research and Design.
109. Fonteyne, M., Correia, A., De Plecker, S., Vercruyssen, J., Ilic, I., Zhou, Q., Vervaet, C., Remon, J. P., Onofre, F., Bulone, V., and De Beer, T., *Impact of microcrystalline cellulose material attributes: a case study on continuous twin screw granulation*. Int J Pharm, 2015. **478**(2): p. 705-17.
110. Zografi, G. and Kontny, M. J., *The interactions of water with cellulose- and starch-derived pharmaceutical excipients*. Pharm Res, 1986. **3**(4): p. 187-94.
111. Parker, M. D., York, P., and Rowe, R. C., *Binder-Substrate Interactions in Wet Granulation .1. The Effect of Binder Characteristics*. International Journal of Pharmaceutics, 1990. **64**(2-3): p. 207-216.
112. Osborne, J. D., Sochon, R. P. J., Cartwright, J. J., Doughty, D. G., Hounslow, M. J., and Salman, A. D., *Binder addition methods and binder distribution in high shear and fluidised bed granulation*. Chemical Engineering Research & Design, 2011. **89**(5A): p. 553-559.
113. Tan, Bernice Mei Jin, Loh, Zhi Hui, Soh, Josephine Lay Peng, Liew, Celine Valeria, and Heng, Paul Wan Sia, *Distribution of a viscous binder during high shear granulation—Sensitivity to the method of delivery and its impact on product properties*. International Journal of Pharmaceutics, (0).

114. Tan, M. X. L. and Hapgood, K. P., *Foam granulation: Binder dispersion and nucleation in mixer-granulators*. Chemical Engineering Research & Design, 2011. **89**(5A): p. 526-536.
115. Afrassiabian, Zahra, Leturia, Mikel, Benali, Mohamed, Guessasma, Mohamed, and Saleh, Khashayar, *An overview of the role of capillary condensation in wet caking of powders*. Chemical Engineering Research and Design, 2016. **110**: p. 245-254.
116. Rumpf, H., *The strength of granules and agglomerates*. n Knepper WA, ed. Agglomeration. New York: John Wiley and so, 1962: p. pp. 379-418.
117. Chitu, T. M., Oulahna, D., and Hemati, M., *Wet granulation in laboratory-scale high shear mixers: Effect of chopper presence, design and impeller speed*. Powder Technology, 2011. **206**(1-2): p. 34-43.
118. Briens, L. and Logan, R., *The effect of the chopper on granules from wet high-shear granulation using a PMA-1 granulator*. AAPS PharmSciTech, 2011. **12**(4): p. 1358-65.
119. Flore, K., Schoenherr, M., and Feise, H., *Aspects of granulation in the chemical industry*. Powder Technology, 2009. **189**(2): p. 327-331.
120. Dawes, J., Gamble, J. F., Greenwood, R., Robbins, P., and Toby, M., *An investigation into the impact of magnesium stearate on powder feeding during roller compaction*. Drug Dev Ind Pharm, 2012. **38**(1): p. 111-22.
121. Smith, P. G. and Nienow, A. W., *Particle growth mechanisms in fluidised bed granulation—I: The effect of process variables*. Chemical Engineering Science, 1983. **38**(8): p. 1223-1231.
122. Hamdan, Intan Munirah, Reklaitis, Gintaras V., and Venkatasubramanian, Venkat, *Exceptional Events Management Applied to Roller Compaction of Pharmaceutical Powders*. Journal of Pharmaceutical Innovation, 2010. **5**(4): p. 147-160.
123. Iveson, S. M. and Litster, J. D., *Fundamental studies of granule consolidation - Part 2. Quantifying the effects of particle and binder properties*. Powder Technology, 1998. **99**(3): p. 243-250.
124. Bakalis, S. and Karwe, M. V., *Velocity distributions and volume flow rates in the nip and translational regions of a co-rotating, self-wiping, twin-screw extruder*. Journal of Food Engineering, 2002. **51**(4): p. 273-282.
125. Bakalis, S. and Karwe, M. V., *Measuring of velocity distributions in the nip region of a co-rotating twin-screw extruder*. Food and Bioproducts Processing, 1999. **77**(C3): p. 205-212.
126. Carneiro, O. S., Covas, J. A., Ferreira, J. A., and Cerqueira, M. F., *On-line monitoring of the residence time distribution along a kneading block of a twin-screw extruder*. Polymer Testing, 2004. **23**(8): p. 925-937.
127. J. Diemert, C. Chilles, et al, *Flow Visualisation in Co-rotating Twin Screw Extruders: Positron Emission Particle Tracking and Numerical Particle Trajectories*. International Polymer Processing, 2011: p. 540-550.

128. Nilpawar, A. M., Reynolds, G. K., Salman, A. D., and Hounslow, M. J., *Surface velocity measurement in a high shear mixer*. Chemical Engineering Science, 2006. **61**(13): p. 4172-4178.
129. Koester, M. and Thommes, M., *Analysis of particle kinematics in spheronization via particle image velocimetry*. Eur J Pharm Biopharm, 2013. **83**(2): p. 307-14.
130. Zhao, X. L., Li, S. Q., Liu, G. Q., Song, Q., and Yao, Q., *Flow patterns of solids in a two-dimensional spouted bed with draft plates: PIV measurement and DEM simulations*. Powder Technology, 2008. **183**(1): p. 79-87.
131. Juan G. Osorio, Ridade Sayin, Arjun V. Kalbag, Laura Martinez-Marcos, Dimitrios A. and Lamprou3, Gavin W. Halbert and James D. Litster., *Scaling of Continuous Twin Screw Wet Granulation*. Particle Technology and Fluidization, 2016.
132. Nobuhito Mori and K.-A Chang, . "*INTRODUCTION TO MPIV– PIV toolbox in MATLAB –version 0.97*". 2009.
133. Haphood, KP. *Pharmaceutical Excipients*. 2016 [cited 2016 October]; Available from: [https://www.medicinescomplete.com/mc/excipients/current/1001936653.htm?q=SYLOID&t=search&ss=text&tot=3&p=3#\\_hit](https://www.medicinescomplete.com/mc/excipients/current/1001936653.htm?q=SYLOID&t=search&ss=text&tot=3&p=3#_hit).
134. Fluoro. *Fluoro Precision PTFE Teflon Xylan Coatings*. Available from: <http://www.fluoroprecision.co.uk/>.
135. Clark, Jim. *THE BEER-LAMBERT LAW*. 2007 [cited 2016 July]; Available from: <http://www.chemguide.co.uk/analysis/uvvisible/beerlambert.html#top>.

# Appendix A

## A.1 Size distribution of primary particles

All powders were supplied by GSK, where some details of their size is shown in the table below. The size distribution of the powder components was measured using Malvern Mastersizer S (Malvern Instruments Ltd., UK).

Data on the components of the powder mixture used in this study.

Size/Component name	D <sub>10</sub> (μm)	D <sub>50</sub> (μm)	D <sub>90</sub> (μm)
α-Lactose monohydrate (Pharmatose 200M)	6	41	110
microcrystalline cellulose (Avicel PH 101)	29	78	322
crosscarmellose sodium (Ac-di-Sol)	19	59	308
Hypromellose 2910 (Pharmacoat 603)	37	83	322

## A.2 Droplet analysis

### A.2.1 Lactose

HPMC%/magnification

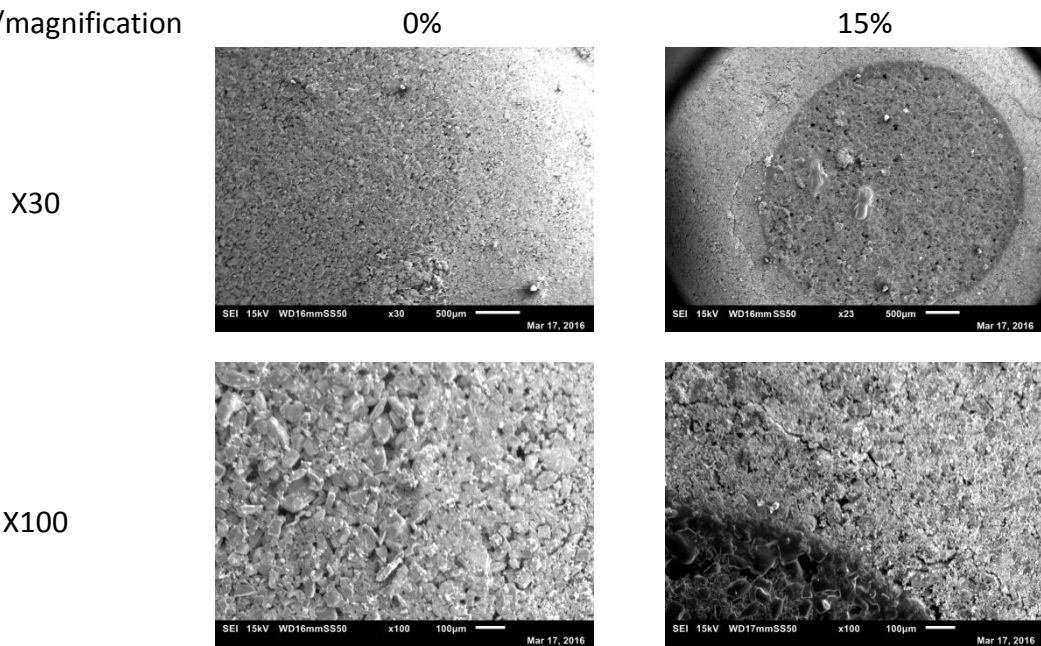


Figure A-1: More images under the SEM showing the wet and dry section of the tablet after the droplet penetrated through the compact of Lactose material, at different magnification.

### A.2.2 MCC HPMC%/magnification

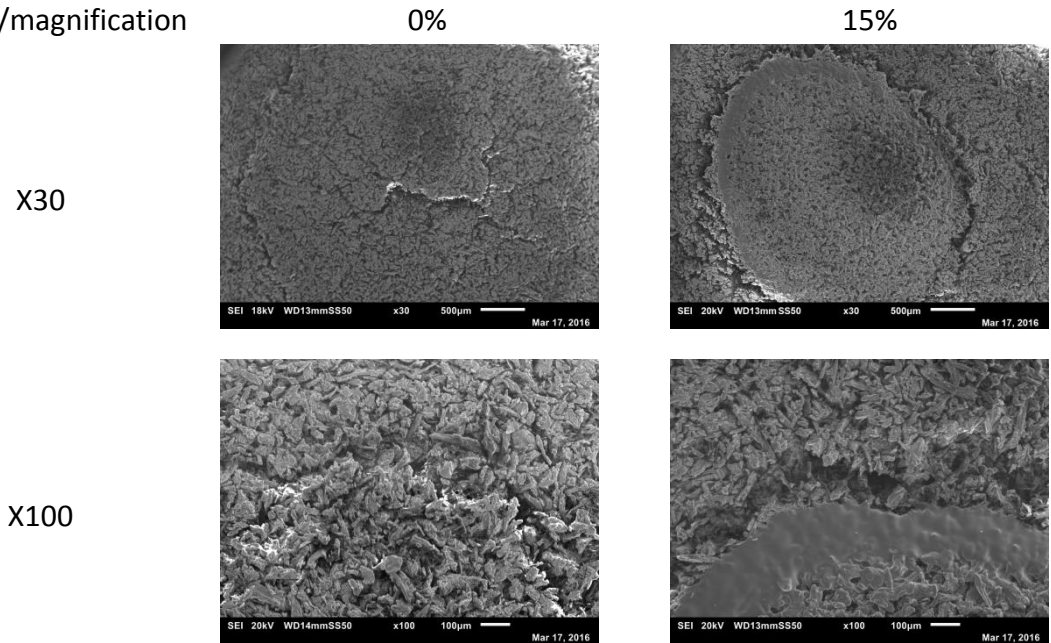


Figure A-2: More images under the SEM showing the wet and dry section of the tablet after the droplet penetrated through the compact of MCC material, at different magnification

### A.3 Compressibility Index

To further our understanding of the two powders their compressibility index and was investigated, where it was found that the compression Index of both materials (lactose and MCC) gradually increases as the compression force applied goes up as it is indicated by Figure shown below. This was as result of the further compression of the primary particles as the compression force was increased. However, MCC showed a lower compressibility index at all the compression forces (300-500N) in comparison with the Lactose. This is an indication of the better follow-ability of the powder.



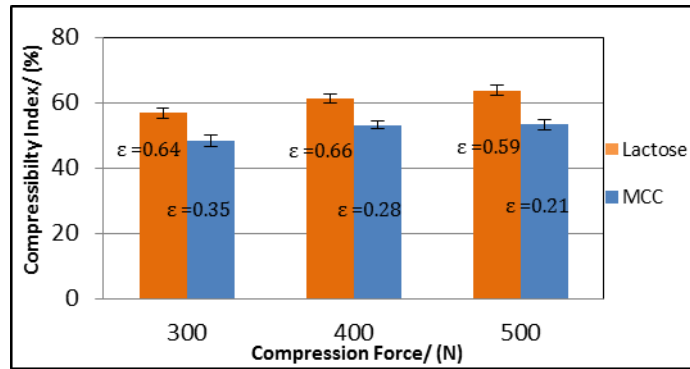


Figure A-3: The Compressibility Index and Porosity of compressed beds Of Lactose and MCC change as the compression force varies.

The increase of the compression force also caused a decrease in porosity ( $\epsilon$ ) as particles compacted together more firmly, which resulted in less voidage within the compressed bed. This is more apparent when considering the lowest compression force (300N) and the highest (500N), for both materials.

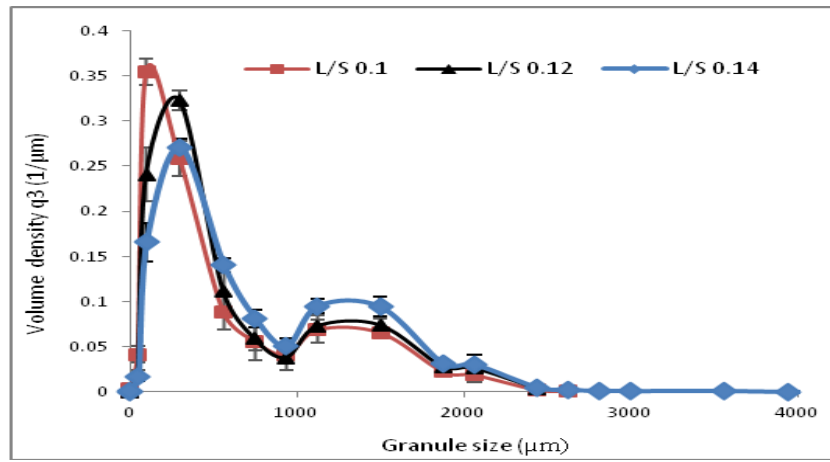
Due to the smaller size of primary particles of the Lactose powder, the small particles have a lot of air surrounding them and this allows the powder bed to compress further (also the shape of particle affect the compressibility too). Therefore the lactose is expected to have a lower void (porosity) as well as poor flowing properties. Furthermore, the production of tablets from lactose alone showed to give a very dense and solid tablet [83]

#### A.4 Independent process and formulation parameters:

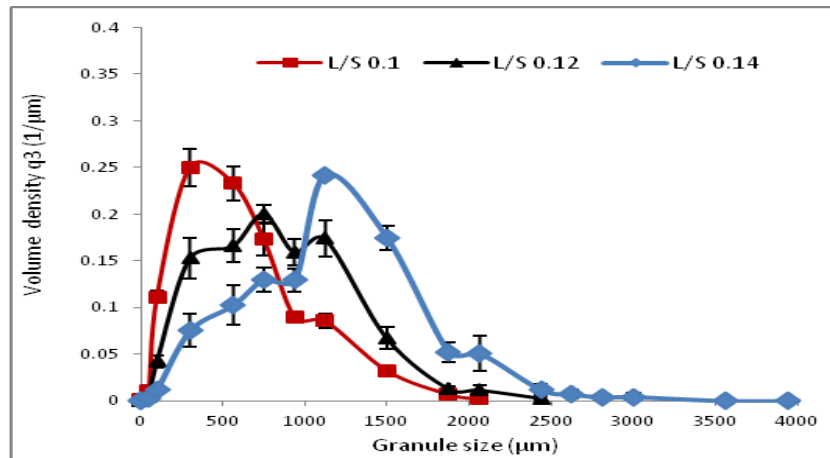
During this section the effect of L/S ratio, Powder Feed rate (PF) and Screw Speed (ss) on the size distribution and granular's shape as the starting material was varied between lactose and MCC. Each condition was performed on two screw configuration (conveying elements only and conveying and kneading elements together).

##### A.4.1 The effect of changing the L/S ratio

###### Lactose



(a)



(b)

Screw speed 100 rpm, Feed rate 1kg/h, 25 °C

L/S ratio

Conveying elements only

Conveying and kneading elements

0.1

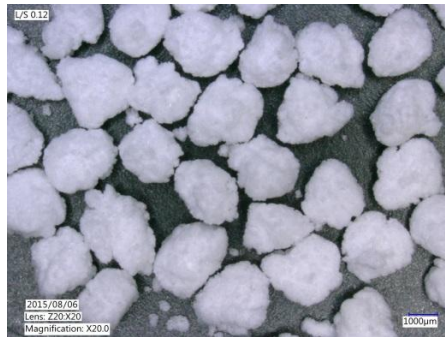


(a)



(d)

0.12



(b)



(e)

0.14

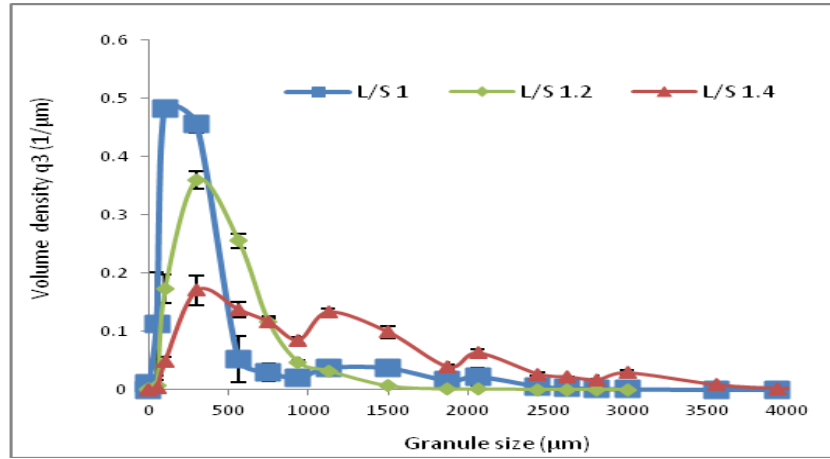


(c)

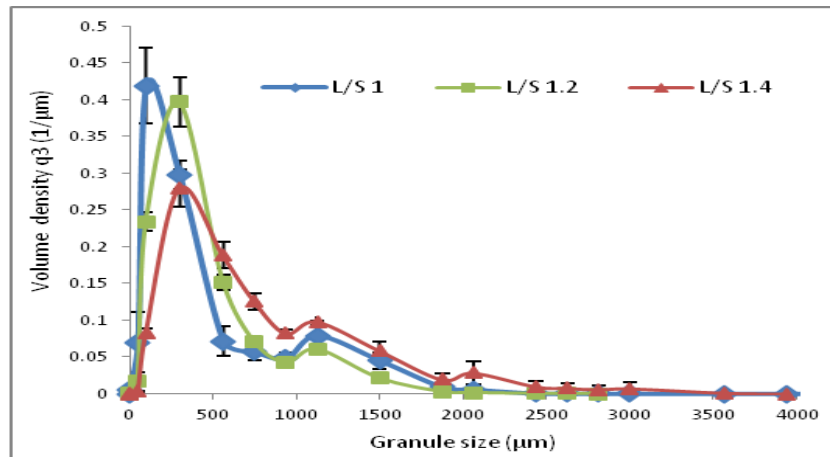


(f)

MCC



(a)



(b)

Screw speed 100 rpm, Feed rate 1kg/h, 25 °C

L/S ratio

Conveying elements only

Conveying and kneading elements

1



(a)



(d)

1.2

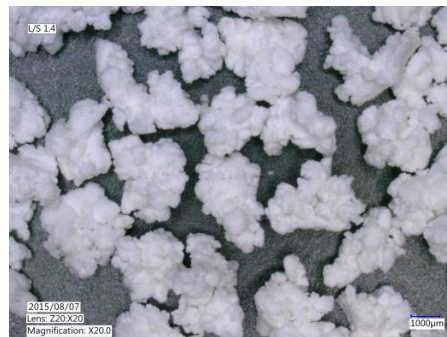


(b)



(e)

1.4



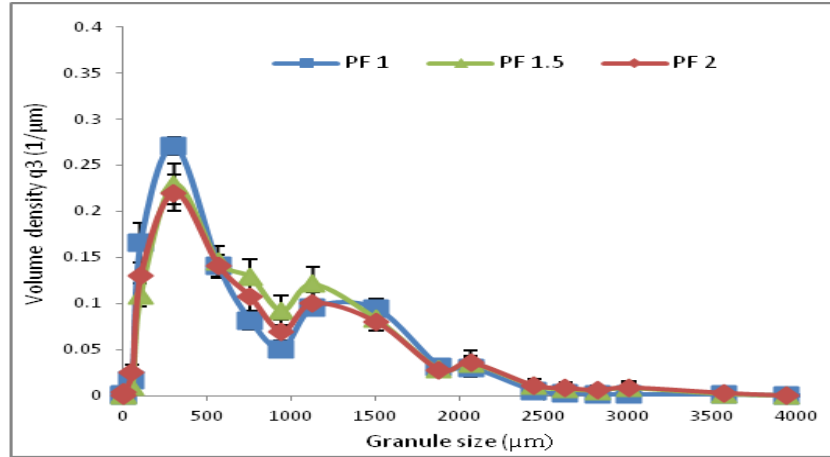
(c)



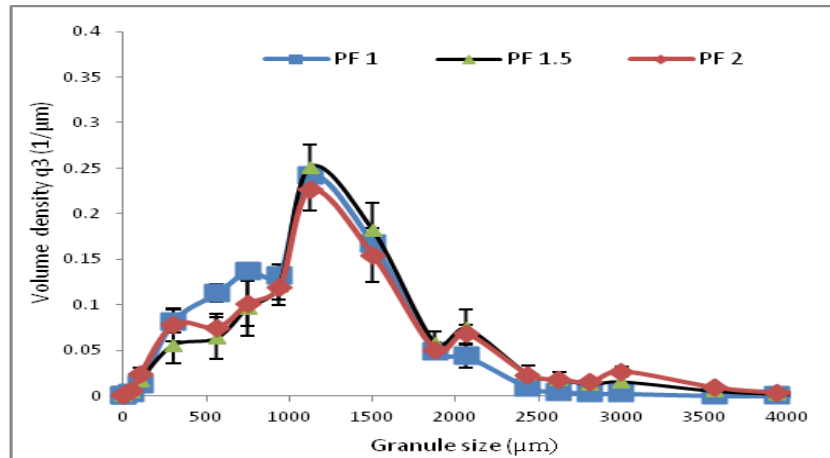
(f)

## A.4.2 Powder Feed rate

Lactose



(a)



(b)

Screw speed 100 rpm, L/S 0.14, 25 °C

Powder feedrate

Conveying elements only

Conveying and kneading elements

1

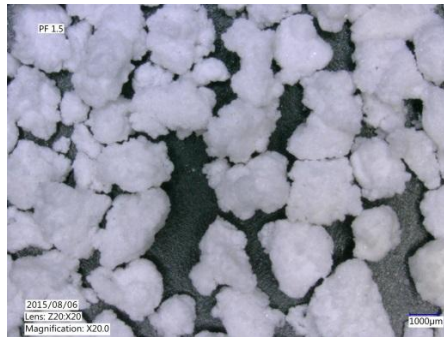


(a)



(d)

1.5



(b)



(e)

2

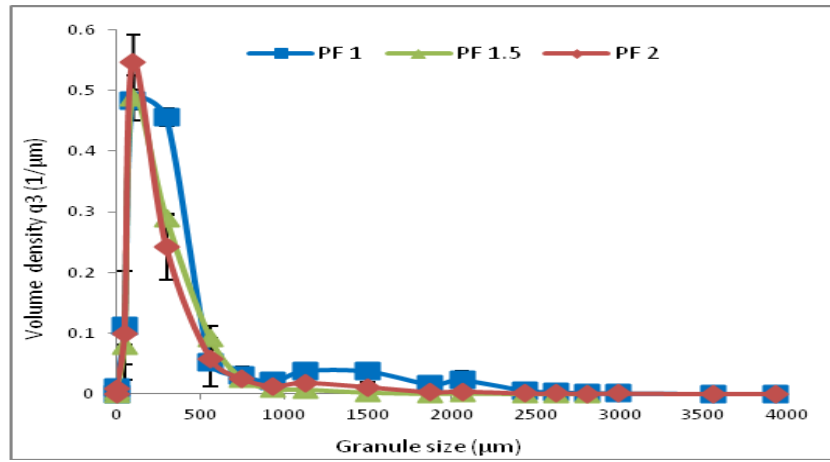


(c)

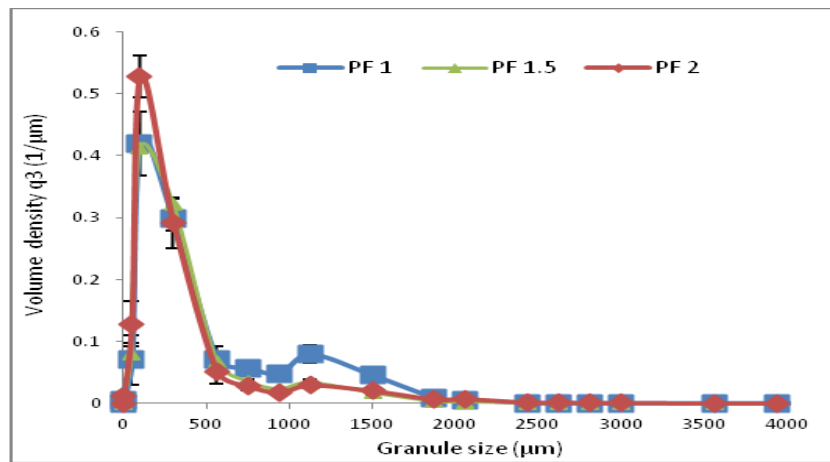


(f)

MCC



(a)



(b)

Screw speed 100 rpm, L/S 1, 25 °C



Powder feedrate

Conveying elements only

Conveying and kneading elements

1



(a)



(d)

1.5



(b)



(e)

2



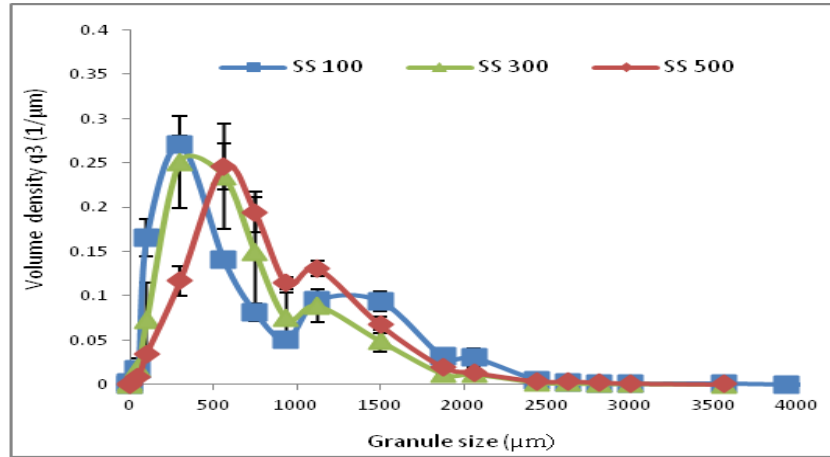
(c)



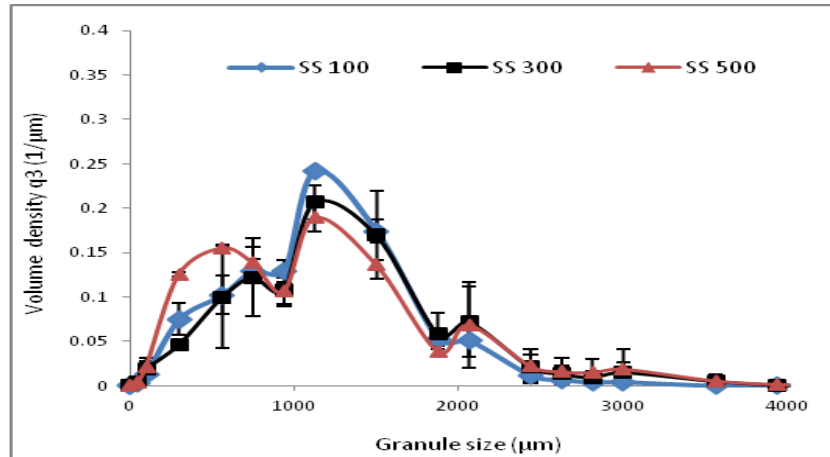
(f)

### A.4.3 Effect of Screw Speed

#### Lactose



(a)



(b)

Feed rate 1kg/h, L/S 014, 25 °C

Screw Speed

Conveying elements only

Conveying and kneading elements

100



(a)



(d)

300



(b)



(e)

500

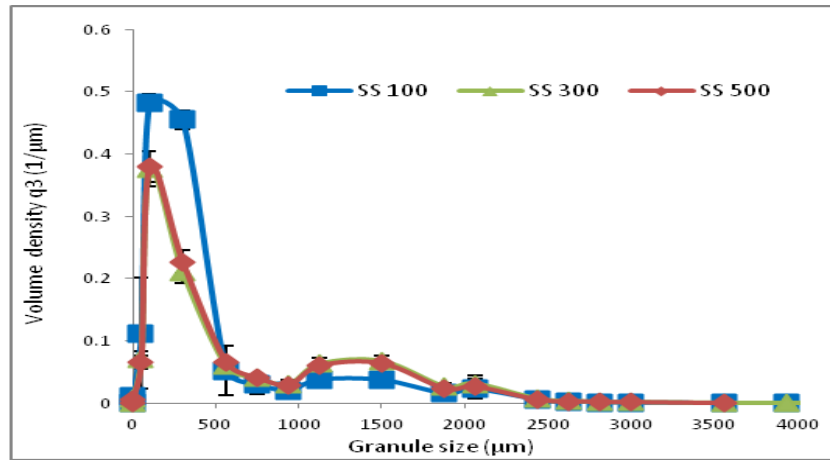


(c)

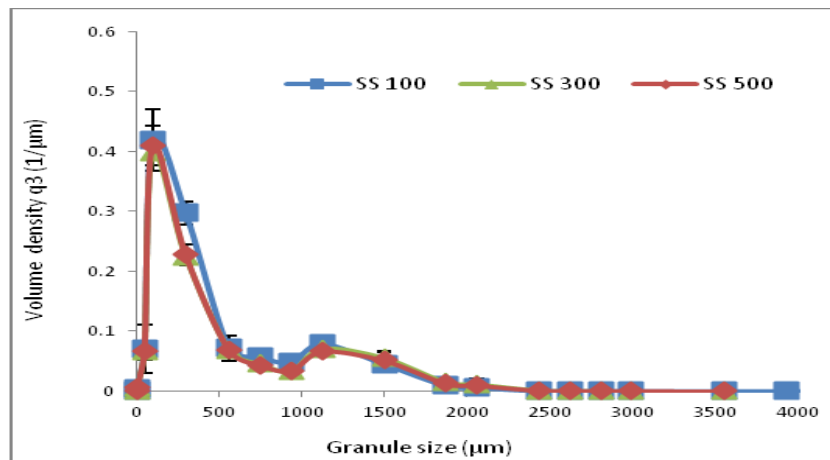


(f)

MCC



(a)



(b)

Feed rate 1kg/h, L/S 1, 25 °C

Screw Speed

Conveying elements only

Conveying and kneading elements

100



(a)



(d)

300



(b)



(e)

500



(c)



(f)

## Appendix B

### B.1 Experimental set-up and process parameters

#### B.1.1 Experimental set-up

Three different experiments namely; Experiment 1, Experiment 2 and Experiment 3 were chosen to investigate the binder delivery effect on granule properties. In each experiment, the binder will be delivered in there different ways:

**Set 1** – All solid binder is mixed with the powder mixture

**Set 2** – 50% of the solid binder in powder mixture and 50% in the granulation liquid media (Water)

**Set 3** - All solid binder in granulation liquid (water)

In Experiment 1, the L/S ratio changed accordingly to ensure the same water content is used in the granulation liquid throughout the three sets. In Experiment 2, all the variables were considered, e.g. the the individual material within the composition, and water content. In Experiment 3, the minimal difference in the formulation composition and L/S ratio is neglected to give the same L/S ratio. The conditions of each experiment are shown as follows:

#### 1. Experiment 1

In this experiment, the mass flow rate of powder mixture was set to 1 kg/h in three sets. However, the granulation liquid was varied to ensure the same amount of water was used in each set. Therefore, the mass flow rate of the water and binder was the same throughout the three sets, giving the compositions shown below:

The formulation variables, used in each set, during experiment 1.

Component	Lactose in powder mixture (w/w%)	MCC in powder mixture (w/w%)	crosscarmellose sodium in powder mixture (w/w%)	Solid Binder in powder mixture (w/w%)	Granulation liquid (kg/h)	Water in granulation liquid (w/w%)	Solid Binder in granulation liquid (w/w%)	L/S ratio
<b>Set 1</b>	73.5	20	1.5	5	0.35	100	0	0.35
<b>Set 2</b>	75.43	20.53	1.54	2.5	0.375	93.33	6.67	0.375
<b>Set 3</b>	77.37	21.05	1.58	0	0.4	87.2	12.5	0.4

## 2. Experiment 2

Experiment 2 was designed to consider the binder delivery while ensuring all the components flowing into the granulator are of the same mass flow rate. To achieve this, the mass flow rate of the powder mixture and granulation liquid was changed accordingly in each set, giving a different L/S ratio. The mass flow rate in each set is presented below.

The formulation variables, used in each set, during experiment 2.

Component	Powder Mixture (kg/h)	Lactose in powder mixture (w/w%)	MCC in powder mixture (w/w%)	crosscarmellose sodium in powder mixture (w/w%)	Solid Binder in powder mixture (w/w%)	Granulation liquid (kg/h)	Water in granulation liquid (w/w%)	Solid Binder in granulation liquid (w/w%)	L/S ratio
<b>Set 1</b>	1	73.5	20	1.5	5	0.35	100	0	0.35
<b>Set 2</b>	0.975	75.39	20.51	1.54	2.56	0.38	93.33	6.67	0.38
<b>Set 3</b>	0.95	77.4	21.1	1.5	0	0.4	87.5	12.5	0.42

## 3. Experiment 3

In this experiment, the mass flow rate of powder mixture and granulation liquid was kept consistent at 1 kg/h and 0.4 kg/h respectively for the three sets (giving L/S ratio of 0.4). This neglected the variation of the water component to minimize the variables used. Therefore, the only component varied is the form of the binder. This is shown below:

The formulation variables, used in each set, during experiment 3.

Component	Lactose in powder mixture (w/w%)	MCC in powder mixture (w/w%)	crosscarmellose sodium in powder mixture (w/w%)	Solid Binder in powder mixture (w/w%)	Water in granulation liquid (w/w%)	Solid Binder in granulation liquid (w/w%)
<b>Set 1</b>	73.5	20	1.5	5	100	0
<b>Set 2</b>	75.43	20.53	1.54	2.5	93.75	6.25
<b>Set 3</b>	77.37	21.05	1.58	0	87.5	12.5

### B.1.2 Size distribution:

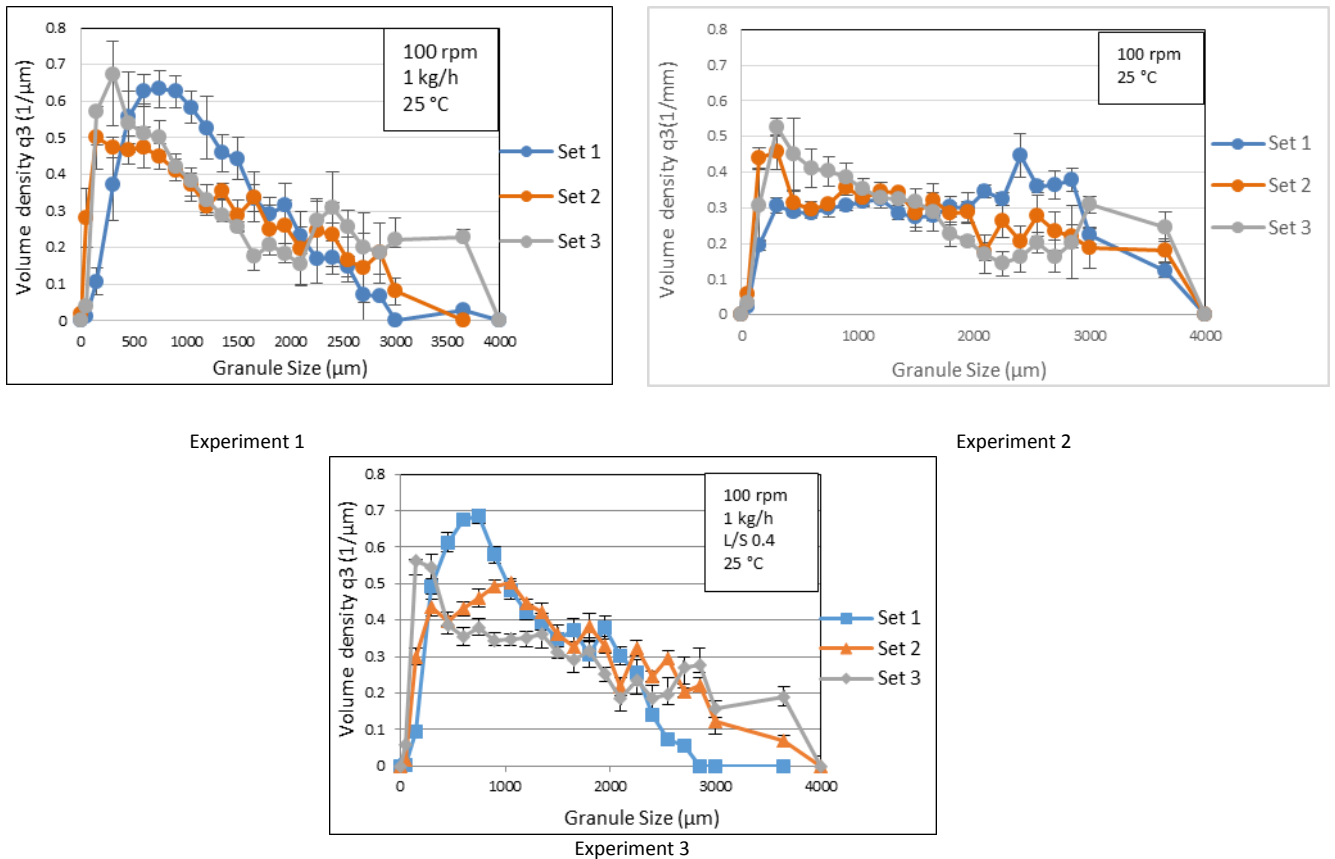


Figure B-1: The size distribution from each experiment may differ but the overall trends remain similar.

### B.1.3 Further analysis for Experiment 3:

#### B.1.3.1 Conveying elements only.

##### *Size distribution*

The study of how the binder delivery will affect the dependent variables (Residence time, Torque and Barrel fill level) was not shown in literature using the twin screw granulator, as El Hagrasy, Hennenkamp [78] only discussed the binder delivery effect on size distribution. In section, an attempt was carried out to explore this effect. It was observed that changing the binder delivery brought about a huge change in the dependent variables, as shown in Figure below.



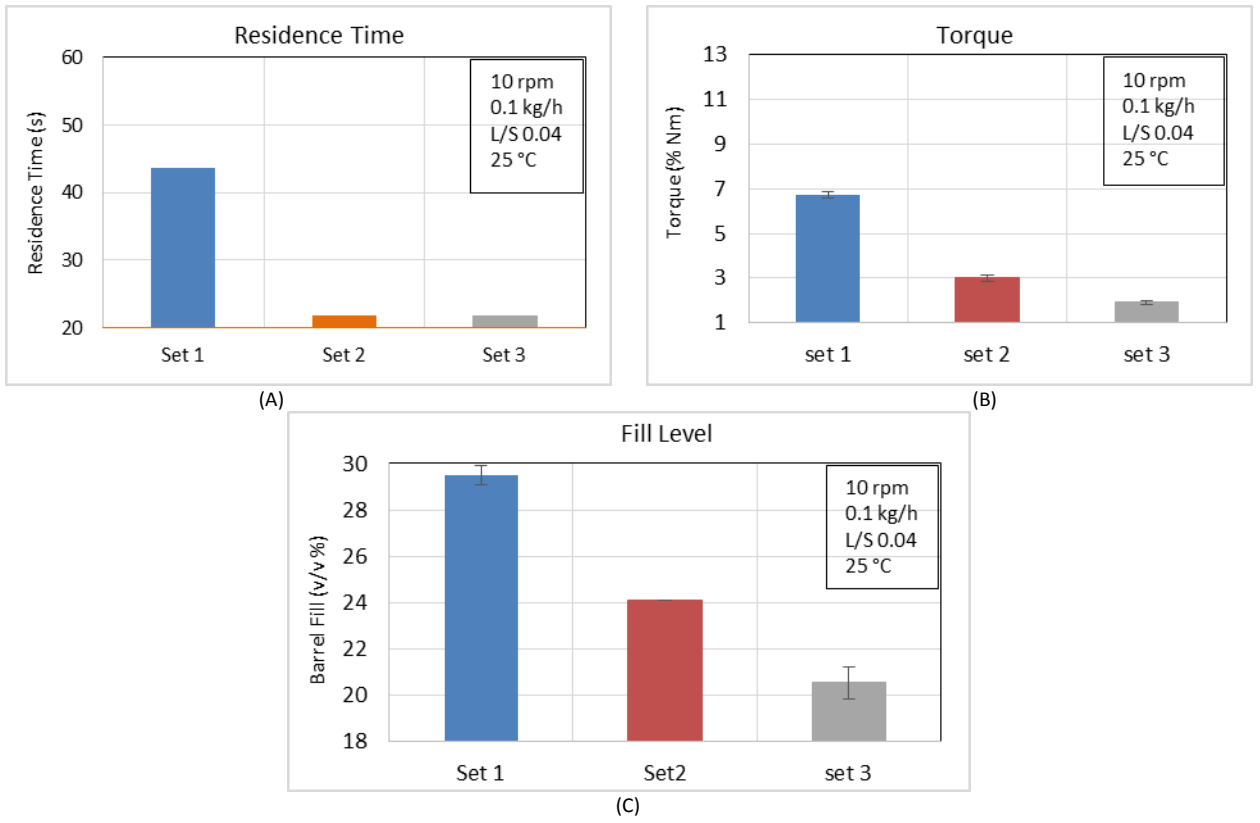


Figure B-2: The effect of binder delivery in Set 1, 2 & 3 on Residence time (A), Torque (B) and Barrel Fill Level, while applying the condition in for experiment 2.

### Granular shape

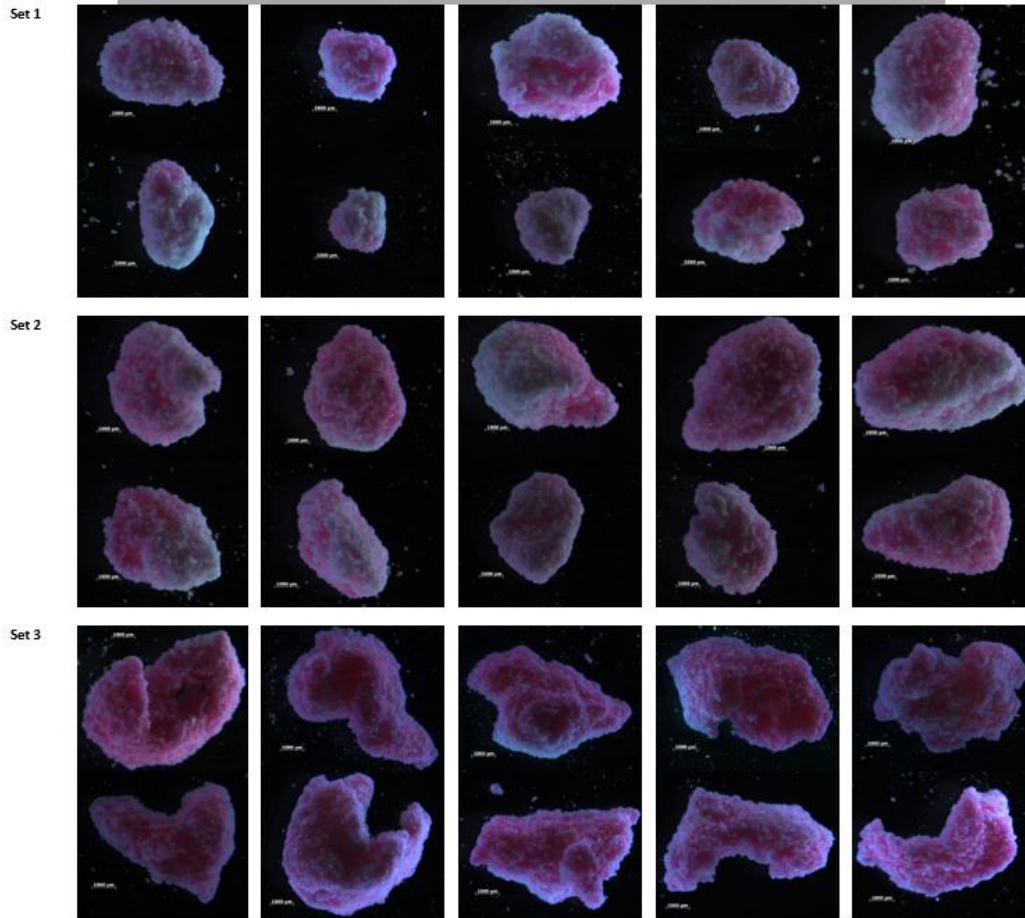


Figure B-3: shows the change in granular's shape as more HPMC delivered in the liquid phase.

### Granular's strength:

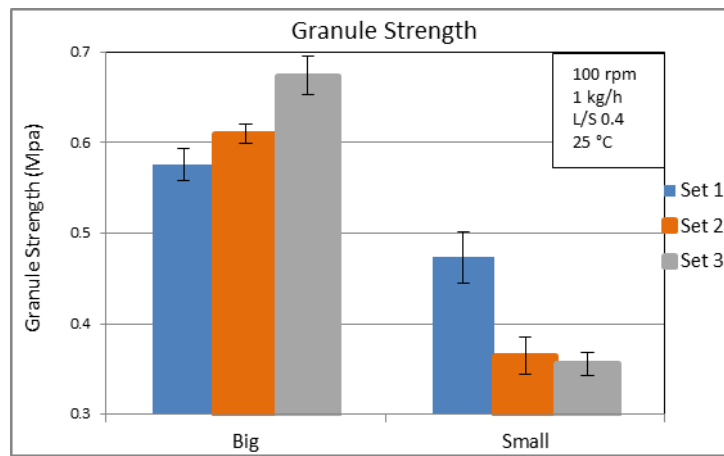


Figure B-4: the strength of granules in the big and small classes produced at different binder delivery.

It can be seen that regardless of the binder method chosen, the bigger granules will possess more strength than the small granules. This is owing to the amount of binder attained by the big granules compared to the small ones. Therefore, the amount of binder determines the strength of the granules, since it is responsible for the strong liquid bridges created between primary particles.

*Granules flowability:*

Set 1 had an angle of repose of approximately 34°, which gives a ‘good’ flow according to the results in literature. The angle of repose for Set 3 was approximately 36°, which gave a ‘fair’ flowing characteristics, as shown in the figure (A) below.

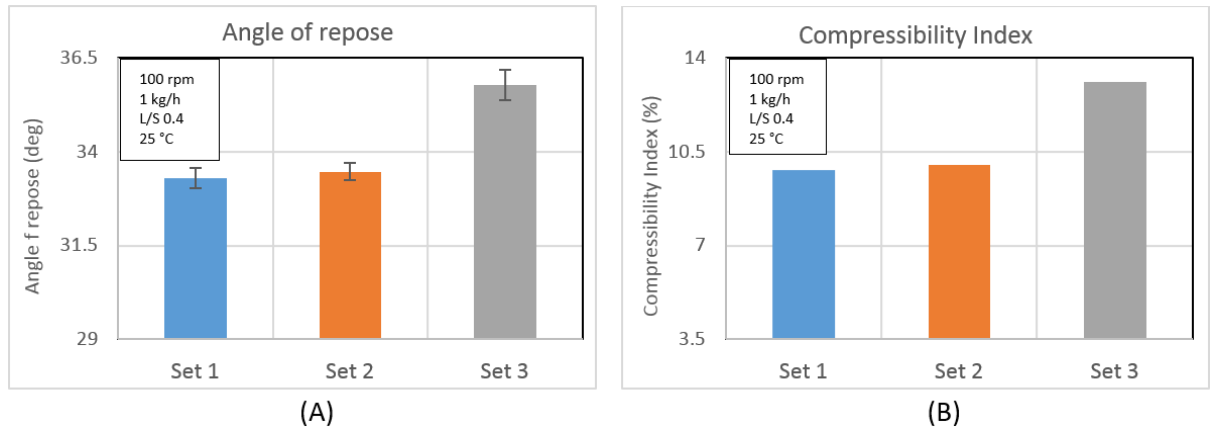


Figure B-5: The effect of binder delivery on the Angle of repose (A), and Compressibility Index (B.).

The compressibility index values in the above figure (B), are used as an indirect indication of the flowability of the granules; the higher the compressibility index, the lower the flowing ability. This indicates a reduction of volume under tapping was significant, as a result of higher amount of fines present within the sample. Comparing those result against the results given in the literature, which characterises the granules in Set 1 as ‘excellent’ flowing character, and Set 3 as only ‘good’ flowing character. This is due to wide size distribution in Set 3.

### B.1.3.2 Kneading elements:

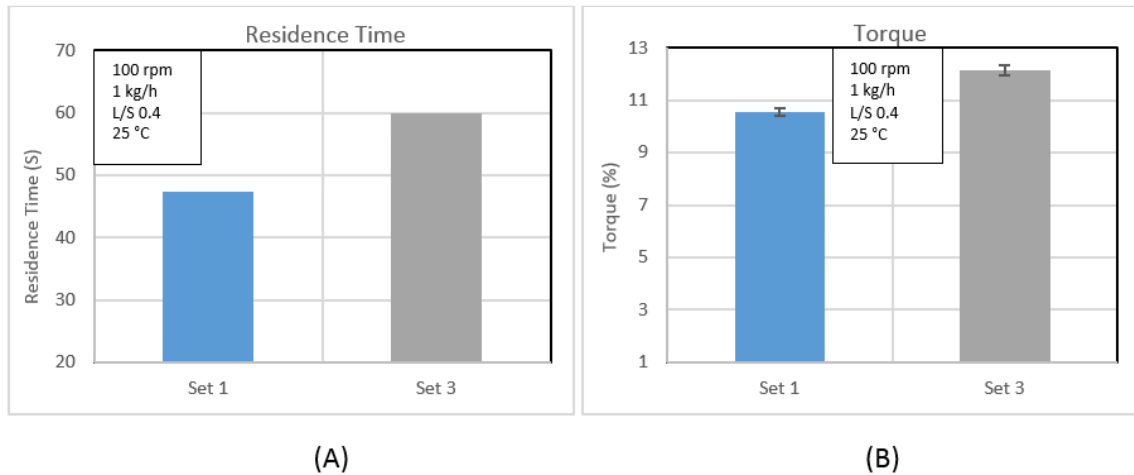


Figure B-6: The effect of binder delivery in Set 1 & 3 on the Residence time (A) & Torque (B), while applying the condition in for experiment 2, with kneading element

It can be seen that the residence time has increased for both sets (Set 1 & 3) with kneading elements than when using only conveying elements. This is because the conveying ability of the kneading element is lower than the conveying elements. This caused the materials to accumulate and, therefore, a delay in material being moved forward [17], which enhanced the mixing between powder mixture and granulation liquid *granules flowability*:

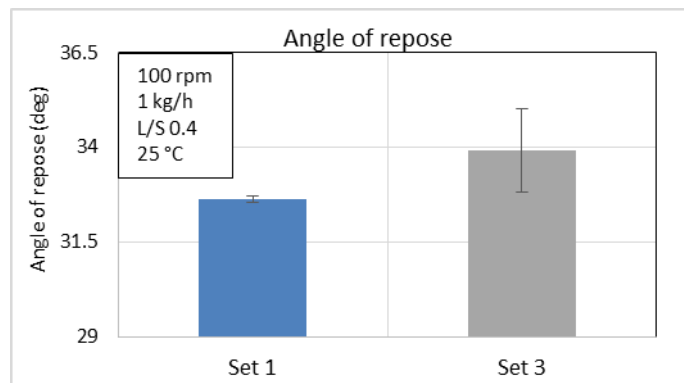


Figure B-7: The effect of binder delivery on the angle of repose, while using kneading element.

The granules in Set 1 and Set 3 possess the same flowing characteristic, when comparing these results with those given in literature.

## B.2 Liquid binder spreading:

### B.2.1 Methodology

To be able to monitor the distribution of binder the solid binder was dissolved in distilled water and then mixed with red dye (erythrosine B, acid red 51, Sigma–Aldrich) which was used as a tracer (Osborne, et al., 2011). The assumption made that dyed solid binder can be traced using the UV-spectrometer. The UV-spectrometer used, is Thermo Genesys 6 UV-Vis spectrophotometer. The wave-length of the beam was chosen by scanning a light of 400-600 nm at an increment of 2 through the solution of red dye and the wave-length, at which the light was absorbed the most, was taken. This wave-length was found to equal to 525nm. The scan was repeated five times.

Because the instrument only gave the amount of light was absorbed by solution, a calibration of the absorption of light to the amount of the concentration of dye was essential. To do so, different amounts of a known concentration of dye were prepared by considering the number of moles of the dye (where the  $M_r = 881.82 \text{ g/mol}$ ) and volume of solution. These solutions (with different concentrations) were run through the UV-spectrometer and the amount of absorbed light was obtained. This method has generated the calibration curve shown in below.

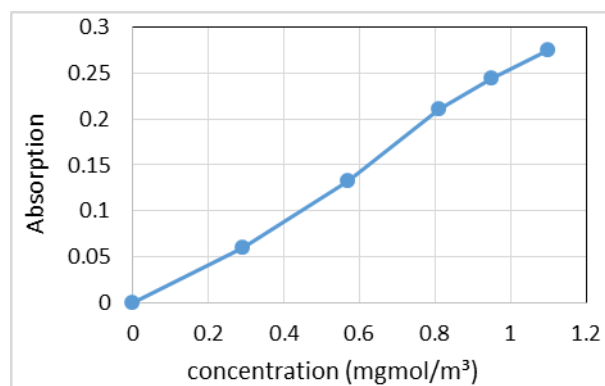


Figure B-8: calibration of light absorption to the concentration of red dye in the solution.

The Y-axis in Figure above represents the amount of light absorbance at a given concentrations (X-axis). The absorption of light is directly proportional to the

concentration of the dye and the thickness of the dye in the light path according to Beer's Law. The combination of Beer's law and Lambert's law (Beer-Lambert's law) enabled to define the amount of light absorbed in relation to the light transmitted as shown in Equation 0-1 [135].

$$A = - \log\left(\frac{I}{I_0}\right) \quad \text{Equation 0-1}$$

Where A is the absorption (no unit),  $I$  is the intensity of transmitted light,  $I_0$  is the intensity of incident light from the source.

The solution (dissolved solid binder and red dye in distilled water) was left in an oven at 120°C to evaporate all the water content for a day. The coloured dried binder was milled using a Ball mill to produce fine particles (<250µm). The reduction of size was necessary to reduce the disparity of raw materials when mixed with the powder mixture). After the granules production, 1 g of granules from each class (big, medium and small) was dissolved in 50 mL deionised distilled water (time was given until all the dye is released and the MCC sediment at the bottom). Then scanning at wavelength of 525 using the thermo Genesys 6 UV-Vis spectrophotometer, the dye concentration was determined. The selected wavelength was chosen so that the materials do not interfere with the absorbance of the dye. The dye concentration was considered as an indication of the binder quantity present within the sample. Each measurement was conducted a minimum of three times.

### **B.2.2 Results and discussion**

The Figure below shows the binder distribution through different class (as described in 5.2.3), namely; small, medium and big, as the binder delivery changed (Set 1-3), while using conveying elements only as screw configuration, as shown in Figure 3-4. It can be seen that granules in the big class (>2000 µm) produced during Set 1, had the least amount of binder in them compared to those produced using Set 2 and Set 3, while the small class (<500 µm) showed that the granules of Set 1 have retained more binder than

the other sets . This suggests that the binder spread was more even in Set 1, which agrees well with images presented in Figure 5-5, where Set 3 showed to have regions on concentrated red, hence the localization of the liquid.

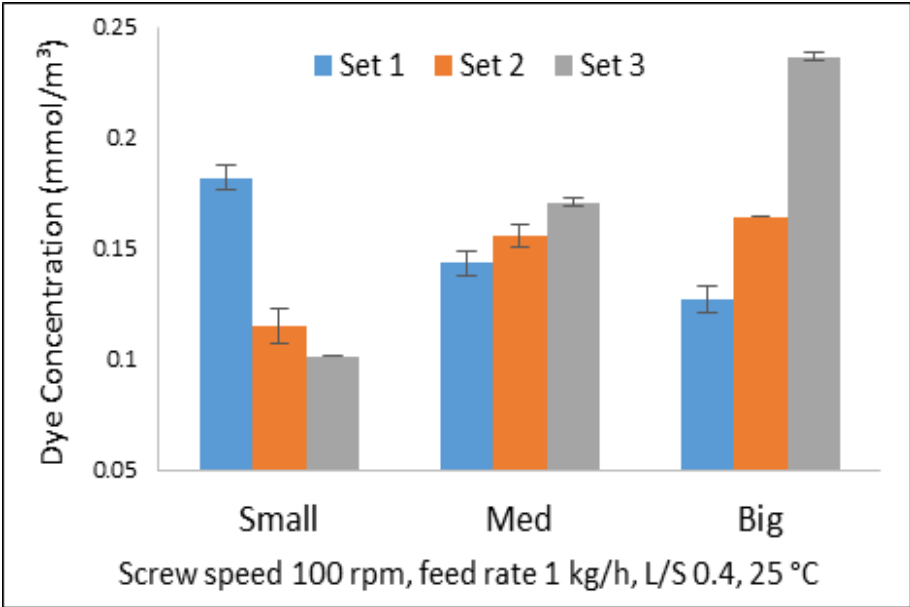
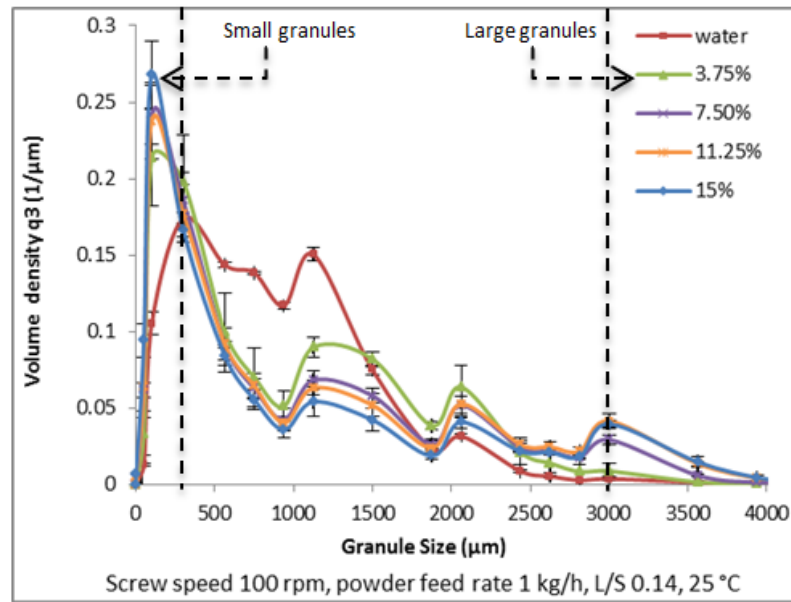


Figure B-9 Concentration of the dye in the three different classes of each set.

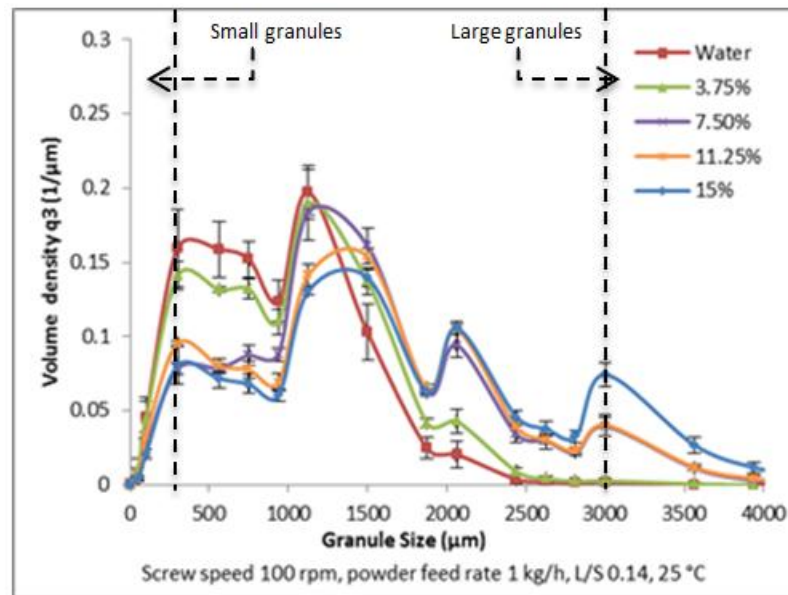
# Appendix C

## C.1 Size distribution

### C.1.1 Lactose



(a)

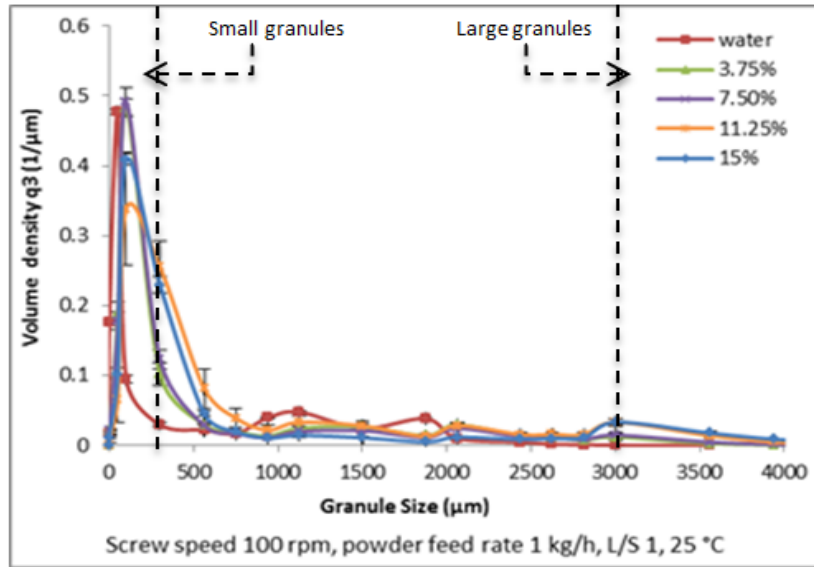


(b)

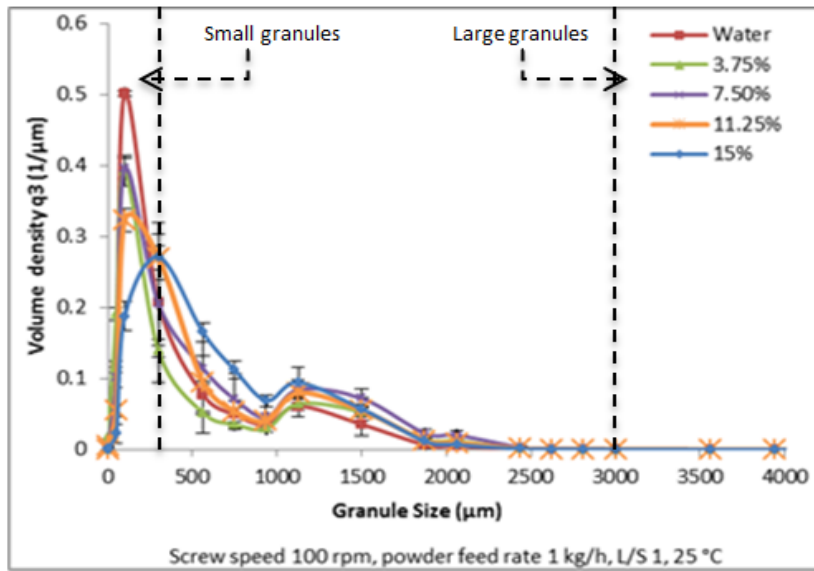
Figure C-1 Effect of variation of HPMC (% w/w) in the granulation liquid on size distribution of granules using lactose powder. (a) Using conveying elements only and (b) using conveying and kneading element as screw configuration.



### C.1.2 MCC



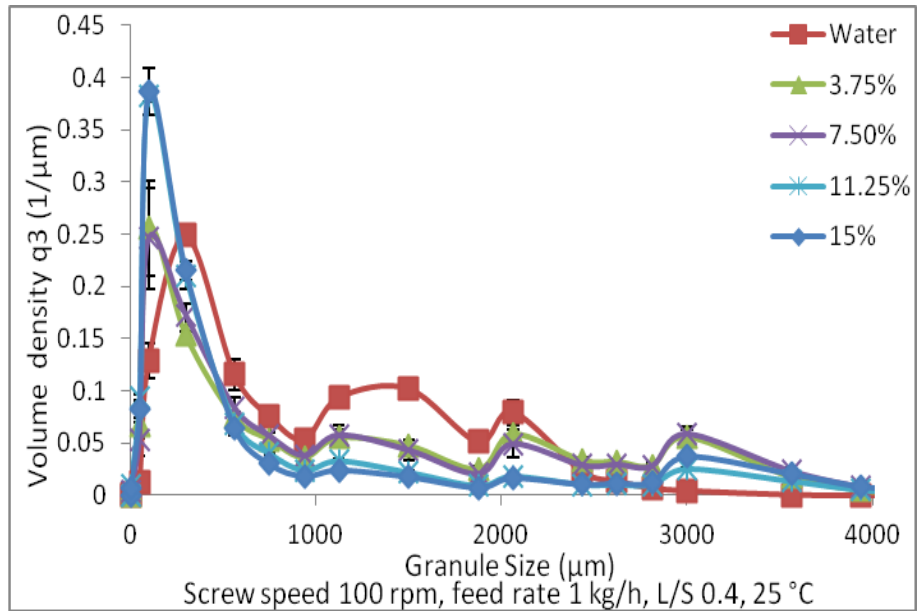
(a)



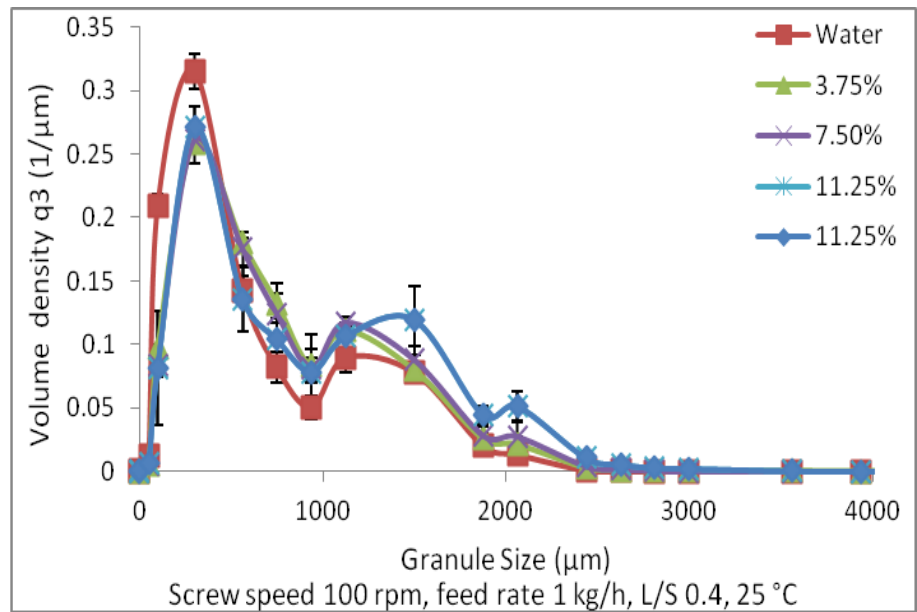
(b)

Figure C-2 Effect of variation of HPMC (% w/w) in the granulation liquid on size distribution of granules using MCC powder. (a) Using conveying elements only and (b) using conveying and kneading element as screw configuration.

### C.1.3 Formulation



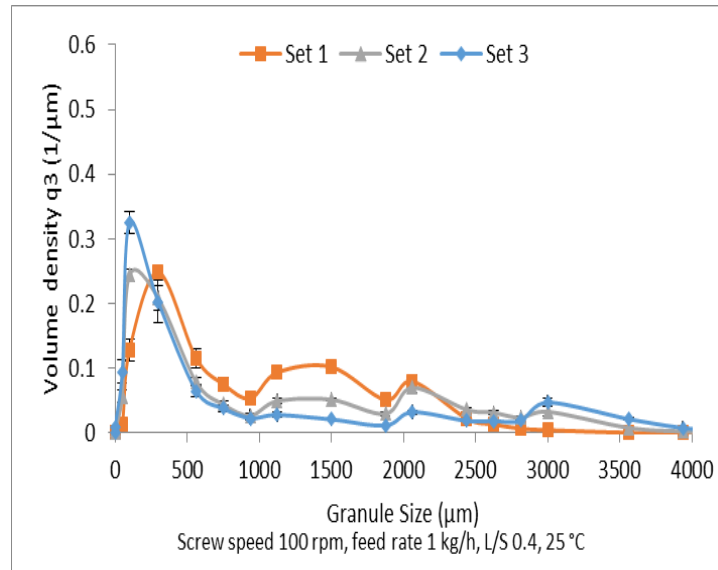
(a)



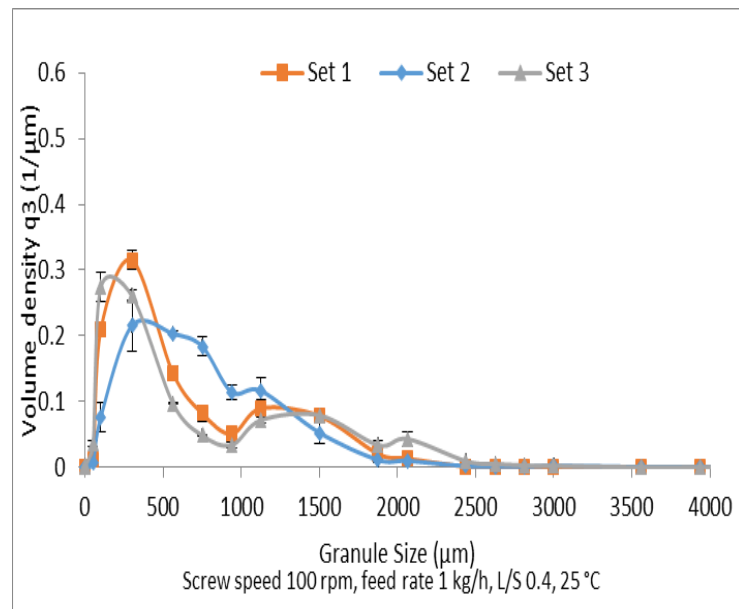
(b)

Figure C-3 Effect of variation of HPMC (% w/w) in the granulation liquid on size distribution of granules using lactose powder. (a) Using conveying elements only and (b) using conveying and kneading element as screw configuration.

### C.1.4 Binder delivery



(a)



(b)

Figure C-4 Effect of variation of binder delivery on size distribution of granules. (a) Using conveying elements only and (b) using conveying and kneading element as screw configuration.

## **C.2 Crushing force**

### **C.2.1 Experimental method**

Brinell ball indenter with diameter of 1.6 mm fitted to a material testing machine (BDO-FB, 0.5 TS, Zwick / Roell, Germany) is used to measure the force needed to break the ribbon. The Figure below shows the indenter used in the measurement. The preload of 0.01 N was applied before starting the test then the indenter moved down with speed of 0.1 mm/min. the maximum force was recorded for each test run and referred to as the crushing force. Although, the thickness of ribbon will influence its resistance to breakage, the results showed that MCC was stronger despite having a thinner ribbon, as shown in Appendix C.

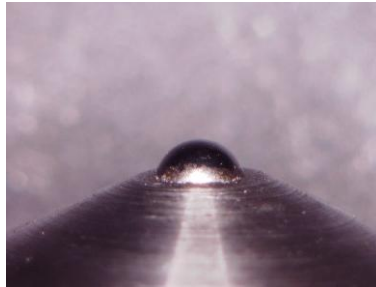


Figure C-5 images of the indenter used to break the ribbon of cakes.

## C.2.2 Experimental method

### Lactose

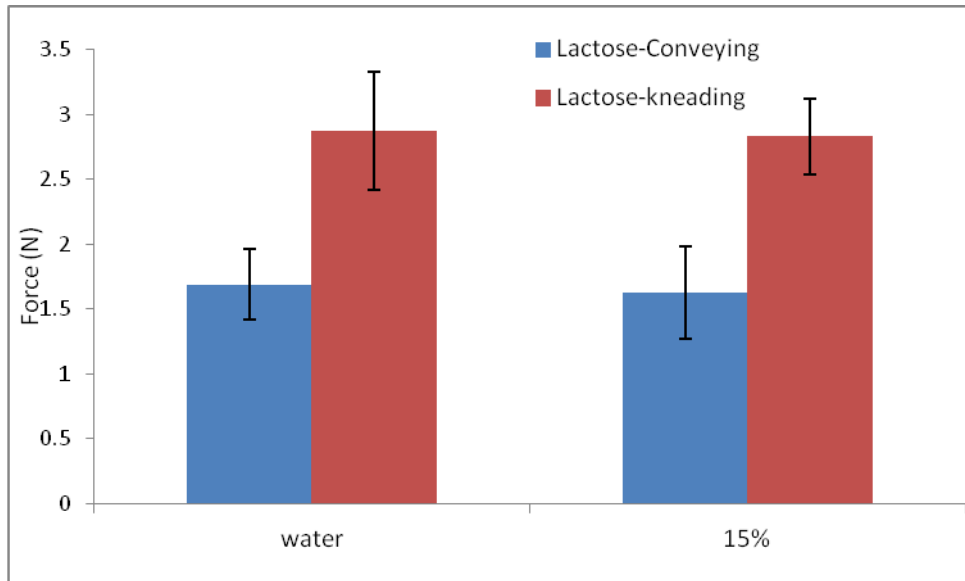


Figure C-6 Crushing forces required to break the ribbon of lactose cakes as the viscosity of the granulation liquid and screw configuration changes.

### MCC

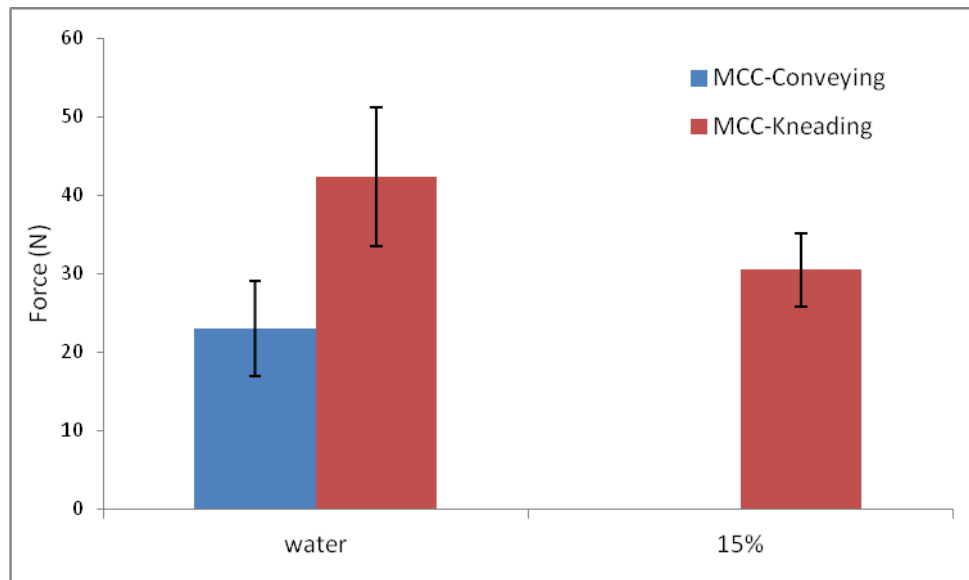


Figure C-7 Crushing forces required to break the ribbon of MCC cakes as the viscosity of the granulation liquid and screw configuration changes.

**Formulation**

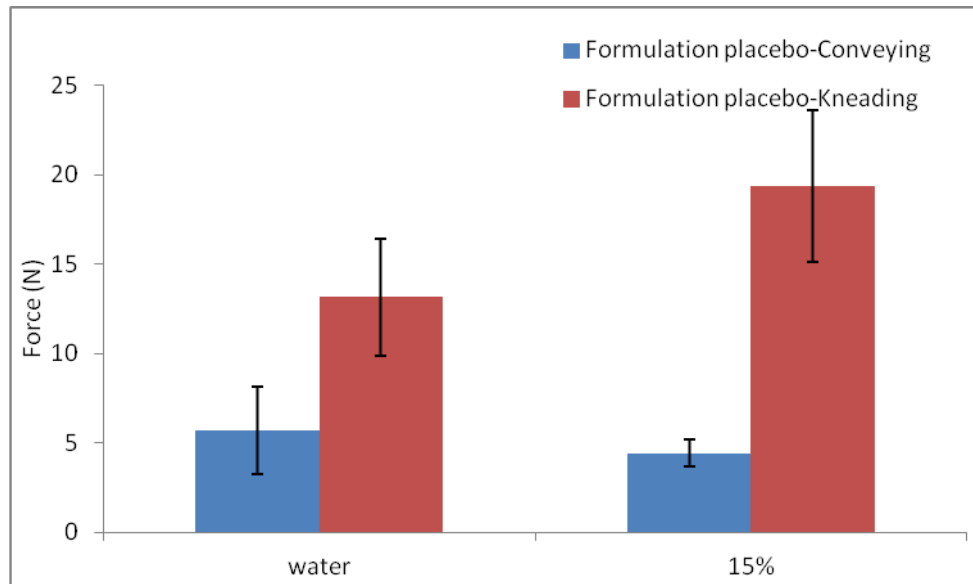


Figure C-8 Crushing forces required to break the ribbon of formulation placebo cakes as the viscosity of the granulation liquid and screw configuration changes.

**Binder delivery**

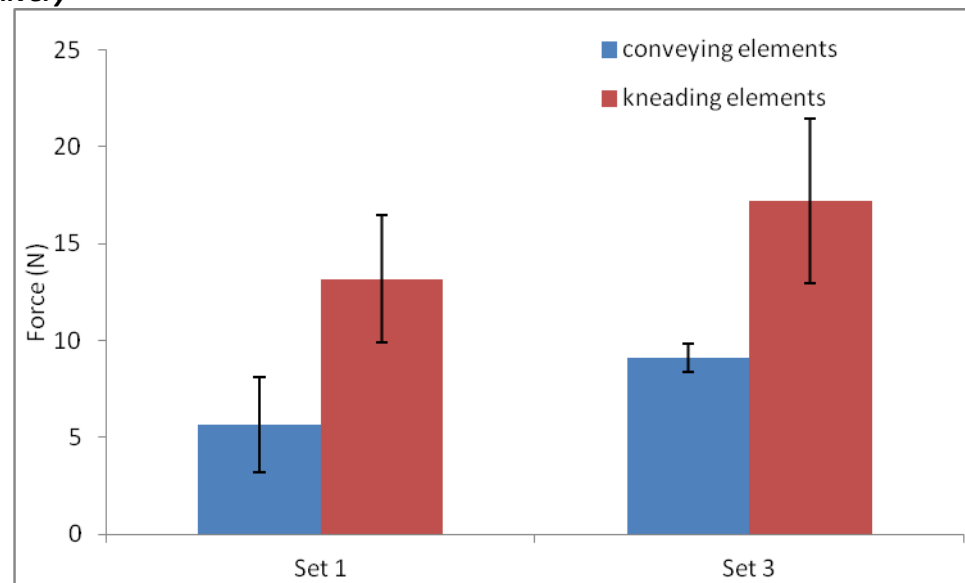


Figure C-9 Crushing forces required to break the ribbon of formulation placebo cakes as binder delivery and screw configuration changes.

### C.3 Powder caking/stickiness on the bottom barrel

Within this sections result (images and mass (g)) shows powder caking/stickiness at the bottom of the barrel after 6 minutes while varying the screw configuration. This is done for lactose and MCC.

#### C.3.1 Lactose

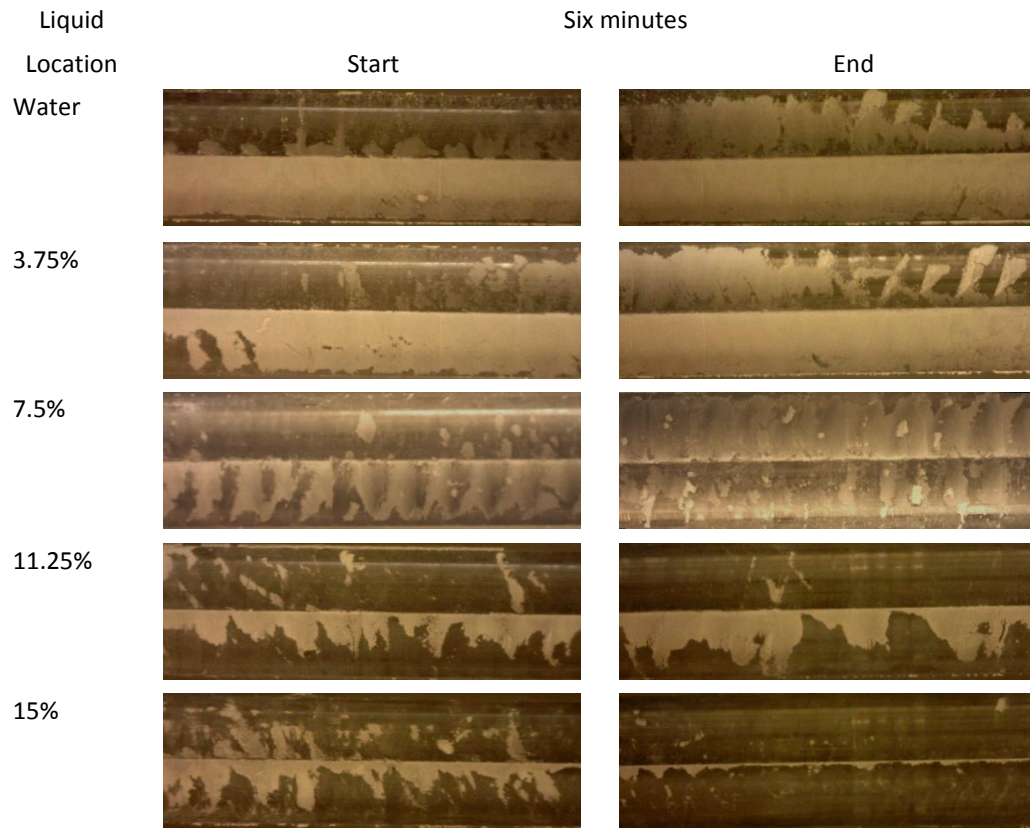


Figure C-10 Effect of granulation liquid viscosity on Lactose powder caking/stickiness on the bottom of the barrel after 6 minutes, using conveying elements only.

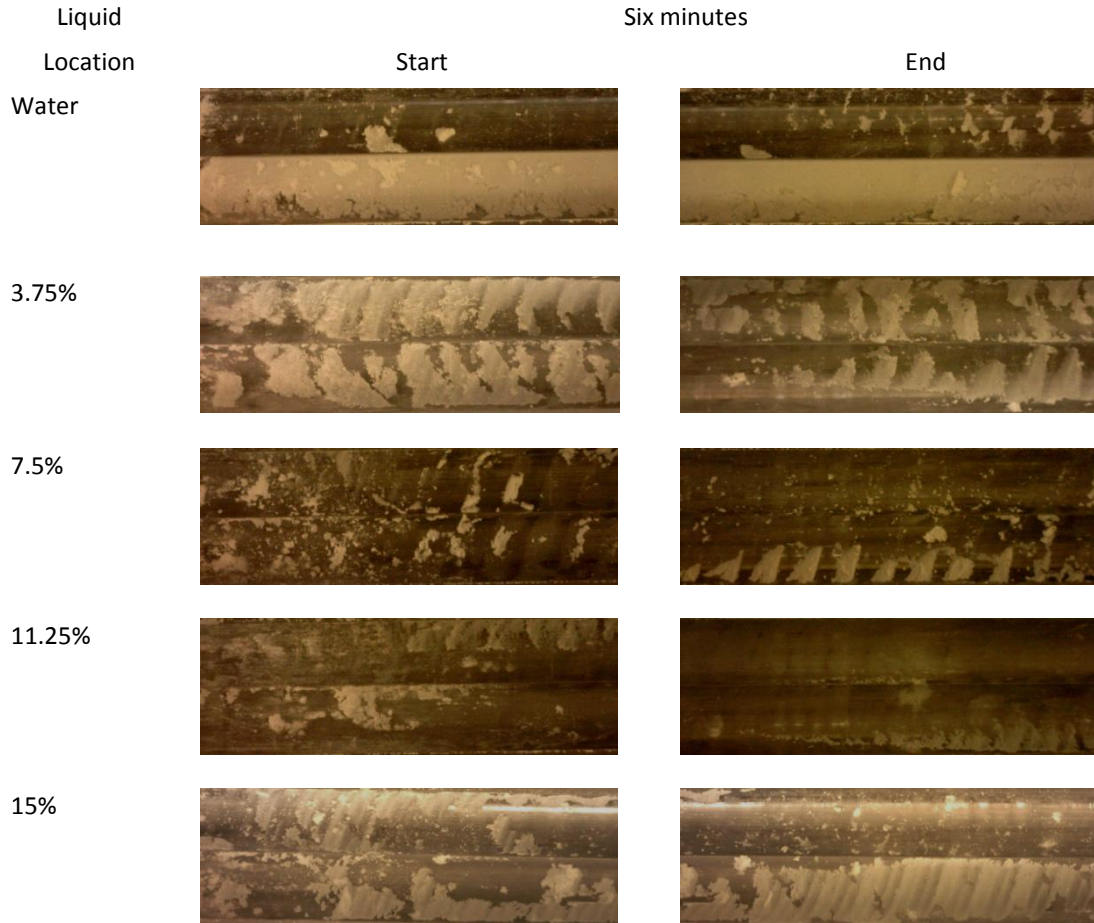


Figure C-11 Effect of granulation liquid viscosity on Lactose powder caking/stickiness on the bottom of the barrel after 6 minutes, using conveying elements and kneading elements.

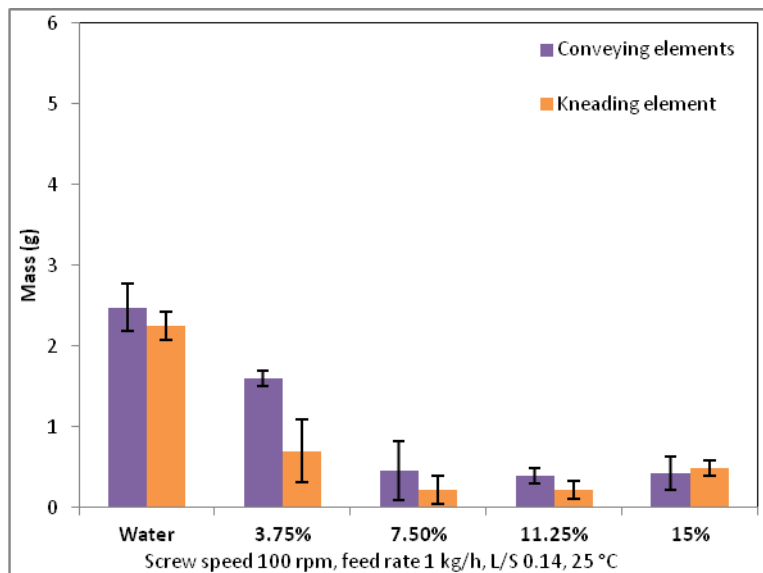


Figure C-12 Effect of granulation liquid viscosity on the mass of caking on the bottom of the barrel using: conveying elements only (■) and conveying with kneading elements (■).



### C.3.2 MCC

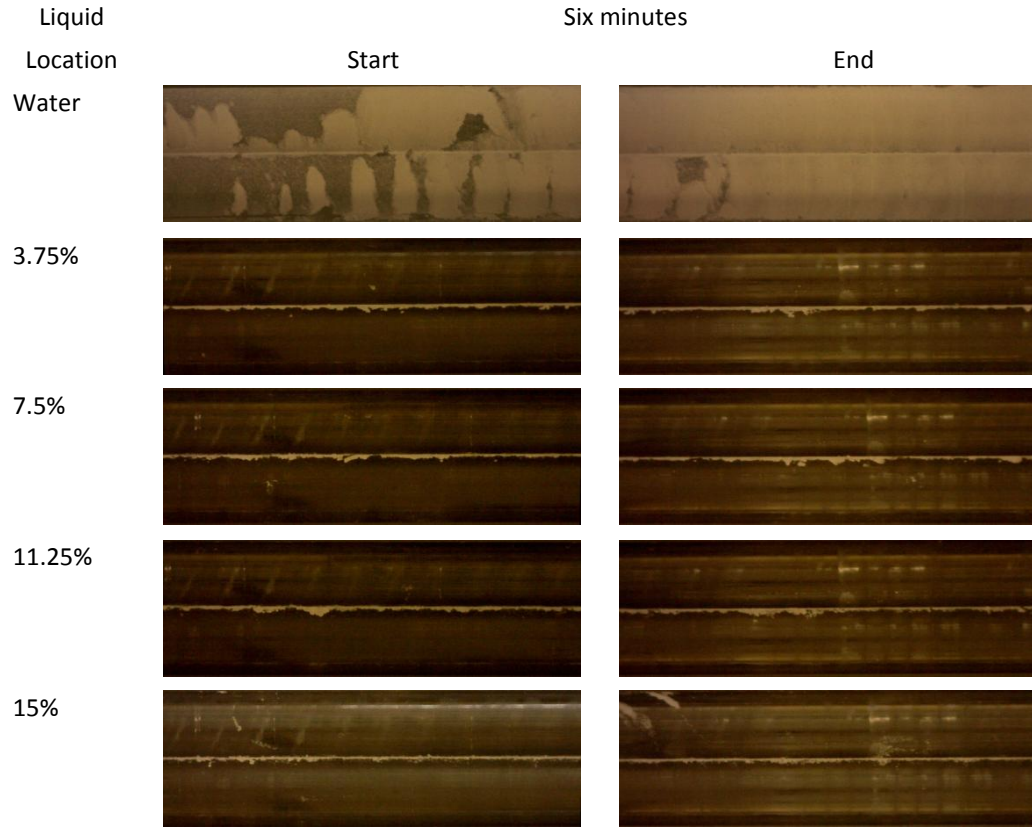


Figure C-13 Effect of granulation liquid viscosity on MCC powder caking/stickiness on the bottom of the barrel after 6 minutes, using conveying elements only.

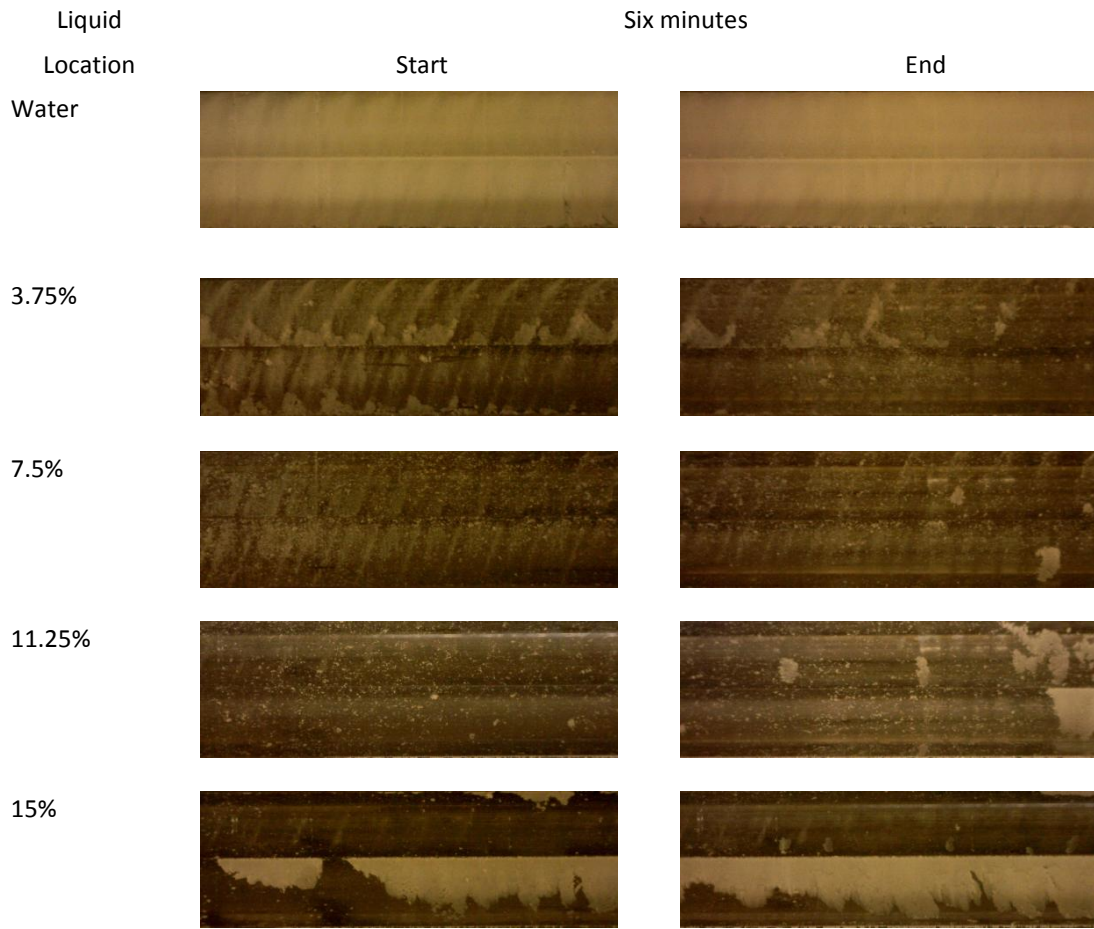


Figure C-14 Effect of granulation liquid viscosity on MCC powder caking/stickiness on the bottom of the barrel after 6 minutes, using conveying elements and kneading elements.

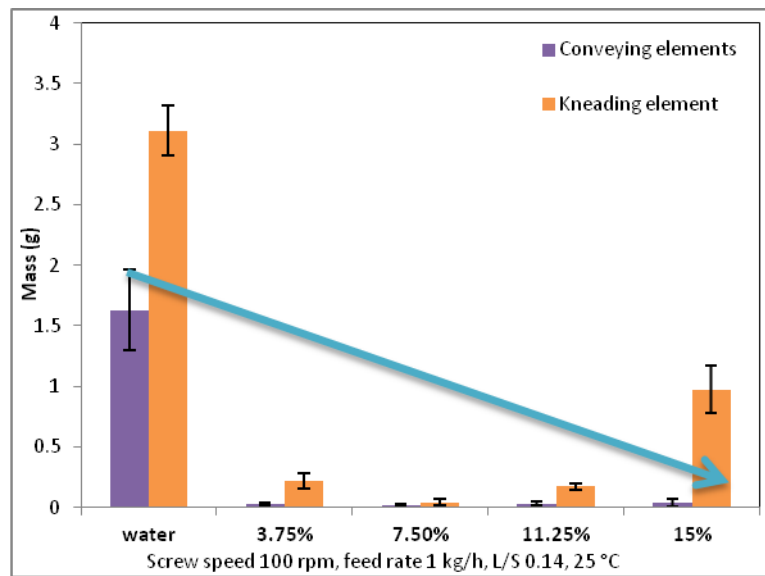


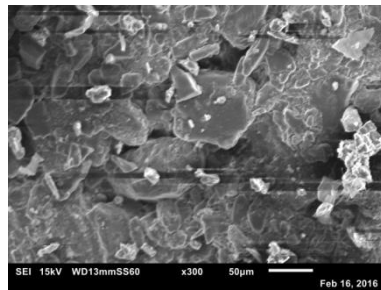
Figure C-15 Effect of granulation liquid viscosity on the mass of caking on the bottom of the barrel using: conveying elements only (■) and conveying with kneading elements (■).

## C.4 SEM

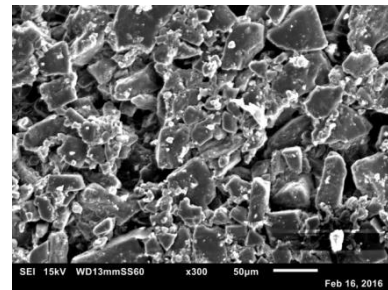
The resulted blow showed the SEM images of the ribbon of cakes for lactose and MCC produced using conveying elements only while using granulation liquid of water. This is to show the difference in compaction and deformation of the both side of the ribbon. Front side is the side facing the granulator and continuously under shear forces as the material is conveyed forward. Back side is the side attached to the steel barrel.

% of HPMC  
Lactose

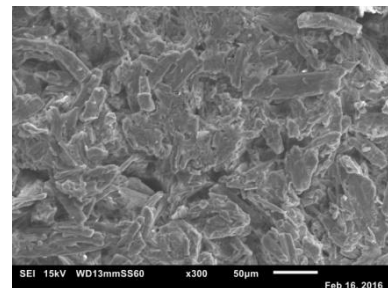
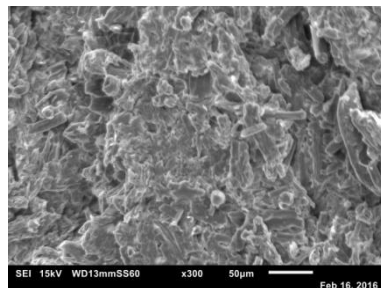
Front



Back



MCC



### C.5 Thickness of caked ribbons

% of HPMC

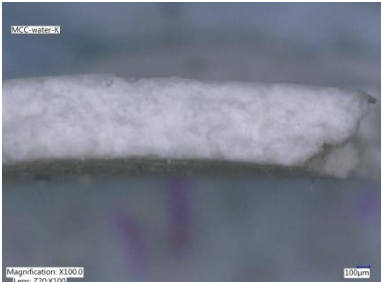
0%

15%

Lactose



MCC



## Appendix D

### D.1 Visual On-line Sizing (VOS)

#### D.1.1 Method

The aim is to try to construct a method of measuring the granule size on-line. There have been several attempts to produce images of granules in focus whilst being well dispersed in the air; some of them are described below.

Visual Online Sizing system involves the use of a higher speed camera, granule dispenser and appropriate lighting. These were set-up at the end of the barrel, where granules are produced as show Figure D- 1:

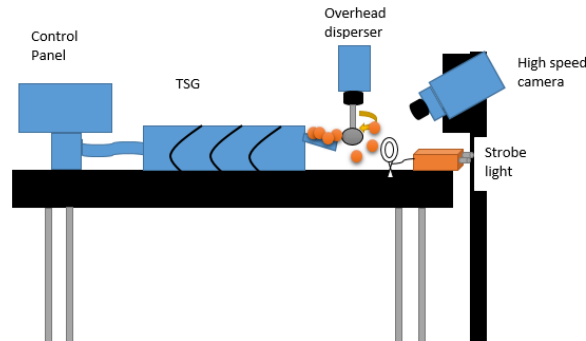


Figure D- 1 system set-up for VOS with overhead mixer.

The overhead disperser is placed in front of the strobe light; the speed of overhead disperser was adjusted to allow granules to be well-dispersed in the air, while reducing the speed to mitigate any damage or deformation to the granules as result. The strobe light, at 60 hz, and the camera frame –rate, at 60fps, were synchronized. This was very important, as the strobe light was used to eliminate any blurriness of granules as a result of the motion.

In another attempt to improve the sharpness of the image and narrow the path of the free falling granules, the overhead disperser was removed and replaced with a vibrator that had chute attached to it at the end. The camera settings were kept the same.

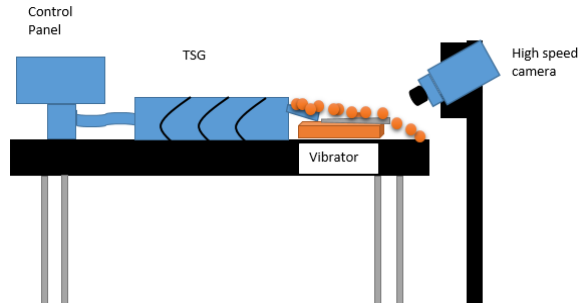


Figure D- 2 system set-up for VOS with vibrator

Figure D- 2 shows the set-up how the granules, produced using a TSG, are being dispersed by using a vibrator. This helped to narrow the path of the free falling granules.

### D.1.2 Results

Using the set-up shown in Figure D- 2 , with the overhead disperser was used to dispense the granules in the air. Granules were produced using a TSG, at 100rpm, 1kg/h and 25°C, where the configuration of the screw consisted of only conveying elements. The aim was to produce granules with broader size range and see if the camera can detect them all both small and big granules. This produced the image shown in Figure D- 3.

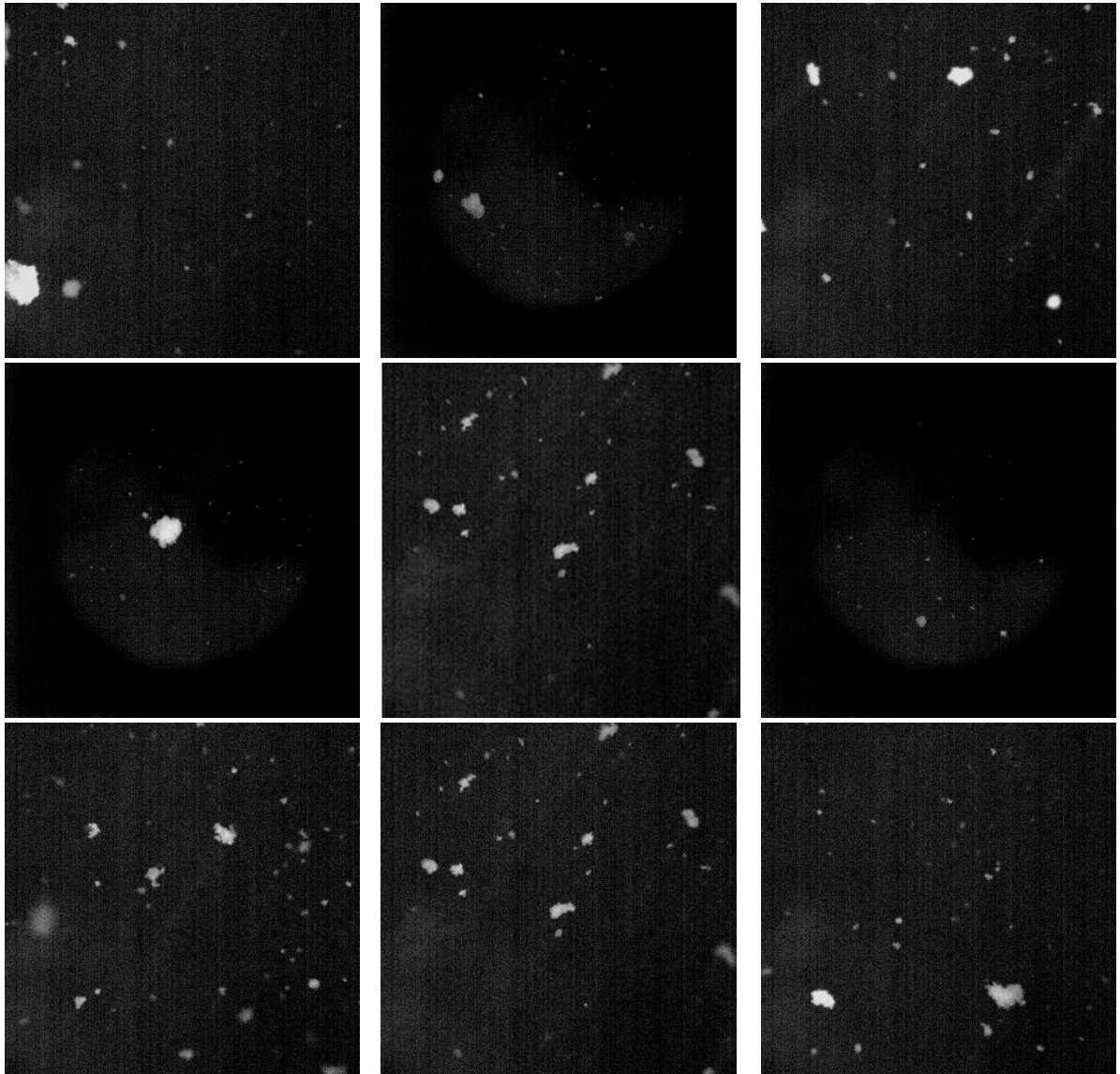


Figure D- 3 image taken using overhead mixer.

From Figure D- 3, it shows that the granules were dispersed well in the air. This is very important as otherwise a misleading results can be drawn, where two small attaching granules can be seen as one big granule. However, some of the granules are out of focus,

and the small granules seen in the images are not clear whether they are far or small in size. This is due to the fact that the overhead disperser spread the granules in the air in all directions, and hence making it difficult for the camera to focus on all the dispersed granules.

Therefore to narrow the flowing channel available for the produced granules, the overhead disperser was replaced with a vibrator. The vibrator had a narrow chute, which gave an image shown in Figure D- 4.

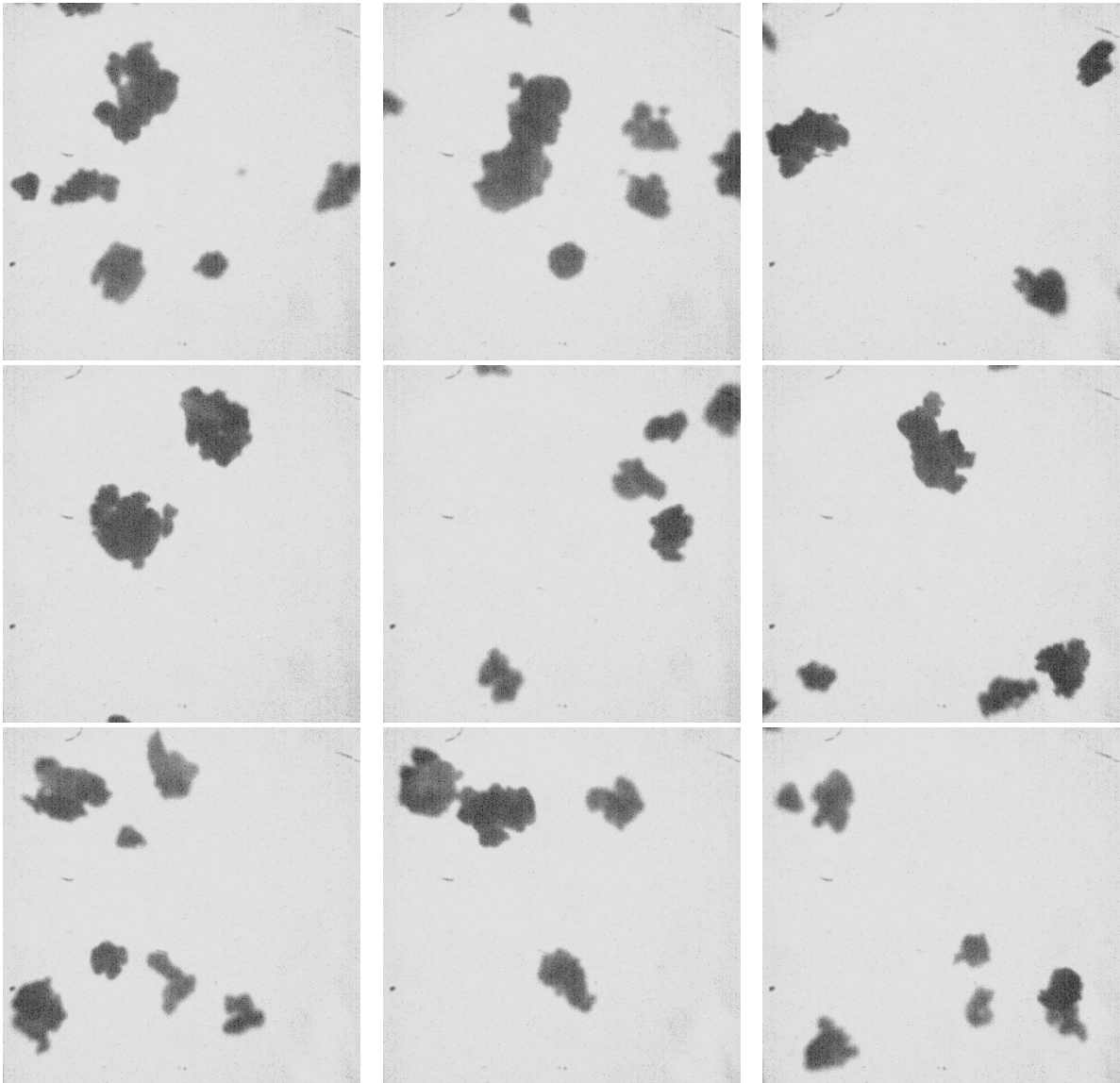


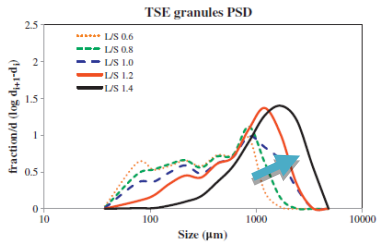
Figure D- 4 image of granules as the fall off the vibrator.



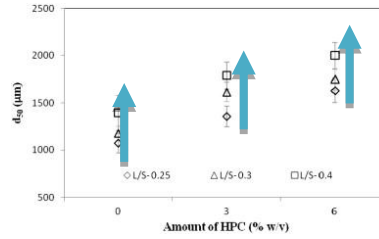
From Figure D- 4., it can be seen that the dispersing of granules in the air is also achievable by using a vibration system with a chute. In addition to the dispersing, the vibrating system was also able to narrow the path of granules. This helped to bring more granules into focus, where the edges of the granules are more defined. However, there is a need for alteration to avoid the accumulation of granules on the chute of vibrator. This is because the granules produced were still wet and therefore adhered to the chute of the vibrator, where they formed a pile of granules. The speed of the vibrator was regulated to ensure a continuous flow of the granules, however, increasing the vibration speed to prevent the accumulation resulted in an overlap of the free falling granules. Therefore, the aim is to design a chute that will allow the angle and height to be adjusted easily, while attaching a vibration source to it.

# Appendix E

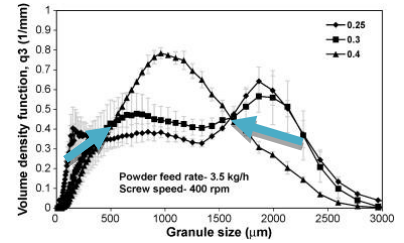
## E.1 Effect of L/S on granule size



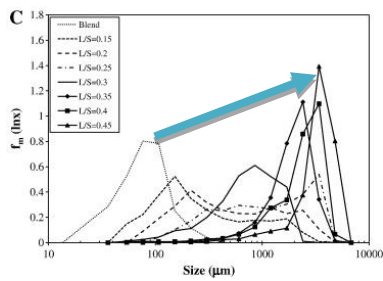
(Kai T. Lee)



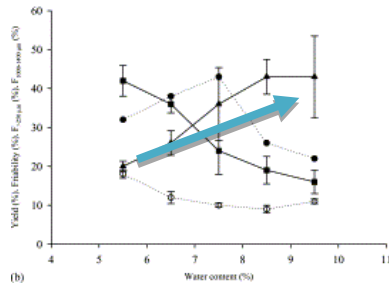
(Dhenge)



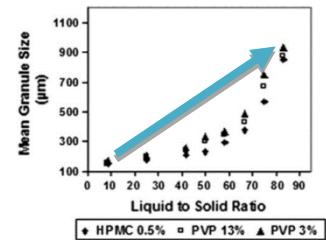
(Dhenge)



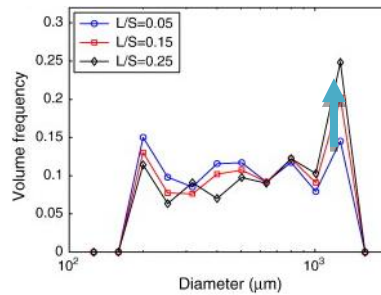
(Hagrasy)



(E.I Keleb)

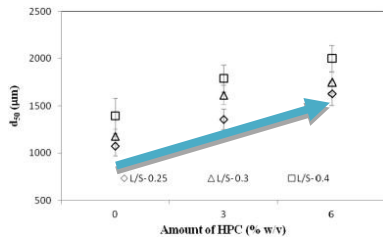


(Chitu)

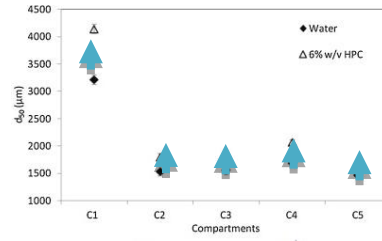


(Dana Barrasso)

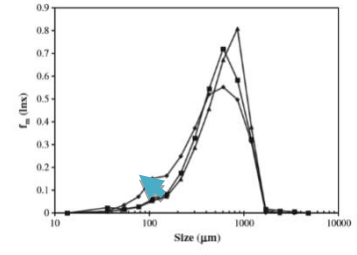
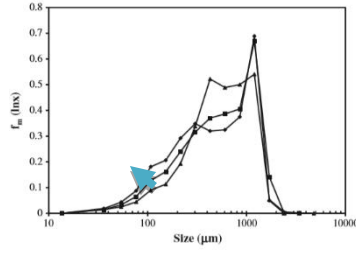
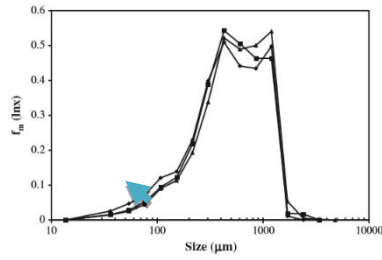
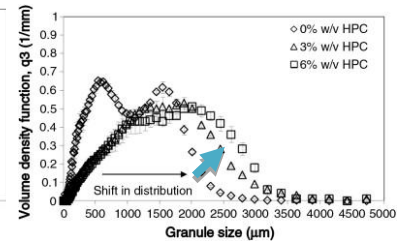
## E.2 Effect of Viscosity on granule size



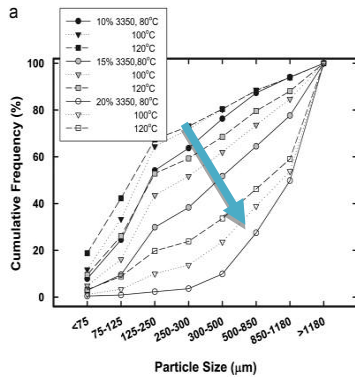
(Dhenge)



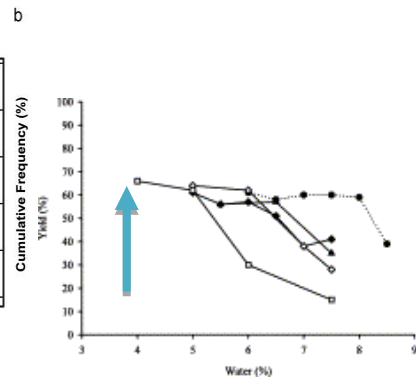
(Dhenge)(Dhenge)



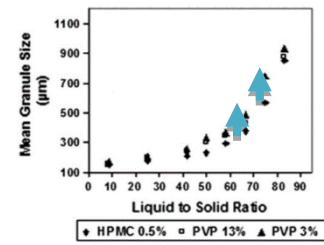
(Hagrasy)



(Mu and Thompson)

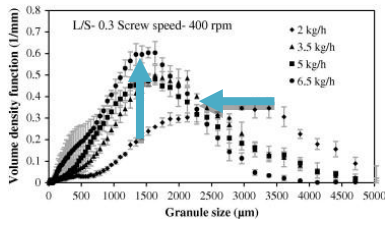


(E.I Keleb)

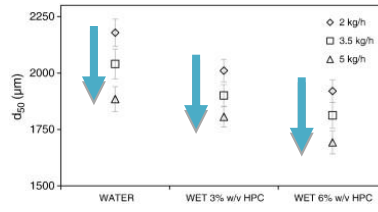


(Chitu)

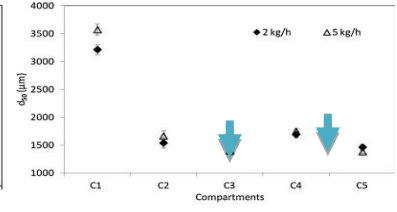
### E.3 Effect of Feed-rate on granule size



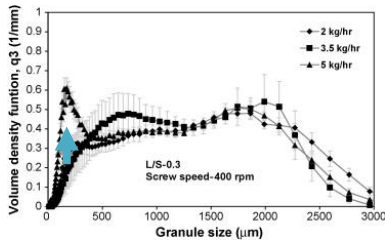
(Dhenge)



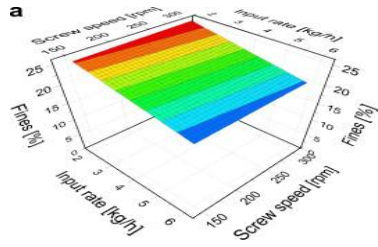
(Dhenge)



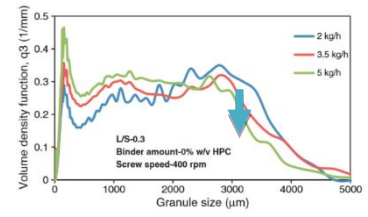
(Dhenge)



(Dhenge)

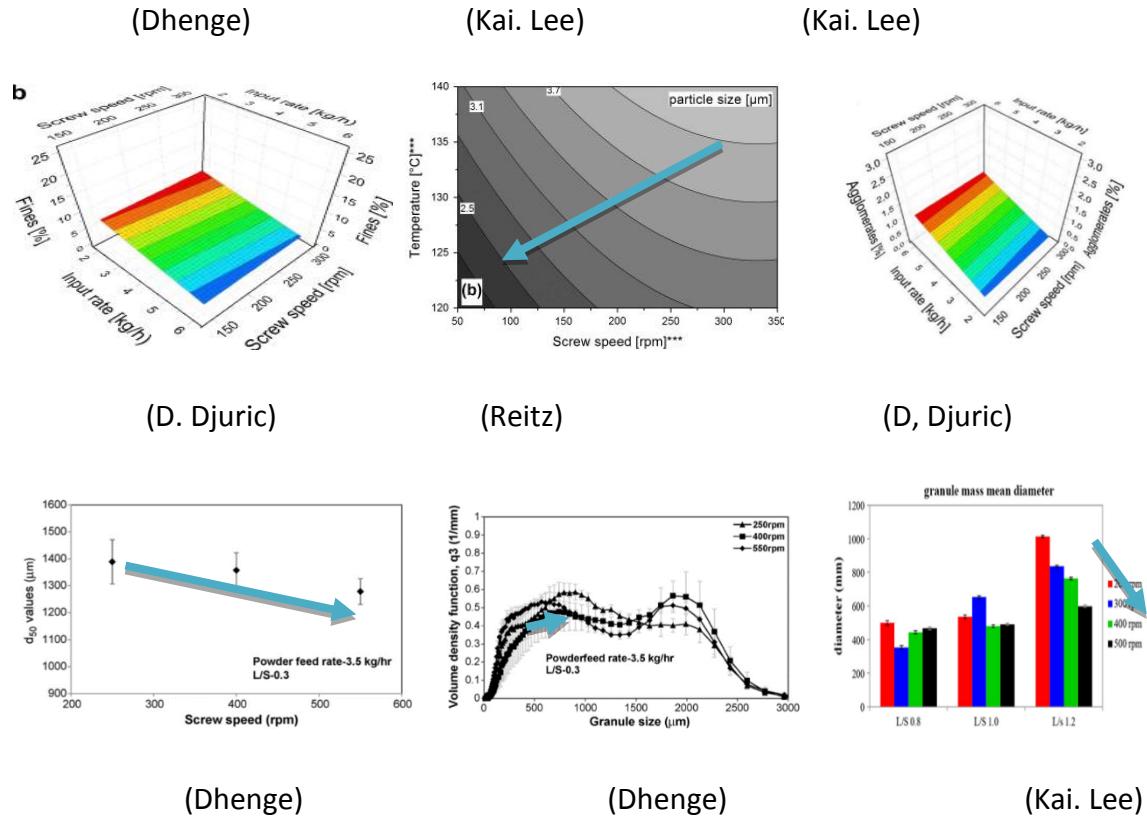


(D. Djuric)

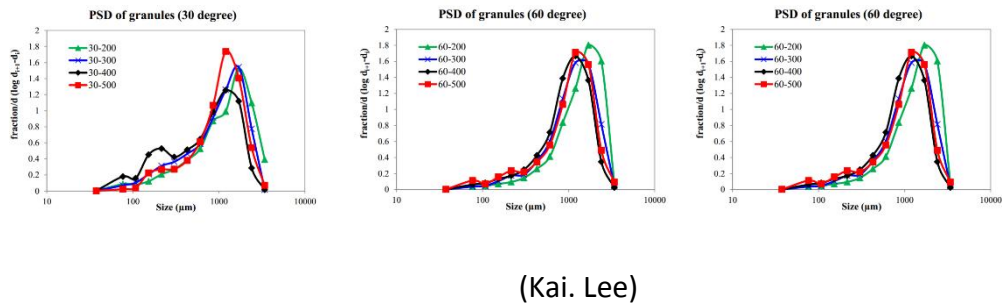


(Dhenge)

## E.4 Effect of screw-speed on granule size



## Effect of screw-configuration on granule size



Ref	Arthur	Material	Variable	TSG set-up	Measurements	Comment
[75]	E.I. Keleb	$\alpha$ -Lactose monohydrate PVP Hydrochlorothiazide	Screw speed Input-rate Screw set-up	L : D ratio of 25:1 Varying configuration	Influence of extruder setup Influence of formulation Influence of processing parameters	Removal of die increases the yield Water is required in a certain range to make a feasible granulation Decreasing water concentration increased the fraction of large particles ( $F_{<250\ \mu\text{m}}$ ) Adding PVP decreases water concentration requirement Increasing the speed did not have a significant effect Increasing input-rate increased the granulation yield
[2]	R.M Dhenge	$\alpha$ -Lactose monohydrate Crosscarmellose Sodium Microcrystalline cellulose HPC Water was used as granulation liquid	Screw speed Powder feed-rate L/S ration	L : D ratio of 25:1 Screw consisted of kneading and conveying element	Influence on residence time and torque Influence on size distribution Influence on granule properties.	Increasing feed-rate, decreases residence time and increases the torque. Where the size distribution shifts from bi-modal to mono-modal, as well as increasing the granule's strength Increasing L/S ratio, increases residence time and torque. While decreasing the granule size as well as increase the granule strength. Increasing the screw speed, decreased the residence time and torque. Screw speed did not affect the size distribution, flowability and the strength of granule.
[7]	E.I. Keleb	$\alpha$ -Lactose monohydrate PVP	Liquid viscosity	L : D ratioe of 25:1 Conveying materials with two mixing	Influence of viscosity of liquid granulation	Addition of PVP improved tablet properties. Addition of PVP reduced the requirement of water concentration for wet granulation.

sections						
Die block is fixed to the extruder barrel						
[17]	Kai T.Lee	$\alpha$ -Lactose monohydrate. HPC Crosscarmelluose Water as granulation liquid	Feed-rate Screw speed	L : D ratio of 10:1 Modified barrel used Conveying zones Mixing zones (discs arranged at an angle of 30°, 60° or 90°)	Positron emission particle tracking (PEPT) Residence time distribution Overall fill fraction of TSE granulator	Flowing velocity of materials in mixing zones is lower than in conveying zones. Increase in screw speed moves RTD slightly to the left and become narrower at high L/S ratio. Increasing feeder-rate decreases the mean residence time Increasing the kneading element angle increase the level fill. The level fill is proportional to powder feed-rate and inversely proportional to screw speed. Materials are conveyed by dispersion mechanism through the 90° mixing zone
[52]	J. Vercruysea	$\alpha$ -Lactose monohydrate. PVP Theophylline anhydrate Magnesium stearate Water (as granulation liquid)	Feed-rate Screw speed	L : D ratio of 25:1 1 <sup>st</sup> segment consist of only conveying elements 2 <sup>nd</sup> consists of the kneading elements.	Influence of process variables on granule quality Influence of process variable on tablet quality Evaluation of granulation process	Conveying element are used with minimal mechanical energy imparted. Kneading elements intensively mix the solid and liquid components. No significant relationships for angle of kneading and screw speed were found. Increase in feed-rate and kneading elements gave a rise in temperature of the barrel and less fines. The binder is more effective when it is already dissolved in the material. The number of kneading elements affected the tensile strength, disintegration time and dissolution profile of the tablet.
[36]	R.M Dhenge	$\alpha$ -Lactose monohydrate HPC	Feed-rate	L : D ratio of 25:1 Conveying elements used only	Influence of viscosity of granulation liquid on penetration time.	High viscosity granulation liquid has a longer penetration time. Decrease in viscosity and increase in feed-rate gave a rise in torque. Granules size increased as the both feed-rate and viscosity increased.

0.5 of blue dye as a colour  
Microcrystalline cellulose  
Crosscarmellose  
Sodium

Influence of viscosity of granulation liquid and powder feed-rate on torque and SME  
Influence of granulation liquid and powder feed-rate on granule properties.

Small granules were stronger at low viscosity.  
Large granules were stronger at high viscosity.  
Increase in viscosity, decreased the deformation value.

[3]	Kai T.Lee	Microcrystalline Cellulose Distilled water used as granulation liquid.	L/S ratio Screw speed	L : D ratio of 25:1 Conveying elements were used Two mixing zones (each of five kneading element oriented at 90°)	Particle size distribution (PSD) Shape and morphology Estimated granule fracture strength	TSE produce porous granules, with multi-modal size distribution. Consolidation stage in TSE is absent Using L/S ratio of 1 and varying screw speed gave bimodal distribution. Increase in L/S ratio shifted the PSD from bimodal to mono-modal Change in L/S ratio and screw speed had no effect on the porosity of particles. The strength of granule produced by TSE is 3-4 times stronger than the granules produced in HSM
[88]	R.M Dhenge	$\alpha$ -Lactose monohydrate HPC Crosscarmellose Sodium Microcrystalline cellulose Sodium Cholride Water was used as	Feed-rate	L : D ratio of 25:1 Screw consisted of conveying and intermeshing elements.	The mechanisms of granulation in each compartment (5Cs) Influence on residence time distribution and torque Influence on properties of	The granules porosity changed along the length of the screw. The surface of the granules changed from rough to smooth.



---

granulation liquid

granules.

<b>[33]</b>	R.M Dhenge	$\alpha$ -Lactose monohydrate Erythrosine was used as red die Crosscarmellose Sodium Microcrystalline cellulose Sodium Cholride Water was used as granulation liquid	Feed-rate (2, 3.5, 5 and 6.5 Kg/h)	L : D ratio of 25:1 Screw consisted of conveying and intermeshing elements only	Influence of the amount of HPC and SDS on viscosity and surface tension Influence of the amount of HPC and SDS on the residence time and torque Influence of the amount of HPC and SDS on granule properties.	As HPC increased the viscosity of liquid increased. SDS changed the surface tension of the liquid. However, when the liquid was viscous (HPC of 6%w/w), SDS didn't affect the surface tension of the liquid. Increasing HPC increased residence time and torque, while SDS was ineffective. Increasing HPC shift the size distribution from bimodal to mono-modal, while SDS had no influence. Increasing HPC produced fewer elongated granules, less porosity, stronger granules as well as improving the flow-ability of granules.
-------------	------------	--	------------------------------------	--	---	--

